NATIONAL SCIENCE FOUNDATION

Print ISSN 1391-4588
E - ISSN 2362-0161
Volume 51 No. 4
December 2023

Journal of the National Science Foundation of Sri Lanka

www.nsf.gov.lk

NATIONAL SCIENCE FOUNDATION

JOURNAL OF THE NATIONAL SCIENCE FOUNDATION OF SRI LANKA

Publication : Published quarterly (March, June, September and December) by the National Science Foundation of Sri Lanka.

Manuscripts: Research Articles, Research Communications, Reviews and Correspondences in all fields of Science and Technology may be submitted for consideration for publication. A guide to the preparation of manuscripts is provided in each issue. The guidelines may also be obtained by visiting the NSF website.

Manuscripts and all correspondence relating to them should be sent to the Editorial Office, National Science Foundation, 47/5, Maitland Place, Colombo 07, Sri Lanka.

Fax: 94-11- 2694754
E-mail: jnsf@nsf.gov.lk
JNSF home page: *http://www.nsf.gov.lk/ index.php/nsfscience-magazine*

Publication : free — A publication fee of US$ 250 will be levied for each manuscript except, when the corresponding author is affiliated to a Sri Lankan institution, in two stages.

- A processing fee of US$ 20 will belevied for each manuscript at peer-review stage.
- Remaining US$ 230 will be charged for accepted articles at the time of publication.

Indexing : **The JNSF is indexed in Science Citation Index Expanded, Journal Citation Reports/ Science Edition, BIOSIS Previews, Zoological Record, Biological A bstracts, Chemical Abstracts, Scopus, DOAJ, TEEAL, Ulrich's, AGRICOLA and EBSCOhost, CAB Abstracts**

JOURNAL OF THE
NATIONAL SCIENCE FOUNDATION
OF SRI LANKA

Volume 51 Number 4 December 2023

CONTENTS

Cover: Cover caption – Some commercially available Anthurium cultivars collected from Japan
See *J.Natn.Sci.Foundation Sri Lanka* 2023 **51**(4): 629 – 641

J.Natn.Sci.Foundation Sri Lanka 2023 51 (4): 571
DOI: http://dx.doi.org/10.4038/jnsfsr.v51i4.11991

EDITORIAL

Reliability of the primary scientific literature

The confidence that scientists and the public have in the reliability of the primary scientific literature stems from a cardinal feature of scientific knowledge itself; that it is public knowledge open to verification by anyone independently, and that its validity does not depend upon the authority of the individual/persons reporting the knowledge. Thus, it has been the norm that extravagant claims made on deliberately falsified data (or wrongly interpreted data driven by an overabundance of enthusiasm) were rare, and exposed early on after publication. Retractions, when made by authors due to honest errors, served to enhance the confidence in scientific knowledge, and is considered a demonstration of the inherent nature of scientific knowledge to correct itself, as it progresses.

However, the large number of retractions by publishers that are now being reported has made a dent in this confidence. It was recently reported in Nature that there were over 10,000 retractions in 2023. The reasons for the retractions were multifarious, and included papers identified as coming from paper mills, papers where images and data had been manipulated and papers published after fraudulent peer review.

Of special interest was the observation that the largest number of retractions were from special issues related to specific topics or conference proceedings. There is a legitimate view that special issues serve a purpose and can enhance the profile of a journal. Nevertheless, it is ironical that special issues today are not special, but have become common, and have lost the original high purpose for which they were intended; to bring together a limited number of papers by established scientists on an emerging topic of relevance and current interest, which could spur on further development.

Editorial boards need to be alert to the increasing amount of malpractice among unethical practitioners professing to be scientists. The COPE documents on retractions provide sound and practical guidelines to minimize the publication of dubious papers which would need to be retracted later.

Ajit Abeysekera

J.Natn.Sci.Foundation Sri Lanka 2023 51 (4): 573 - 587
DOI: http://dx.doi.org/10.4038/jnsfsr.v51i4.11473

RESEARCH ARTICLE

Ecotoxicology

Risk assessment of heavy metals in the freshwater lake sediments around Eppawala phosphate deposit, Sri Lanka

NM Batapola[1], NP Dushyantha[2*], NP Ratnayake[1], HMR Premasiri[1], H Panagoda[1], CL Jayawardena[1], R Chandrajith[3], IMSK Ilankoon[4], LPS Rohitha[1], AS Ratnayake[2], JB Koongolla[5], AMBK Abeysinghe[1], DMDOK Dissanayake[1] and RMP Ratnayake[1]

[1] *Department of Earth Resources Engineering, Faculty of Engineering, University of Moratuwa, Moratuwa, Sri Lanka.*
[2] *Department of Applied Earth Sciences, Faculty of Applied Sciences, Uva Wellassa University, Passara Road, Badulla, Sri Lanka.*
[3] *Department of Geology, Faculty of Science, University of Peradeniya, Peradeniya, Sri Lanka.*
[4] *School of Engineering, Monash University Malaysia, Selangor, Malaysia.*
[5] *Key Laboratory of Tropical Marine Bio-resources and Ecology, South China Sea Institute of Oceanology, Chinese Academy of Science, Guangzhou, China.*

Submitted: 23 November 2022; Revised: 03 March 2023; Accepted: 28 April 2023

Abstract: The Eppawala area in Sri Lanka has an agricultural-based economy. As a result, the recent agricultural intensification could increase the risk of heavy metal contamination in lakes in the area as the main water canal in the area, *i.e.*, Jaya Ganga, flows across these lakes. Therefore, this study focuses on the risk assessment of heavy metals in the freshwater lake sediments in the Eppawala area and the identification of potential sources for heavy metal contamination in the lakes. Nine heavy metals (Cr, Mn, Co, Ni, Cu, Zn, As, Cd, and Pb) were investigated in surface sediments (n = 22) of the upstream and downstream lakes of the Eppawala Phosphate Deposit (EPD). The average heavy metal concentrations in the upstream lake sediments were higher than those downstream. Eppawala lake sediments were heavily polluted by As along with moderate to high Cr pollution. However, only As and Cd indicated considerable to moderate ecological risk levels to the local environment. The downstream lake sediments showed lower heavy metal contents compared to those upstream and had negative correlations between heavy metals and P_2O_5 contents. This reveals that the EPD does not contribute to the heavy metal contamination in the Eppawala lake sediments. However, the statistical analysis showed that heavy metals were mostly derived from similar pollution sources. Agrochemicals used in paddy cultivation in the vicinity might be a potential source of heavy metals. This study highlights the importance of implementing remediation to control the heavy metal pollution prevailing in the Eppawala lakes.

Keywords: Agricultural intensification, ecological risks, Eppawala, heavy metals, sediments.

INTRODUCTION

Heavy metals in aquatic ecosystems are a pressing global concern due to their adverse characteristics, such as toxicity, persistence, non-biodegradability, and bioaccumulation (Dai *et al*., 2018). In this context, heavy metal pollution in freshwater lakes has acquired significant attention as lakes are responsible for providing numerous ecosystem services (*e.g.*, water cycling, climate regulation, and habitats for aquatic flora, fauna, and microorganisms) and play a vital role in human lifestyle (*i.e.*, providing water for irrigation, drinking, and other various purposes) (Thevenon *et al*., 2013; Jahromi *et al*., 2021). Lake sediments are crucial indicators for monitoring heavy metal contamination levels in lakes since they act as both carriers and sinks for heavy metals (Li *et al*., 2013; Jin *et al*., 2021). Heavy metals get easily absorbed and accumulated in the lake sediments due to their low solubility. However, the settled heavy metals in the lake sediments could remobilize to water under various changing environmental conditions, such as pH,

* Corresponding author (nimila.dush@uwu.ac.lk; https://orcid.org/0000-0002-3871-6851)

temperature, and redox potential. It causes secondary contamination of heavy metals in the water column and aquatic organisms, posing severe risks to the ecology of the environment and to human health (Malferrari *et al*., 2009; Varol, 2020).

Heavy metals are introduced into lakes either by natural sources, such as geological weathering, volcanic eruptions, and airborne dust, or anthropogenic sources including agricultural activities (application of fertilizers/pesticides), smelting/processing of metal ores, mining, sewage discharge, industrial effluents, and urban construction (Magni *et al*., 2021). Typically, agricultural activities are overlooked as a source of heavy metal contamination in lake sediments due to relatively low content of heavy metals in agricultural runoffs (*e.g.*, Cd, Ni, and Pb contents in Wagon Train agricultural watershed, Nebraska are about 0.00045, 0.0063 and 0.0013 mg/L) (Elrashidi *et al*., 2007) compared to other anthropogenic sources, especially industrial discharges (*e.g.*, Cd, Ni, and Pb contents in an iron and steel industrial effluent from India are about 0.051, 0.303 and 0.082 mg/L) (Ladwani *et al*., 2012). However, long-term usage of agrochemicals in agricultural lands may lead to excessive accumulations of heavy metals in close-by waterbodies (Tang *et al*., 2014). Furthermore, rapid population growth and the scarcity of land have induced an agricultural intensification (*i.e.*, high levels of inputs (*e.g.*, agrochemicals, water, labour, etc.) or outputs (*e.g.*, harvest, plant growth, etc.) per unit area of land), which is significant to increase the food security in the world but causes high heavy metal accumulations in lake sediments, posing severe impacts to ecosystems and human health (Alauddin & Quiggin, 2008).

The North-Central Province of Sri Lanka has an agriculture-based economy and a centuries-old history of paddy cultivation. In the past few decades, agriculture in Sri Lanka has been intensified with an increased quantity of agrochemicals to secure the food supply within the country. However, it has been carried out improperly without following the guidelines and standards imposed by the Agriculture Department of Sri Lanka (De Costa, 2021). Eppawala in the North-Central Province is such an area where intensified agriculture is being carried out. Consequently, the ecological environment in lakes adjacent to the agricultural fields is vulnerable to heavy metal contamination through fertilizer/pesticide leaching.

Therefore, three lakes, namely Koon, Ihalahalmilla, and Kiralogama were selected to investigate the heavy metal contamination in lake sediments of the Eppawala area. In addition, these three lakes are adjacent to the Eppawala Phosphate Deposit (EPD) and since phosphate deposits contain significant amounts of heavy metals (*e.g.*, the concentrations of Cd, Cr, Ni, V, U, and Zn in the Al-Jiza phosphate deposit of Central Jordan are 15 ± 8, 109 ± 21, 34 ± 6, 211 ± 55, 142 ± 55, and 161 ± 57 mg/kg, respectively) (Al-Hwaiti *et al*., 2014; Siddique *et al*., 2018), the EPD could be a natural source for heavy accumulation in the lake sediments via geological weathering. The specific objectives of this research are (1) investigating the spatial distribution of heavy metals in surface lake sediments of the Eppawala area; (2) assessing the degree of contamination and evaluating the potential ecological risk to the environment; and (3) identifying the possible natural and anthropogenic sources for heavy metal contamination in the lake sediments.

MATERIALS AND METHODS

Study area

The EPD is the only phosphate mine in Sri Lanka with an annual production of 50,000 tonnes of rock phosphate fertilizers (Dushyantha *et al*., 2019; 2020). It lies in the Eppawala area of the North-Central province, which belongs to the Wanni Complex (Figure 1) of Sri Lanka. Moreover, a man-made water canal named 'Jaya Ganga' flows across the EPD connecting these three lakes and it distributes water over an area of 470 km^2 while feeding about 46 km^2 of paddy fields and 120 small lakes (Dushyantha, 2018). In addition, the lifestyle of people in this area is closely related to these lakes through fishing, irrigation, and agriculture.

Based on the location of the EPD, the present study area is divided into upstream (Ihalahalmilla and Koon lakes) and downstream (Kiralogama lake) regions (Figure 1b) (Dushyantha *et al*., 2017; 2021). The lakes are located in the dry climatic zone of Sri Lanka, and thus water levels of the lakes are raised dramatically during the rainy season, particularly in the north-eastern monsoon (December to February). However, during the dry season, most of the lake water volume is drastically reduced while turning some lakes into huge grasslands.

Sample collection and preparation

A total of 22 surface lake sediment samples were collected from the upstream (n = 12) and downstream (n = 10) lakes by using a Van Veen grab sampler (Figure 2). All the sediment samples were oven-dried at 105˚C for 24 hours to remove the moisture and powdered using an agate mortar and a pestle. The pulverized samples were then sieved using a 63 µm sieve to obtain undersize fractions of the samples. Finally, representative samples were prepared by the coning and quartering method for further analyses.

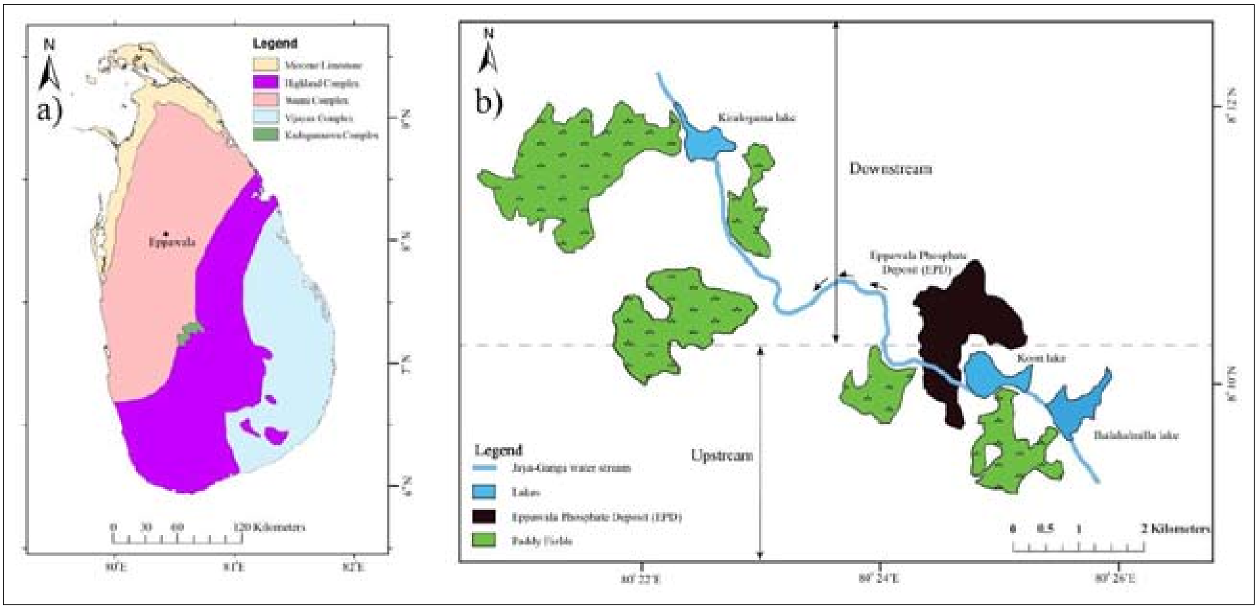

Figure 1: (a) The simplified geological map of Sri Lanka with major lithotectonic complexes (after Cooray, 1984); (b) the study area illustrating Ihalahalmilla, Koon, and Kiralogama lakes along with the Eppawala phosphate deposit (EPD) (Dushyantha *et al*., 2019).

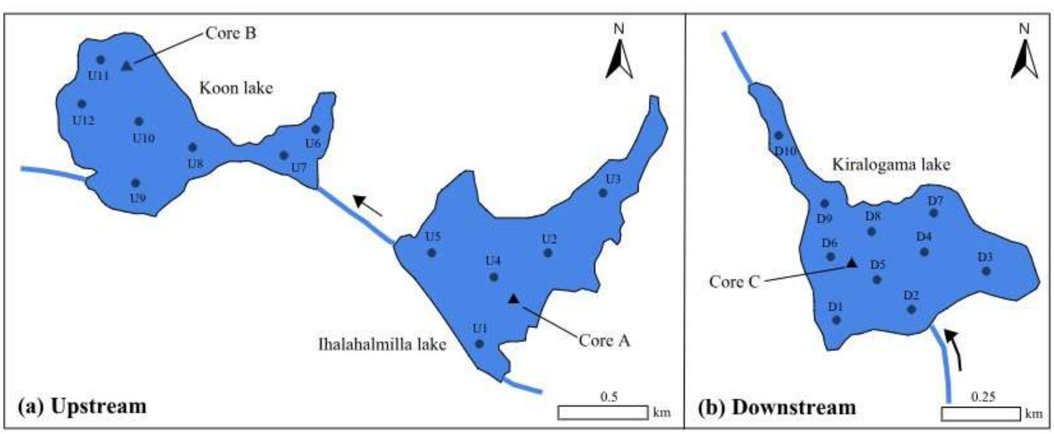

Figure 2: The surface sediment sampling locations at Eppawala (a) upstream lakes; (b) downstream lakes

Heavy metal analysis

Representative samples were digested using a mixture of HCl, HNO_3, and H_2O_2 with a ratio of 1:3:1 in a MARS-6 microwave digester (CEM; Mathews, NC) equipped with EasyPrep Plus high-pressure vessels. The digested samples were then diluted with de-ionized water and analyzed for heavy metals (Cr, Mn, Co, Ni, Cu, Zn, As, Cd, and Pb) using a Thermo ICapQ Inductively Coupled Plasma Mass Spectrometer (ICP-MS) (Thermo Fisher, Bremen, Germany), with the use of multi-elemental ICP-MS standards (Sigma-Aldrich, Germany). In addition, the certified international reference samples and blanks were used to control the accuracy and precision of the analysis.

Assessment of sediment contamination and potential ecological risk

It is not ideal to identify and compare the individual heavy metal contamination levels in the environment solely by their concentrations since the crustal abundances of each heavy metal are different. Therefore, some indices such as the geoaccumulation index are used to assess the actual contamination of heavy metals in the environment. In addition, the potential ecological risk index is used to determine the ecological risks posed by heavy metals to the aquatic environment.

Geoaccumulation index

The geoaccumulation index (I_{geo}) is used to verify the magnitude of the contamination caused by an individual heavy metal (Varol, 2011) (equation 1).

$$I_{geo} = \mathrm{Log}_2 \frac{C_s^i}{1.5\, C_n^i} \qquad ...(1)$$

C_s^i is the concentration of the element i in the lake sediment sample, C_n^i is the geochemical background concentration of the element i, and n is the number of heavy metals analyzed (n = 9). However, due to the absence of background data on heavy metals in the Eppawala lakes, the upper continental crust (UCC) values were used as the reference values (Wedepohl, 1995). The constant 1.5 is the background matrix correction factor due to lithospheric effects.

Potential ecological risk index

The potential ecological risk index (RI) is a quantitative measurement of the degree of ecological risks caused by the heavy metals in aquatic sediments (Hakanson, 1980) and it is obtained by equations 2 and 3.

$$E_r^i = T_r^i \times C_f^i = T_r^i \times \frac{C_s^i}{C_n^i} \qquad ...(2)$$

$$RI = \sum_{i=1}^{n} E_r^i \qquad ...(3)$$

E_r^i is the potential ecological risk factor of the heavy metal i and T_r^i is the toxic response factor of the element i, while C_f^i is the contamination factor of the element i. C_s^i and C_n^i are similar to the parameters defined in Equation 1. T_r^i for Cr, Mn, Co, Ni, Cu, Zn, As, Cd, and Pb are 2, 1, 5, 5, 5, 1, 10, 30, and 5, respectively (Hakanson, 1980).

RESULTS AND DISCUSSION

Heavy metal contents in surface lake sediments

The heavy metal concentrations in all the upstream and downstream surface lake sediment samples are presented in Table S1, whereas Table 1 shows the corresponding range and average values. According to the Table 1, the heavy metal concentrations showed a decreasing order of Mn > Cr > Zn > Ni > Cu > Co > As > Pb > Cd in the upstream surface lake sediments and Mn > Cr > Zn > Cu >Ni > As > Co > Pb > Cd in the downstream surface lake sediments. The average concentrations of all the heavy metals analysed in this study were high in the upstream surface lake sediments compared to the respective downstream values (Table 1). Therefore, it is evident that there are no point sources of heavy metals between the upstream and downstream lakes. However, based on Dushyantha *et al*. (2019, 2020), there is a phosphate-rich sediment contribution from the EPD to the downstream

Table 1: Ranges and averages (mg/kg) of heavy metals in the upstream and downstream, surface lake sediments

Heavy metal	Upstream		Downstream	
	Range	Avg.	Range	Avg.
Cr	90.42 – 427.34	263.0	69.58 – 394.38	241.3
Mn	187.61 – 2706.96	1420.7	176.62 – 2212.94	1141.1
Co	5.87 – 49.89	32.6	5.50 – 43.86	23.8
Ni	33.64 – 273.63	97.5	20.43 – 120.46	53.2
Cu	10.12 – 108.00	72.5	5.91 – 101.90	63.6
Zn	40.78 – 449.30	186.4	49.73 – 213.46	133.7
As	2.81 – 46.77	25.1	14.14 – 33.08	24.9
Cd	0.07 – 2.19	0.5	0.01 – 0.67	0.2
Pb	3.48 – 26.23	14.7	3.47 – 24.81	12.9

Avg.: Average

lake sediments, and the subsequent dilution could be the cause for the respective low contents of heavy metals. In this study, Mn displayed the highest concentration levels in the surface lake sediments. Generally, Mn is ubiquitous in the earth's crust (*e.g.*, basalt - 1300 mg/kg, gneiss - 600 mg/kg, and limestone - 550 mg/kg) and thus, it is found in higher concentrations in surface lake sediments compared to other heavy metals (Queiroz *et al*., 2021).

Table 2 presents the average heavy metal concentrations of surface lake sediments in this study compared to a few other lakes in Sri Lanka and other countries in the world. Compared to the local studies, reservoirs in Anuradhapura, Polonnaruwa, and Kilinochchi districts have reported higher concentrations of heavy metals in sediments than in the present study. Since Anuradhapura and Polonnaruwa are agriculture-based areas, especially for paddy cultivation, the extensive use of agrochemicals may be the possible reason for these high concentrations (Wijesinghe *et al*., 2018; Perera *et al*., 2021). However, heavy metal concentrations in the Bolgoda lake sediments were relatively low compared to the present study. In the global context, the reported high heavy metal concentrations of surface lake sediments in India, Egypt, and China may be due to local industrial developments, urbanization, and intense agricultural activities in the area (Suresh *et al*., 2012; Ma *et al*., 2016b; Ji *et al*., 2019). In contrast, most of the heavy metal concentrations in the surface lake sediments of Lake St. Clair and Hope Lake in the USA were found to be the lowest compared to the other lakes (Table 2). The low concentration levels in these lakes are possibly due to strict legislative frameworks in developed countries that control and monitor heavy metal discharges and emissions from industrial, urban, and agricultural sources (Dai *et al*., 2018). Therefore, legislative frameworks on heavy etals would alleviate the heavy metal pollution in freshwater lakes.

Table 2: A comparison of average heavy metal concentrations in surface lake sediments (mg/kg) in this study and a few other lakes in the world

Lake		Cr	Mn	Co	Ni	Cu	Zn	As	Cd	Pb
Local										
Eppawala	Upstream	263.0	1420.7	32.6	97.5	72.5	186.4	25.1	0.5	14.7
Lake	Downstream	241.3	1141.1	23.8	53.2	63.6	133.7	24.9	0.2	12.9
Mahakanadarawa, Anuradhapura [1]		1842	NA	NA	NA	744	1346	25.6	0.0	138.0
Iranamadu, Kilinochchi [1]		355.0	NA	NA	NA	169.0	758.0	27.3	0.0	221.0
Mahadiwulwewa, Anuradhapura [1]		1836	NA	NA	NA	207.0	894.0	188.0	26.3	231.0
Bolgoda Lake,	North Lake	109.5	NA	NA	NA	33.8	130.6	NA	2.3	36.8
Colombo [2]	South Lake	119.7	NA	NA	NA	13.4	61.8	NA	1.9	26.5
Minneriya Reservoir, Polonnaruwa [3]		97.3	NA	NA	NA	105.0	67.0	NA	105.0	722.0
Parakrama Samudraya, Polonnaruwa [3]		64.3	NA	NA	NA	55.0	41.0	NA	66.0	845.3
Global										
Veeranam Lake, India [a]		88.2	NA	NA	63.6	94.1	180.1	NA	0.8	30.1
Dongting Lake, South China [b]		70.2	781.0	NA	33.0	30.2	121.6	4.5	0.8	34.1
Baiyangdian Lake, North China [c]		30.1- 6.0	NA	NA	22.0- 44.0	16.1-204.0	41.6-263.0	5.3-24.3	0.2-2.5	25.3-99.3
Lake St. Clair, USA [d]		8.6	NA	NA	10.1	11.6	40.0	5.9	<1.0	7.9
Hope Lake, USA [e]		37.8	3903.4	20.1	38.6	21.0	128.0	NA	0.4	17.1
Lake Nasser, Egypt [f]		30.8	279.6	NA	27.6	21.8	35.4	NA	0.2	10.9

NA - Not Available

[1] (Perera *et al*., 2021); [2] (Senarathne & Pathiratne, 2007); [3] (Wijesinghe *et al*., 2018)

[a] (Suresh *et al*., 2012); [b] (Ma *et al*., 2016a); [c] (Ji *et al*., 2019); [d] (Gewurtz *et al*., 2007); [e] (López *et al*., 2010); [f] (Goher *et al*., 2014)

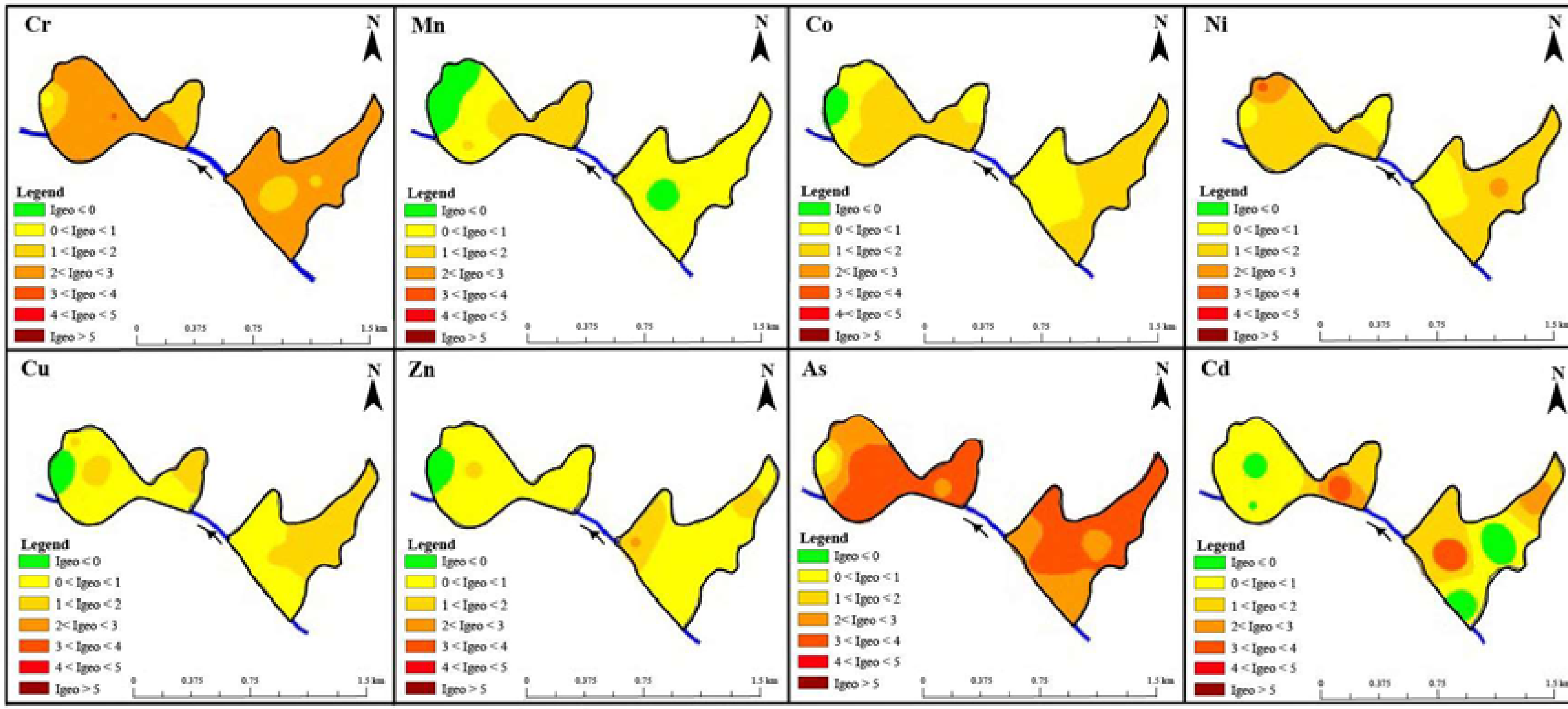

Figure 3: The spatial distribution of I_{geo} of heavy metals in the upstream surface lake sediments of the Eppawala area: $I_{geo} \leq 0$: practically unpolluted; $0 < I_{geo} < 1$: unpolluted to moderately polluted; $1 < I_{geo} < 2$: moderately polluted; $2 < I_{geo} < 3$: moderately to heavily polluted; $3 < I_{geo} < 4$: heavily polluted; $4 < I_{geo} < 5$: heavily to extremely polluted; $I_{geo} > 5$: extremely polluted

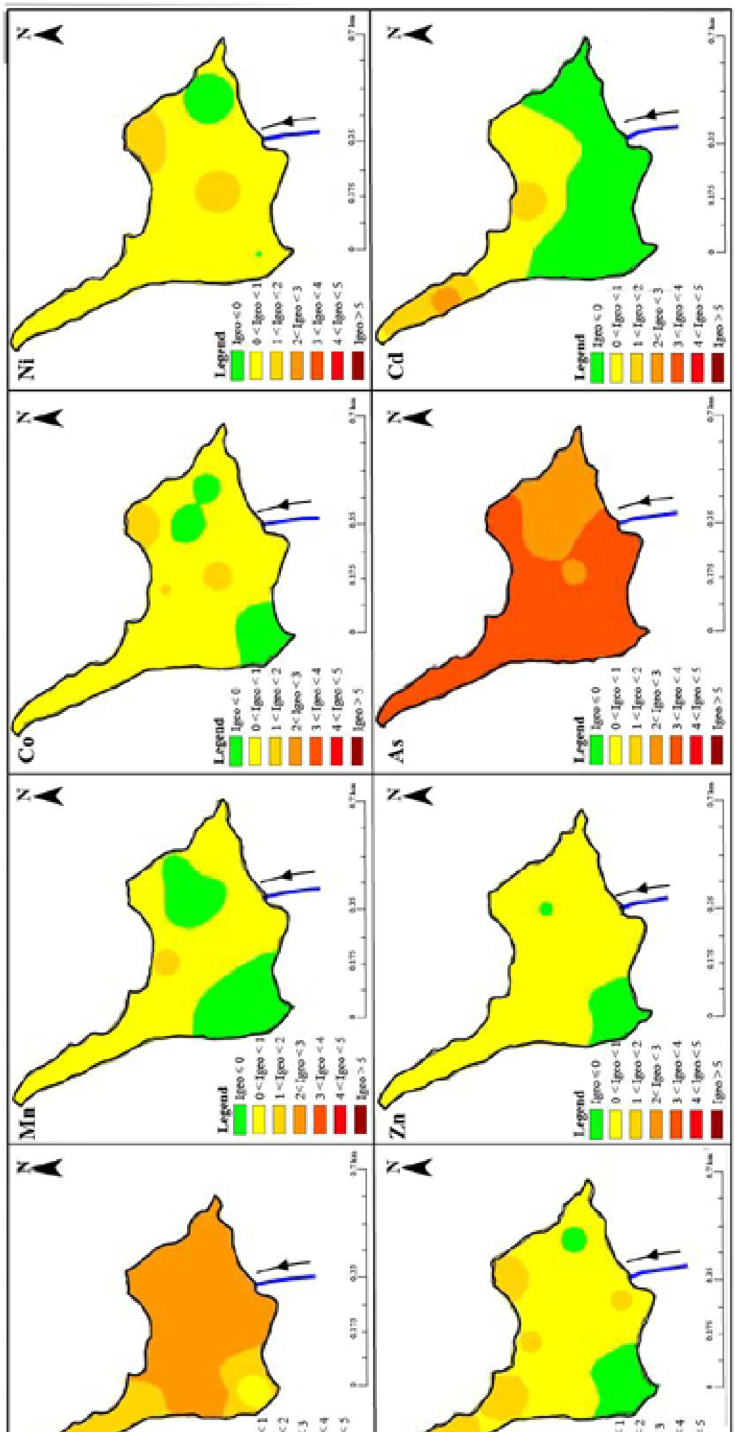

Figure 4: The spatial distribution of I_{geo} of heavy metals in the downstream surface lake sediments of the Eppawala area: $I_{geo} \leq 0$: practically unpolluted; $0 < I_{geo} < 1$: unpolluted to moderately polluted; $1 < I_{geo} < 2$: moderately polluted; $2 < I_{geo} < 3$: moderately to heavily polluted; $3 < I_{geo} < 4$: heavily polluted; $4 < I_{geo} < 5$: heavily to extremely polluted; $I_{geo} > 5$: extremely polluted

Assessment of heavy metal contamination

The classification criteria of I_{geo} are shown in Table S2. The spatial distributions of I_{geo} of each heavy metal in the upstream and downstream surface lake sediments are illustrated in Figures 3 and 4, respectively. These figures indicate that both the upstream and downstream surface lake sediments were heavily polluted by As (I_{geo} = -0.09–3.96) and moderately to heavily polluted by Cr (I_{geo} = 0.41–3.02). However, only the upstream surface lake sediments were moderately contaminated by Ni (I_{geo} = 0.46–3.19) and Co (I_{geo} = 0.10–1.73). Other heavy metals (Mn, Cu, Zn, Cd, and Pb) generally displayed unpolluted or unpolluted to moderately polluted levels in the Eppawala surface lake sediments

On the other hand, Mn, Cu, Zn, and Cd showed relatively high contamination levels in several locations at both the upstream and downstream areas (Figures 3 and 4). This heavy metal accumulation could be related to the sedimentation patterns of the lakes, and the nature of sedimentation depends on the grain size (Liang *et al*., 2019). The mean grain size distribution of the same samples in the Eppawala surface lake sediments was obtained from Dushyantha *et al*. (2019). However, Figure 5 illustrates no significant correlation between heavy metals and grain size. It elucidates that the grain size did not affect the degree of heavy metal accumulation in the Eppawala surface lake sediments, thus a local point source could be the reason for the arbitrarily high contamination levels of Mn, Cu, Zn, and Cd.

Table 3: Average potential ecological risk factors in the Eppawala surface lake sediments

Heavy metals	Upstream avg. potential ecological risk factor (E^i_r)	Downstream avg. potential ecological risk factor (E^i_r)
Cr	15.03	13.79
Mn	2.37	1.90
Co	16.30	11.82
Ni	24.38	13.31
Cu	14.49	12.71
Zn	2.63	1.88
As	125.84	124.65
Cd	137.93	66.06
Pb	3.66	3.21

Potential ecological risks

Table 3 presents the average potential ecological risk factors (E^i_r) of individual heavy metals in both the upstream and downstream surface lake sediments. E^i_r values of the heavy metals in the upstream surface lake sediments varied in the following order: Cd > As > Ni > Co > Cr > Cu > Pb > Zn > Mn. By contrast, E^i_r values of the heavy metals in the downstream surface lake sediments followed the order of As > Cd > Cr > Ni > Cu > Co > Pb > Mn > Zn. According to E^i_r classification criteria (Table S3), As and Cd posed considerable to moderate ecological risk levels in the surface lake sediments of the

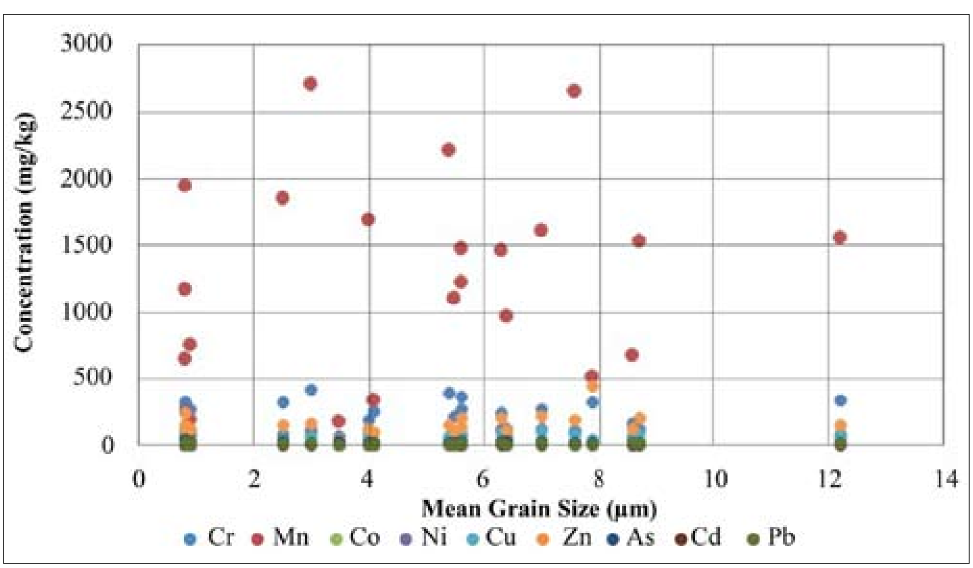

Figure 5: The variation of heavy metals with the grain size of Eppawala surface lake sediments

Eppawala area, whereas other heavy metals remained at low-risk levels. The potential ecological risks caused by As in both the upstream and downstream surface lake sediments were consistent with the I_{geo} results obtained for As (Figures 3 and 4). However, Cd showed a considerable to moderate ecological risk level despite its low degree of contamination in the surface lake sediments (Figures 3 and 4). Furthermore, despite high to moderate contamination levels of Cr, Ni, and Co in both the upstream and downstream surface lake sediments (Figures 3 and 4), they did not pose any considerable threat to the ecological environment in the Eppawala area.

The potential ecological risk of heavy metals in sediments depends on both their contents and their speciation. There are six categories of speciation of heavy metals in sediments, namely (1) exchangeable (EXC), (2) bound to carbonate (CARB), (3) bound to easily reducible oxides (ERO), (4) bound to organic matter (OM), (5) bound to residual oxides (RO), and (6) residual fraction (RES-R). Under changing environmental conditions, such as pH or redox potential, these categories behave differently with respect to remobilization. Therefore, the reason for having ecological risk levels that were inconsistent with the results of I_{geo} for Cd, Cr, Ni, and Co may be due to their speciation in the Eppawala surface lake sediments. For example, if the percentage of CARB-Cd in the Eppawala surface lake sediments were high, Cd could be released into water under low pH conditions, causing high pollution to the surrounding environment (Yang *et al*., 2009).

Figure 6 shows the spatial distribution of RI values in both the upstream and downstream surface lake sediments, which represents the overall ecological risks posed by the investigated heavy metals in the Eppawala surface lake sediments (Equation 3). The potential ecological risk levels of heavy metals in the upstream surface lake sediments were considerable compared to the downstream surface lake sediments, which had moderate risk levels. Since the heavy metal accumulation in the upstream surface lake sediments was higher, heavy metals may have yielded comparatively greater levels of ecological risk to the local upstream environment.

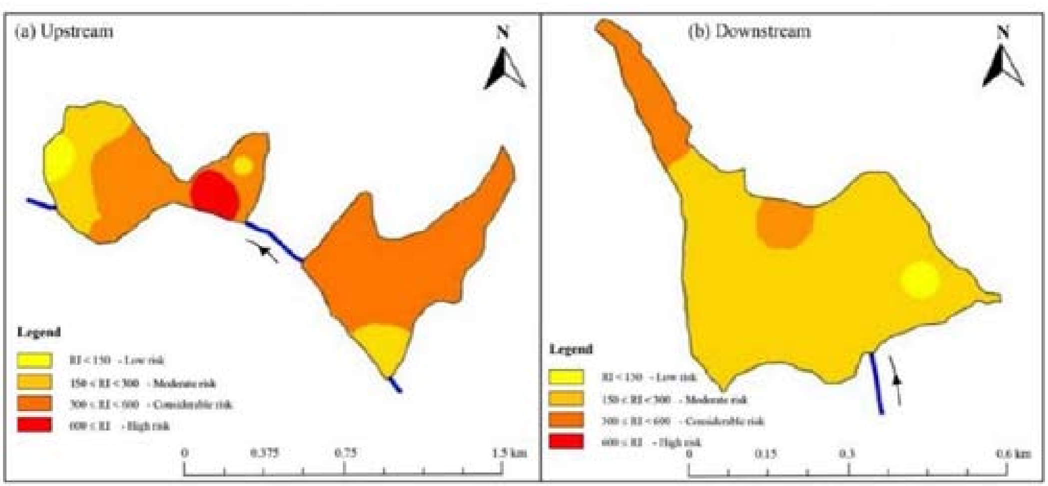

Figure 6: The spatial distribution of RI in the (a) upstream and (b) downstream surface lake sediments of the Eppawala area

Potential sources of heavy metals

Pearson's correlation coefficient matrix of heavy metals and phosphate (P_2O_5) content in the Eppawala lake sediments was derived (Table 4) since it reveals the potential sources and pathways in the environment. The P_2O_5 content of these samples was taken from Dushyantha *et al*. (2019). In the upstream surface lake sediments, significant and positive correlations were observed between Co and Cu (r = 0.773), Co and Pb (r = 0.836), Cu and As (r = 0.701), Cu and Pb (r = 0.748), and As and Pb (r = 0.765), whereas Co and As showed only a moderate positive correlation (r = 0.595). Since only Cu, As, and Pb were significantly intercorrelated, they may have derived from a similar pollution source, whereas Co could have a different origin or controlling factors in the upstream surface lake sediments (Tang *et al*., 2014).

Table 4: The correlation coefficient (r) matrix (n = 12) for heavy metals in the Eppawala surface lake sediments

		Cr	Mn	Co	Ni	Cu	Zn	As	Cd	Pb	P_2O_5
Upstream	Cr	1									
	Mn	0.267	1								
	Co	0.526	0.658	1							
	Ni	0.417	-0.062	0.384	1						
	Cu	0.132	0.409	**0.773**	0.324	1					
	Zn	0.341	-0.077	0.065	-0.135	0.199	1				
	As	0.339	0.373	0.595	-0.039	**0.701**	0.392	1			
	Cd	-0.048	0.155	0.016	-0.169	0.011	-0.019	0.065	1		
	Pb	0.363	0.417	**0.836**	-0.006	**0.748**	0.274	**0.765**	0.061	1	
	P_2O_5	-0.309	-0.511	-0.598	0.168	-0.624	-0.457	-0.648	-0.393	**-0.724**	1
		Cr	Mn	Co	Ni	Cu	Zn	As	Cd	Pb	P_2O_5
Downstream	Cr	1									
	Mn	0.578	1								
	Co	0.517	0.608	1							
	Ni	0.306	0.371	**0.890**	1						
	Cu	0.427	0.756	**0.833**	0.663	1					
	Zn	0.515	0.675	**0.952**	**0.852**	**0.792**	1				
	As	0.062	0.165	0.353	0.428	0.421	0.129	1			
	Cd	0.070	0.300	0.075	-0.065	0.431	0.113	0.074	1		
	Pb	0.523	0.223	**0.701**	**0.808**	0.372	**0.713**	0.246	-0.419	1	
	P_2O_5	0.063	0.062	0.080	-0.041	0.072	-0.116	0.571	-0.121	-0.101	1

r > 0 - positive correlation; r < 0 - negative correlation; r > ±0.7 - significant correlation (highlighted in bold)

In contrast, Co and Ni (r = 0.890), Co and Zn (r = 0.952), Ni and Zn (r = 0.852), Ni and Pb (r = 0.808), Zn and Pb (r = 0.713), and Pb and Co (r = 0.701) in the downstream surface lake sediments showed significant positive correlations. It indicated that Co, Ni, Zn, and Pb were positively correlated among themselves in the downstream surface lake sediments, thus they may be discharged from a similar pollution source. However, negative and very low positive correlations among P_2O_5 and the heavy metals suggested that the phosphate-bearing materials accumulated in these lake sediments might not be a source for heavy metals.

The application of agrochemicals (*i.e.*, pesticides and chemical fertilizers) to the regional paddy cultivations may be a potential source of As, Pb, and Cu. It is also supported by the field investigations as intense agricultural activities, especially paddy cultivations were observed in the vicinity of these three lakes. According to Jayasumana *et al*. (2015), the most commonly used chemical fertilizers in Sri Lanka contain significantly high concentrations of As, Pb, and Cu (*e.g.*, Triple Superphosphate (TSP): As = 26.5–31.9 mg/kg, Pb = 251.7–263.9 mg/kg and Cu = 14.2–16.0 mg/kg, and Muriate of Potash (MOP): As = 0.2–0.4 mg/kg, Pb = 0.8–0.9 mg/kg and Cu = 0.3–0.4 mg/kg). Moreover, despite being illegal to import, As-containing agrochemicals available in Sri Lanka contain considerable levels of As (*e.g.*, Glyphosate: 0.9–2.6 mg/kg, Dimethoate: 1.0–2.4 mg/kg, and Fenoxaprop-p-ethyl: 1.2–2.6 mg/kg) (Jayasumana *et al*., 2015). Therefore, extensive usage of TSP and pesticides in the local paddy fields may be a potential source of As contamination in the Eppawala lake sediments. However, further studies are recommended, especially for heavy metal contamination in the agricultural fields and runoffs in the vicinity of these lakes, to determine the impact of agricultural activities in the region on the observed heavy metal pollution in the Eppawala lake sediments.

CONCLUSIONS

The present study demonstrated that both the upstream and downstream surface lake sediments of the Eppawala area were moderately to heavily contaminated by As and Cr, whereas Co and Ni showed moderate contamination levels only in the upstream area. However, based on the RI analysis, only As and Cd displayed considerable to moderate ecological risk levels in the surface lake sediments, in which the highest potential ecological risk was caused by As. Based on the correlation coefficient relationships of heavy metals, the possible pollution source for heavy metals might be the intense agrochemical use in paddy cultivation. The average heavy metal concentrations were higher in the upstream lake sediments compared to the downstream, and this, together with the negative correlation between heavy metals and P_2O_5 content, suggested that the weathered materials from the EPD could not be a potential source for the heavy metal contamination in lakes. The results of this research reveal important findings that can be used to recommend proper ecological management of aquatic ecosystems while controlling the heavy metal pollution in the Eppawala lakes.

Conflict of interest statement

The authors declare that there is no conflict of interest.

Acknowledgements

The authors wish to acknowledge the financial support by the Accelerating Higher Education and Development (AHEAD) Operation of the Ministry of Higher Education, Sri Lanka, funded by the World Bank (AHEAD/ DOR/6026-LK/8743-LK). The core sampling in this study was funded by the University of Moratuwa through the Senate Research Grant (SRC/CAP/2015/02). We thank Mrs. A.R. Amarasinghe (Technical Officer), Mr. S.S.U. Silva (Laboratory Assistant) of the Oceanography laboratory of the Department of Earth Resources Engineering, the University of Moratuwa for their assistance in field visits and laboratory tests.

REFERENCES

Abrahim G.M.S. & Parker R.J. (2008). Assessment of heavy metal enrichment factors and the degree of contamination in marine sediments from Tamaki Estuary, Auckland, New Zealand. *Environmental Monitoring and Assessment* **136**: 227–238.
DOI: https://doi.org/10.1007/s10661-007-9678-2

Al-Hwaiti M., Al Kuisi M., Saffarini G. & Alzughoul K. (2014). Assessment of elemental distribution and heavy metals contamination in phosphate deposits: potential health risk assessment of finer-grained size fraction. *Environmental Geochemistry and Health* **36**: 651–663.
DOI: https://doi.org/10.1007/s10653-013-9587-y

Alauddin M. & Quiggin J. (2008). Agricultural intensification, irrigation and the environment in South Asia: Issues and policy options. *Ecological Economics* **65**: 111–124.
DOI: https://doi.org/10.1016/j.ecolecon.2007.06.004

Chai L., Li H., Yang Z., Min X., Liao Q., Liu Y., Men S., Yan Y. & Xu J. (2017). Heavy metals and metalloids in the surface sediments of the Xiangjiang River, Hunan, China: Distribution, contamination, and ecological risk assessment. *Environmental Science and Pollution Research* **24**: 874–885.
DOI: https://doi.org/10.1007/s11356-016-7872-x

Cooray P.G. (1984). *An Introduction to the Geology of Sri Lanka (Ceylon)*. Department of National Museums, Colombo, Sri Lanka.

Dai L., Wang L., Li L., Liang T., Zhang Y., Ma C. & Xing B. (2018). Multivariate geostatistical analysis and source identification of heavy metals in the sediment of Poyang Lake in China. *Science of the Total Environment* **621**: 1433–1444.
DOI: https://doi.org/10.1016/j.scitotenv.2017.10.085

De Costa W.A.J.M. (2021). *'Fertilizer Saga' in Sri Lanka: A Considered Opinion*. Available at *https://island.lk/fertilizer-saga-in-sri-lanka-a-considered-opinion/.*

Dushyantha N.P. (2018). Alternative phosphorus sources in lake bottom sediments around Eppawala phosphate deposit in Sri Lanka. *M.Phil thesis*, University of Moratuwa, Sri Lanka.

Dushyantha N.P., Hemalal P.V.A., Jayawardena C.L., Ratnayake A.S., Premasiri H.M.R. & Ratnayake N.P. (2017). Nutrient characteristics of lake sediments around Eppawala phosphate deposit, Sri Lanka. *Journal of Geological Society of Sri Lanka* **18**(2): 33–42.

Dushyantha N.P., Hemalal P.V.A., Jayawardena C.L., Ratnayake A.S. & Ratnayake N.P. (2019). Application of geochemical techniques for prospecting unconventional phosphate sources: A case study of the lake sediments in Eppawala area Sri Lanka. *Journal of Geochemical Exploration* **201**: 113–124.
DOI: https://doi.org/10.1016/j.gexplo.2019.02.010

Dushyantha N., Batapola N., Ilankoon I.M.S.K., Rohitha S., Premasiri R., Abeysinghe B., Ratnayake N. & Dissanayake K. (2020). The story of rare earth elements (REEs): Occurrences, global distribution, genesis, geology, mineralogy and global production. *Ore Geology Reviews* **122**:.103521.
DOI: https://doi.org/10.1016/j.oregeorev.2020.103521

Dushyantha N., Ratnayake N., Panagoda H., Jayawardena C. & Ratnayake A.S. (2021a). Phosphate mineral accumulation in lake sediment to form a secondary phosphate source: A case study in lake sediment around Eppawala phosphate deposit (EPD) in Sri Lanka. *International Journal of Sediment Research* **36**: 532–541.

DOI: https://doi.org/10.1016/j.ijsrc.2020.12.001

Dushyantha N.P., Ratnayake N.P., Premasiri H.M.R., Ilankoon I., Hemalal P.V.A., Jayawardena C.L., Chandrajith R., Rohitha L.P.S., Abeysinghe A. & Dissanayake D. (2021b). Leaching of rare earth elements (REEs) from lake sediments around Eppawala phosphate deposit, Sri Lanka: A secondary source for REEs. *Hydrometallurgy* **205**: 105751. DOI: https://doi.org/10.1016/j.hydromet.2021.105751

Elrashidi M.A., Hammer D., Fares A., Seybold C.A., Ferguson R. & Peaslee S.D. (2007). Loss of heavy metals by runoff from agricultural watersheds. *Soil Science* **172**: 876–894. DOI: https://doi.org/10.1097/ss.0b013e31814cec7b

Gewurtz S.B., Helm P.A., Waltho J., Stern G.A., Reiner E.J., Painter S. & Marvin C.H. (2007). Spatial distributions and temporal trends in sediment contamination in Lake St. Clair. *Journal of Great Lakes Research* **33**: 668–685. DOI: https://doi.org/10.3394/0380-1330(2007)33[668:SDATTI]2.0.CO;2

Goher M.E., Farhat H.I., Abdo M.H. & Salem S.G. (2014). Metal pollution assessment in the surface sediment of Lake Nasser, Egypt. *Egyptian Journal of Aquatic Research* **40**: 213–224. DOI: https://doi.org/10.1016/j.ejar.2014.09.004

Hakanson L. (1980). An ecological risk index for aquatic pollution control. A sedimentological approach. *Water Research* **14**: 975–1001. DOI: https://doi.org/10.1016/0043-1354(80)90143-8

Jahromi F.A., Keshavarzi B., Moore F., Abbasi S., Busquets R., Hooda P.S. & Jaafarzadeh N. (2021). Source and risk assessment of heavy metals and microplastics in bivalves and coastal sediments of the Northern Persian Gulf, Hormogzan Province. *Environmental Research* **196**: 110963. DOI: https://doi.org/10.1016/j.envres.2021.110963

Jayasumana C., Fonseka S., Fernando A., Jayalath K., Amarasinghe M., Siribaddana S., Gunatilake S. & Paranagama P. (2015). Phosphate fertilizer is a main source of arsenic in areas affected with chronic kidney disease of unknown etiology in Sri Lanka. *Springer Plus* **4**: 1–8. DOI: https://doi.org/10.1186/s40064-015-0868-z

Ji Z., Zhang H., Zhang Y., Chen T., Long Z., Li M. & Pei Y. (2019). Distribution, ecological risk and source identification of heavy metals in sediments from the Baiyangdian Lake, Northern China. *Chemosphere* **237**: 124425. DOI: https://doi.org/10.1016/j.chemosphere.2019.124425

Jin C., Li Z., Huang M., Wen J., Ding X., Zhou M. & Cai C. (2021). Laboratory and simulation study on the Cd (II) adsorption by lake sediment: Mechanism and influencing factors. *Environmental Research* **197**: 111138. DOI: https://doi.org/10.1016/j.envres.2021.111138

Ladwani K.D., Ladwani K.D., Manik V.S. & Ramteke D.S. (2012). Impact of industrial effluent discharge on physico-chemical characteristics of agricultural soil. *International Research Journal of Environment Sciences* **1**: 32–36.

Li F., Huang J., Zeng G., Yuan X., Li X., Liang J., Wang X., Tang X. & Bai B. (2013). Spatial risk assessment and sources identification of heavy metals in surface sediments from the Dongting Lake Middle China. *Journal of Geochemical Exploration* **132**: 75–83. DOI: https://doi.org/10.1016/j.gexplo.2013.05.007

Liang J., Liu J., Xu G. & Chen B. (2019). Distribution and transport of heavy metals in surface sediments of the Zhejiang nearshore area, East China Sea: sedimentary environmental effects. *Marine Pollution Bulletin* **146**: 542–551. DOI: https://doi.org/10.1016/j.marpolbul.2019.07.001

López D.L., Gierlowski-Kordesch E. & Hollenkamp C. (2010). Geochemical mobility and bioavailability of heavy metals in a lake affected by acid mine drainage: Lake Hope, Vinton County, Ohio. *Water, Air, and Soil Pollution* **213**: 27–45. DOI: https://doi.org/10.1007/s11270-010-0364-6

Ma R., Wang B., Lu S., Zhang Y., Yin L., Huang J., Deng S., Wang Y. & Yu G. (2016a). Characterization of pharmaceutically active compounds in Dongting Lake, China: occurrence, chiral profiling and environmental risk. *Science of the Total Environment* **557**: 268–275. DOI: https://doi.org/10.1016/j.scitotenv.2016.03.053

Ma X., Zuo H., Tian M., Zhang L., Meng J., Zhou X., Min N., Chang X. & Liu Y. (2016b). Assessment of heavy metals contamination in sediments from three adjacent regions of the Yellow River using metal chemical fractions and multivariate analysis techniques. *Chemosphere* **144**: 264–272. DOI: https://doi.org/10.1016/j.chemosphere.2015.08.026

Magni L.F., Castro L.N. & Rendina A.E. (2021). Evaluation of heavy metal contamination levels in river sediments and their risk to human health in urban areas: A case study in the Matanza-Riachuelo Basin, Argentina. *Environmental Research* **197**: 110979. DOI: https://doi.org/10.1016/j.envres.2021.110979

Malferrari D., Brigatti M.F., Laurora A. & Pini S. (2009). Heavy metals in sediments from canals for water supplying and drainage: mobilization and control strategies. *Journal of Hazardous Materials* **161**: 723–729. DOI: https://doi.org/10.1016/j.jhazmat.2008.04.014

Perera W., Dayananda M., Dissanayake D., Rathnasekara R., Botheju W.S.M., Liyanage J.A., Weragoda S.K. & Kularathne K.A.M. (2021). Risk assessment of trace element contamination in drinking water and agricultural Soil: a study in selected chronic kidney disease of unknown etiology (CKDu) endemic areas in Sri Lanka. *Journal of Chemistry* **2021**: 6627254. DOI: https://doi.org/10.1155/2021/6627254

Queiroz H.M., Ying S.C., Abernathy M., Barcellos D., Gabriel F.A., Otero X.L., Nobrega G.N., Bernardino A.F. & Ferreira T.O. (2021). Manganese: The overlooked contaminant in the world largest mine tailings dam collapse. *Environment International* **146**: 106284. DOI: https://doi.org/10.1016/j.envint.2020.106284

Senarathne P. & Pathiratne K.A.S. (2007). Accumulation of heavy metals in a food fish, Mystus gulio inhabiting

Bolgoda Lake, Sri Lanka. *Sri Lanka Journal of Aquatic Sciences* **12** : 61–75.
DOI: https://doi.org/10.4038/sljas.v12i0.2214

Siddique A., Hassan A., Khan S.R., Inayat A., Nazir A. & Iqbal M. (2018). Appraisal of heavy metals and nutrients from phosphate rocks, Khyber Pakhtunkhwa, Pakistan. *Chemie International* **4**: 1.

Suresh G., Sutharsan P., Ramasamy V. & Venkatachalapathy R. (2012). Assessment of spatial distribution and potential ecological risk of the heavy metals in relation to granulometric contents of Veeranam lake sediments, India. *Ecotoxicology and Environmental Safety* **84**: 117–124.
DOI: https://doi.org/10.1016/j.ecoenv.2012.06.027

Tang W., Ao L., Zhang H. & Shan B. (2014). Accumulation and risk of heavy metals in relation to agricultural intensification in the river sediments of agricultural regions. *Environmental Earth Sciences* **71**: 3945–3951.
DOI: https://doi.org/10.1007/s12665-013-2779-z

Thevenon F., de Alencastro L.F., Loizeau J-L., Adatte T., Grandjean D., Wildi W. & Poté J. (2013). A high-resolution historical sediment record of nutrients, trace elements and organochlorines (DDT and PCB) deposition in a drinking water reservoir (Lake Brêt, Switzerland) points at local and regional pollutant sources. *Chemosphere* **90**: 2444–2452.
DOI: https://doi.org/10.1016/j.chemosphere.2012.11.002

Varol M. (2011). Assessment of heavy metal contamination in sediments of the Tigris River (Turkey) using pollution indices and multivariate statistical techniques. *Journal of Hazardous Materials* **195**: 355–364.
DOI: https://doi.org/10.1016/j.jhazmat.2011.08.051

Varol M. (2020). Environmental, ecological and health risks of trace metals in sediments of a large reservoir on the Euphrates River (Turkey). *Environmental Research* **187**: 109664.
DOI: https://doi.org/10.1016/j.envres.2020.109664

Wedepohl K.H. (1995). The composition of the continental crust. *Geochimica et Cosmochimica Acta* **59**: 1217–1232.
DOI: https://doi.org/10.1016/0016-7037(95)00038-2

Wijesinghe H., Idroos F.S. & Manage P.M. (2018). Heavy metal contamination status in seven fish species from reservoirs of Polonnaruwa district, Sri Lanka. *Sri Lanka Journal of Aquatic Sciences* **23**(1): 95-104.
DOI: https://doi.org/10.4038/sljas.v23i1.7550

Yang Z., Wang Y., Shen Z., Niu J. & Tang Z. (2009). Distribution and speciation of heavy metals in sediments from the mainstream, tributaries, and lakes of the Yangtze River catchment of Wuhan, China. *Journal of Hazardous Materials* **166**: 1186–1194.
DOI: https://doi.org/10.1016/j.jhazmat.2008.12.034

Zhu X., Ji H., Chen Y., Qiao M. & Tang L. (2013). Assessment and sources of heavy metals in surface sediments of Miyun Reservoir, Beijing. *Environmental Monitoring and Assessment* **185**: 6049–6062.
DOI: https://doi.org/10.1007/s10661-012-3005-2

Supplementary Information

Table S1: Concentrations, ranges, and averages of heavy metals in the upstream and downstream surface lake sediments in the Eppawala area

Heavy metal	Upstream													
	U1	U2	U3	U4	U5	U6	U7	U8	U9	U10	U11	U12	Range (mg/kg)	Average (mg/kg)
Cr	343.8	208.5	277.5	168.2	324.8	115.4	264.1	427.3	325.4	282.7	327.8	90.4	(90.42- 427.34)	263.0
Mn	1556.0	1525.0	1611.1	669.4	515.3	2655.3	1949.0	2707.0	1857.0	1165.1	651.0	187.6	(187.61-2706.96)	1420.7
Co	38.8	44.6	49.9	21.9	16.0	29.2	34.2	46.7	33.5	40.9	29.5	5.9	(5.87-49.89)	32.6
Ni	83.4	131.5	120.0	56.0	34.4	33.6	99.2	111.8	87.4	98.1	273.6	41.2	(33.64-273.63)	97.5
Cu	70.5	95.5	108.0	77.6	43.1	91.5	63.3	67.9	57.2	108.0	77.0	10.1	(10.12-108.00)	72.5
Zn	159.0	203.5	217.2	121.4	449.3	193.7	132.8	161.4	149.6	249.4	158.6	40.8	(40.78-449.30)	186.4
As	22.4	23.6	31.9	25.0	23.7	26.1	23.9	24.2	35.7	46.8	16.0	2.8	(2.81-46.77)	25.1
Cd	0.1	0.1	0.7	1.0	0.6	0.3	2.2	0.3	0.1	0.1	Bdl	Bdl	(0.07- 2.19)	0.5
Pb	18.8	22.2	25.1	13.8	10.3	10.0	13.5	18.8	13.6	26.2	3.5	Bdl	(3.48-26.23)	14.7

Table S1: Concentrations, ranges, and averages of heavy metals in the upstream and downstream surface lake sediments in the Eppawala area

Downstream											
D1	D2	D3	D4	D5	D6	D7	D8	D9	D10	Range (mg/kg)	Average (mg/kg)
69.6	371.6	220.4	256.0	267.7	276.3	245.2	394.4	190.2	121.3	(69.58- 394.38)	241.3
176.6	1226.2	1103.3	336.8	1478.9	759.8	1464.5	2212.9	1687.4	964.1	(176.62- 2212.94)	1141.1
5.5	25.5	14.2	10.6	35.8	27.2	43.9	30.5	23.6	19.7	(5.50- 43.86)	23.8
29.8	57.3	20.4	35.7	76.7	59.3	120.5	51.0	41.1	40.7	(20.43- 120.46)	53.2
5.9	80.2	34.5	37.7	75.1	52.7	101.9	79.5	85.0	83.1	(5.91- 101.90)	63.6
49.7	136.4	107.6	102.1	206.1	123.8	213.5	155.7	123.6	118.1	(49.73- 213.46)	133.7
28.6	33.1	14.1	16.0	20.8	27.1	30.0	26.2	25.9	27.5	(14.14- 33.08)	24.9
0.0	0.1	0.1	0.3	0.1	0.0	0.2	0.5	0.2	0.7	(0.01- 0.67)	0.2
8.1	20.5	11.1	10.2	19.4	14.4	24.8	10.5	6.2	3.5	(3.47- 24.81)	12.9

*Bdl – Below detection limit

Table S2: Classification criteria for the degree of heavy metal contamination by geo-accumulation index (I_{geo}) (Abrahim & Parker, 2008; Ma *et al*., 2016)

I_{geo}	Class	Quality of sediment
$I_{geo} \leq 0$	0	Practically unpolluted
$0 < I_{geo} < 1$	1	Unpolluted to moderately polluted
$1 < I_{geo} < 2$	2	Moderately polluted
$2 < I_{geo} < 3$	3	Moderately to heavily polluted
$3 < I_{geo} < 4$	4	Heavily polluted
$4 < I_{geo} < 5$	5	Heavily to extremely polluted
$I_{geo} > 5$	6	Extremely polluted

Table S3: Potential ecological risk classification criteria for heavy metal contamination (Chai *et al*., 2017; Zhu *et al*., 2013)

Potential ecological risk factor (E^i_r)	Class	Level of single heavy metal ecological risk	Potential ecological risk index (RI)	Class	Level of total potential ecological risk
$E^i_r < 40$	1	Low risk	RI < 150	1	Low risk
$40 \leq E^i_r < 80$	2	Moderate risk	150 ≤ RI < 300	2	Moderate risk
$80 \leq E^i_r < 160$	3	Considerable risk	300 ≤ RI < 600	3	Considerable risk
$160 \leq E^i_r < 320$	4	High risk	RI ≥ 600	4	Very high risk
$E^i_r \geq 320$	5	Very high risk			

J.Natn.Sci.Foundation Sri Lanka 2023 51 (4): 589 - 595
DOI: http://dx.doi.org/10.4038/jnsfsr.v51i4.11438

RESEARCH ARTICLE

Horticulture

Genetic control of fruit length, external colour and number of fruits per vine in bitter gourd studied using *Charantia* × *Muricata* crosses

HMPS Kumari[1*], PU Nisansala[1], EP Wijewardhana[1], DP Sumanasinghe[1], DS De Z Abeysiriwardena[2] and TLCN Kusalani[1]

[1] *Horticultural Crops Research and Development Institute, Gannoruwa, Peradeniya, Sri Lanka.*
[2] *CIC Agribusinesses, Pelwehera, Dambulla, Sri Lanka.*

Submitted: 01 December 2022; Revised: 20 February 2023; Accepted: 28 April 2023

Abstract: The present study was undertaken to ascertain the genetic control of external fruit colour, fruit length, and the number of fruits per vine in bitter gourd using reciprocal crosses of *Momordica charantia* var. *muricata* and *M. charantia* var. *charantia* and to identify suitable lines of *M. charantia* var. *muricata* to be used in bitter gourd improvement programmes. *Muricata* accession collected from Girandurukotte (GK), Sri Lanka, was selected as a suitable accession for crop improvement based on higher gynoecy and consistency of characteristics. Crossing success between *Charantia* and *Muricata* varieties was 100 % indicating cross-compatibility between the two types. External fruit colour, fruit length and the number of fruits per vine of bitter gourd were found to be quantitative traits, potentially controlled by many genes, each with a small effect. The number of fruits per vine was found to show cytoplasmic inheritance, as the F_1 generation recorded fruit numbers per vine similar to those of C*harantia* varieties, when C*harantia* varieties were used as the female parent of the reciprocal crosses made between *Charantia* and *Muricata* varieties. However, the suspected cytoplasmic effect was not useful, as it influenced to reduce the number of fruits per vine. In addition, the number of fruits per vine showed several transgressive segregants in both extremes of the F_2 populations. In bitter gourd improvement programmes, GK *Muricata accession* may be used to improve cultivated *Charantia* varieties with respect to fruit characteristics such as external fruit colour, fruit length and the number of fruits per vine through a breeding program with the directional selection made towards obtaining the desired characters.

Keywords: Bitter gourd, *Charantia* and *Muricata* varieties, fruit length, fruit colour, genetic control, number of fruits per vine.

INTRODUCTION

Bitter gourd (*Momordica charantia* L.) is one of the most important vegetables which belongs to the family Cucurbitaceae. Based on fruit size, shape, colour, and surface texture, bitter gourd is classified into two botanical varieties, *viz.*, *M. charantia var. charantia* and *M. charantia var. muricata* (wild progenitor). *Momordica charantia* var. *charantia* has large fusiform fruits, while *M. charantia* var. *muricata* develops small and round fruits with tubercles having tapered ends (Chakravarty, 1990).

Widely cultivated bitter gourd *M. charantia var. charantia* bears 8–10 fruits per vine and has desirable fruit characteristics such as large fruits preferred by farmers and consumers. Though limited in the extent of commercial cultivation and not popular, the small-fruited edible bitter gourd *M. charantia var. muricata* bears a large number of fruits (15–25) per vine and carries field-level resistance to leaf curl viruses.

The fruit length, number of fruits per vine, and fruit colour are important fruit and yield characteristics for

* Corresponding author (hmpskumari2021@gmail.com; https://orcid.org/0000-0002-5935-9646)

improving bitter gourd for high yield and consumer preference. Fruit length and the number of fruits per vine are controlled by additive factors and have direct positive effects on fruit yield (Sharma & Bhutani, 2001). Rao *et al.* (2021) also reported that fruit length and the number of fruits per vine are controlled by quantitative trait loci (QTL). Zhang *et al.* (2008) reported that fruit length is incompletely dominant and is controlled by a minimum of five genes. According to Kumari *et al*. (2015), fruit length in the bitter gourd is quantitatively inherited and is controlled by four genes. Fruit colour of bitter gourd (green vs. white) is highly heritable and is controlled by two genes, in which green is dominant over white (Liu *et al*., 2005). A recent finding reported that the expression of chlorophyll has complex interactions and thus the fruit colour of bitter gourd is a quantitative trait (Huang & Hsieh, 2017).

The utilization of potentially important wild bitter gourd varieties in varietal improvement programs has been reported (Behera *et al*., 2008). Thus, hybridization between *M. charantia* var. *muricata* and *M. charantia* var. *charantia* appears to be an effective approach in bitter gourd improvement programmes for fruit length, the number of fruits per vine, and external fruit colour. For this purpose, further studies on the genetic control of fruit characteristics of bitter gourd using crosses between *M. charantia* var. *muricata* and *M. charantia* var. *charantia* will be important. Thus, the objectives of the present study were to identify the best out of five *M. charantia* var. *muricata* accessions collected from different regions in Sri Lanka, and to ascertain the genetic control of important fruit characteristics, *viz.*, fruit length, the number of fruits per vine, and external fruit colour, using direct and reciprocal crosses between *M. charantia* var. *muricata* and *M. charantia* var. *charantia.*

MATERIALS AND METHODS

Identification of promising *Muricata* accessions

The small-fruited bitter gourd accessions (*M. charantia* var. *muricata*) were collected from five different regions in Sri Lanka, *viz.*, Giradurukotte (GK), Polonnaruwa (PN), Dehiatthakandiya (DK), and Hambanthota (HT), representing the Low Country Dry zone, and Muruthalawa (MT) representing the Mid Country Wet zone of Sri Lanka. The accessions were compared in an experiment conducted in a protected house at the Horticultural Crops Research and Development Institute (HORDI), Gannoruwa, Sri Lanka. Thirty plants from each accession were potted with one plant per pot and kept in the protected house in a Randomized Complete Block Design (RCBD), with three replications against the sunlight intensity gradient observed in the protected house. Each accession had 10 pots per replicate.

Morphological characteristics important for bitter gourd crop improvements such as mature vine length, days to flower initiation, number of fruits per vine, and external fruit colour were evaluated to select the best accessions. Green and yellowish-white are the two main fruit colours so that Matale Green and Thinnaweli White varieties were used as the green and yellowish-white fruit colour standards, respectively. Accessions were evaluated over three consecutive seasons (2016 Dry, 2016/17 Wet, and 2017 Dry seasons) to observe stability and uniformity of characteristics within accessions. Data were analysed using ANOVA and mean separation was performed using Duncan's Multiple Range Test at $p \leq 0.05$ using SAS software version 9.1. Before the analyses, each data set was tested for normality, error homogeneity, the correlation between means and variances, and additivity of main effects to ensure the non-violation of the assumptions of ANOVA. None of the data sets was found to be violating any of the assumptions so that the use of ANOVA on the original (non-transformed) data could be justified.

Genetic control study

The *Muricata* accession from Giradurukotte was used to make distant crosses with recommended bitter gourd *Charantia* varieties 'Matale Green' and 'Thinnaweli white'. Seeds of all possible crosses of *Muricata* × Matale Green and *Muricata* × Thinnaweli White and their reciprocal crosses (altogether four crosses) were planted to raise the F_1 generations. All the F_1 seeds from each cross (four F_2 populations) were used to establish an F_2 population in the field and were maintained according to the recommended cultural practices by the Department of Agriculture (DOA).

Fruit length, number of fruits per vine, and the external fruit colour were recorded in all F_1 and F_2 populations. From each F_2 population, a sample of 150 to 220 individual plants was used to study the genetic control of each of the three characteristics measured in the F_2 populations using segregation patterns by plotting frequency distributions in terms of histograms.

RESULTS AND DISCUSSION

Identification of promising *Muricata* accessions

More than 90% within line uniformity was ascertained on observational basis in all the accessions in all three seasons for external fruit colour, length of matured vine, and the number of fruits per vine. The length of the matured vine, days to flower initiation, number of fruits per vine, and external fruit pericarp colour of *Muricata* accessions over three consecutive seasons of 2016 Dry, 2016/17 Wet, and 2017 Dry, are presented in Tables 1 and 2.

The cross, accession × season interaction was found to be not significant ($p \leq 0.05$) for vine length, days to flower initiation, and the number of fruits per vine so that the means of those characteristics over seasons could be compared among accessions. The differences in vine length, days to flower initiation, and the number of fruits per vine observed among selected accessions were consistent over seasons; so that differences between accessions could mainly be attributed to genetic effects. Thus, accessions were genetically different and making selection among them appeared effective. The GK accession was selected as the comparatively better-performing accession for the crossing programme for introgression of important traits, as it recorded the highest number of fruits per vine, the longest mature vine length, the lowest number of days to initiate female flowers, and green external fruit colour over all three seasons (Table 1).

Table 1: Mature vine length and days to flower initiation of site based *Muricata* accessions over three consecutive seasons of 2016 Dry, 2016/17 Wet and 2017 Dry.

Site based Accession	Vine length (m)[#]				Days to flower initiation[#]								Number. of fruits/vine[#]				External fruit colour[# £]		
					Male				Female										
	S1	S2	S3	Mean*	S1	S2	S3	Mean*	S1	S2	S3	Mean*	S1	S2	S3	Avg.*	S1	S2	S3
Girandurukotte	2.5	2.8	2.7	2.66a	33	32	33	32.70a	45	40	44	43.0c	18	22	29	23.0a	G	G	G
Muruthalawa	1.4	1.5	1.4	1.43c	35	33	34	3.00a	50	50	49	49.7a	11	10	8	9.6c	LG	LG	LG
Dehiattakandiya	1.5	1.6	1.5	1.53c	30	32	32	1.30a	45	45	44	44.7b	15	13	13	13.3b	LG	LG	LG
Polonnaruwa	1.2	1.4	1.4	1.33c	32	33	32	2.33a	45	44	45	44.7b	10	12	10	10.0c	G	G	G
Hambantota	1.8	2.0	1.9	1.90b	33	33	32	2.70a	50	48	50	49.3a	12	12	15	13.0b	G	G	G

[#] S1- 2016 Dry Season, S2- 2016/17 Wet Season, S3- 2017 Dry Season

* Means with the same letter within a column are not significantly different at 0.05 probability level

Table 2: External fruit colour, fruit length and number and mid-parent value of fruits/vine of GK *Muricata* accession, Matale green and Thinnaweli white parental lines and their F_1 cross combinations

Population	External fruit colour	Fruit length* (cm)	Fruits/vine* (number)	Mid-parent value
GK Muricata accession	Green	3.5c	20.0a	
Matale Green	Green	32.0a	12.0bc	
Thinneweli White	Yellowish White	37.0a	8.0d	
GK Muricata acc. × Matale green (F_1)	Green	6.0b	17.0a	16
Matale green × GK *Muricata* acc.(F_1)	Green	6.5b	12.0bc	16
GK Muricata acc. × Thinneweli white (F_1)	Light green	8.0b	14.0b	14
Thinneweli white × GK *Muricata acc.* (F_1)	Light green	8.2b	9.0cd	14
CV %		14.0	12.5	

*Values with the same letter within a column are not significantly different at 5% probability level.

Determination of the genetic control of traits

In each cross, more than 95% of female flowers set fruits following crossing, and this revealed the genetic compatibility and close relationship between the GK *Muricata* accession and *Charantia*. Thus, the use of GK *Muricata* accession as promising germplasm for bitter gourd improvement would be possible. This is in agreement with Rathod *et al*. (2019), who reported a high percentage of fruit set (> 85%) with abundant seeds per fruit and seedling survivability of the cross between *M. Charantia var. Charantia* and *M. Charantia var. Muricata.* They also suggested that *Charantia* and *Muricata* are genetically close to each other and compatible. Bai & Beevy (2012) and Bharathi *et al*. (2012) explained the closeness between these two botanical varietal groups based on conventional crossing methods.

External fruit colour

The external fruit colour of parental lines of GK *Muricata* accession Matale Green and Thinnaweli White and their F_1 cross combinations of GK *Muricata* accession × Matale green, Matale green × GK *Muricata accession,* GK *Muricata* accession × Thinneweli white and Thinneweli white × GK *Muricata accession* are presented in Table 3. Both the F_1 cross combinations involving the cross between Thinnaweli White with yellowish-white fruit colour and GK *Muricata* accession with green fruit colour and the reciprocal cross showed light green fruit colour, so that incomplete dominance could be operating. This was in agreement with Lion *et al*. (2002) who also speculated that the light green colour in F_1 is due to incomplete dominance or modifiers.

The external fruit colour of both the F_2 populations derived from the cross between GK *Muricata* accession and Thinnaweli White and the reciprocal cross showed a continuous variation approaching normal distribution from green to yellowish-white (Figure 1). Thus, the external fruit colour appeared to be a quantitative characteristic controlled by many genes, each with a possible small additive effect. This is in agreement with Huang & Hsieh (2017), who reported that the external fruit colour of bitter gourd is controlled by many genes as expression of chlorophyll has complex interactions. Liu *et al.* (2005) and Lion *et al*. (2002) reported that fruit colour (green vs. white) in bitter guard is controlled by two genes, where green is dominant over white. Therefore, the desired fruit colour may be achieved through directional selection.

As no F_2 segregation was observed for external fruit colour of the cross between the GK *Muricata* accession and Matale Green, while all parents and F_1 plants had the same green external fruit colour, both the parents, GK *Muricata* accession and Matale Green, may carry the same gene/genes alleles for green fruit colour.

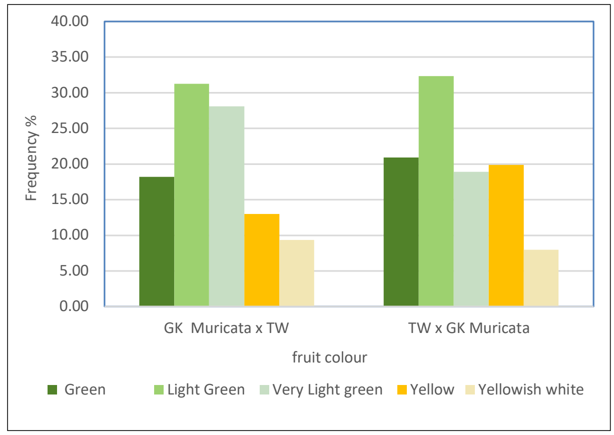

Figure 1: Percentage distribution of external fruit colour in two F_2 populations derived from the cross of GK *Muricata* accession × Thinnaweli White, and the reciprocal cross.

Fruit length

The fruit length of the GK *Muricata* accession, Matale Green and Thinnaweli White parental lines, and their F_1 cross combinations are presented in Table 2. All four F_1 cross combinations recorded significantly ($p \leq 0.05$) shorter fruit length than Matale Green and Thinnaweli White, however, significantly ($p \leq 0.05$) longer fruit length than that of the GK *Muricata* accession. The fruit length of F_1 was very close to that of GK *Muricata* accession and showed incomplete dominance for short fruit length. This is in agreement with Kim *et al*. (1990) and Zhang *et al.* (2008), who reported that the fruit length of bitter gourd showed incomplete dominance and Kumari *et al*. (2015) who reported that short fruit length is partially dominant over long fruit length. Furthermore, Behera *et al*. (2008) reported that the fruit length of bitter gourd is controlled by a single dominant gene or few genes, as *Muricata* parental characteristics are expressed in the fruit length of F_1.

Fruit length in four F_2 populations derived from the crosses of GK *Muricata* accession × Matale Green and its reciprocal cross and cross of GK *Muricata* accession × Thinnaweli White and its reciprocal cross showed continuous variations from short (0–5 cm) to long (35–40 cm) fruits (Figure 2). Thus, the current study is in agreement with the previous studies (Sharma & Bhutani, 2001; Zhang *et al*., 2008; Kumari *et al*., 2015) verifying that fruit length of bitter gourd may be a quantitative characteristic controlled by many genes, each with an effect varying in size. For genetic improvement of the trait, directional selection may be used for the desired direction as the trait is quantitative. Kumari *et al*. (2015) reported that selection for fruit length is effective as it has a high broad-sense heritability.

In all F_2 populations, longer fruit lengths than that of the parents with the longest fruit length were observed, and they are suspected to be transgressive segregants which may be effectively utilized for bitter gourd improvement.

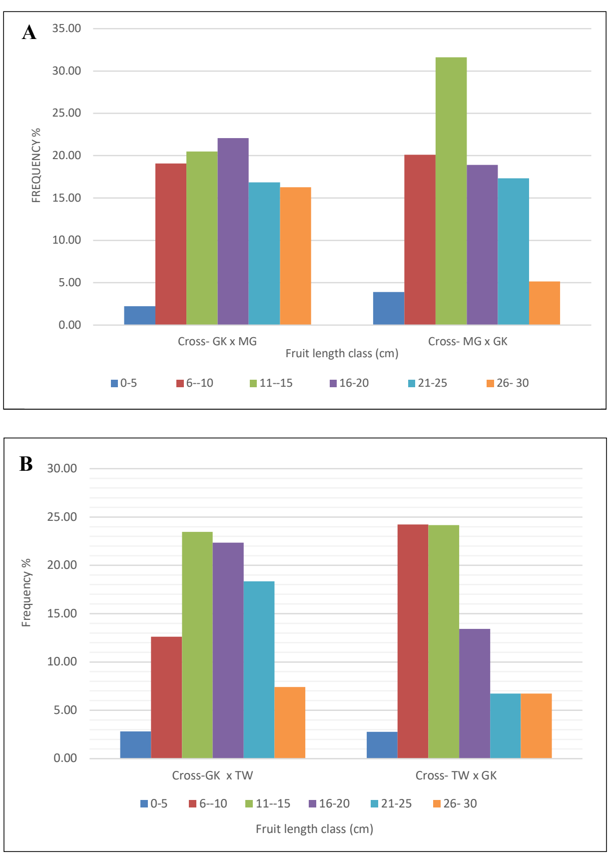

Figure 2: Histogram of fruit length in four F_2 populations derived from the crosses of (A) Girandurukotte *Muricata* accession (GK) × Matale Green, its reciprocal (Matale green × GK), (B) Girandurukotte *Muricata* accession × Thinnaweli White, and its reciprocal (Thinnaweli white × GK).

Number of fruits per vine

The number of fruits per vine of GK *Muricata* accession Matale Green, and Thinnaweli White parental lines and their F_1 cross combinations are presented in Table 3. The behavior of F_1 progenies of GK *Muricata* accession × Thinnaweli White and GK *Muricata* accession × Matale Green cross combinations indicated that the number of fruits per vine may be controlled by many genes with additive effects. However, the F_1 progenies of the reciprocal crosses of the above-indicated crosses, *viz*., Thinnaweli White × GK *Muricata* accession and Matale Green × GK *Muricata* accession recorded nine fruits pre vine and 12 fruits per vine, respectively which were not significantly ($p \leq 0.05$) different from that of the respective female parents, while much lower than the mid-parent value (Table 3). Thus, the number of fruits per vine in bitter gourd may be controlled by both nuclear gene effects as well as a cytoplasmic effect depending on the female parent used in the cross combination.

GK *Muricata* accession had no cytoplasmic effect but both Matale Green and Thinnaweli White (*Charantia* varieties) may have a cytoplasmic effect on the number of fruits per vine. However, this cytoplasmic effect may not be useful as its influence was to reduce the number of fruits per vine. As no previous studies are available on such a cytoplasmic effect on the number of fruits per vine in bitter gourd, further studies are needed to confirm this.

The number of fruits per vine of all four F_2 populations derived from the crosses of GK *Muricata accession* × Matale Green and its reciprocal cross and cross of GK *Muricata* accession × Thinnaweli White and its reciprocal cross segregated in the same pattern showing a continuous variation from the lowest fruit number (0–5) to the highest fruit number (26–30) per vine (Figure 3). Based on the segregation pattern of the respective F_2 populations, the number of fruits per vine in bitter gourd appeared to be a quantitative characteristic that is mainly controlled by many genes with additive effects. This is in agreement with Sharma & Bhutani (2001) who reported that the number of fruits per vine is a quantitative trait controlled by additive factors, and Rao *et al*. (2021) who reported that the number of fruits per vine is controlled by QTL. The cytoplasmic effect may have been nullified in all F_2 populations where female parents were Matale Green and Thinnaweli White. All four F_2 distributions had segregants with values much lower and higher than the lowest and highest parents, respectively and these may be transgressive segregants appearing in both extremes (Figure 3).

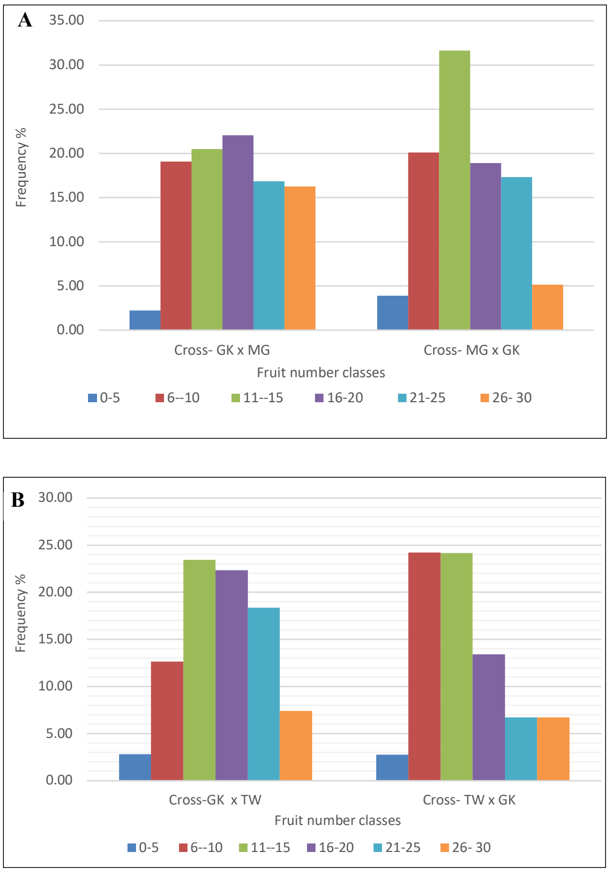

Figure 3: Distribution of the number of fruits per vine in four F_2 populations derived from the crosses (A) *Muricata* (GK) × Matale Green, and its reciprocal cross (Matale Green × GK), (B) *Muricata* × Thinnaweli White and its reciprocal cross (Thinnaweli White × GK).

Although the highest number of fruits per vine recorded among parents was 20, F_2 segregants suspected to be transgressive with the number of fruits per vine as high as 26-30 were recorded, so that potential for improving the number of fruits per vine in bitter gourd through directional selection appears very high. This may be comparatively more efficient in the F_2 population derived from the cross between GK *Muricata* accession × Matale Green as the number of plants with 26-30 fruits per vine was the highest (about 27) in that population.

CONCLUSIONS

The bitter gourd accession of GK *Muricata* collected from the Giradurukotte region in Sri Lanka was identified as a rich genetic source for bitter gourd improvement due to its consistency in characters and higher gynoecy. External fruit colour, fruit length, and the number of fruits per vine of bitter gourd appeared to be quantitative characteristics controlled by many genes, each with a potential small effect. GK *Muricata* accession may be used to improve presently cultivated varieties Matale Green and Thinnaweli White, with respect to the above fruit characteristics, through a breeding programme with the directional selection made towards the desired direction.

The cytoplasmic effect of Matale Green and Thinnaweli White varieties on the number of fruits per vine is considered to be not useful as its influence was to reduce the number of fruits per vine. The appearance of transgressive segregants in fruit length and the number of fruits per vine in respective F_2 populations were about 3% and 10%, respectively, and they are of interest for further improvement.

Conflict of interest statement

The authors declare no conflict of interest regarding the publication of this article.

Acknowledgements

The authors wish to thank the Council for Agriculture Research Policy, Sri Lanka for providing financial support for the present study through NARP Research Grants.

REFERENCES

Bai N.H. & Beevy S.S. (2012). Characterization of intraspecific F1 hybrids of *Momordica charantia* L. based on morphology, cytology, and palynology. *Cytologia* **77**(3): 301–310. DOI: https://doi.org/10.1508/cytologia.77.301

Bharathi L.K., Munshi A.D, Behera T.K., Joseph J.K.V., Bhat K.V., Das A.B. & Sidhu A.S. (2012). Production and preliminary characterization of novel inter-specific hybrids derived from *Momordica* species. *Current Science* **103**: 178–186.

Behera T.K., Staub J.E., Behera S. & Simon P.W. (2008). Bitter gourd and human health. *Medicinal and Aromatic Plant Science and Biotechnology* **1**(2): 224–226.

Chakravarty H.L. (1990). Cucurbits of India and their role

in the development of vegetable crops. In: *Biology and Utilization of CucvrbiLoceao* (eds. D.M. Bates, R.W. Robinson & C. Jeffrey), pp. 325–334. Cornell University Press, Ithaca, New York, USA.
DOI: https://doi.org/10.7591/9781501745447-028

Huang H.Y. & Hsieh C.H. (2017). Genetic research on fruit colourants of the bitter gourd (*Momordica charantia* L.) *The Horticulture Journal* **86**(2): 238–243.
DOI: https://doi.org/10.2503/hortj.MI-159

Kim Z.H., Kim Y.R. & Urn S.K. (1990). Inheritance of fruit weight in bitter-gourd (*Momordica charantia* L.). *Journal of Korean Society for Horticultural Science* **31**: 238–246.

Kumari M., Behera T.K., Munshi A.D. & Talukadar A. (2015). Inheritance of fruit traits and generation mean analysis for estimation of horticultural traits in bitter gourd. *Indian Journal of Horticulture* **72**(1): 43–48.
DOI: https://doi.org/10.5958/0974-0112.2015.00008.0

Lion T.D., Chen K.S., Lee S.F., Lin J.N., Tsao S.J. & Yang Y.W. (2002). Tangshan 036', a white bitter gourd cultivar. *Horticultural Science* **37**: 1142–1143.
DOI: https://doi.org/10.21273/HORTSCI.37.7.1142

Liu Z.G., Long M.M., Qin R.Y. & Wang X.Y. (2005). Studies on genetic variation, correlation and path analysis in bitter gourd (*Momordica charantia* L.). *Guangxi Botany* **25**: 426–430.

Rao P.G., Behera T.K., Gaikwad A.B., Munshi A.D., Srivastava A. & Boopalakrishnan G. (2021). Genetic analysis and QTL mapping of yield and fruit traits in bitter gourd (*Momordica charantia* L.). *Scientific Reports* **11**(1): 1–10.
DOI: https://doi.org/10.1038/s41598-021-83548-8

Rathod V., Behera T.K., Munshi A.D., Vinod V. & Singh G. (2019). Crossability studies among *Momordica charantia* var. charantia and *Momordica charantia* var. muricata. *Indian Journal of Agricultural Sciences* **89**(11): 1900–1905.
DOI: https://doi.org/10.56093/ijas.v89i11.95339

Sharma N.K. & Bhutani R.D. (2001). Correlation and path analysis studies in bitter gourd (*Momordica charantia* L.). *Haryana Journal of Horticultural Sciences* **30**: 84–86.

Zhang C., Luo S., Goo J., Zheng X., Lao H. & Man J. (2008). Study on the genetic effects of fruit length of bitter gourd. *Guangdong Agricultural Sciences* **1**: 34–35.

J.Natn.Sci.Foundation Sri Lanka 2023 51 (4): 597 - 614
DOI: http://dx.doi.org/10.4038/jnsfsr.v51i4.11500

RESEARCH ARTICLE

Agriculture

Screening eighty traditional and improved rice genotypes in Sri Lanka for salinity tolerance at the seedling stage in *Yoshida* solution

HAPA Shyamalee and AL Ranawake*
Department of Agricultural Biology, Faculty of Agriculture, University of Ruhuna, Mapalana, Kamburupitiya, Sri Lanka.

Submitted: 21 December 2022; Revised: 22 July 2023; Accepted: 25 August 2023

Abstract: A total of eighty different rice genotypes consisting of fifty-three traditional rice accessions and twenty-seven improved rice varieties were evaluated for salinity tolerance. To identify the tolerant genotypes and the relationship between tolerance level with plant height and dry matter accumulation, the seedlings were subjected to electrical conductivity (EC) ~12 dSm^{-1} for ten and sixteen days separately at the seedling stage. The salinity tolerance of the seedlings was evaluated by standard evaluation scores (SES). Plant height, and total, shoot, and root-dry matter were evaluated in stressed and controlled plants. *Rathuheenati4992* was highly tolerant at salinity stresses, and *Heenati4618, Kaluwee3728, Mawee (5531, 3618)*, and *Pokkali3573* were highly tolerant at the 10-day and tolerant at the 16-day salinity stress. *Pokkali3881* was moderately tolerant at both stress conditions. Improved rice varieties *At354* and *Bg250* were highly tolerant at 10-day salinity stress and tolerant at 16-day salinity stress. Cultivation of highly susceptible improved rice varieties, *Bg360, At306, At362, Ld368 At405, At402, Ld371, Bw272-6b, Ld365*, and *Bg352* must be avoided in salinized soils. There was no correlation between plant height and salinity tolerance (r = -0.381, α = 0.000), salinity tolerance and total dry matter (r = 0.325 α = 0.002), salinity tolerance and root dry matter (r = 0.294, α = 0.008), or salinity tolerance and shoot dry matter (r = 0.061, α = 0.594). Plant height or dry matter accumulation can be considered unreliable parameters for salinity tolerance screening since they differ with the genotype. The highly tolerant and tolerant genotypes must be further studied at different growth stages.

Keywords: Improved rice, salinity tolerance, seedling stage, Sri Lanka, traditional rice accessions.

INTRODUCTION

More than 50% of the world's population consumes rice as their primary calorie source, with 80% carbohydrates (USDA, 2018). Latin American countries, the USA, Europe, Africa, and Asia grow rice worldwide, while an average Asian consumes around 150 kg yearly (Papademetriou, 2000).

Rice cultivation experiences various environmental stresses, such as salinity, drought, flood, heat, cold, topography, and soil factors (Mitin, 2009). Salinity is the second most important abiotic stress that decreases rice productivity worldwide (Isayenkov, 2012), next to drought (Gregorio *et al*., 1997). Though some lands are naturally salinized by rock weathering (Moreira-Nordemann, 1984), climate change and inappropriate land usage collectively cause the salinization of one-third of the irrigated lands (Machado & Serralheiro, 2017; Ullah *et al*., 2021). Excessive irrigation accumulates salts, and limited drainage intensifies salinity in the fields (Van der Zee *et al*., 2017). Evaporation accelerates salinization in dry zone fields (Vidal, 2019).

About sixty million hectares of rice-cultivating lands are affected by salinity in Asia (Papademetriou, 2009). Due to the absence of data on actual salinity-affected areas, the economic impact of salinization has not been

* Corresponding author (lankaranawake@hotmail.com; https://orcid.org/0000-0003-0517-9911)

reported in Sri Lanka (Thiruchelvam & Pathmarajah, 1999). Being an island, Sri Lanka experiences both inland (Rengasamy, 2016) and coastal salinity in different districts (Kendaragama & Bandara, 2000). Rice fields near the coastal belts develop salinity due to seawater intrusion (Opatha & Lokupitiya, 2019). By 1978, around 0.112 million ha of rice lands had been affected by salinity with electrical conductivity over 4 dSm^{-1} (Panabokke, 1978). After the tsunami in 2004, 4000 ha of the coastal belt in Sri Lanka developed salinity (Sirisena & Wanigasundera, 2021).

Salinity stress reduces plant growth and yield by reducing water and nutrient uptake (Corwin, 2021). Salinity stress badly affects germination (Vibhuti *et al*., 2015) seedling growth (Vibhuti *et al*., 2015; Senanayake *et al*., 2017), and survival ability (Mishra *et al*., 2021), at vegetative (Zeng *et al*., 2001), panicle initiation (Rad *et al*., 2011) and heading (Rad *et al.*, 2011; Gerona *et al*., 2019) stages. Yield components, such as the number of spikelets (Shereen *et al*., 2005), filled grain percentage (Abdullah *et al.*, 2001), and per plant yield have also been reduced under salinity stress (Zeng *et al*., 2001; Raza *et al*, 2005; Singh & Sengar, 2014).

The effect of salinity is minimized by soil amendment (Minhas & Sharma, 2003), proper drainage (Rhoades, 2016), plant transplanting and minimizing evaporation (Gurung & Azad, 2013). Improving rice varieties with salinity stress significantly increases rice production (Haque *et al*., 2021). Identifying new tolerant genetic materials by screening genotypes for salinity tolerance is essential for directly introducing or incorporating elite lines in rice varietal improvement programmes (Vasudevan *et al*., 2014). Breeders must integrate yield and salinity tolerance into the same genotype by eliminating unfavourable traits for commercial cultivation. Broadening the existing genetic base of rice expands the possibilities of new gene combinations for breeding programmes (Brozynska *et al*., 2016). In such a study, out of 185 rice genotypes, fifteen genotypes at the germination stage and twenty-eight at the seedling stage were salinity-tolerant (Sakina *et al*., 2016). Several other studies have been conducted to find salinity tolerance in different genetic sources (Supplementary Table I). Indonesian researchers (Hairmansis *et al.*, 2017) and the International Rice Research Institute (IRRI, 2006) have developed salinity-tolerant rice varieties. Improved rice varieties *Bw400*, *Bg369*, *At353*, and *At354,* have been recommended for differently saline soils in Sri Lanka (RRDI, 2018).

Sri Lankan traditional rice accessions, *Mas samba, Galpawee, Mahasuduwee, Godawee, Rathkara,* and *Handiran,* have scored more than 35% survival rates under salinity stress (Pradeepika *et al*., 2014), and *Sudu Karayal* (Pradeepika *et al*., 2014), *Godawee* and *Alwee* (Dahanayaka *et al.*, 2015), *Pachchaperumal* (Pradheeban, 2014), *Herath* and *Ranhiriyal* (Ranawake & Dahanayake, 2012) are some of the traditional rice accessions which have performed better than the other accessions under salinity stress.

Imposing salinity stress has been done by using different electrical conductivity (EC) levels or Na^+ concentrations, and different morphological and biochemical parameters have been used to evaluate the materials compared to positive control and sensitive check varieties (Supplementary Table I).

Salinity-tolerant character in rice is not a single-factor trait; thus, screening for salinity tolerance and improving salinity tolerance in rice face several difficulties. Genetic factors and genetic environment interactions significantly affect salinity tolerance (Krishnamurthy *et al*., 2016; Rasel *et al*., 2021). Salinity tolerance links with poor quality characteristics such as low yield, poor grain quality, and long age in rice (Ravikiran *et al*., 2018). Field screening procedures are impractical for salinity screening due to uncontrolled environmental factors in the field. Hence, preliminary screening must be done under controlled environmental conditions to determine the tolerant genotypes (Gregorio *et al*., 1997). Laboratory or greenhouse screening experiments (Souleymane *et al*., 2015), manipulation of *Yoshida* solution at EC 5 dSm^{-1} (Ranawake *et al*., 2014) and EC 7 dSm^{-1} (Chen *et al.*, 2020), or hydroponic systems (Hakim *et al*., 2010; Kranto *et al*., 2016; Tabassum *et al*., 2021) are commonly applied techniques for salinity tolerance screening (Supplementary Table I).

Morphological or physiological changes in rice due to salinity stress have been used to evaluate the level of tolerance or susceptibility of rice to salinity stress. Several salinity-affected traits are leaf length, leaf folding leaf tip burning, dry or dead leaves, burned patches on leaves (Gregorio *et al*., 1997), and reduced chlorophyll contents in the leaves (Singh *et al*., 2014; Tabassum *et al.*, 2021). Further, rice reduces leaf elongation and new leaf emergences (Hakim *et al.*, 2010; Kranto *et al.*, 2016; Tabassum *et al.*, 2021). The plant survival rate, reduction of plant height, tillering ability (Razzaque *et al*., 2009), and days to flowering (Joseph, 2013) have also been altered under salinity stress. Reduction in the number of spikelets per panicle and seed yield per panicle (Zeng *et al*., 2001), panicle length, spikelets number, and fertility percentage have also been altered during the salinity stress (Joseph, 2013).

Pokkali and *Nona-Bokara* are used as the positive control, and *IR29* and *IR29* are used as the sensitive genotype in many salinity-tolerant studies in rice (Supplementary Table I).

Further, rice has been evaluated in different growth stages for salinity tolerance: at germination (Pradheeban *et al*., 2015), seedling (Gregorio *et al*., 1997; Khan *et al*., 1997), vegetative (Ranawake *et al*., 2014) and maturity (Tabassum *et al*., 2021) stages (Supplementary Table I). The seedling and early seedling stages are the most sensitive stages for salinity stress in rice (Grattan *et al*., 2002).

Screening genotypes for salinity tolerance at the early growth stages ensures crop establishment and survival at the latter growth stages. The parameters considered for salinity tolerance screening must be reliable and convenient. Since the salinity-induced morphological and physiological changes in rice are complex, visual characters are evaluated in salinity tolerance screening in rice (Gregorio *et al*., 1997).

Plant shoot and root weight are reduced under salinity stress at the seedling and vegetative stage (Razzaque *et al*., 2009). Tolerant and susceptible genotypes have recorded different reduction rates in total biomass, and shoot and root dry matter under salinity stress (Lutts *et al*., 1995; Zeng *et al.*, 2001; Souleymane *et al.*, 2015; Tabassum *et al.*, 2021). The reliability of such characteristics as parameters in salinity tolerance screening is doubtful. In the present study, while screening salinity tolerance in improved and traditional rice genotypes using IRRI adapted technique (Gregorio *et al*., 1997), the possibility of using plant height, total dry matter weight, and shoot and root dry matter weight as evaluation parameters was assessed.

MATERIALS AND METHODS

Plant materials

Eighty rice genotypes, including fifty-three traditional rice accessions and twenty-seven improved varieties, were collected from the Plant Genetic Resources Centre, Gannoruwa, Sri Lanka (PGRC, 1999). Tolerant and susceptible check varieties used in the study were Pokkali and IR, respectively.

Experimental design and procedure

The experiment was conducted according to a randomized complete block design with four replicates, and ten plants were included in each replicate. Dormancy broken surface-sterilized rice seeds were germinated in distilled water for three days and transferred to *Yoshida* solution (Gregorio *et al*., 1997). Using sodium chloride, the Yoshida solution's electrical conductivity (EC) was increased up to EC ~ 6 dSm^{-1}. The calibration curve was plotted to manage the EC of the *Yoshida* solution. After three days at EC 6 dSm^{-1}, the salinity level was increased to 12 dSm^{-1}, and seedlings were kept in the same condition for 16 days. The medium was renewed at intervals of two days. The *Yoshida* solution was prepared according to Yoshida *et al*. (1972).

Scoring visual salt injuries using standard evaluation scores (SES)

Plants were evaluated according to the IRRI standard scores for visible salt injury (Gregorio *et al*., 1997) at ten and sixteen days of salinization (Supplementary Figure I).

Determination of plant height and biomass accumulation

After visual scoring, plant height was measured. The stressed plants and control plants were kept at 70^{o}C for five days until a constant dry matter weight was recorded, and the per-plant shoot dry weight, root dry weight, and total dry weight were measured. The shoot, root, and total dry weight reduction percentages were calculated as a percentage of the difference between the dry weight of the salinity-stressed plants (DWSP) and the control plants (DWCP); {(DWSP-DWCP)/DWCP}*100.

Data analysis

Data were analyzed using ANOVA with Statistical Analysis System (SAS Institute Inc., 2000). Duncan's multiple range test separated means.

RESULTS AND DISCUSSION

Salinity tolerance of traditional rice accessions as scored by standard evaluation scores (SES)

According to the SES, *Dahanala3917, Heenati4618, Kaluwee3728, Mawee (8497, 5531, 3618), Murungakayan3921, Pokkali3573, Rathuwee3905*, and *Rathuheenati (6249, 4992),* and improved varieties *Bg250* and *At354* were highly tolerant at the10-day salinity stress at EC 12 dSm^{-1}. However, among traditional rice accessions highly tolerant at the 10-day salinity stress, only *Rathuheenati6229* was highly tolerant at the 16-day salinity stress. *Heenati4618, Kaluwee3728, Pokkali3573,* and *Mawee (5531, 3618)* were tolerant, and *Mawee3487* and *Rathuwee3905* were moderately tolerant at the 16-day salinity stress though they were highly tolerant at the 10-day salinity stress. Finding *Rathuheenati4992* as a highly tolerant accession at both 10-day and 16-day salinity stresses is a promising finding in the present study. The most tolerant accessions next to *Rathuheenati4992* were *Heenati4618, Kaluwee3728, Mawee (5531, 3618)*, and *Pokkali3,* which were highly tolerant at the 10-day and tolerant at the 16-day salinity stress. Among the tolerant accessions at the 10-day salinity stress, only *Kaluheenati7802* was tolerant at 16 days. In contrast, all other traditional accessions that were tolerant at the 10-day salinity stress were moderately tolerant, susceptible or highly susceptible at the 16-day salinity stress. *Kaluheenati7802* would be a promising accession to withstand the salinity stress better than many of the highly salinity tolerant accessions at the 10-day salinity stress, that were not highly tolerant or tolerant at the 16-day salinity stress (Table 1).

There are several *Pokkali* accessions in the farmer fields and the germplasm collections. These accessions could be the same or different in their genetic make-up. In the present study, two *Pokkali* accessions *(3881, 3573)* were evaluated, and *Pokkali3573* was highly tolerant at the 10-day salinity stress while moderately tolerant at the 16-day salinity stress. However, *Pokkali3881* was moderately tolerant at both stress conditions (Table 1). Dahanayaka *et al.* (2015) reported that *Pokkali5556* is salinity tolerant, and Noorzuraini *et al.* (2021) reported that two different *Pokkali* lines (accession numbers were not given) are salinity tolerant. *Pokkali* has been reported as salinity tolerant at the seedling stage (Heenan *et al*., 1988; Wijerathna *et al*., 2011; de Costa *et al*., 2012b; Senanayake *et al*., 2017) and the panicle stage (Heenan *et al*., 1988). *Pokkali* serves as the tolerant check variety for salinity tolerance studies (El-Shabrawi *et al.*, 2010; Chunthaburee *et al*., 2016; Sampangi-Ramaiah *et al*., 2020). De Costa *et al*. (2012a) used *Pokkali* as the check variety in an osmotic and ionic stress tolerance study; El-Shabrawi *et al.* (2010) as a positive control for a salinity tolerant physiological marker; and Sampangi-Ramaiah *et al.* (2020) as a reference for a salinity tolerant endophyte producer.

Salinity tolerance of improved rice varieties as scored by standard evaluation scores (SES)

Improved rice varieties *At354* and *Bg250* were highly tolerant at the 10-day salinity stress, and both were tolerant at the 16-day salinity stress (Table 1). *At354* has been recorded as salinity tolerant at the seedling stage (Senanayake *et al*., 2017) and used as the standard check variety in a study carried out to evaluate the varietal performances under salinity stress (de Costa *et al*., 2012a; Pradeepika *et al*., 2014). Under experimental conditions, *At354* has performed better than *Pokkali* (de Costa *et al.*, 2012b) and has recorded a 77% survival rate under salinity stress at the seedling stage (Dahanayaka *et al*., 2015). Pradheeban *et al*. (2014) has reported that *At354* is a highly salinity-tolerant accession at the germination stage, the same as *Pokkali*. Highly salinity tolerant *Bg250* is a short-day variety (85 days) with an average yield of 4.5 t/ha in Sri Lanka. It has been recommended for drought and flood-prone fields to escape the stress (RRDI, 2018). *Bg250* has been recorded as a highly salinity-tolerant accession to the level of *Pokkali* at the germination stage (Pradheeban *et al*., 2014) and at the seedling stage after the seeds were treated with *Imidacloprid* 70% WS (Gaucho), *Thiamethoxam* 70% WS (Cruiser), and *Nitrophenolate* 0.5% WS (Atonik) (Ranawake *et al*., 2013).

Among the improved rice varieties, *Bw400, Bg369*, and *At353* were tolerant at the 16-day salinity stress, along with *Bg250* and *At354* were highly salinity-tolerant at the 10-day salinity stress. *Bg369* and *At353* were tolerant at both stress conditions. *Bg45*5 and *Swarnasub1* were moderately tolerant at 16-day salinity stress, and *Bg350* was moderately tolerant at both 10-day and 16-day salinity stresses. *Bg369* has been reported as a salinity-tolerant rice variety (Senanayake *et al*., 2017). *At354*, *Bw400, Bg369*, and *At353* have been recommended for differently salinized fields in Sri Lanka and have fallen into different yield and age categories (RRDI, 2018).

Four improved rice varieties, namely *Bg360, At306, At362,* and *Ld368,* were highly susceptible even at the 10-day salinity stress, while ten accessions including the same varieties that were highly susceptible at 10-day and *At405, At402, Ld371, Bw272-6b, Ld365*, and *Bg352* were highly susceptible at 16-day salinity stress (Table 1). These varieties should not be grown in saline-prone areas in Sri Lanka.

Table 1: Salinity tolerance of rice genotypes on the 10th and 16th day salinity stress at the seedling stage

		Highly tolerant	Tolerant	Moderately tolerant	Susceptible		Highly susceptible
Salinity stress at 6 dS/m for 10 days	Traditional rice accessions	*Dahanala3917*	*Kalubalawee5479*	*Dikwee3741*	*Dikwee3504*	*Murungakayan6263*	*Kuruwee3552*
		Heenati4618	*Kaluheenati5191*	*Dikwee2203*	*Heenati6402*	*Murungakayan3490*	
		Kaluwee3728	*Kaluheenati7802*	*Kalubalawee3976*	*Heenati4935*	*Dahanala3304*	
		Mawee8497	*Kaluheenati4621*	*Kalubalawee5480*	*Heenati3936*	*Podiwee3109*	
		Mawee5531	*Murungakayan 3492*	*Kaluheenati4991*	*Heenati3707*	*Rathuheenati5486*	
		Mawee3618	*Polayal3661*	*Mawee8552*	*Heenati4524*	*Suduheenati3932*	
		Murungakayan 3921	*Ratawee3466*	*Mawee4145*	*Mawee8551*	*Sudurusamba2202*	
		Pokkali3573	*Rathuwee3473*	*Murungakayan 3809*	*Mawee3683*	*Kaluwee3876*	
		Rathuwee3905	*Suduheenati7799*	*Pokkali3881*	*Mawee5384*	*Kaluheenati3471*	
		Rathuheenati6249	*Kuruwee3982*	*Ratawee3655*	*Kuruwee3898*		
		Rathuheenati4992		*Sudurusamba3671*	*Kuruwee3465*		
	Improved	*Bg250*	*Bg359, Bg369*	*Bg350*	*Bg350*	*Bw453*	*Bg360*
		At354	*Bg455, At353*	*Ld371*	*At308*	*Ld365*	*At306*
			Bw367, Bw400	*IRRI64*	*At402*	*Ld408*	*At362*
			IRRI64		*At405*	*Sambamasuri*	*Ld368*
			Swarnasub1		*Bw272-6b*	*Bg352*	
			Heenati4618	*Dikwee3504*	*Dahanala3917*	*Kalubalawee3976*	*Dikwee2203*
Salinity stress at 6 dSm-1 for 16 days	Traditional rice accessions	*Rathuheenati4992*	*Kaluwee3728*	*Heenati4935*	*Dahanala3304*	*Murungakayan3921*	*Heenati3707*
			Kaluheenati7802	*Heenati3936*	*Dikwee3741*	*Murungakayan3492*	*Mawee3683*
			Mawee5531	*Kalubalawee5479*	*Heenati6402*	*Murungakayan3490*	*Murungakayan 3495*
			Mawee3618	*Kaluheenati4991*	*Heenati4524*	*Ratawee3466*	*Podiwee3109*
			Pokkali3573	*Kaluheenati4621*	*Kaluheenati 5191*	*Rathuwee3473*	*Rathuheenati6249*
				Kaluheenati3471	*Kuruwee3982*	*Suduheenati7799*	*Rathuheenati5486*
				Mawee8497	*Kuruwee3552*	*Suduheenati3932*	*Sudurusamba2202*
				Murungakayan 3809	*Kuruwee3465*	*Sudurusamba3671*	*Mawee8551*
				Pokkali3881	*Kuruwee3898*	*Kaluwee3876*	*Murungakayan 6263*
				Polayal3905	*Mawee8552*		
				Ratawee3655	*Mawee3704*		
				Rathuwee3905			
	Improved		*Bw400*	*Bg350*	*Bg300*	*Ld408*	*At405, Bg360*
			Bg250	*Bg455*	*Bg359*	*IRRI64*	*Bw272-6b, Ld371*
			Bg369	*Swarnasub1*	*At308*	*IRRIsub1*	*Ld365, At306*
			At353		*Bw367*	*Sambamasuri*	*Ld368, At362*
			At354		*Bw453*	*Ld368*	*Bg352, At402*

Yield and agronomic characteristics of studied key genotypes were greatly varied under field conditions (*Unpublished data by the authors*).

Ientification of the tolerance category into which the rice genotype is included is convenient for future practices. Among the traditional genotypes, 20.7% was highly tolerant, 16.9% tolerant, 20.7% moderately tolerant and 39.6% susceptible or highly susceptible at the 10-day salinity stress, while the values changed to 1.9, 11.3, 24.5, and 62.2% respectively at the 16-day salinity stress.

Identifying different tolerance categories in salinity stress studies in rice is a common practice. Three categories, namely tolerant, moderately tolerant, and sensitive, have been identified based on physio-morphological indices evaluated at EC 10 dSm^{-1} salinity stress in the rice seedling stage by Pongprayoon *et al.* (2019). They reported that the variety *Riceberry* is salinity tolerant, five cultivars are moderately tolerant, and two cultivars are susceptible. Germplasm consisting of 114 genotypes recorded 7% highly tolerant, 20.14% tolerant, 36.84% moderately tolerant, 28.95% susceptible, and 7% highly susceptible at the germination stage in a Petri dish method under a 120 mM salt concentration (Zhang *et al.*, 2021). Another continued study from 2012 to 2021 in India reported that out of 1500 different rice genotypes, only 5% were salinity tolerant and out of 7500 rice lines, only 3.2% were salinity tolerant at the seedling stage under 10 dSm^{-1} salinity stress (Krishnamurthy *et al.*, 2022). A collection of another 110 Sri Lankan genotypes consisting of both improved and traditional rice accessions has also recorded 5.9% highly tolerant, 24.5% tolerant, 29.4% moderately tolerant, 31.4% susceptible, and 8.8% highly susceptible genotypes under a hydroponic system at a salinity level of 100 mM Na^+ (de Costa *et al.*, 2012a). The percentages of highly salinity tolerant and tolerant rice genotypes in the studied Sri Lankan rice germplasm are significantly greater than those of the other studies.

Salinity tolerance in traditional rice accessions

Salinity tolerance levels in traditional rice accessions are more sustainable than improved rice varieties. Only *Kuruwee3552* was highly susceptible to 10-day salinity stress among the traditional rice accessions. Around 40% acquired at least a minimum tolerance level, proving the adaptability of naturally evolved traditional genotypes for saline fields (Table 1). Although highly tolerant improved rice varieties and traditional rice accessions at the 10-day salinity stress have been downgraded to lower-level salinity tolerant/susceptible groups at the 16-day salinity stress, *Rathuheenati4992* was able to withstand severe 16-day salinity stress as well as the 10-day salinity stress. The sustainability of traditional rice accessions under salinity stress was exhibited in many traditional rice accessions by remaining at the same tolerance level at both 10-day and 16-day salinity stresses: *Rathuheenati6229* was highly tolerant, *Kaluheenati7802* was tolerant, *Kaluheenati4991*, *Murungakayan3809*, *Pokkali3881*, *Murungakayan3809,* and *Rathuwee3655* were moderately tolerant at both stresses (Table 1). The broad genetic diversity in Sri Lankan traditional rice gene pool gives a great chance to select promising accessions other than *Pokkali* for future breeding programmes.

Dry matter reduction and salinity tolerance of studied rice genotypes

When subjected to extended periods of salinity, plants undergo ionic stress, resulting in early aging of mature leaves and subsequently reducing the available photosynthetic area, which, in turn, affects leaf water potential and the production and distribution of assimilated dry matter (Cramer & Nowak, 1992; Bradford, 1994). However, there is no unique relationship between salinity tolerance level and dry matter accumulation or reduction, compared to that of control plants at the salinity stress in the studied genotypes. The shoot, root, and total dry matter reduction and accumulation varied in different ranges regardless of the tolerance level: shoot dry matter 24.53% reduction to 63.14% accumulation, root dry matter 36.15% reduction to 6.61% accumulation, total dry matter 31.76% reduction to 15.39% accumulation.

Dry matter reduction and accumulation under salinity stress were evident in the highly tolerant or tolerant groups. *Pokkali3573* reported dry matter reduction in the shoot (24.53%), root (36.15%), and total dry matter (31.76%). *Mawee3618* and *At353* reported the highest shoot (63.14%), and root (63.14%) dry matter accumulation, and *Pokkali3573* reported the highest shoot dry matter reduction (24.53%). Further, *Kaluwee3728* and *Bg250* accumulated the highest root dry matter (6.61%), and *Pokkali3573* reduced the root dry matter by 36.15%. Highly salinity tolerant *Rathuheenati4992* reduced the shoot and total dry matter. Still, it increased the root dry weight at salinity stress, indicating that its root system grows under salinity stress while shoot growth is limited (Table 2).

Dry matter reduction and dry matter accumulation in shoot, root, or both were significantly changed in the moderately salinity tolerant group. Among thirteen traditional rice accessions and three modern varieties, *Kaluheenati4621* reported the highest significant shoot dry matter reduction (58.13%) and *Bg350* recorded the highest shoot dry matter accumulation (84.55%).

The highest root dry matter reduction was reported in *Dikwee3504* (62.07%), and *Heenati3936* recorded the highest root dry matter accumulation (59.87%). Traditional rice accession *Polayal3661* recorded the lowest total dry matter accumulation (0.94%), and *Kalubalawee5479* recorded the highest total dry matter accumulation (59.87%). However, *Ratawee3655* and *Pokkali3881* reduced the dry matter accumulation in both shoots and roots. These values emphasize the variations in shoot, root or total dry matter accumulation and reduction in rice genotypes at the seedling stage under the salinity stress even though they belong to the same tolerance level. Usually, the root dry matter accumulation is reduced under salinity stress (Singam *et al*., 2011). Though the slightest reduction of dry matter in salinity-tolerant genotypes under salinity stress is evident (Ashraf & Bhatti, 2000; Souleymane *et al*., 2015; Tabassum *et al*., 2021a), the studied genotypes behaved differently. A broad diversity exists in dry matter partitioning and dry matter reduction and accumulation in highly tolerant, tolerant or moderately tolerant rice genotypes at the salinity stress.

Table 2: Shoot dry matter, root dry matter, and total dry matter reduction in highly tolerant, tolerant, and moderately tolerant rice genotypes in the seedling stage at the 16-day salinity stress

HT & T genotypes	SD	RD	TD	MT genotypes	SD	RD	TD
Rathuhenati4992(HT)	8.97 ^{c}	-1.05 ^{c}	2.99 ^{d}	*Dikwee3504*	-31.93 ^{e}	62.07 ^{a}	48.48 ^{a}
Heenati4618	-4.48 ^{d}	4.63 ^{b}	1.13 ^{d}	*Heenati4935*	40.67 ^{b}	-1.70 ^{g}	12.95 ^{d}
Kaluwee3728	-0.90 ^{d}	-6.61 ^{d}	-4.50 ^{e}	*Heenati3936*	-7.36 ^{d}	-59.87 ^{j}	-4.85 ^{h}
Kalubalawee5480	-33.13 ^{e}	35.05 ^{a}	23.20 ^{b}	*Kalubalawee5479*	-84.27 ^{g}	-48.28 ^{i}	-61.23 i
Mawee5531	-60.25 ^{f}	2.70 ^{bc}	-14.34 ^{f}	*Kaluheenati4991*	17.85 ^{c}	-1.97 ^{g}	4.09 ^{e}
Mawee3618	-63.14 ^{f}	6.31 ^{b}	-15.39 ^{f}	*Kaluheenati4621*	58.13 ^{a}	-4.57 ^{g}	25.25 ^{c}
Pokkali3573	24.53 ^{a}	36.15 ^{a}	31.76 ^{a}	*Kaluheenati3471*	-11.54 ^{d}	24.24 ^{d}	13.66
Bg250	-0.90 ^{d}	-6.61 ^{d}	-4.50 ^{e}	*Mawee8497*	19.84 ^{c}	-4.65 ^{g}	4.04 ^{e}
Bg369	5.37 ^{b}	1.73 ^{bc}	6.71 ^{c}	*Murungakayan3809*	-37.15 ^{e}	-0.99 ^{g}	-10.56 ^{g}
At353	-63.14 ^{f}	6.31 ^{b}	-15.39 ^{f}	*Pokkali3881*	14.60 ^{c}	42.24 ^{c}	35.73 ^{b}
At354	15.37 ^{b}	1.72 ^{bc}	6.71 ^{c}	*Polayal3661*	24.92 ^{c}	-24.79 ^{h}	-0.94 f
Bw400	15.36 ^{b}	1.73 ^{bc}	6.71 ^{c}	*Ratawee3655*	46.19 ^{b}	53.49 ^{b}	49.58 ^{a}
CV	-23.46	15.13	9.9	*Rathuwee3905*	19.88 ^{c}	-3.97 ^{g}	6.25 ^{e}
				Bg350	-84.55 ^{g}	15.01 ^{e}	-7.89 ^{g}
				Bg455	-2.27 ^{d}	6.33 ^{f}	4.03 ^{e}
				Swarnasub1	-60.89 ^{f}	22.27 ^{d}	13.73 ^{d}
				CV	-13.8	17.39	38.22

HT: Highly tolerant, T: Tolerant, MT: Moderately tolerant SD: Shoot dry matter, RD: Root dry matter, TD: Total dry matter

In the susceptible group, 62.5% of genotypes reduced the shoot dry matter at the salinity stress, but there is a significant variation in the degree of reduction or accumulation. The highest root dry matter reduction (81.68%) was observed in *IRRIsub1,* and the highest root dry matter accumulation (49.04%) was observed in *IRRI64* (Table 3). Traditional rice accessions *Kaluwee3876, Kuruwee* (*3898, 3552, 3465*), *Suduheenati3932,* and improved variety *Bg300* increased the total dry matter while other genotypes reduced the total dry matter under salinity stress. Traditional rice accession *Dahanala3917* had not reduced the total dry matter under salinity stress. Genotypes in the salinity susceptible group record a spectrum of dry matter reduction or accumulation patterns in root, shoots, or both under salinity stress.

In the highly susceptible group, only four accessions, *Murungakayan3495* (35.78%), *Sudurusamba2202* (64.18%), *Bg360* (15.41%), and *Bw272-6b* (75.30%) accumulated the shoot dry matter and two traditional rice accessions, *Murungakayan3495* (2.82%), and *Rathuheenati6249* (48.16%), and improved variety *At402* (14.01%) accumulated root dry matter under salinity stress. All other rice genotypes showed shoot and root dry matter reductions under salinity stress. Being highly susceptible, *Murungakayan3495* was the only highly susceptible genotype that increased the total dry matter accumulation under salinity stress.

Table 3: Shoot dry matter, root dry matter, and total dry matter reduction of susceptible and highly susceptible rice genotypes in the seedling stage at the 16-day salinity stress

S Genotypes	SD	RD	TD	HS Genotypes	SD	RD	TD
Dahanala3917	9.21 ^{gh}	-5.23 ^{k}	0.00 ^{j}	*Dikwee2203*	39.48 ^{b}	22.90 ^{gh}	28.67 ^{e}
Dahanala3304	-15.18 ^{l}	32.07 ^{g}	19.27 ^{efg}	*Heenati3707*	20.88 ^{d}	56.50 ^{b}	45.66 ^{b}
Dikwee3741	56.81 ^{d}	-17.67 ^{l}	25.44 ^{d}	*Mawee3683*	25.67 ^{d}	2.83 ^{k}	12.10 ^{j}
Heenati6402	14.45 ^{g}	51.26 d	44.39 ^{a}	*Mawee8551*	37.52 ^{bc}	40.80 ^{d}	39.53 ^{c}
Heenati4524	4.29 ^{hi}	-1.98 ^{k}	0.34 ^{j}	*Murungakayan6263*	40.28 ^{b}	22.62 ^{gh}	25.65 ^{f}
Kaluwee3876	-3.00 ^{ij}	-31.05 ^{m}	-22.92 ^{k}	*Murungakayan3495*	-35.78 ^{f}	-2.82 ^{l}	-12.54 ^{l}
Kalubalawee3976	58.33 ^{cd}	11.18 ^{j}	37.28 ^{b}	*Podiwee3109*	69.41 ^{a}	16.33 ^{ij}	23.59 ^{fj}
Kaluheenati5191	16.11 ^{g}	15.70 ^{j}	15.89 ^{gh}	*Rathuheenati6249*	60.16 ^{a}	-48.16 ^{n}	14.74 ^{i}
Kuruwee3982	34.55 ^{f}	-12.96 l	10.87 ^{i}	*Rathuheenati5486*	37.52 ^{bc}	40.80 ^{d}	39.55 ^{c}
Kuruwee3898	-71.43 ^{o}	-34.06 ^{m}	-44.68 ^{l}	*Sudurusamba2202*	-64.18 ^{g}	104.15 ^{a}	35.02 ^{d}
Kuruwee3552	66.07 ^{bc}	66.07 ^{c}	-24.83 ^{k}	*Bg352*	69.41 ^{a}	16.33 ^{ij}	23.59 ^{fg}
Kuruwee3465	74.18 ^{ab}	74.18 ^{b}	-52 15 ^{m}	*Bg360*	-15.41 ^{e}	32.67 ^{e}	24.62 ^{fg}
Mawee8552	-39.17 ^{m}	38.80 ^{f}	20.67 ^{ef}	*At306*	27.88 ^{cd}	14.58 ^{j}	17.98 ^{h}
Mawee3704	4.33 ^{hi}	30.16 ^{gh}	22.29 ^{de}	*At362*	23.17 ^{d}	54.40 ^{b}	47.32 ^{ab}
Mawee5384	-1.41 ^{ij}	32.33 g	18.72 ^{efg}	*At402*	44.63 ^{b}	-14.01 ^{m}	5.74 ^{k}
Murungakayan3921	11.16 ^{gh}	-2.79 ^{k}	1.99 ^{j}	*At405*	60.11 ^{a}	46.03 ^{c}	49.27 ^{a}
Murungakayan3492	-14.23 ^{kl}	31.31 ^{g}	19.15 ^{efg}	*Bw272-6b*	-75.30 ^{h}	30.80 ^{ef}	22.48 ^{g}
Murungakayan3490	4.29 ^{hi}	-1.98 ^{k}	0.34 ^{j}	*Ld365*	39.49 ^{b}	20.46 ^{hi}	25.70 ^{f}
Ratawee3466	13.25 ^{gh}	31.59 ^{g}	25.81 ^{d}	*Ld368*	37.35 ^{bc}	26.57 ^{fg}	28.50 ^{e}
Rathuwee3473	42.80 ^{e}	34.85 ^{fg}	36.59 ^{b}	*Ld371*	40.28 ^{b}	22.62 ^{gh}	25.65 ^{f}
Suduheenati7799	-6.52 ^{jk}	24.49 ^{hi}	15.44 ^{gh}	*CV*	27.09	13.5	6.74
Suduheenati3932	-71.43 ^{o}	-34.06 m	-44.68 ^{nl}				
Sudurusamba3671	-16.26 ^{l}	51.34 d	33.56 ^{bc}				
Bg300	-3.00 ^{ij}	-31.05 ^{m}	-22.92 ^{k}				
Bg359	44.61 ^{e}	44.64 ^{e}	44.62 ^{a}				
At308	60.76 ^{cd}	21.35 ^{i}	36.73 ^{b}				
Bw367	-60.61 ^{n}	30.60 ^{g}	13.89 ^{hi}				
Bw453	61.81 ^{cd}	11.59 ^{j}	31.06 ^{c}				
Ld408	47.13 ^{e}	29.35 ^{gh}	35.41 ^{b}				
IRRIsub1	-73.44 ^{o}	81.68 ^{a}	24.92 ^{d}				
IRRI64	79.74 ^{a}	-49.04 ^{n}	34.64 ^{bc}				
Sambamasuri	66.09 ^{bc}	-0.65 ^{k}	16.76 ^{fgh}				
CV	46.63	24.11	21.44				

S: Susceptible, HS: Highly susceptible, SD: Shoot dry matter, RD: Root dry matter, TD: Total dry matter

The presence of salinity has notably diminished the heights of all paddy cultivars throughout the specified growth stages when compared to the control treatments (Puvanitha & Mahendran, 2017). The seedling growth has reduced in salinity-susceptible varieties (Razzaque *et al*., 2009), and salinity has reduced dry matter by about 90% (Asch *et al*., 2000), including root dry matter (Singam *et al*., 2011). The level of salinity tolerance and dry matter reduction are genetically decided (Narayanan & Sree Rangasamy, 2008), and the degree of variation in dry matter reduction or accumulation changes with the genotype (Suriyan *et al.*, 2009). Efficiency reduction of photosynthesis, expression changes in transporter genes whose expression depends on Na^+ and K^+ availability, inability to absorb soil nutrition, and changes in ethylene biosynthesis directly reduce plant dry matter under salinity stress (El-Shabrawi *et al*., 2010; Puteh & Mondal, 2015; Kaur *et al*., 2016; Li *et al*., 2018; Mishra *et al*., 2021b). Overall dry matter reduction or accumulation may change once these salinity tolerance mechanisms are differently affected in different genotypes.

Table 4: Correlation between different parameters studied in screening for salinity tolerance at the seedling stage

Parameters	r	p
Susceptible level on 10th day × Total dry matter reduction (%)	0.151	0.182
Susceptible level on 10th day × Root dry matter reduction (%)	-0.068	0.550
Susceptible level on 10th day × Shoot dry matter reduction (%)	0.184	0.102
Susceptible level on 10th day × Plant height treatment	-0.334**	0.002
Total dry matter reduction (%) × Root dry matter reduction (%)	0.297**	0.007
Total dry matter reduction (%) × Shoot dry matter reduction (%)	0.405*	0.000
Root dry matter reduction (%) × Shoot dry matter reduction (%)	-0.105	0.353
Plant height × Shoot dry matter reduction (%)	-0.330**	0.003
Plant height × Total dry matter reduction (%)	-0.170	0.125
Plant height × Shoot dry matter reduction (%)	-0.330**	0.003
Plant height treatment × Plant height control	0.400**	0.000
Susceptible level on 16th day × Total dry matter reduction (%)	0.325**	0.003
Susceptible level on 16th day × Shoot dry matter reduction (%)	0.061	0.594
Susceptible level on 16th day × Root dry matter reduction (%)	0.294**	0.008
Susceptible level on 16th day × Plant height treatment	-0.381**	0.000
Susceptible level on 10th day × Tolerant level on 16th day	0.634**	0.001

r: Pearson's correlation coefficient, p: probability, *correlation is significant at the 0.05 level (2-tailed). **Correlation is significant at the 0.01 level (2-tailed).

Correlation of dry matter accumulation and salinity tolerance

Correlation analysis was performed to understand the relationship between dry matter accumulation or reduction and salinity tolerance or susceptible levels at the seedling stage at the 10-day and 16-day salinity stress (Table 4). The correlation was positive and nonsignificant ($r = 0.152$, $\alpha = 0.182$) between the susceptible level and total dry matter reduction of seedlings at the 10-day salinity stress and at the 16-day salinity stress ($r = 0.325$, $\alpha = 0.003$). A prolonged period of salinity stress is needed for a significant change in plant dry matter reduction under salinity stress (François *et al*., 1994). The type of correlation depends on the studied genetic materials and their tolerance mode at salinity stress.

There was a significant weak correlation ($r = 0.405$, $\alpha = 0.000$) between the total dry matter reduction and shoot dry matter reduction, which was greater than the correlation coefficient (r = 0.297, α = 0.007) of total dry matter reduction and root dry matter reduction, which suggests that shoots is more severely affected by salinity stress than roots. A positive, weak, but significant correlation between total dry matter reduction and root dry matter reduction at both 10-day salinity stress (r = 0.297, α = 0.007) and 16-day salinity stress (r = 0.294, α = 0.008) explains that the decrease in root dry matter is distinct under salinity stress (Durga *et al*., 2021).

Table 5: Plant height of genotypes in different salinity tolerant groups at the control condition and the salinity stress condition

Tolerant & highly tolerant		
Genotype	T	C
*Rathuheenati4992**	18.79 b	17.64 c
Heenati4618	22.28 a	17.61 c
Kaluwee3728	15.60 c	20.78 a
Kalubalawee5480	11.44 e	16.85 d
Mawee5531	14.71 d	18.82 b
Mawee3618	8.24 g	20.71 a
Pokkali3573	22.23 a	15.54 e
Bg250	15.60 c	20.78 a
Bg369	10.66 f	13.06 f
At353	8.24 g	20.71 a
At354	10.66 f	13.06 f
Bw400	10.66 f	13.06 f
CV	7.66	9.55

Moderately tolerant		
Genotype	T	C
Dikwee3504	21.11 ^{a}	13.07 ^{f}
Heenati4935	15.30 ^{d}	14.72 ^{e}
Heenati3936	18.33 ^{b}	18.25 ^{c}
Kalubalawee5479	15.54 ^{cd}	14.45 ^{e}
Kaluheenati4991	13.69 ^{f}	9.76 ^{h}
Kaluheenati4621	10.86 ^{g}	22.51 ^{a}
Kaluheenati3471	16.00 ^{c}	10.43 ^{g}
Mawee8497	14.98 ^{de}	16.47 ^{d}
Murungakayan3809	21.15 ^{a}	14.59 ^{e}
Pokkali3881	18.19 ^{b}	14.64 ^{e}
Polayal3661	13.72 ^{f}	14.95 ^{e}
Ratawee3655	15.96 ^{c}	22.61 ^{a}
Rathuwee3905	14.49 ^{e}	21.50 ^{b}
Bg350	14.44 ^{e}	8.05 ^{i}
Bg455	10.46 ^{g}	9.21 ^{h}
Swarnasub1	6.81 ^{h}	8.11 ^{i}
cv	12.88	3.08

Susceptible		
Genotype	T	C
Dahanala3917	14.97 ^{g}	10.82 ^{q}
Dahanala3304	16.41 ^{e}	15.64 ^{i}
Dikwee3741	18.00 ^{cd}	29.50 ^{b}
Heenati6402	18.14 ^{cd}	20.28 ^{d}
Heenati4524	21.42 ^{a}	15.62 ^{i}
Kaluwee3876	8.64 ^{jk}	12.16 ^{o}
Kalubalawee3976	20.11 ^{b}	25.78 ^{c}
Kaluheenati5191	16.45 ^{e}	17.78 ^{f}
Kuruwee3982	18.13 ^{cd}	16.66 ^{g}
Kuruwee3898	14.70 ^{g}	9.94 ^{r}
Kuruwee3552	11.54 ^{h}	7.47 ^{u}
Kuruwee3465	10.17 ^{i}	6.99 ^{w}
Mawee8552	21.16 ^{a}	19.18 ^{e}
Mawee4145	14.72 ^{g}	17.64 ^{f}
Mawee5384	19.89 ^{b}	41.20 ^{a}
Murungakayan3921	10.01 ^{i}	15.52 ^{i}
Murungakayan3492	17.63 ^{d}	16.50 ^{h}
Murungakayan3490	21.92 ^{a}	15.62 ^{i}
Ratawee3466	14.63 ^{g}	9.62 ^{s}
Rathuwee3473	16.17 ^{ef}	15.24 ^{j}
Suduheenati7799	18.75 ^{c}	12.08 ^{o}
Suduheenati3932	15.42 ^{fg}	9.94 r
Sudurusamba3671	15.52 ^{efg}	9.59 s
Bg300	8.63 ^{jk}	12.16 ^{o}
Bg359	9.42 ^{ij}	13.97 ^{l}
At308	8.32 ^{vk}	12.48 ^{n}
Bw367	9.97 ^{i}	7.97 ^{t}
Bw453	8.09 ^{k}	11.57 ^{p}
Ld408	6.64 ^{l}	9.62 s
IRRIsub1	18.98 ^{c}	13.38 ^{m}
IRRI64	7.98 ^{k}	15.10 ^{k}
Sambamasuri	5.32 ^{m}	7.15 ^{v}
CV	4.47	7.3

Highly susceptible		
Genotype	T	C
Dikwee2203	12.32 ^{g}	17.13 ^{e}
Heenati3707	14.42 ^{e}	22.17 ^{b}
Mawee3683	16.00 ^{d}	22.48 ^{a}
Mawee8551	16.36 ^{c}	19.85 ^{c}
Murungakayan6263	7.77 ^{l}	9.68 ^{j}
Murungakayan3495	23.16 ^{a}	18.84 ^{d}
Podiwee3109	5.55 ^{q}	18.94 ^{d}
Rathuheenati6249	22.08 ^{b}	10.93 ^{h}
Rathuheenati5486	16.36 ^{c}	19.85 ^{c}
Sudurusamba2202	6.87 ^{n}	14.50 f
Bg352	5.55 ^{q}	18.94 ^{d}
Bg360	7.50 ^{m}	6.77 ^{m}
At306	11.34 ^{h}	6.43 ^{n}
At362	13.55 f	13.00 ^{g}
At402	11.17 ^{i}	10.86 ^{h}
At405	9.34 ^{j}	10.44 ^{i}
Bw272-6b	9.18 ^{k}	7.10 l
Ld365	6.64 ^{o}	9.45 ^{k}
Ld368	6.16 ^{p}	4.33 ^{0}
Ld371	7.77 ^{l}	9.68 ^{j}
CV	5.38	10.66

*Highly tolerant genotype, T: Salinity treated plants, C: Control plants

Plant height and salinity tolerance

A plant height reduction is expected at salinity stress due to the decreases in chlorophyll content (Hakim *et al*., 2014), but some genotypes behaved differently in the present study (Table 5). Some salinity-stressed genotypes increased the plant height more than the control plants in each different salinity tolerant or susceptible group. In the highly salinity tolerant and tolerant group, out of twelve genotypes, three genotypes (*Rathuheenati4992, Heenati4818,* and *Pokkali3573*) increased the plant height at salinity stress compared to that of their control plants. In the moderately tolerant group, out of sixteen genotypes, eight genotypes increased the plant height (*Dikwee3504, Heenati4935, Kalubalawee5479, Kaluheenati4991, Murungakayan3809, Pokkali3881,* and *Bg455)* under salinity stress more than that of control plants. Sixteen genotypes out of twenty-eight in the susceptible group and eight out of twenty in the highly susceptible group performed similarly (Table 5). Generally, the plant height of the rice varieties decreases under salinity stress compared to control plants (Hakim *et al*., 2010; Umar, 2016). Different genetic constituents that are responsible for growth and salinity tolerance mechanisms respond to salinity stress at different rates in rice.

According to the correlation analysis, there were a significant yet weak and negative correlation between the tolerance level and the plant height at the 10-day ($r = -0.334$, $\alpha = 0.002$) and 16-day ($r = -0.381$, $\alpha = 0.000$) salinity stress (Table 4). A significant negative correlation between plant height and salinity tolerance has been reported in many studies (Khan *et al*., 1997; De Leon *et al*., 2015; Razzaq *et al*., 2020; Durga *et al*., 2021). However, *Pokkali* performed differently (Dionisio-Sese & Tobita, 1998), and a nonsignificant positive correlation between the same has also been reported (Asch *et al*., 2000), which supports the idea that different genotypes respond to salinity differently yet retain the same tolerance level. Plant height cannot be considered as an accurate salinity-tolerant selection criterion since individual rice genotypes respond differently to salinity stress.

CONCLUSIONS

The present study screened eighty traditional rice accessions and modern rice varieties in Sri Lanka for salinity tolerance at EC ~12 dSm^{-1} for ten and sixteen days at the seedling stage. The standard evaluation scoring method was used to evaluate the salinity tolerance, and shoot, root, and total dry matter in salinity-stressed and control plants were assessed to understand the relationship between salinity tolerance and dry matter accumulation or reduction. The traditional rice accession, *Rathuheenati4992,* was highly salinity tolerant, and *Henati4618, Kaluwee3728, Mawee (5531, 3618)*, and *Pokkali3573* were salinity tolerant at the 16-day salinity stress. There are genetically different *Pokkali* accessions with different salinity tolerance levels; *Pokkali3573* was highly tolerant, and *Pokkali3881* was moderately tolerant. Sri Lankan improved rice varieties *Bg250*, *At354, Bw400, Bg369*, and *At353* were tolerant at 16-day salinity stress. Improved rice varieties, *Bg360, At306, At362, Ld368 At405, At402, Ld371, Bw272-6b, Ld365*, and *Bg352* were highly susceptible to salinity, and their cultivation must be avoided in salinized soils. Salinity tolerance in traditional rice accessions is more sustainable: Around 40% of traditional rice accessions were moderately tolerant or highly tolerant. Dry matter reduction and accumulation varied with the genotype under the salinity stress. According to the correlation analysis, plant height ($r = -0.381$, $\alpha = 0.00$) cannot be considered a selection criterion for salinity stress, and salinity stress affects the plant height of the individual rice genotype at the seedling stage. There was no correlation ($r = 0.325$, $\alpha = 0.003$) between the tolerant or susceptible level and total dry matter reduction or accumulation under salinity stress; dry matter accumulation or reduction is not a criterion to use as a parameter for salinity tolerance at the seedling stage. These findings would differ in prolonged stresses or other growth stages. Further studies at different growth stages are needed to confirm the results.

Acknowledgements

The authors would like to acknowledge NRC12-027, Indo-Sri Lanka Program of cooperation and ICGEB/CRP/SRI/13-01 for financial assistance and Plant Genetic Resources Centre, Gannoruwa, Sri Lanka for providing planting materials.

REFERENCES

Abdullah Z., Khan M.A. & Flowers T.J. (2001). Causes of sterility in seed set of rice under salinity stress. *Journal of Agronomy and Crop Science* **187**: 25–32. DOI: https://doi.org/10.1046/j.1439-037X.2001.00500.x

Asch F., Dingkuhn M. & Dorffling K. (2000). Salinity increases CO_2 assimilation but reduces growth in field-grown, irrigated rice. *Plant and Soil* **218**: 1–10. DOI: https://doi.org/10.1023/a:1014953504021

Ashraf M.Y. & Bhatti A.S. (2000). Effect of salinity on growth and chlorophyll content in rice. *Pakistan Journal of Scientific and Industrial Research* **43**: 130–131.

DOI: https://doi.org/10.22092/AJ.2014.100920

Bradford K.J. (1994). Water stress and the water relations of seed development: a critical review. *Crop Science* **34**(1): 1–11.

Brozynska M., Furtado A. & Henry R.J. (2016). Genomics of crop wild relatives: Expanding the gene pool for crop improvement. *Plant Biotechnology Journal* **14**(4): 1070–1085.
DOI: https://doi.org/10.1111/pbi.12454

Chen C., Norton G.J. & Price A.H. (2020). Genome-wide association mapping for salt tolerance of rice seedlings grown in hydroponic and soil systems using the Bengal and Assam Aus panel. *Frontiers in Plant Science* **11**: 576479.
DOI: https://doi.org/10.3389/fpls.2020.576479

Chunthaburee S., Dongsansuk A., Sanitchon J., Pattanagul W. & Theerakulpisut P. (2016). Physiological and biochemical parameters for evaluation and clustering of rice cultivars differing in salt tolerance at seedling stage. *Saudi Journal of Biological Sciences* **23**(4): 467–477.
DOI: https://doi.org/10.1016/j.sjbs.2015.05.013

Corwin D.L. (2021). Climate change impacts on soil salinity in agricultural areas. *European Journal of Soil Science* **72**: 842–862.
DOI: https://doi.org/10.1111/ejss.13010

Cramer G.R. & Nowak R.S. (1992). Supplemental manganese improves the relative growth, net assimilation and photosynthetic rates of salt-stressed barley. *Physiologia Plantarum* **84**(4): 600–605.

Dahanayaka B., Gimhani D., Kottearachchi N. & Samarasinghe W. (2015). Assessment of salinity tolerance and analysis of SSR markers linked with saltol QTL in Sri Lankan rice (*Oryza sativa*) genotypes. *American Journal of Experimental Agriculture* **9**: 1–10.
DOI: https://doi.org/10.9734/ajea/2015/20255

De Costa W.A.J.M., Wijeratne M.A.D. & de Costa D.M. (2012a). Identification of Sri Lankan rice varieties having osmotic and ionic stress tolerance during the first phase of salinity stress. *Journal of the National Science Foundation of Sri Lanka* **40**: 251–280.
DOI: https://doi.org/10.4038/jnsfsr.v40i3.4699

De Costa W.A.J.M., Wijeratne M.A.D., de Costa D.M. & Zahra A.R.F. (2012b). Determination of the appropriate level of salinity for screening of hydroponically grown rice for salt tolerance. *Journal of the National Science Foundation of Sri Lanka* **40**: 122–135.
DOI: https://doi.org/10.4038/jnsfsr.v40i2.4440

De Leon T.B., Linscombe S., Gregorio G. & Subudhi P.K. (2015). Genetic variation in Southern USA rice genotypes for seedling salinity tolerance. *Frontiers in Plant Science* **6**: 1–13.
DOI: https://doi.org/10.3389/fpls.2015.00374

Dionisio-Sese M.L. & Tobita S. (1998). Antioxidant responses of rice seedlings to salinity stress. *Plant Science* **135**(1): 1–9.
DOI: https://doi.org/10.1016/S0168-9452(98)00025-9

Durga K.V., Rao P.V.R., Satyanarayana P., Rao V.S., Jayalalitha K. & Kasturi T. (2021). Correlation studies in seedling and reproductive stage salinity tolerance in rice (*Oryza sativa* L.) under salinity. *International Journal of Chemical Studies* **9**: 2140–2143.
DOI: https://doi.org/10.22271/chemi.2021.v9.i1ad.11538

El-Shabraw H., Kumar B., Kaul T., Reddy M.K., Singla-Pareek S.L. & Sopory S.K. (2010). Redox homeostasis, antioxidant defense, and methylglyoxal detoxification as markers for salt tolerance in Pokkali rice. *Protoplasma* **245**: 85–96.
DOI: https://doi.org/10.1007/s00709-010-0144-6

François L.E., Maas E.V. & Lesch S.M. (1994). Time of salt stress affects growth and yield components of irrigated wheat. *Agronomy Journal* **86**(1): 100–107.
DOI: https://doi.org/10.2134/agronj1994.00021962008600010019x

Gerona M.E.B., Deocampo M.P., Egdane J.A., Ismail A.M. & Dionisio-Sese M.L. (2019). Physiological responses of contrasting rice genotypes to salt stress at reproductive stage. *Rice Science* **26**: 207–219.
DOI: https://doi.org/10.1016/j.rsci.2019.05.001

Grattan S.R., Zeng L., Shannon M.C. & Roberts S.R. (2002). Rice is more sensitive to salinity than previously thought. *California Agriculture*. **56**: 189–198.
DOI: https://doi.org/10.3733/ca.v056n06p189

Gregorio G.B., Senadhira D. & Mendoza R.D. (1997). *Screening Rice for Salinity Tolerance*. Plant Breeding, Genetics and Biotechnology Division, International Rice Research Institute, Manila, Philippines.

Gurung T.R. & Azad A.K. (2013). *Best Practices and Procedures of Saline Soil Reclamation Systems in SAARC Countries*. SAARC Agriculture Centre, Dhaka, Bangladesh.

Hairmansis A., Nafisah N. & Jamil A. (2017). Towards developing salinity tolerant rice adaptable for coastal regions in Indonesia. *2nd International Conference on Sustainable Agriculture and Food Security* **2**: 72–79.
DOI: https://doi.org/10.18502/kls.v2i6.1021

Hakim M.A., Juraimi A.S., Begum M., Hanafi M.M., Ismail M.R. & Selamat A. (2010). Effect of salt stress on germination and early seedling growth of rice (*Oryza sativa* L.). *African Journal of Biotechnology* **9**: 1911–1918.
DOI: https://doi.org/10.5897/ajb09.1526

Hakim M.A., Juraimi A.S., Hanafi M.M., Ismail M.R., Selamat A., Rafii M.Y. & Latif M.A. (2014). Biochemical and anatomical changes and yield reduction in rice (*Oryza sativa* L.) under varied salinity regimes. *Biomed Research International* **2014**: 1–11.
DOI: https://doi.org/10.1155/2014/208584

Haque M.A., Rafii M.Y., Yusoff M.M., Ali N.S., Yusuff O., Datta D.R., Anisuzzaman M. & Ikba M.F. (2021). Advanced breeding strategies and future perspectives of salinity tolerance in rice. *Agronomy* **2021**: 11.
DOI: https://doi.org/10.3390/agronomy11081631

Heenan D.P., Lewin L.G. & McCaffery D.W. (1988). Salinity tolerance in rice varieties at different growth stages. *Australian Journal of Experimental Agriculture* **28**: 343–349.
DOI: https://doi.org/10.1071/EA9880343

IRRI (2006). Breeding for salt tolerance in rice. *Stress and Disease Tolerance-Module 4,* International Rice Research Institute, Manila, Philippines.

Isayenkov S. V. (2012). Physiological and molecular aspects of salt stress in plants. *Cytology and Genetics* **46**: 302–318. DOI: https://doi.org/10.3103/S0095452712050040

Joseph E.A. (2013). A Study on the effect of salinity stress on the growth and yield of some native rice cultivars of Kerala State of India. *Agriculture Forestry and Fisheries* **2**: 141. DOI: https://doi.org/10.11648/j.aff.20130203.14

Kaur N., Dhawan M., Sharma I. & Pati P.K. (2016). Interdependency of reactive oxygen species generating and scavenging system in salt sensitive and salt tolerant cultivars of rice. *BMC Plant Biology* **16**(1): 1–31. DOI: https://doi.org/10.1186/s12870-016-0824-2

Kendaragama K.M.A. & Bandara T.M.J. (2000). Changes in land use pattern in paddy lands. In: *Rice Congress 2000*. Department of Agriculture, Peradeniya, Sri Lanka, p. 251.

Khan M.S.A., Hamid A., Salahuddin A.B.M., Quasem A. & Karim M.A. (1997). Effect of sodium chloride on growth, photosynthesis and mineral ions accumulation of different types of rice (*Oryza sativa* L.). *Journal of Agronomy and Crop Science* **179**: 149–161. DOI: https://doi.org/10.1111/j.1439-037X.1997.tb00511.x

Kranto S., Chankaew S., Monkham T., Theerakulpisut P. & Sanitcho, J. (2016). Evaluation for salt tolerance in rice using multiple screening methods. *Journal of Agricultural Science and Technology* **18**: 1921–1931.

Krishnamurthy S.L., Lokeshkumar B.M., Rathor S., Warraich A.S., Yadav S., Gautam R.K., Singh R.K. & Sharma P.C. (2022). Development of salt-tolerant rice varieties to enhancing productivity in salt-affected environments. *Proceedings of the 2nd International Laayoune Forum on Biosaline Agriculture* **16**(1): 30. DOI: https://doi.org/10.3390/environsciproc2022016030

Krishnamurthy S.L., Sharma P.C., Ravikiran K.T., Basak N., Vineeth T. V., Singh Y.P. & Sarangi S.K. (2016). G×E interaction and stability analysis for salinity and sodicity tolerance in rice at reproductive stage. *Journal of Soil Salinity and Water Quality* **8**: 162–172.

Li *et al.* (13 authors) (2018). Comparative transcriptome and translatome analysis in contrasting rice genotypes reveals differential mRNA translation in salt-tolerant Pokkali under salt stress. *BMC Genomics* **19**(S10): 935. DOI: https://doi.org/10.1186/s12864-018-5279-4

Lutts S., Kinet J.M. & Bouharmont J. (1995). Changes in plant response to NaCl during development of rice (*Oryza sativa* L.) varieties differing in salinity resistance. *Journal of Experimental Botany* **46**: 1843–1852. DOI: https://doi.org/10.1093/jxb/46.12.1843

Machado R.M.A. & Serralheiro R.P. (2017). Soil salinity: Effect on vegetable crop growth. Management practices to prevent and mitigate soil salinization. *Horticulture* **3(2)**: 1–13. DOI: https://doi.org/10.3390/horticulturae3020030

Minhas P.S. & Sharma O.P. (2003). Management of soil salinity and alkalinity problems in India. *Journal of Crop Production* **7**(1–2): 181–230. DOI: https://doi.org/10.1300/J144v07n01_07

Mishra M., Wungrampha S., Kumar G., Singla-Pareek S.L. & Pareek A. (2021). How do rice seedlings of landrace Pokkali survive in saline fields after transplantation? Physiology, biochemistry, and photosynthesis. *Photosynthesis Research* **150**: 117–135. DOI: https://doi.org/10.1007/s11120-020-00771-6

Mitin A. (2009). *Documentation of Selected Adaptation Strategies to Climate Change in Rice Cultivation*. East Asia Rice Working group, Quezon City, Philippine.

Moreira-Nordemann L.M. (1984). Salinity and weathering rate of rocks in a semi-arid region. *Journal of Hydrology* **71**: 131–147. DOI: https://doi.org/10.1016/0022-1694(84)90074-X

Narayanan K.K. & Sree Rangasamy S.R. (2008). Genetic analysis for salt tolerance in rice. *Rice Genetics II*: 167–173. DOI: https://doi.org/10.1142/9789812814272_0016

Noorzuraini A.R., Mohd Ramdzan O., Nur Idayu A.R. & Muhammad Hafiz M.S. (2021). Evaluating the rice germplasm for salinity tolerance based on phenotypic traits. *IOP Conference Series: Earth and Environmental Science* **736**(1): 012067 DOI: https://doi.org/10.1088/1755-1315/736/1/012067

Opatha K.N. & Lokupitiya E. (2019). Impacts of salt water intrusion in coastal paddy areas of wet zone of Sri Lanka. *Proceedings of the 24th international Forestry and Environment Symposium,* Department of Forestry and Environmental Science, University of Sri Jayewardenepura, Sri Lanka.

Panabokke C.R. (1978). A case study of tropical Alfisols in Sri Lanka. In: *Soil Resource Data for Agricultural Development* (eds L.D. Swindale), pp. 155-162. Hawaii Agricultural Experimental Station, USA.

Papademetriou M.K. (2000). Rice production in the Asia-Pacific region: Issues and perspectives. In: *Food and Agriculture Organization Report of The United Nations*. Regional Office for Asia and the Pacific, Bangkok, Thailand.

Papademetriou M.K. (2009). *Bridging the Rice Yield Gap in the Asia-Pacific Region*. Food and Agriculture Organization of the United Nation, Regional Office for Asia and Pacific, Bangkok, Thailand.

PGRC (1999). *Characterization Catalogue on Rice (Orysa sativa L.) Germplasm*. Plant Genetic Resources Centre, Sri Lanka.

Pongprayoon W., Tisarum R., Theerawittaya C. & Cha-um S. (2019). Evaluation and clustering on salt-tolerant ability in rice genotypes (*Oryza sativa* L. subsp. indica) using multivariate physiological indices. *Physiology and Molecular Biology of Plants* **25**: 473–483. DOI: https://doi.org/10.1007/s12298-018-00636-2

Pradeepika N.G.J., Ranawake A.L. & Wanniarachchi S.D. (2014). *Screening Traditional Rice Cultivars for Salinity Tolerance at Vegetative Stage*. 11th Academic Sessions, University of Ruhuna, Sri Lanka.

Pradheeban L., Nissanka S.P., Suriyagoda L.D.B., Agri I.J. & Agri R. (2015). Screening commonly cultivated rice cultivars in Sri Lanka with special reference to Jaffna for salt tolerance at seedling stage under hydroponics. *International Journal of Agronomy and Agricultural Research* **7**: 1–13.

Pradheeban L., Nissanka N.A.A.S.P. & Suriyagoda L.D.B. (2014). Clustering of rice (*Oryza sativa* L.) varieties cultivated in Jaffna District of Sri Lanka based on salt tolerance during germination and seedling stages. *Tropical Agricultural Research* **25**(3): 358 – 375.

Puteh A. & Mondal M. (2015). Salinity effect on dry mass partitioning in different plant parts and ion uptake in leaves of rice mutants. *Journal of Environmental Science and Natural. Resources* **6**: 239–245.
DOI: https://doi.org/10.3329/jesnr.v6i1.22073

Puvanitha S. & Mahendran S., (2017). Effect of salinity on plant height, shoot and root dry weight of selected rice cultivars. *Scholars Journal of Agriculture and Veterinary Sciences* **4**(4): 126–131.
DOI: https://doi.org/10.13140/RG.2.2.10540.72322

Rad H.E., Aref F., Rezaei M., Amiri E. & Khaledian M.R. (2011). The effects of salinity at different growth stages on rice yield. *Ecology, Environment and Conservation* **17**: 455–462.

Ranawake A.L. & Dahanayake N. (2012). Understanding abiotic stress tolerant levels and mechanisms in some traditional rice cultivars in Sri Lanka. *9th Academic Session,* University of Ruhuna, Sri Lanka.

Ranawake A.L., Amarasinghe U.G.S. & Senanayake S.G.J.N. (2014). Submergence tolerance of some modern rice cultivars at seedling and vegetative stages. *Journal of Crop Weed* **10**: 240–247.

Ranawake A.L., Rodrigo U.T.D. & Senanayake S.G.J.N. (2013). Revealing effect of selected agrochemicals on salinity stress tolerance of rice cultivars at seedling stage. *Journal of Crop Weed* **9**: 57–60.

Rasel M., Tahjib-Ul-Arif M., Hossain M.A., Hassan L., Farzana S. & Brestic M. (2021). Screening of salt-tolerant rice landraces by seedling stage phenotyping and dissecting biochemical determinants of tolerance mechanism. *Journal of Plant Growth Regulators* **40**: 1853–1868.
DOI: https://doi.org/10.1007/s00344-020-10235-9

Ravikiran K.T., Krishnamurthy S.L., Warraich A.S. & Sharma P.C. (2018). Diversity and haplotypes of rice genotypes for seedling stage salinity tolerance analyzed through morpho-physiological and SSR markers. *Field Crop Research* **220**: 10–18.
DOI: https://doi.org/10.1016/j.fcr.2017.04.006

Raza S. Shereen A., Mumtaz S., Khan M.A. & Solangi S. (2005). Salinity effects on seedling growth and yield components of different inbred rice lines. *Pakistan Journal of Botany* **37**(1): 131–139.

Razzaq A., Ali A., Bin Safdar L., Zafar M.M., Rui Y., Shakeel A., Shaukat A., Ashraf M., Gong W. & Yuan Y. (2020). Salt stress induces physiochemical alterations in rice grain composition and quality. *Journal of Food Science* **85**(1): 14–20.
DOI: https://doi.org/10.1111/1750-3841.14983

Razzaque M.A., Talukder N.M., Islam M.S., Bhadra A.K. & Dutta R.K. (2009). The effect of salinity on morphological characteristics of seven rice (*Oryza sativa*) genotypes differing in salt tolerance. *Pakistan Journal Biological Science* **12**(5): 406–412.
DOI: https://doi.org/10.3923/pjbs.2009.406.412

Rengasamy P. (2016). Soil Salinization. In: *Oxford Research Encyclopedia of Environmental Science*. Oxford University Press, UK.
DOI:https://doi.org/10.1093/acrefore/9780199389414.013.65

Rhoades J.D. (2016). Drainage for salinity control. In: *Drainage for Agriculture* (ed. J. Schilfgaarde), pp 433–468.
DOI: https://doi.org/10.2134/agronmonogr17.c21

RRDI (2018). *Recommended Rice Varieties in Sri Lanka (1958–2016)*. Rice Research and Development Institute, Sri Lanka.

Sakina A., Ahmed I., Shahzad A., Iqbal M. & Asif M. (2016). Genetic variation for salinity tolerance in Pakistani rice (*Oryza sativa* L.) germplasm. *Journal of Agronomy and Crop Science* **202**: 25–36.
DOI: https://doi.org/10.1111/jac.12117

Sampangi-Ramaiah *et al*. (2020). An endophyte from salt-adapted Pokkali rice confers salt-tolerance to a salt-sensitive rice variety and targets a unique pattern of genes in its new host. *Science Report* **10**: 3237 (2020)
DOI: https://doi.org/10.1038/s41598-020-59998-x

SAS Institute Inc. (2000). SAS Online Doc, version 8.

Senanayake R.M.N.H., Herath H.M.V.G., Wickramesinghe I.P., Udawela U.A.K.S. & Sirisena D.N. (2017). Phenotypic screening of rice varieties for tolerant to salt stress at seed germination, seedling and maturity stages. *Tropical Agriculture Research* **29**(1): 90–100.
DOI: https://doi.org/10.4038/tar.v29i1.8300

Shereen A., Mumtaz S., Raza S., Khan M.A. & Solangi S. (2005). Salinity effects on seedling growth and yield components of different inbred rice lines. *Pakistan Journal of Botany* **37**: 131–139.

Singam K., Juntawong N., Cha-Um S. & Kirdmanee C. (2011). Salt stress induced ion accumulation, ion homeostasis, membrane injury and sugar contents in salt-sensitive rice (*Oryza sativa* L. spp. indica) roots under iso osmotic conditions. *African Journal of Biotechnology* **10**: 1340–1346.

Singh A. & Sengar R.S. (2014). Salinity stress in rice: An overview. *Plant Archives* **14**(20): 643–648.

Singh S., Mackill D.J. & Ismail A.M. (2014). Physiological basis of tolerance to complete submergence in rice involves genetic factors in addition to the SUB1 gene. *AoB Plants* **6**: 1–20.
DOI: https://doi.org/10.1093/aobpla/plu060

Sirisena D.N. & Wanigasundera W.A.D.P. (2021). Blog 165: Soil salinity in paddy fields of Sri Lanka and best practices to avoid crop failures due to soil salinity. *Agriculture Extension in South Asia*. Centre for Research on Innovation and Science Policy (CRISP), India

Souleymane O., Nartey E., Manneh B., Danquah E. & Ofori K. (2015). Phenotypic variability of 20 rice genotypes under salt stress. *International Journal of Plant Breeding and Genetics* **10**: 45–51.
DOI: https://doi.org/10.3923/ijpbg.2016.45.51

Suriyan C.U., Supaibulwattana K. & Kirdmanee C. (2009). Comparative effects of salt stress and extreme pH stress combined on glycinebetaine accumulation, photosynthetic abilities and growth characters of two rice genotypes. *Rice Science* **16**(4): 274–282.

Tabassum R., Tahjib-Ul-Arif, Hasanuzzaman, Sohag A.A.M., Islam M.S., Shafi S.M.S.H., Islam M.M. & Hassan L. (2021). Screening salt-tolerant rice at the seedling and reproductive stages: An effective and reliable approach. *Environmental and Experimental Botany* **192**: 104629. DOI: https://doi.org/10.1016/j.envexpbot.2021.104629

Thiruchelvam S. & Pathmarajah S. (1999). An economic analysis of salinity problems in the Mahaweli river system H irrigation scheme in Sri Lanka. *EEPSEA Research Report rr1999082*. Economy and Environment Program for Southeast Asia (EEPSEA), International Center for Living Aquatic Resources Management, Inc., Malaysia.

Ullah A., Bano A. & Khan N. (2021). Climate change and salinity effects on crops and chemical communication between plants and plant growth-promoting microorganisms under stress. *Frontiers in Sustainable Food Systems* **5**: 1–16. DOI: https://doi.org/10.3389/fsufs.2021.618092

Umar S. (2016). Awareness, manifestation and information sources on climate change among irrigation farmers in Katsina State, Nigeria. *Journal of Agriculture and Veterinary Science* **3**: 37–41. DOI: https://doi.org/10.21276/sjavs

USDA (2018). *Food Data Central*. Department of Agriculture, Agriculture Research Service. United States.

Van der Zee S.E.A.T.M., Stofberg S.F., Yang X., Liu Y., Islam M.N. & Hu Y.F. (2017). Irrigation and drainage in agriculture: a salinity and environmental perspective. In: *Current Perspectives of Irrigation and Drainage*. IntechOpen Limited, London, UK. DOI: https://doi.org/10.5772/66046

Vasudevan K., Vera Cruz C.M., Gruissem W. & Bhullar N.K. (2014). Large scale germplasm screening for identification of novel rice blast resistance sources. *Frontiers in Plant Science* **5**: 505. DOI: https://doi.org/10.3389/fpls.2014.00505

Vibhuti, Shahi C., Bargali K. & Bargali S.S. (2015). Seed germination and seedling growth parameters of rice (*Oryza sativa*) varieties as affected by salt and water stress. *Indian Journal of Agricultural Science* **85**: 102–108.

Vidal J. (2019). Irrigation, drought, sea level rise and more are causing salt to build up in soils around the world. What can we do? Available at *https://www.eco-business.com/news/irrigation-drought-sea-level-rise-and-more-are-causing-salt-to-build-up-in-soils-around-the-world-what-can-we-do/*

Wijerathna Y.M.A.M., Kottearachchi N.S., Gimhani D.R. & Sirisena D.N. (2011). Sri Lankan fragrant rice (*Oryza Sativa* L.) varieties are associated with decreased salt tolerance. *Proceedings of 11th Agriculture Research Symposium*. Wayamba University Sri Lanka, pp. 51–55.

Yoshida S., Forno D.A., Cock J.H. & Gomez K. (1972). *Laboratory Manual for Physiological Studies of Rice*, pp. 53–57, 2nd edition, International Rice Research Institute, Los Baños, Philippines.

Zeng L., Shannon M.C. & Lesch S.M. (2001). Timing of salinity stress affects rice growth and yield components. *Agriculture Water Management* **48**: 191–206. DOI: https://doi.org/10.1016/S0378-3774(00)00146-3

Zhang R., Hussain S., Wang Y., Liu Y., Li Q., Chen Y., Wei H., Gao P. & Dai Q. (2021). Comprehensive evaluation of salt tolerance in rice (*Oryza sativa* L.) germplasm at the germination stage. *Agronomy* **11**(8): 1569. DOI: https://doi.org/10.3390/agronomy11081569

Supplementary files

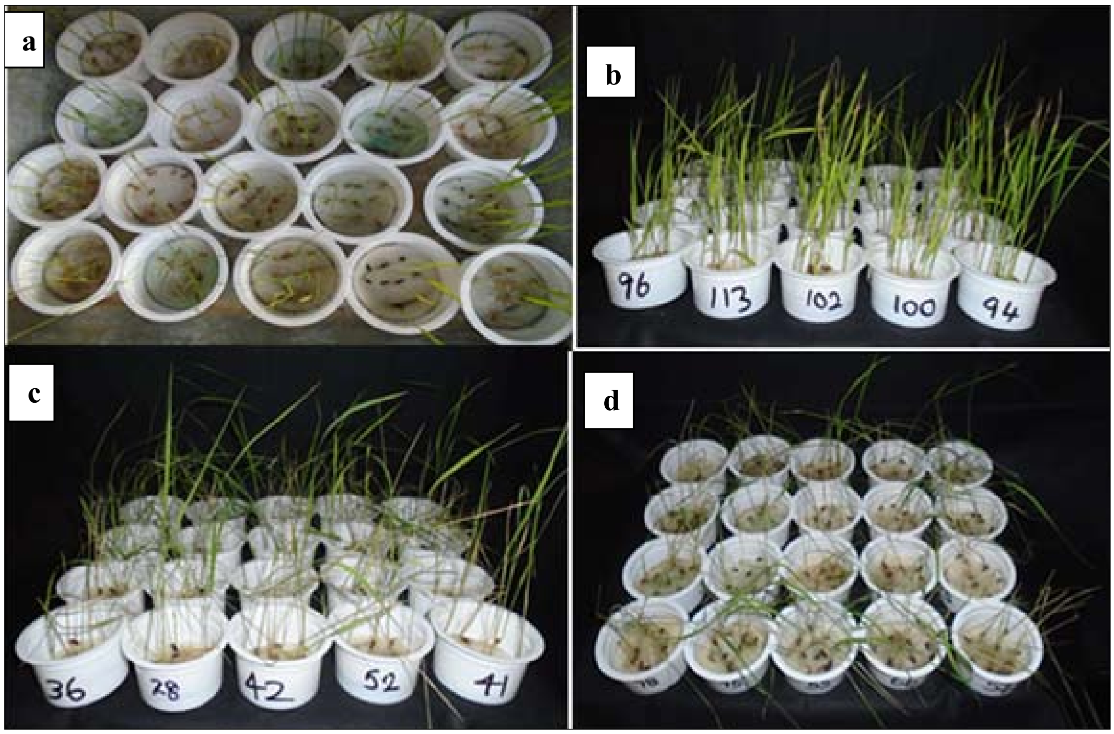

Supplementary figure 1: Some different stages of testing for salinity tolerance at the seedling stage
(a): Starting stage for salinity treatment, (b): Control seedlings after sixteen days, (c): Seedlings after ten days in salinity treatment, (d) Seedlings after sixteen days in salinity treatment.

Supplementary table I: Experimental conditions used for salinity tolerant studies in rice

Materials	Tolerant genotypes	St	Salinity stress	Results	Parameters	References
Nine thousand rice germplasm	*IR29* (T) *FL478* (T)	S	EC ~10 dSm^{-1}	Identified 241 salinity-tolerant rice lines	Thirty qualitative and quantitative traits	(Krishnamurthy *et al.,* 2022)
Five rice cultivars		S	Hydroponic culture with a deep flow technique (DFT)	Hydroponic DFT is a screening technique	Agronomic characters	(Arifuddin *et al.*, 2021)
Seventy-four rice lines		S,R	Pot culture with sand six dSm^{-1} and 12 dSm^{-1}	Tolerant 13 lines- with FED 473 and IR85427	Shoot and root morpho-physiological traits	(Kakar *et al*., 2019)
Twenty-one improved rice varieties.		R	Germination, seedling and maturity stages in Petri dishes, in a hydroponic system and soil-filled pots, respectively.	At the germination stage, *Bg406* and *Pokkali* (HT) At seedling *Pokkali* (HT) *At402, Bg369* and *At354* (T)	Seed viability, growth performance, plant survival%, growth performance and grain yield reduction at maturity	(Senanayake *et al*., 2017)
Two hundred and thirty-one rice genotypes	*FL478* *NSIC Rc222* (S)	S	IRRI standard evaluation system EC ~12 dSm^{-1}	Tolerant -1.73% Moderately tolerant-18.18%	Plant damage%	(Mondal and Borromeo, 2016)
Sixteen traditional rice cultivars		G S	A Petri dish method- control, 50-, 100- and 150-mM Na^{+}	Fifteen at germination and twenty-eight at the seedling stage were salinity tolerant.		(Sakina *et al*., 2016)
Twenty germplasm-traditional and improves.	*Pokkali*		12 dS/m saline stress and five SSR markers located	*Goda Wee, At354,* and *Al Wee* varieties were highly salinity tolerant	Weighted indicator, Salinity survival index	(Dahanayaka *et al.,* 2015)
Twenty traditional rice accessions	*At354* (T) *Pokkali*	S	A hydroponic system with *Yoshida* solution EC~10 dSm^{-1}	*Sudu-Karayal* recorded the highest survival percentage	Green plant height and survival percentage	(Pradeepika *et al*., 2014)
Pokkali, Nona-Bokra and *Bicol, IR29*	*Pokkali, Nona-Bokra* and *Bicol* (T), *IR29* (S)	S	The non-destructive image-based method	The success of the technique	Total shoot area and senescent shoot area, using images.	(Hairmansis *et al*., 2014)
Five Malaysian rice varieties	*Pokkali*	V	Pot experiments EC~4-, 8-,12 dSm^{-1}	Two Malaysia varieties, *MR211* and *MR232* performed better	Plant height, leaf area, and dry matter accumulation	(Hakim *et al*., 2014a)
Japonica rice-Hyogokithanishiki and Indica rice Hokuriku-142 (Hokuriku)		S	EC solution method and MS (Murashige and Skoog) medium method	*Hyogokithanishiki* is more salt tolerant than *Hokuriku*	Green shoot length, dry matter weight and root length	(Ranawake and Nakamura, 2013)

St: Growth stage (T): Tolerant check, (S): Sensitive check, S: Seedling stage, R: Reproductive stage, G: Germination stage V: Vegetative stage, M: Tillering, panicle-initiation, heading, and harvesting stages, RILs: Recombinant inbred lines

Continued on page *dcxiv* -

- continued from page - *dcxiii*

Materials	Tolerant genotypes	St	Salinity stress	Results	Parameters	References
Nine rice lines			EC ~5 dSm^{-1}salinized solution and let them grow in 8 days.	*Bg 250, Bg 352 and Bg 379/2* are better than others	Plant height, fresh and dry weight, survival%	(Ranawake *et al*., 2013)
Twenty-improved rice varieties			Seedling stage	*At402 (89%)*	Survival%	(Weragodavidana, *et al.*, 2012)
Eight varieties	*At354* and *Pokkali*	S	Hydroponic culture, 100 mM Na^+	*At354,* salt tolerant than *Pokkali*,	Plant growth: Leaf width fresh and dry weight, shoot and root Na^+ concentration.	(de Costa *et al*., 2012b)
One hundred and sixty-three RILs			EC~5 dSm^{-1} salinized	*Herath* and *Ranhiriyal* were salinity tolerant	Plant survival percentages	(Ranawake and Dahanayake, 2012)
Eight improved rice cultivars		S	A 50 mM NaCl and 0.2 trisodium-8-hydroxy-1,3,6-ppyrene-tri sulphonacacids (PTS)		Seedling survival%, Na^+% in shoots	(Faiyue *et a*l., 2012)
Thirty-three traditional rice cultivars		M	EC ~2-, 4-, 6-, and 8 dSm^{-1}	Salinity sensitivity among different growth stages	Plant height, biomass, harvest index, yield and yield components	(Faiyue *et al*., 2012)
Thirty rice genotypes	*Pokkali*	SR	Three levels of NaCl 0-, 60-, 100 mM at reproductive stage, EC ~12 dSm^{-1} at seedling stage		Plant growth and yield components	(Mohammadi-Nejad *et al*., 2010)
	Nona-Bokra and *Pokkali,* and *IR28* (S)*IR35657-33-2* (S)	S,R	Under controlled conditions by using the solution and pot culture techniques at EC ~12 dSm^{-1}		Shoot -length, -Na^+, Ca^{++} content and -dry weight	(Akbar *et al.,* 2008)
IR55178	*Pokkali, Nona-Bokra* and *Bicol (T) IR29* (S)	S	Primers		DNA	(Xie *et al*., 2000)
Five Malaysian rice varieties	*Pokkali*	S, VR	Standard evaluation system EC ~6 dSm^{-1} and EC ~12 dSm^{-1}	Tolerant level/score	Visual scoring system	(Gregorio *et al.,* 1997)
		S	Silica gravel culture 50-200 mol m^{-3} NaCI	Technique validation	Shoot fresh and dry weights, mortality%	(Aslam *et al.,* 1993)
		GS	EC ~10-, 15-, and 20 dSm^{-1} (5:1 NaCl and $CaCl_2$ solution)	One hundred and thirteen fairly tolerant genotypes	Germination index dry seedling weight	(Islam and Karim, 1970)

St: Growth stage (T): Tolerant check, (S): Sensitive check, S: Seedling stage, R: Reproductive stage, G: Germination stage V: Vegetative stage, M: Tillering, panicle-initiation, heading, and harvesting stages, RILs: Recombinant inbred lines

J.Natn.Sci.Foundation Sri Lanka 2023 51 (4): 615 - 628
DOI: http://dx.doi.org/10.4038/jnsfsr.v51i4.11331

RESEARCH ARTICLE

Structural Engineering

A kurtosis-based parameter for classifying elliptical hollow sections under bending

KIU Nanayakkara* **and WPS Dias**
Department of Civil Engineering, Faculty of Engineering, University of Moratuwa, Moratuwa, Sri Lanka.

Submitted: 19 August 2022; Revised: 19 June 2023; Accepted: 28 July 2023

Abstract: A novel section parameter termed *normalized excess kurtosis of a section*, inspired by the same parameter used in probability distributions, is introduced to characterize the rotation capacity of a hollow section under bending. The proposed normalization accounts for variations in yield stress and Young's modulus too. A linear relationship is observed between rotation capacity and the normalized excess kurtosis of circular hollow sections (CHS), rectangular/square hollow sections (RHS) and elliptical/oval hollow sections (EHS), under constant and linearly varying moment conditions, based on experimental and finite element model (FEM) data. It is found that, the rotation capacity variation of hollow sections is better explained by using normalized excess kurtosis than by the conventional section slenderness. The gradient of the above linear relationship varies with the section type and provides an estimate of the rotation capacity of a hollow section with a known shape and aspect ratio. It also provides insights into the section classification of EHS sections, with aspect ratios closer to unity ($0.67 < a/b < 1.5$) being suitable for an equivalent diameter approach and those with aspect ratios further from unity ($a/b < 0.5$ and $a/b > 2.0$) for an equivalent RHS approach. The difference between the moment and rotation capacities of linearly varying moment conditions (3-point bending) and constant moment conditions (4-point bending) is also elucidated.

Keywords: Bending of beams, elliptical hollow sections, kurtosis, rotation capacity, slenderness.

INTRODUCTION

Classification of steel hollow sections

Steel tubular sections are used extensively in the construction industry, from projects such as the Sydney Olympic Stadium to steel framed houses in North America, and in scale from space trusses and frames to wind turbine towers. Along with the rapid rise in usage, research into the same has also picked up during the past couple of decades.

Section classification is central to the design of steel elements (Chen *et al*., 2013). Most of the major design guidelines classify sections into three classes: (i) Class 1, capable of reaching and exceeding full plastic capacity, (ii) Class 2, capable of reaching yield stress at extreme fibres but not full plasticisation, and (iii) Class 3, failing in local collapse before yielding occurs. Slenderness parameters based on section geometry and material yield strength are used for this classification.

However, the existing design codes do not provide guidelines on classification of EHS, although they are now being used extensively in construction. Haque *et al*. (2012) propose an equivalent RHS approach for the

* Corresponding author (isuru_nanayakkara@live.com; https://orcid.org/0000-0003-2630-7724)

classification and design of EHS in axial compression and bending, where EHS sections are transformed to an equivalent RHS and section classification based on RHS slenderness limits. On the other hand, Theofanous *et al*. (2009), Zhu & Wilkinson (2007), Gardner & Chan (2006) and Gardner & Chan (2007) have successfully used an equivalent diameter approach where an EHS is converted to an equivalent CHS.

Furthermore, current codified section classifications use section geometry and material strength as the only input variables, although other parameters have been observed to influence the rotation capacity of a beam and hence the section classification. Sherman (1976) observes that moment gradient and stiffness due to end fixities influence the rotation capacity; and Wang *et al*. (2016) identify aspect ratio, strain hardening and moment gradient as parameters influencing the rotation capacity of RHS. Seif & Schafer (2010) redefine the section slenderness parameter to take web-flange interaction into account.

Classification of sections for plastic frame analysis (*i.e.*, class 1 limit) is based on the available rotation capacity of a beam of uniform section exceeding some pre-defined plastic rotation capacity requirement, the value of which is not clearly intimated to users in current codes of practice. It is the authors' view that a continuous relationship between rotation capacity and section geometry, as opposed to a single point value, allows for better utilization of the capacity available in a beam of a uniform hollow section (*i.e.*, to optimize the section geometry). To maintain the simplicity expected of a design process, it is prudent to relate the rotation capacity to a simple section parameter.

Three primary methods have been used to predict the rotation capacity of beams: (i) empirical methods (*e.g.*, Kato, 1988; Castaldo *et al*., 2017), (ii) analytical solutions, and (iii) soft computing methods (*e.g.*, D'Aniello *et al*., 2015). Empirical methods are hindered by limitations of the data set while analytical solutions face the trade-off between the need for simplicity in design usage and the need to account for complex behaviour. D'Aniello *et al*. (2015) use genetic programming and neural networks to build a predictive model which is both efficient and not influenced by simplifying assumptions; however the model will only be as good as the quality and the breadth of the training set.

The current paper introduces a new section parameter with a view to presenting a simplified relationship with rotation capacity, and to clarify the quandary in classifying EHS as either CHS or RHS. We present a novel section parameter based on the statistical parameter kurtosis. Experimental and finite element model (FEM) data on CHS, EHS/OHS and RHS are studied on the basis of this novel parameter. In particular, we use the parameter to shed light on the dilemma of the section classification for EHS. Finally, we note further insights that can be provided by this novel parameter and the advantages thereof.

Rotation capacity and kurtosis

In mechanics, the zeroth raw moment of area of a cross section gives the area of the section; the first raw moment of area of the cross section as a fraction of the area gives the distance to the centroid; and the second raw moment of area as a fraction of the area yields the well-known definition of radius of gyration.

Moments of area are parameters that appear in both statistics and mechanics. The first order raw moment, second order central moment, third order standardized moment and fourth order standardized moment of a probability distribution function are called the mean, variance, skewness, and kurtosis of the probability distribution, respectively.

Kurtosis is the most misunderstood statistical parameter of the four mentioned above and the hardest to grapple with (DeCarlo, 1997). Kurtosis is an indicator of the shape of a statistical distribution. Kurtosis values for some common distributions are 3.0 for a normal distribution, 1.8 for a uniform distribution of unit variance and 4.2 for a logistic distribution. As DeCarlo (1997) notes, kurtosis should be clearly distinguished from variance and "represents a movement of mass that does not affect the variance." When applied to hollow cross sections, excess kurtosis (see below) acts as a parameter representing the wall thickness of the section, with variance (hence the stress distribution) and area of section being made irrelevant.

Kurtosis of a section (*Kt*) is defined as in equation 1; where I_{x^4} is the fourth moment of area about the x-x axis, which is chosen to coincide with the axis of bending; *A* is the gross cross-sectional area and r_{xx} is the radius of gyration of the cross-section with reference to the x-x axis (*i.e.*, the axis of bending).

$$Kt = \frac{I_{x^4}}{A\, r_{xx}{}^4} \qquad \text{...(1)}$$

where $I_{x^4} = \int_A y^4 \, dA$

The bimodal reference kurtosis (Kt_b) is defined as the kurtosis of the section at an infinitesimally small wall thickness *(t)* (see equation 2). The physical representation of this condition for a hollow section is the concentration of the total area of section at infinitesimally small points at either end along the y-axis; hence a bimodality.

$$Kt_b = \lim_{t \to 0} \frac{I_{x^4}}{A\, r_{xx}{}^4} \qquad \text{...(2)}$$

The parameter suggested for the classification of hollow steel sections is $\widehat{Kt}$– *i.e.*, the normalized excess kurtosis of a section (see equation 3); or kurtosis in excess of a pure bimodal distribution, normalized with respect to yield strength (f_y) and modulus of elasticity (E) of the material.

$$\widehat{Kt} = (Kt - Kt_b)\left(\frac{235}{f_y}\right)^{n_1}\left(\frac{E}{210}\right)^{n_2} \qquad \text{...(3)}$$

with f_y in MPa and E in GPa.

The reference values of yield strength (f_y) and modulus of elasticity (E) are chosen as 235 MPa and 210 GPa respectively, based on EN 1993-1-1 (2005). The normalization with f_y as denominator and E as numerator follows EN 1993-1-4 (2006) and EN 1993-1-12 (2007). The values n_1 and n_2 are chosen based on the section type (CHS, RHS, or EHS) and loading pattern (constant moment or linearly varying moment).

The concept of excess kurtosis over and above the reference bimodal kurtosis (which is related to thickness concentration at the bimodal points) gives us a parameter related to the wall thickness of the section. In essence, this simplifies the buckling of a hollow section to a single plate buckling problem. It is important to recognize that excess kurtosis has this theoretical basis, and is not merely a parameter that has a fortuitous relationship with rotation capacity. However, the parameter does not take into account the transverse curvature along the wall of the section, which must be accounted for by section shapes and aspect ratios.

Table 1 and Table 2 summarize section slenderness and excess kurtosis values for a series of CHS and RHS. As section slenderness decreases, excess kurtosis increases, as does the rotation capacity. Also, as indicated above, sections with larger thickness have larger excess kurtosis values, provided other section properties are identical. However, a CHS of diameter 150 mm and wall thickness 2 mm gives an excess kurtosis of 365 $\times 10^{-6}$ whereas RHS of section depth 150 mm and same wall thickness gives excess kurtosis values of range around 3,500 to 6,000 $\times\ 10^{-6}$. This dependence on shape and aspect ratio will become very evident in the ensuing analysis of data.

Table 1: Excess kurtosis value for typical CHS of different outer diameter and thickness.

Outer diameter (*D* in mm)	Wall thickness (*t* in mm)	Section slenderness (*D/t*)	Excess kurtosis ($Kt - Kt_b$ in 10^{-3})
300	2	150.0	0.09
150	2	75.0	0.37
150	4	37.5	1.50

Table 2: Excess kurtosis value for typical RHS of different section breadth, depth and thickness.

Section breadth (*B* in mm)	Section height (*D* in mm)	Wall thickness (*t* in mm)	Section slenderness *B/t*	*D/t*	Excess kurtosis ($Kt - Kt_b$ in 10^{-3})
50	150	1.25	40.0	120.0	3.57
75	150	2.00	37.5	75.0	3.54
50	150	2.00	25.0	75.0	5.94
75	150	4.00	18.8	37.5	8.08

Table 3: Summary of data sources used in the current study

Author(s)	Year	Section type	Experiments / FEM	No. tests
Jiao & Zhao	2004	CHS	4-point bending test (4PB)	12
			Pure bending test	
Guo *et al.*	2013	CHS	4-point bending test	8
Elchalakani *et al.*	2002	CHS	Pure bending test	12
Elchalakani *et al.*	2002	CHS	Pure bending test	9
Kiyamaz	2005	CHS	4-point bending	8
Sedlacek *et al.*	1998	CHS	4-point bending	61
		RHS	3-point bending (only CHS)	18
Sherman	1976	CHS	4-point bending test Cantilever tests	28
Sherman	1986	CHS	Constant moment tests	
			Cantilever tests	
Rasmussen & Hancock	1993	CHS	4-point bending	2
		RHS		
Zheng *et al.*	2016	CHS	4-point bending	8
		RHS		
Theofanous *et al.*	2009	EHS	3-point bending (3PB)	6
			FEM(3PB)	36
Chan & Gardner	2008	EHS	4-point bending	18
			3-point bending	
Wilkinson & Hancock	1998	RHS	4-point bending	44
Korol & Hudoba	1972	RHS	4-point bending	22
Gardner *et al*.	2006	RHS	4-point bending	6
Zhou & Young	2005	RHS	4-point bending	15
Theofanous & Gardner	2010	RHS	3-point bending	8
			FEM (3PB)	36
Huang & Young	2013	RHS	4-point bending	10
			FEM (4PB)	125
Afshan & Gardner	2013	RHS	3-point bending	8
			4-point bending	
Bock *et al.*	2015	RHS	3-point bending	9
			4-point bending	
Theofanous *et al*.	2014	RHS	3-point bending	5
Zhao *et al*.	2015	RHS	4-point bending	5
Zhao *et al*.	2016	RHS	4-point bending	2
Zhao *et al*.	2016	RHS	4-point bending	2
Wang *et al.*	2016	RHS	3-point bending	22
			4-point bending	216
			FEM (3PB/4PB)	
Su *et al.*	2014	RHS	3-point bending	22
			4-point bending	128
			FEM (3PB/4PB)	

MATERIALS AND METHODS

Data collection

Experimental and FEM data were collected from published studies by various authors (see Table 3). The data collected include tests on CHS, RHS, and EHS under both constant and linearly varying moment conditions, and covers a range of geometrical parameters, yield strengths, and material types, as summarized in Table 4.

The geometrical parameters are (i) slenderness ratios – *i.e.*, *D/t* for CHS, *B/t* for RHS and ab/t^2 for EHS; and (ii) aspect ratios – *i.e.*, *H/B* for RHS and a/b for EHS. Here, *D* is the outer diameter of a CHS; *H* and *B* are the height and breadth of an RHS; *a* and *b* are the lengths of the major and minor axes of an EHS; and *t* is the wall thickness (see Figure 1)

.

Table 4: Summary of ranges of geometrical parameters, yield strengths and materials covered in the data set.

Section type	Geometry parameter*	Parameter range	Yield strength (MPa)	Materials
CHS	*D/t*	6.2–75	190–1,398	Steel (cold formed / hot rolled), stainless steel
RHS	*B/t* *H/B*	3.6–61 1.0–6.0	139–813	Steel (cold formed/hot rolled) stainless steel (austenitic, ferritic, duplex, cold worked and annealed), aluminium
EHS	ab/t^2 *a/b*	83–655 1.0–2.0	317–441	Steel (hot rolled), stainless steel

* The corresponding dimensions are as shown in Figure 1.

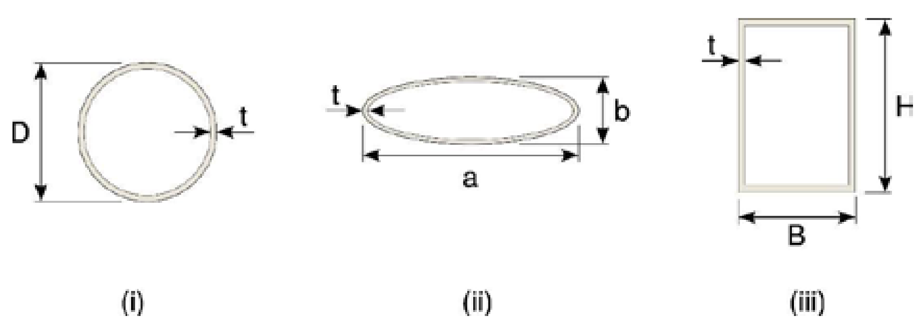

Figure 1: Dimensions of (i) circular hollow sections, (ii) elliptical hollow sections and (iii) rectangular hollow sections.

All the sources of FEM results above have used the ABAQUS software package and the S4R four node doubly curved shell element in their models. Residual stresses were not explicitly included and Theofanous *et al*. (2009) note that the yield strength values used may include this effect. Local geometric imperfections were incorporated in the FE models via the lowest elastic buckling mode shape obtained from linear eigenvalue buckling analysis with appropriate imperfection amplitudes. The imperfection amplitudes used in the above models are summarized in Table 5. Wang *et al*. (2016), Theofanous *et al*. (2014) and Theofanous & Gardner (2010) have tested multiple imperfection amplitudes before selecting those noted in Table 5.

It was observed that the peak moment is not significantly influenced by the imperfections (*i.e.*, mean errors of about 5% in comparison to experimental results) but the rotation capacity is. The amplitudes selected by Wang *et al*. (2016), Theofanous *et al*. (2009) and Theofanous & Gardner (2010) resulted in mean errors of -6%, + 10% and +12% respectively.

Huang & Young (2019) and Su *et al*. (2014) have not reported corresponding error values. Note that these are not necessarily the smallest average errors observed for rotation capacities in the respective studies, since the imperfection amplitudes had been selected to minimize the errors for the peak moments.

Table 5: Imperfection amplitudes used in FEM models referenced in this study

Author(s)	Imperfection amplitude	Notes
Wang *et al*. (2016)	*t*/50	
Theofanous *et al*. (2009)	*t*/10	
Theofanous & Gardner (2010)	$0.023(\sigma_{0.2}/\sigma_{cr})t$	Dawson and Walker solution as adapted by Theofanous & Gardner (2010)
Huang & Young (2013)	*t*/10	Average measured local imperfection was t/11
Su *et al*. (2014)	0.2 mm	This is the average measured local imperfection

Rotation capacity

Two different ways are used to define the rotation capacity. The two definitions—R_1 and R_2—are as presented in equation 4 and equation 5, where κ_p and κ_u are bending curvatures corresponding to full plastic moment (M_p) and ultimate moment (M_u) while $\vartheta_y, \vartheta_p, \vartheta_{max}$ and ϑ_u are bending rotations corresponding to moment at onset of yield (M_y), full plastic moment (M_p), maximum moment (M_{max}) and the ultimate moment (M_u) as shown in the moment-rotation (curvature) graph in Figure 2.

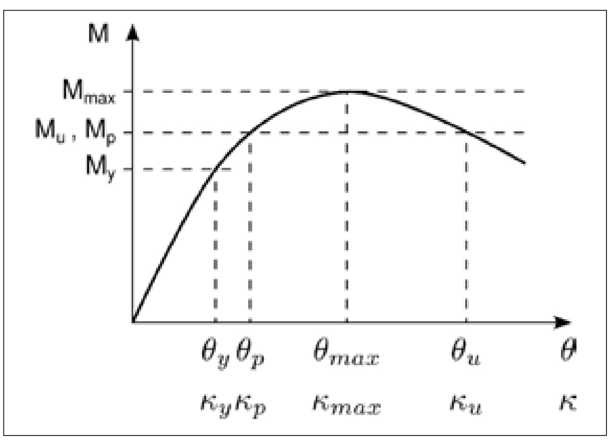

Figure 2: Typical moment - rotation (curvature) plot with reference notation for equations 4 and 5.

$$R_1 = \begin{cases} \frac{\kappa_u}{\kappa_p} - 1, & curvature\ measured \\ \frac{\vartheta_u}{\vartheta_p} - 1, & rotation\ measured \end{cases} \quad ...(4)$$

$$R_2 = \frac{\vartheta_{max}}{\vartheta_y} - 1 \quad ..(5)$$

In the equation 4 definition, the choice of curvature or rotation is based on the method of measuring deformation; curvature is primarily used in constant moment tests, and rotation in tests with linearly varying moment.

The equation 5 definition based on Sherman (1976) normalizes the plastic rotation by elastic rotation at first yield (ϑ_y) as opposed to elastic rotation at full plastic moment (ϑ_p) used in the equation 4 definition. Although the numerical values are comparable, the data presented using the equation 5 definition are omitted for the sake of data consistency. Furthermore, the equation 4 definition is superior in that the measurement is of the rotation while maintaining full plastic moment, which is consistent with the definition of Class 2 sections under section classification in EN 1993-1-1 (2005).

RESULTS AND DISCUSSION

Study of experimental and FEM data

The behaviour of rotation capacity against normalized excess kurtosis for CHS, RHS, and EHS under linearly varying moment was studied (CHS - Figure 3, RHS - Figure 4, EHS - Figure 5). Data points considered are from experimental data, complemented by FEM data where available.

Only experimental data were available for CHS while both experimental and FEM data were available for the study of RHS and EHS. Some experimental data were available from constant moment tests on EHS; however only four valid data points were available for the trendline and this was deemed too few for any reasonably conclusive study. As such this study is focused on linearly varying moment conditions. However, the authors would anticipate a similar behaviour under the constant moment condition, as explained later.

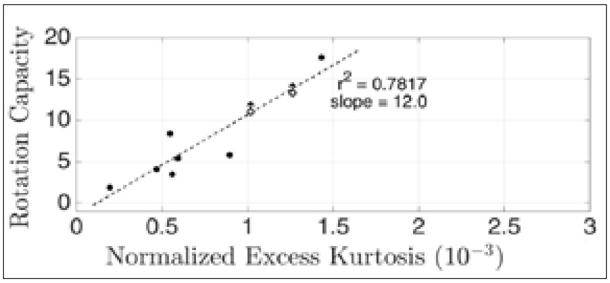

Figure 3: Rotation capacity vs normalized excess kurtosis of experimental data from linearly varying moment tests on CHS. The dashed line indicates the trendline. Markers with arrows indicate that tests stopped prematurely (*i.e.*, full rotation capacity not achieved).

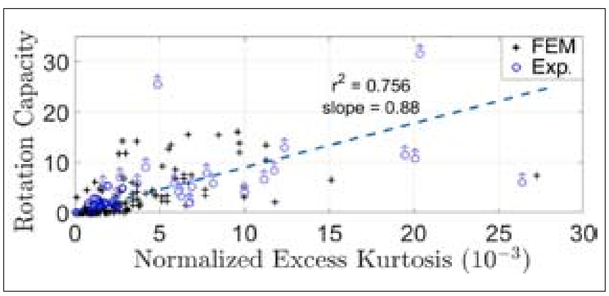

Figure 4: Rotation capacity vs normalized excess kurtosis of experimental and FEM data from linearly varying moment tests on RHS. Dashed line indicates the linear trend of the combined data. Markers with arrows indicate tests stopped prematurely (*i.e.*, full rotation capacity not achieved).

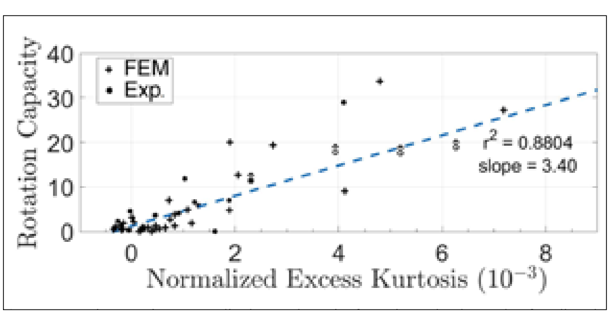

Figure 5: Rotation capacity vs normalized excess kurtosis of experimental and FEM data from linearly varying moment tests on EHS. Dashed line indicates the linear trend of the combined data. Markers with arrows indicate tests stopped prematurely (*i.e.*, full rotation capacity not achieved).

For CHS, $n_1 = n_2 = 2.2$ was used and for RHS, $n_1 = n_2 = 1.0$. The value for CHS is based on the semi-empirical equation derived in the Appendix – under the selected value the rotation capacity vs normalized excess kurtosis relationship is insensitive to yield strength and modulus of elasticity. A similar semi-empirical equation for RHS gives a variable function for n_1 and n_2, but a constant value of unity is chosen for simplicity. This value gives the highest coefficient of correlation for the rotation capacity versus normalized excess kurtosis linear regression line. For EHS, $n_1 = n_2 = 2.2$ was borrowed from CHS since the semi-empirical equation cannot be derived, with no reliable base curve being available for EHS in the current literature. It is noted that using $n_1 = n_2 = 1.0$ —the value used for RHS—would result in the same general conclusions, albeit different slopes for excess kurtosis-rotation capacity relationship of EHS.

The linear trendline was plotted using the data points, subject to the data qualification processes described in the following paragraphs. A robust least-squares fitting process with bisquare weights was used to minimize the effect of outliers.

In both the experimental and FEM data sets there were several tests in which the sections did not reach the plastic moment capacity, and consequently a rotation capacity of zero was recorded. At the other extreme there were points where the full rotation capacity was not achieved due to limitations in the experimental set up: *e.g.*, limits on loading and/or deflection measurements and/or limitations on the loading apparatus. The latter values are noted in the graphs with an upward arrow marker to indicate that the actual rotation capacities would be higher than the recorded value. Both these types of data are ignored in trendlines.

It was also observed that rotation capacities (for both experimental and FEM data) start to drop from the linear trend at very high $\widehat{Kt}$. These rotations could be low due to two reasons. At very high $\widehat{Kt}$, very high rotation capacities are expected. This in turn means that deflections may no longer satisfy small deformation assumptions, thus invalidating curvature calculations. Furthermore, at higher deflections the ductility requirement of the material may have been exceeded, possibly leading to failure of material by reaching the ultimate strain. As such the data points beyond $\widehat{Kt} = 3 \times 10^{-3}$ in CHS and 10×10^{-3} in RHS are ignored in the trendlines. In any case these sections would be having rotation capacities well beyond the rotation capacity demands for common structural engineering applications, therefore having no impact on the usage of the simple linear relationship for the purpose of section classification.

For both RHS and EHS (Figures 4 and 5 respectively), experimental data were observed to be consistent with the FEM data even though the data came from multiple sources. FEM data were not available for comparison in CHS data.

For all three section types studied, a monotonic trend was observed, with rotation capacity increasing as normalized excess kurtosis increases. At the same time, a considerable scatter is observed in the data.

A primary reason for the scatter observed in the data is the geometrical imperfections in the members. The FE model by Theofanous *et al*. (2009) shows that omitting imperfections in the model would result in the overestimation of rotation capacity by 38% on average (compared to experimental results used for the verification of the corresponding FE model); and using the measured imperfections would underestimate the rotation capacity by 8%. Furthermore, individual errors in the range of 67% were observed.

Still higher discrepancies were observed in experimental results even where the same nominal section of the same material was tested under the same loading systems. Guo *et al.* (2013) observed rotation capacities of 1.2, 1.6 and 3.2 for three CHS specimens of outer diameter 300 mm, thickness 2 mm and yield strength 190 MPa; and Sherman (1986) observed rotation capacities of 5.9 and 8 for two CHS specimens of outer diameter 458 mm, thickness 10.29 mm and yield strength 341 MPa. Similarly, Theofanous *et al*. (2009) observed rotation capacities of 2.28 and 4.59 for EHS sections of nominal major and minor axes 121 mm and 76 mm, thickness 2 mm and yield strength 380 MPa.

A significant number of such discrepancies were observed in RHS sections as well. Wilkinson and Hancock (1998) observed rotation capacities of 5.9 and 0 (failure before reaching plastic moment capacity) for two RHS specimens of breadth 25 mm, depth 75 mm, thickness 2 mm and yield strength 467 MPa. They further report rotation capacities of 1.1, 1.2, 1.4 and 2.2 for a series of RHS specimens of breadth 50 mm, depth 150 mm, thickness 2.3 mm and yield strength 456 MPa. Zheng *et al*. (2016) report rotation capacities of 5.4 and >10.7 (no failure at termination of experiment) for a series of square hollow section (SHS) specimens of breadth and depth of 100 mm, thickness 3 mm and yield strength 408 MPa. The above are only a sample of individual data points that show the inherent scatter of the data and they are most likely due to the geometrical imperfections in the beams tested.

Another minor reason for the scatter is the experimental procedures followed. The data are collected from experiments conducted with varying facilities, equipment, procedures, and personnel. As such we should give due recognition to the fact that there is the possibility of inconsistencies between some data sets. Attempts to account for all minor discrepancies will lose the generality of possible conclusions. As mentioned earlier a robust least square fitting with bisquare weights was used to allow for these outliers.

The same data set was considered to study the relationship between the rotation capacity and the section slenderness as defined in EN 1993-1-1 (2005). We have compared the corresponding R-squared values under a linear regression with bisquare robust fitting (see Table 6) and found that excess kurtosis fits better to a linear relationship with rotation capacity. Note that rotation capacity increases monotonically with excess kurtosis while decreasing monotonically with section slenderness.

Since there are two section slenderness parameters for RHS – for the web and flange – the critical slenderness was considered. The critical slenderness was determined based on the section slenderness as a fraction of the corresponding upper class 2 limit on section slenderness, as given in EN 1993-1-1 (2005) – *i.e.*, 83ε and 38ε for web and flange respectively.

Table 6: Comparison of R-squared values for (i) rotation capacity vs section slenderness and (ii) rotation capacity vs excess kurtosis relationships, for linear regression with bisquare robust fitting

	Rotation capacity against	
	Section slenderness	Excess kurtosis
CHS (experimental)	0.397	0.782
RHS (experimental and FEM)	0.613	0.756

Table 7: Gradients of rotation capacity vs normalized excessive kurtosis for major axis bending of RHS under varying D/B ranges.

Nominal *D/B*	*D/B* range	Number of data points	Gradient	r^2
0.714	0.714	7	2.16	0.6312
1.00	0.8–1.0	55	2.34	0.7331
1.50	1.25–1.5	13	1.94	0.8691
2.00	2.0	30	1.27	0.9546
2.50	2.4–2.6	21	1.16	0.9151

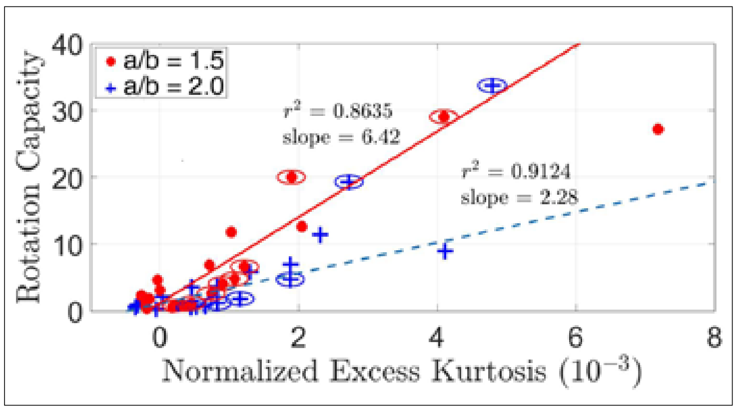

Figure 6: Rotation capacity of EHS under linearly varying moment condition, from experimental and FEM data, differentiated based on aspect ratio. A circle around data point marker indicates bending about major axis.

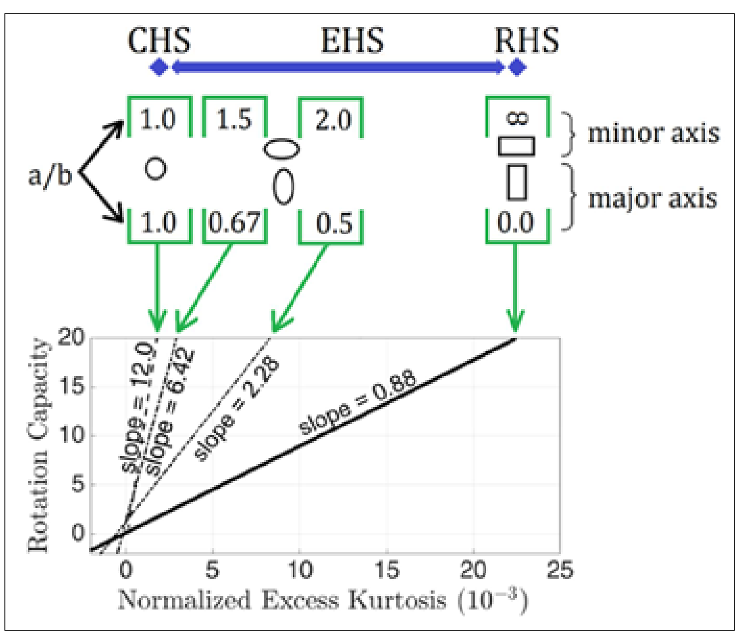

Figure 7: Trend lines observed from data (both experimental and FEM) for CHS, EHS and RHS under linearly varying moment conditions.

Effect of aspect ratio and axis of bending on rotation capacity

Examination of data for RHS show an ordering of the gradient when grouped based on the aspect ratio (*D/B*) (see Table 7). Under major axis bending RHS sections show decreasing gradient with increasing aspect ratio. (from *D/B* = 1.0 to 2.5). There is also a slight decrease in gradient from *D/B* = 1.0 to 0.714, indicating that gradient decreases as *D/B* moves away (in either direction) from unity. This is reflected in the EHS data below too.

Experimental and FEM data of EHS display a much more obvious ordering and significant change in gradient when grouped based on aspect ratio, with a change of gradient from 2.28 to 6.42 in EHS as compared to 1.27 to 1.94 in RHS, for a change in aspect ratio from 2.0 to 1.5. Furthermore, there is no discernible effect due to axis of bending (Figure 6). Note that Figure 6 includes both major and minor axis bending, with symbols enclosed in a loop indicating bending about major axis.

The above collation of data—both experimental and FEM—on CHS, RHS and EHS, based on multiple aspect ratios, leads to an interesting observation, where in essence EHS can be thought of as an intermediate state between RHS and CHS – see Figure 7 for the linearly varying moment condition. Note that the RHS slope is based on all the data in Figure 4, but disaggregated in Table 7. Because slopes are obtained by bisquare fitting the overall RHS slope in Figures 4 and 7 does not fall within the slopes in Table 7, but is similar in magnitude.

The above observations (clearly visible in Figure 7) counter the claims for using a single equivalent RHS or equivalent CHS approach for the classification of EHS, and shows that the EHS behaviour varies between CHS and RHS as the aspect ratio changes; an aspect ratio closer to 1 indicates more CHS-like behaviour while an aspect ratio closer to 0.0 or infinity (or practically < 0.5 or > 2.0) indicates more RHS like behaviour. Interestingly, most of the data used by Haque *et al*. (2012) to validate the equivalent RHS behaviour are of aspect ratio of 2.0 (or 0.5).

It is obvious that minor and major axis lengths (*a* and *b*) for an equivalent CHS are equal to unity (1.0), but this is less clear for an equivalent RHS. Note that the values of aspect ratio act as indicators of transverse curvature along the wall of the hollow section. As such we can consider an RHS having a very large breadth to be having an infinitely long horizontal axis – see Figure 1(iii), where the top and bottom flanges will become virtually a single plate with zero curvature. By a similar argument the RHS having a very large height can be considered as having an infinitely long vertical axis and webs once again with zero curvature.

We have noted early on that excess kurtosis does not take into account the effect of geometric transverse curvature of the wall of the hollow section. It is now evident that aspect ratio based on minor and major axis length accounts for the transverse curvature along the wall of the hollow section. Circular sections have the greatest curvatures followed by elliptical sections, with that of rectangular sections approaching zero. As curvatures decrease the slopes in Figure 7 also decrease. Based on Figure 7 we can say that EHS with aspect ratios closer to unity ($0.67 < a/b < 1.5$) should be classified based on an equivalent diameter approach, and those with aspect ratios further from unity ($a/b < 0.5$ and $a/b > 2.0$) based on an equivalent RHS approach. The actual normalized excess kurtosis limits for classification of hollow sections (from CHS to RHS, through EHS) can be based on Figure 7. For this, an appropriate confidence line (where, say 95%, of all values lie above the line) can be used, instead of the average trend line used here for identifying the distinctions across the types of sections.

We only present and discuss the behaviour under the linearly varying moment condition due to limited availability of data – EHS data for constant moment conditions were available for only one aspect ratio. We have observed however similar patterns with the constant moment condition for CHS and RHS, with constant moment conditions giving a higher rotation capacity than the linearly varying moment condition, for a given normalized excess kurtosis.

Excess kurtosis vs slenderness ratio

Slenderness is the currently used parameter in design codes to relate rotation capacity with section geometry. This relationship is such that if the section slenderness is smaller than a given value then the rotation capacity is sufficient for a plastic analysis to be carried out. The value of this 'sufficient rotation capacity' is not clear, but suggested values can be inferred from Korol & Hudoba (1972).

The slenderness parameter and the limiting slenderness value are different for different section types – *e.g.*, *c/t* for each plate in RHS with ($33\sqrt{235/f_y}$) as the limit for parts in compression only and *D/t* for CHS with ($50 \times 235/f_y$) as the limit (EN 1993-1-1: 2005). Furthermore, Jiao & Zhao (2004) note that, even after normalizing for material strength, the relevant slenderness limit for very high strength steel (f_y = 1350 MPa) is different from that for normal strength steel (f_y = 350–450 MPa).

Although both slenderness ratio and excess kurtosis can be used to determine a continuous relationship between rotation capacity and section geometry, the latter is superior as it (i) uses a common equation for CHS, RHS and EHS sections and (ii) gives the same rotation capacity value regardless of the material strength (*e.g.*, valid for both very high strength and normal strength steel).

The rotation capacity of sections, within the range of geometry in commonly used CHS and RHS sections, is influenced by local buckling. As such, using section slenderness to relate to rotation capacity is intuitive (since we use member slenderness to relate to overall buckling). However, although not immediately obvious, the excess kurtosis of a section is a measure of the wall thickness of hollow sections, as stated early on. Use of excess kurtosis simplifies the rotation capacity problem to a plate buckling problem, while the different slopes in Figure 7 account for the curvature of the plate in the transverse direction.

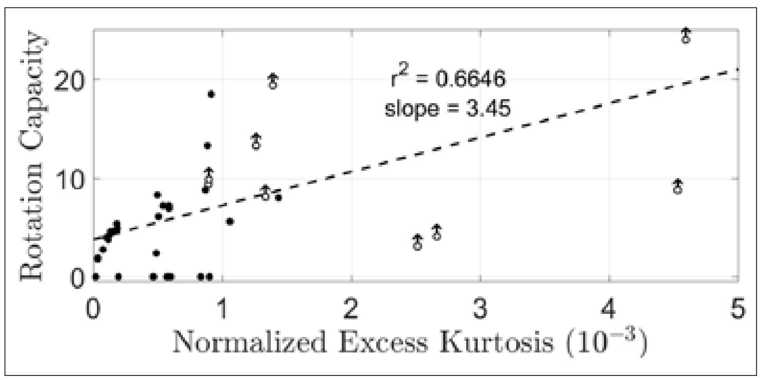

Figure 8: Rotation capacity vs normalized excess kurtosis of experimental data from constant moment tests on CHS. Markers with arrows indicate tests stopped prematurely (*i.e.*, full rotation capacity not achieved).

Effect of loading system

We have so far presented data under the varying moment condition. Figure 8 presents the behaviour of rotation capacity against normalized excess kurtosis under the constant moment condition. Experimental data for CHS indicate a higher rotation capacity under linearly varying moment (Figure 3) than under constant moment conditions (Figure 8).

Most of our data and analysis are for the varying moment condition (*e.g.*, Figure 3 for CHS). Figure 8 however, allows this to be compared with the behaviour under a constant moment condition. The trendlines from the experimental data for CHS indicate a higher rotation capacity under linearly varying moment (Figure 3) than under constant moment conditions (Figure 8), at higher normalized excess Kurtosis values (say > 1×10^{-3}), and vice versa at lower values.

CONCLUSION

In this study, a novel section parameter termed normalized excess kurtosis of a hollow section has been derived. It is inspired by a parameter of similar name in the field of statistics and is a measure of the wall thickness of hollow sections. It demonstrates a linear relationship with the rotation capacity of the section, hence giving a simple method to estimate rotation capacity of circular hollow sections (CHS), rectangular/square hollow sections (RHS) and elliptical/oval hollow sections (EHS).

Given a CHS, an RHS, and an EHS having the same normalized excess kurtosis, the CHS, which has the highest transverse curvature (*i.e.*, a section aspect ratio of 1.0) will have the largest rotation capacity; RHS, with the smallest transverse curvature (*i.e.*, having an aspect ratio tending to infinity) the smallest rotation capacity; and EHS, with an intermediate curvature, a rotation capacity between that of the CHS and the RHS.

It is observed that EHS presents a CHS–like behaviour at aspect ratios (a/b) closer to 1.0 and an RHS-like behaviour at high (say >2.0) or low (say < 0.5) aspect ratios. Thus, the equivalent RHS or equivalent CHS approaches can be appropriately applied to EHS, for use in plastic analysis.

Acknowledgements

The authors sincerely acknowledge the assistance provided by Prof. Ben Young, Dr Marios Theofanous, Dr Mei-Ni Su, and Dr Michaela Gkantou in sharing their FEM data sets; and Prof. Leroy Gardner, Dr Mohamed Elchalakani, and Dr Fulop Ludovic for the additional data and clarifications on data provided. Comments and suggestions from Prof. David Nethercot are especially appreciated.

REFERENCES

Afshan S. & Gardner L. (2013). Experimental study of cold-formed ferritic stainless steel hollow sections. *Journal of Structural Engineering* **139**(5): 717–728.
DOI: https://doi.org/10.1061/(ASCE)ST.1943-541X.0000580

Bock I., Arrayago I. & Real E. (2015). Experiments on cold-formed ferritic stainless steel slender sections. *Journal of Constructional Steel Research* **109**: 13–23.
DOI: https://doi.org/10.1016/j.jcsr.2015.02.005

Castaldo P., Nastri E. & Piluso V. (2017). Ultimate behaviour of RHS temper T6 aluminium alloy beams subjected to non-uniform bending: Parametric analysis. *Thin-Walled Structures* **115**: 129–141.
DOI: https://doi.org/10.1016/j.tws.2017.02.006

Chan T. & Gardner L. (2008). Bending strength of hot-rolled elliptical hollow sections. *Journal of Constructional Steel Research* **64**: 971–986.
DOI: https://doi.org/10.1016/j.jcsr.2007.11.001

Chen Y., Cheng X. & Nethercot D.A. (2013). An overview study on cross-section classification of steel H-sections. *Journal of Constructional Steel Research* **80**: 386–393.
DOI: https://doi.org/10.1016/j.jcsr.2012.10.006

D'Aniello M., Güneyisi E.M., Landolfo R. & Mermerdaş K. (2015). Predictive models of the flexural overstrength factor for steel thin-walled circular hollow section beams. *Thin-Walled Structures* **94**: 67–78.
DOI: https://doi.org/10.1016/j.tws.2015.03.020

DeCarlo L.T. (1997). On the meaning and use of kurtosis. *Psychological Methods* **2**(3): 292–307.
DOI: https://doi.org/10.1037/1082-989X.2.3.292

Elchalakani M. (2014). A closed formed solution for elastic buckling of thin-walled unstiffned circular cylinders in pure flexure. *Thin-Walled Structures* **80**: 120–129.
DOI: https://doi.org/10.1016/j.tws.2014.03.002

Elchalakani M., Zhao X.L. & Grzebieta R. (2002a). Bending tests to determine slenderness limits for cold-formed circular hollow sections. *Journal of Constructional Steel Research* **58**: 1407–1430.
DOI: https://doi.org/10.1016/S0143-974X(01)00106-7

Elchalakani M., Zhao X.L. & Grzebieta R. (2002b). Plastic slenderness limits for cold-formed circular hollow sections. *Australian Journal of Structural Engineering* **3**(3): 127–139.
DOI: https://doi.org/10.1080/13287982.2002.11464900

EN1993-1-1:2005. Eurocode 3: Design of Steel Structures: Part 1-1: General Rules and Rules for Buildings. European Committee for Standardization, Brussels.

EN 1993-1-4:2006. Eurocode 3: Design of steel structures: Part 1-4: General rules - Supplementary rules for stainless steels. European Committee for Standardization, Brussels.

EN 1993-1-12:2007. Eurocode 3: Design of steel structures: Part 1-12: Additional rules for the extension of EN 1993 up to steel grades S 700. European Committee for Standardization, Brussels.

Gardner L. & Chan T. (2006). Cross section classification of elliptical hollow sections. In: *Proceedings of the 11th International Symposium on Tubular Structures*. Québec City, Canada.

Gardner L. & Chan T. (2007). Cross-section classification of elliptical hollow sections. *Steel and Composite Structures* **7**(3): 185–200.

Gardner L., Talja A. & Baddoo N. (2006). Structural design of high-strength austenitic stainless steel. *Thin-Walled Structures* **44**: 517–528.
DOI: https://doi.org/10.1016/j.tws.2006.04.014

Guo L., Yang S. & Jiao H. (2013). Behaviour of thin-walled circular hollow section tubes subjected to bending. *Thin-Walled Structures* **73**: 281–289.
DOI: https://doi.org/10.1016/j.tws.2013.08.014

Haque T., Packer J.A. & Zhao X.L. (2012). Equivalent RHS approach for the design of EHS in axial compression or bending. *Advances in Structural Engineering* **15**(1): 107–120.
DOI: https://doi.org/10.1260/1369-4332.15.1.107

Huang Y. & Young B. (2013). Experimental and numerical investigation of cold-formed lean duplex stainless steel flexural members. *Thin-Walled Structures* **73**: 216–228.
DOI: https://doi.org/10.1016/j.tws.2013.07.019

Jiao H. & Zhao X.L. (2004). Section slenderness limits of very high strength circular steel tubes in bending. *Thin-Walled Structures* **42**: 1257–1271.
DOI: https://doi.org/10.1016/j.tws.2004.03.020

Kato B. (1988). Rotation capacity of steel members subject to local buckling. In: *Proceedings of Ninth World Conference on Earthquake Engineering*. Tokyo – Kyoto, Japan.

Kiyamaz G. (2005). Strength and stability criteria for thin-walled stainless steel circular hollow section members under bending. *Thin-Walled Structures* **43**: 1534–1549.
DOI: https://doi.org/10.1016/j.tws.2005.06.006

Korol R.M. & Hudoba J. (1972). Plastic behaviour of hollow

structural sections. *Journal of The Structural Division* **98**: 1007–1023.
DOI: https://doi.org/10.1061/JSDEAG.0003221

Rasmussen K. & Hancock G. (1993). Design of cold-formed stainless steel tubular members: II - beams. *Journal of Structural Engineering* **119**(8): 2368–2386.
DOI: https://doi.org/10.1061/(ASCE)0733-9445(1993)119:8(2368)

Sedlacek G. *et al*. (1998). *Investigation of the Rotation Behaviour of Hollow Section Beams*. Office for Official Publications of the European Communities, Luxembourg.

Seif M. & Schafer B.W. (2010). Local buckling of structural steel shapes. *Journal of Constructional Steel Research* **66**: 1232–1247.
DOI: https://doi.org/10.1016/j.jcsr.2010.03.015

Sherman D.R. (1976). Tests of circular steel tubes in bending. *Journal of the Structural Division* **95**: 2181–2195.
DOI: https://doi.org/10.1061/JSDEAG.0004478

Sherman D. (1986). Inelastic flexural buckling of cylinders. In: *International Conference on Steel Structures: Recent Research Advances and their Application to Design*. Amsterdam, Netherlands.

Su M.N., Young B. & Gardner L. (2014). Deformation-based design of aluminium alloy beams. *Engineering Structures* **80**: 339–349.
DOI: https://doi.org/10.1016/j.engstruct.2014.08.034

Theofanous M., Chan T. & Gardner L. (2009). Flexural behaviour of stainless steel oval hollow sections. *Thin-Walled Structures* **47**: 776–787.
DOI: https://doi.org/10.1016/j.tws.2009.01.001

Theofanous M. & Gardner L. (2010). Experimental and numerical studies of lean duplex stainless steel beams. *Journal of Constructional Steel Research* **66**: 816–825.
DOI: https://doi.org/10.1016/j.jcsr.2010.01.012

Theofanous M., Saliba N., Zhao O. & Gardner L. (2014). Ultimate response of stainless steel continuous beams. *Thin-Walled Structures* **83**: 115–127.
DOI: https://doi.org/10.1016/j.tws.2014.01.019

Wang J., Afshan S., Gkantou M., Theofanous M., Baniotopoulos C. & Gardner L. (2016). Flexural behaviour of hot-finished high strength steel square and rectangular hollow sections. *Journal of Constructional Steel Research* **121**: 97–109.
DOI: https://doi.org/10.1016/j.jcsr.2016.01.017

Wilkinson T. & Hancock G.J. (1998). Compact or Class 1 limits for rectangular hollow sections in bending. In: *Tubulur Structures* VIII, *Proceedings, 8th International Symposium on Tubular Structures*, Singapore, pp 409–416.

Zhao O., Gardner L. & Young B. (2016). Buckling of ferritic stainless steel members under combined axial compression and bending. *Journal of Constructional Steel Research* **117**: 35–48.
DOI: https://doi.org/10.1016/j.jcsr.2015.10.003

Zhao O., Rossi B., Gardner L. & Young B. (2015). Behaviour of structural stainless steel cross-sections under combined loading - Part I: Experimental study. *Engineering Structures* **89**: 236–246.
DOI: https://doi.org/10.1016/j.engstruct.2014.11.014

Zhao O., Rossi B., Gardner L. & Young B. (2016). Experimental and numerical studies of ferritic stainless steel tubular cross sections under combined compression and bending. *Journal of Structural Engineering* **142**(2): 04015110.
DOI: https://doi.org/10.1061/(ASCE)ST.1943-541X.0001366

Zheng B., Shu G., Xin L., Yang R. & Jiang Q. (2016). Study on the bending capacity of cold-formed stainless steel hollow sections. *Structures* **8**: 63–74.
DOI: https://doi.org/10.1016/j.istruc.2016.08.007

Zhou F. & Young B. (2005). Tests of cold-formed stainless steel tubular flexural members. *Thin-Walled Structures* **43**: 1325–1337.
DOI: https://doi.org/10.1016/j.tws.2005.06.005

Zhu Y. & Wilkinson T. (2007). *Finite Element Analysis of Structural Steel Elliptical Hollow Sections in Compression*. School of Civil Engineering, The University of Sydney, Sydney, Australia.

APPENDIX

Consider a beam of uniform stiffness under 3 point bending. We shall calculate the deflection at mid span of the beam under elastic response (Δ_{el}) from Mohr's second theorem based on the M/EI plot (see Figure A.1), where M is the bending moment, E is the modulus of elasticity, I is the second moment of area and L is the span length.

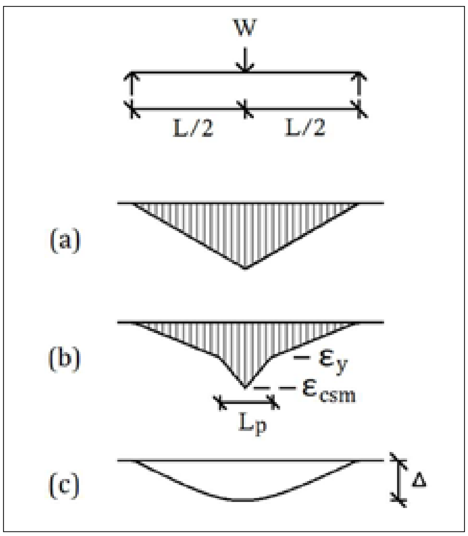

Figure A.1: (a) M/EI diagram within elastic material response, (b) strain plot beyond elastic limit, and (c) deflection pattern, under 3 point bending resulting in linearly varying moment in the mid-span.

Similarly, the deflection at mid span beyond the elastic limit (Δ) is calculated using the strain plot under linearly varying moment conditions, where $\kappa(s)$ is the bending curvature at a distance s from the point of reference, β is the strain capacity, $\bar{\beta}$ is the strain capacity adjusted for linearly varying moment, ε_y is yield strain, S_F is the shape factor, and ρ is the moment ratio.

$$\Delta = \int_0^L \kappa(s)(L-s)ds = \bar{\beta}\varepsilon_y \frac{L^2}{12d}; \qquad \text{...(S1)}$$

where $\bar{\beta} = \left[\left(1 + \frac{1}{\rho S_F}\right) + \beta\left(\frac{(\rho S_F - 1)(2\rho S_F + 1)}{(\rho S_F)^2}\right)\right]$

$$\rho = \frac{M_{csm}}{M_p} = \left[1 + \frac{E_{sh}}{E}\frac{1}{S_F}(\beta - 1) - \left(1 - \frac{1}{S_F}\right)\frac{1}{\beta^2}\right]$$

$$S_F = \frac{M_p}{M_y}$$

The base curve relates the strain capacity to section properties and Buchanan *et al*. (2016) present one for circular hollow sections, where λ is the section slenderness, f_{crt} the elastic buckling strength, ν the Poisson ratio and ε_{csm} the limiting strain under the continuous strength method.

$$\lambda = \sqrt{\frac{f_y}{f_{crt}}} = \sqrt{\frac{f_y\sqrt{3(1-\nu^2)}}{E}\frac{D}{t}} \qquad \text{...(S2)}$$

$$\beta = \frac{\varepsilon_{csm}}{\varepsilon_y} = \frac{4.44\times10^{-3}}{\lambda^{4.5}}\ ; for\ \lambda \leq 0.3 \qquad \text{...(S3)}$$

The mid span deflection is related to bending curvature (κ) using equation (S4) assuming a uniform curvature along the beam. However this is strictly applicable only to a constant moment condition. Note that this assumption overstates the rotation under linearly varying moment conditions, where the rotation is localised due to the moment gradient.

$$\kappa = \frac{1}{R} = \frac{8\Delta}{4\Delta^2 + L^2} \qquad \text{...(S4)}$$

The resulting elastic curvature at full plastic moment (κ_p) and at maximum moment (κ_{max}) can be formed as;

$$\kappa_p = \frac{24 M_p EI}{\left(M_p L\right)^2 + (6EI)^2} \qquad \text{...(S5)}$$

$$\kappa_{max} = \frac{24\bar{\beta}\varepsilon_y d}{\left(\bar{\beta}\varepsilon_y L\right)^2 + (6d)^2} \qquad \text{(S6)}$$

The resulting rotation capacity is;

$$R_3 = \frac{\kappa_{max}}{\kappa_p} - 1 = \frac{2\bar{\beta}}{S_F}\frac{\left[\left(S_F\varepsilon_y L\right)^2 + (3d)^2\right]}{\left[\left(\bar{\beta}\varepsilon_y L\right)^2 + (6d)^2\right]} - 1 \qquad \text{...(S7)}$$

Note that the equation S7 gives rotation capacity only up to the maximum moment (see Figure A.1); the post buckling behaviour is not accounted for. Such behaviour will depend on the collapse mechanisms formed and this in turn would depend on the section type.

APPENDIX REFERENCES

Buchanan C., Gardner L. & Liew A. (2016). The continuous strength method for the design of circular hollow sections. *Journal of Constructional Steel Research* **118**: 207–216. DOI: https://doi.org/10.1016/j.jcsr.2015.11.006

J.Natn.Sci.Foundation Sri Lanka 2023 51 (4): 629 - 641
DOI: http://dx.doi.org/10.4038/jnsfsr.v51i4.11306

RESEARCH ARTICLE

Agricultural Biotechnology

Does an R2R3-MYB transcription factor affect anthurium spathe colour variation via regulation of vacuolar pH?

NVT Jayaprada[1,2], S Fukai[3] and S Geekiyanage[4*]
[1] *Department of Agricultural Technology, Faculty of Technology, University of Colombo, Pitipana, Sri Lanka. (current address)*
[2] *Board of Study in Agriculture, Faculty of Graduate Studies, University of Ruhuna, Matara, Sri Lanka.*
[3] *Department of Horticulture, Faculty of Agriculture, Kagawa University, Miki, Kagawa 761-0795, Japan.*
[4] *Department of Agricultural Biology, Faculty of Agriculture, University of Ruhuna, Mapalana, Kamburupitiya, Sri Lanka.*

Submitted: 26 July 2022; Revised: 11 July 2023; Accepted: 28 July 2023

Abstract: The anthurium is a popular cut flower worldwide having red, pink, coral, white, green, or brown spathes. There is a constant demand for new flower colours in the commercial market. Flower colour in plants is mainly determined by anthocyanins. Understanding anthocyanin variation and other factors affecting anthurium spathe colour is important for genetic engineering approaches. Therefore, our objectives were to assess the factors affecting colour variation of selected commercially available cut flower anthuriums and to determine the associated regulatory networks and transcription factors (TFs). Nineteen commercial cut flower anthurium cultivars were selected for this purpose. The colour of the spathe surface, anthocyanin location, anthocyanidin type and vacuolar pH were recorded. Anthocyanin associated Gene Network Model generation and analysis were carried out. The CIELAB colourimeter procedure indicated the colour variation among the selected 19 cultivars in terms of colour type, colour intensity, chroma, and hue angle. The location of anthocyanin was limited to mesophyll and epidermal cells. Cyanidin was detected in tested anthurium cultivars as the main anthocyanidin. The pH gradient in pigment extracts indicated a variation with a range of 4.6 to 4.94. The gene pathways of anthocyanin biosynthesis and transport were associated with that of the vacuolar pH/H^+ pump according to Gene Network Model. Three pathways were regulated by an R2R3-MYB transcription factor. Although, cyanidin was the only pigment in all the tested cultivars, different pH levels by *R2R3-MYB* regulated V-H^+ synthase was suggested to be the cause of the high colour variation in addition to the anthocyanidin type and location. Our results indicate the application of *R2R3-MYB* transcription factor genes for desirable vacuolar pH maintenance in genetic engineering of the blue anthurium in the future.

Keywords: Anthocyanidin, anthurium, gene pathways, spathe colour, R2R3-MYB transcription factor, vacuolar pH.

INTRODUCTION

The spathe of the anthurium, *Anthurium andraeanum* (Hort) is important as a cut flower. Introduction of interspecific hybrids had contributed to a significant increase in anthurium production in the world (Kamemoto & Sheffer, 1978; Kamemoto & Kuehnle, 1997; Henny, 1999; Elibox & Umaharan, 2008). Red, green, orange, purple, and white are the common spathe colours of commercial varieties (Jayaprada & Geekiyanage, 2017). There is a constant global demand for novel spathe colours (Puchooa, 2005). The genetic basis of spathe colour is determined by two major genes named *M* and *O* in conventional breeding. The *O* gene confers recessive epistatis over *M*; thus red/pink spathes result due to *MmOo, MmOO, MMOo*, and *MMOO* genotypes. Orange-Coral spathes are by *mmOo* and *mmOO* genotypes, and *mmoo*, *Mmoo,* and *MMoo* produce white-spathed phenotypes (Gopaulchan *et al*., 2014). In addition, several other factors influence the colour variation and understanding the factors leading to

* Corresponding author (sudarshanee@agbio.ruh.ac.lk; https://orcid.org/0000-0002-3771-2680)

variation in spathe colour is of great importance in the breeding of new commercial cultivars in the future.

Colours of plants are determined by pigments such as chlorophylls, aurones, anthocyanins, carotenoids, and betalains. The major pigment in the spathe of anthurium is anthocyanin which is a product of the flavonoid biosynthesis pathway (Osorio-Guarín *et al*., 2021). Anthocyanidins are aglycone products of anthocyanins. The anthocyanin biosynthesis pathway is conserved among plants. It has been intensively studied, and the main anthocyanidins, pelagonidin-3-glucoside, cyanidin-3-glucoside, and delphinidin-3-glucoside, which are responsible for the colour variation, are already established (Holton & Cornish, 1995; Morita & Hoshino, 2018; Saigo *et al*., 2020). The early steps of the anthocyanin biosynthesis pathway are catalyzed by structural genes for the enzymes *chalcone synthase*, *chalcone isomerase*, and *flavanone-3-hydroxylase*, whereas the later steps are mediated by the structural genes of *dihydroflavonol-4-reductase*, *anthocyanin synthase*, and *flavonoid-3-O-glucosyltransferase* (*3GT*). In higher plants, the anthocyanin biosynthesis pathway is reportedly regulated by an MBW complex comprising transcription factors of MYB, basic helix-loop-helix (bHLH) domains and W40D repeats (Gonzalez *et al*., 2008; Albert *et al*., 2014). Among them, MYB transcription factors which are the v-myb avian myeloblastosis viral oncogene homologue proteins, play a major role in the regulatory network of anthocyanin biosynthesis (Yan *et al.,* 2021). According to Kobayashi *et al*. (2002), the *UDP glucose flavonoid-3-O-glucosyltransferase* (*UFGT*) gene in anthocyanin pathway is up-regulated by the *VlmybA2* gene from grape. Geekiyanage *et al*. (2007) and Geekiyanage (2010), reported that *VlmybA* genes could induce dark brown seed coats in transgenic tobacco and Arabidopsis in addition to the intense purple pigmentation, in leaves and flowers, suggesting that *VlmybA* genes not only regulated the *UFGT* gene for anthocyanidins but also the genes for proanthocyanidin in seed coat.

The displayed colour depends not only on the pigment present, but also on several factors including vacuolar pH (Rodríguez *et al*., 2020) and the location of pigment (Chen *et al*., 2019). Vacuolar pH had been considered as a major factor in studies to change the flower colour of floricultural crops such as hydrangea, petunia, morning glory, orchids, and roses (Noda, 2018; Okitsu *et al*., 2018; Sangeetha Priya, 2020). In petunia, the inheritance of flower colour is attributed to the combined effect of anthocyanidin pigmentation and vacuolar pH (Berardi *et al*, 2021). In morning glory, flower colour varies from reddish purple buds to blue flowers with an increase in vacuolar pH from 6.6 to 7.7 (Morita & Hoshino, 2018). The wide variation of spathe colour among many commercially available cultivars of anthurium has not been completely explained.

The objectives of the study were to characterize selected anthurium cultivars in terms of spathe colour, vacuolar pH, location of pigments on spathe and pigment type, and to determine the effects of pH regulatory genes on the anthocyanin biosynthesis pathway through Gene Network Models. Therefore, we selected nineteen anthurium cultivars of different colours and checked the effects of pH increase externally on pigment colour *in vitro*. Secondly, types of anthocyanidins in selected *Anthurium andraeanum* accessions were determined. Finally, associated gene pathways were extracted to justify the influence of the above factors on colour variations and to decipher the most influential genes through Gene Network Models.

MATERIALS AND METHODS

Materials

Paradise, Maxima, Tulip Summer, Sharren, Maxima Erigancia, Flabia, Losa green, Eternum, Tropic Night, Maxima, Sabia, T. Sopink, Maxima Berdin, Karisht, T. Arura Pink, and Torenda cultivars with colourful spathes and Wind, Okinawa, Kisstouche, and Maxima Berdin cultivars with green spathes were selected for the study (Figure 1). These cultivars are cut flower anthuriums, which are commercially available in Japan. The study was carried out in the Faculty of Agriculture, Kagawa University, Japan and the Department of Agricultural Biology, Faculty of Agriculture, University of Ruhuna, Sri Lanka.

Colour assessment of spathe surfaces

Nineteen anthurium cultivars were subjected to colour assessment of spathe surfaces. The lightness (L*) and chromatic components a* and b* of CIELAB standards of the spathe were measured by a colourimeter (NR-12B; Nippon Denshoku Industries Co., Ltd., Tokyo, Japan). The L* represents the degree of darkness and brightness, a* represents the degree of green and red, and b* represents the degree of blue and yellow. In the CIELAB, the colour coordinates C^* and H^* were calculated based on the following equations: $C^* = (a^{*2}+b^{*2})$ 1/2 and $H^* = \tan^{-1}(b^*/a^*)$, according to Punangkrit *et al*. (2018).

Figure 1: The commercially available anthurium cultivars collected from Japan for the pigment analysis. (a) Wind, (b) Paradise, (c) Okinawa, (d) Maxima, (e) Tulip Summer, (f) Sharren, (g) Maxima Erigancia, (h) Flabia, (i) Losa green, (j) Eternum, (k) Kisstouche, (l) Torenda, (m) Maxima, (n) Sabia, (o) T. Sopink, (p) Maxima Berdin, (q) Karishth, (r) T. Arura Pink, (s) Tropic Night

Observation of pigment locations in the spathe

Wind, Kissotouch, Maxima, Berdin, Paradise, Sabia, Sharren, Losa Green, Eternum, Torenda, Karishth, Tropic Night, and Flabia cultivars were selected to represent the total colour variation. Pieces of 0.5 cm × 0.5 cm from the middle of the spathe were dipped in 5% agar longitudinally. Spathe pieces were picked with agar using a scalpel. The pieces were put in the micro slicer. The thickness of a longitudinal cross section was 125 µm. The longitudinal cross sections were observed under an enhanced light microscope (Olympus, Japan) to locate the pigments on the spathe.

Sample preparation for high performance liquid chromatography (HPLC)

Paradise, Maxima, Tulip Summer, Sharren, Maxima Erigancia, Flabia, Losa green, Eternum, Tropic Night, Maxima, Sabia, T. Sopink, Maxima Berdin, Karisht, T. Arura Pink, and Torenda cultivars with colourful spathes were selected for the analysis. Green colour cultivars of Wind, Okinawa, Kisstouche, and Maxima Berdin with chlorophyll were not used for the analysis. Five grams from each sample were placed in a test tube. Five milliliters of 5% formic acid in methanol (v/v) were added to each sample. The extraction solution was filtered, and used for HPLC analysis.

Confirmation of the presence of anthocyanidins

The filtered spathe extract was injected into HPLC, in which chromatograms were developed with two LC-20AT pumps (Shimadzu Co. Ltd., Japan), a CTO-10ASvp column oven (Shimadzu Co. Ltd., Japan) equipped with ODS-3 columns (3.0 mm I.D. × 50 mm + 3.0 mm I.D. × 250 mm; GL Science Co. Ltd., Japan) and an SPD-10MAvp detector (Shimadzu Co. Ltd.) set at 530 nm. The column temperature was maintained at 40^0C. A linear gradient elution for 40 min from 25 to 85% solvent B (0.1% trifluoroacetic acid, 20% acetic acid (CH_3COOH) and 25% CH_3CN in H_2O, v/v) in solvent A (0.1 % trifluoroacetic acid in H_2O, v/v) was employed as the solvent system, and the flow rate of 0.4 mL/s was maintained.

Acid hydrolysis of anthocyanidin extracts

For the identification of anthocyanidin type, the same amount of 6 M hydrochloric acid was added to the above spathe extract, and the mixture hydrolysed for 120 min at 90 ^{0}C. The acid hydrolysates were passed through a membrane filter and applied to a Sep-Pak C18 cartridge (Waters). Aglycones (anthocyanidins) trapped on the cartridge were washed with distilled water to eliminate the water-soluble hydrophilic contaminants, and then eluted with small amounts of 5% formic acid (HCOOH) methanolic solution.

Identification of the anthocyanidin type

The filtered elutes were injected into HPLC, in which chromatograms were developed with two LC-20AT pumps (Shimadzu Co. Ltd.), a CTO-10ASvp column oven (Shimadzu Co. Ltd.) equipped with Cosmosil 5C18 AR-2 columns (4.6 mm I.D. × 50 mm + 4.6 mm I.D. × 250 mm; Nakarai Tesque Co. Ltd., Japan) and an SPD-M10Avp detector (Shimadzu Co. Ltd.).The column temperature was maintained at 40 ^{0}C. A mixed solvent of 45% solvent A (1.5% H_3PO_4 in H_2O, v/v) and 55% solvent B (1.5% H_3PO_4, 20% Acetic Acid (CH_3COOH) and 25% CH_3CN in H_2O, v/v) was employed, and a flow rate of 1.0 mL/s was maintained. The retention time of each peak of each accession was compared with the chromatograms of the standards. As the standards, Cyanidin, Pelargonidin, and Delphinidin were used.

Measurement of vacuolar pH of spathe samples

Five grams of spathe samples were crushed using mortar and pestle. The crushed sample was dipped in 5 mL of distilled water overnight. The pH was measured in the final extract. The pH of pigment extract in distilled water was assumed to be representing the vacuolar pH (Verweij *et al.*, 2008).

Adjustment of the pH of the pigment extract

Five grams of spathe pieces were dipped in 5 mL of glacial acetic acid overnight for total pigment extraction of the spathe. In order to assess the colour change with increased pH, the pH of the glacial acetic acid extracts was increased by adding 10 M NaOH. After the establishment of the reaction, the pH was measured. The change in colour in contrast to the control was observed and recorded.

Gene network model generation

Information on genes involved in anthocyanin biosynthesis, trafficking, and vacuolar pH regulation was collected from KEGG (*https://www.genome.jp/kegg/pathway.html*), and STRING (*https://string-db.org/*) databases and from the literature. The network table files were created. Network data were imported into the Cytoscape interface. Interaction parameters were defined by specifying columns of data containing the Source Interaction, Target Interaction, and Interaction Type. Network models were generated using Cytoscape 3.8. In the generated network, nodes (or vertices) represented enzyme genes, while edges represented relationships of interactions. The generated network was analysed to decipher gene interactions. Key transcription factors involved were identified.

RESULTS AND DISCUSSION

Insignificant influence of anthocyanidin type on anthurium spathe colour variation

The nineteen anthurium cut flower cultivars selected had a significant variation in terms of colour intensity, Chroma (C*) and hue angle (H*). According to the CIELAB procedure of colour measurement "L*" with a lower number (0-50) indicates darkness, and a higher number (51-100) indicates brightness. The "a" scale indicates the state of green versus red where a positive number indicates red and a negative number indicates green. Moreover, the "b" scale indicates the state of blue versus yellow where a positive number indicates yellow, and a negative number indicates blue. The "C*" and "H*" describe chroma and the hue angle respectively. The hue angle describes the relative amounts of redness and purpleness where a value around 240 represents blue and a value around 300 represents purple. The purple colour cultivar "Flabia" had a hue angle of around 347, red, brown, pink and orange cultivars had the lowest hue angles residing within a range of 20-40. This confirmed that colours determined through the naked eye coincide with the CIELAB standards. Chroma meant the purity or intensity of the colour. The colours of low chroma are considered to be "weak" while those of high chroma are considered to be "highly saturated" or "strong" when colour is measured using Hunter L, a, b versus CIE L*a*b*. In our collection, red cultivars gave higher chroma ranges of 60-75, indicating the presence of high anthocyanin content in the spathe (Table 1).

The three most common anthocyanidins of delphinidin-3-glycoside for blue and purple colour, cyanidin 3-glucoside for brick red and magenta colour and pelargonidin-3-glycoside for orange and red colour were used as standards in HPLC (Figure 2; Table 2a). Despite the high colour variation and saturation among the cultivars, HPLC identified mainly one anthocyanidin type in them, which was cyanidin (Figure 2; Table 2b).

Table 1: Colour phenotypes, CIELAB parameter values, vacuolar pH and anthocyanin locations of selected anthurium cultivars

Cultivar	Phenotype	L	a*	b*	C*	H*	Vacuolar pH	Anthocyanin Location
Wind	Green	56.19	-15.66	28.28	28.52	82.52	4.94	Mesophyll
Kisstouch	Green	54.6	-8.33	43.27	44.06	100.9	4.94	Mesophyll
Maxima Berdin	Green	58.62	-8.28	22.57	22.64	85.49	4.94	Mesophyll
Paradise	Brown	28.81	38.4	13.01	40.55	18.72	-	Mesophyll
Okinawa	Brown	35.39	14.59	13.74	20.04	43.3	-	-
Maxima	Pink	69.89	18.14	15.22	23.67	40	4.63	-
Maxima Ergancia	Pink	64.57	19.2	19.06	27.06	44.79	4.63	-
Sabia	Pink	45.94	56.2	16.81	58.66	16.65	4.63	Lower Epidermis
T. Sopink	Pink	66.63	26.49	10.49	28.49	21.6	4.75	-
Aurora Pink	Pink	72.26	14.33	2.96	14.63	11.67	4.75	-
Tulip Summer	Orange	62.71	24.79	14.06	28.5	29.55	4.73	-
Sharren	Red	41.24	60.57	34.7	69.8	29.81	4.73	Lower Epidermis
Losa Green	Red	58.8	38.8	12.19	40.67	17.44	4.73	Lower Epidermis
Eternum	Red	52.13	47.7	22.52	52.74	25.27	4.77	Lower Epidermis
Torenda	Red	40.08	67.03	27.02	72.27	21.96	4.77	Mesophyll and Lower Epidermis
Karishth	Red	33.41	53.45	31.68	62.13	30.65	4.77	-
Tropic Night	Red	23.61	29.72	9.09	31.08	17.01	4.77	Lower Epidermis
Flabia	Purple	47.08	43.43	-9.55	44.47	347.59	4.94	Mesophyll
Maxima	White	83.72	-1.55	18.89	18.95	94.69	4.6	-

Variation in pigment location and pH as factors determining colour variation

Anthocyanins are accumulated in the vacuoles. There are reports on vacuolar pH and pigment location as important factors in flower colour variations in several species (Zhang *et al*., 2021). Consequently, the vacuolar pH and pigment localization in spathes of selected anthurium cultivars were assessed using spathe cross sections consisting of epidermal and mesophyll layers (Figure 3). The anthocyanins in pink, red, orange and brown cultivars were mainly localized in the epidermal layer of the spathes. The anthocyanins of the purple cultivar were mainly localized in the mesophyll cells of the spathes (Figure 3; Figure 4; Table 1).

The tested anthurium cultivars exhibited a pH variation among different colours within a range of 4.6 to 4.94. Purple cultivars had the highest pH of 4.94 followed by red and white cultivars of pH of 4.77 and 4.6, respectively. Avila- Rostant *et al.* (2010), who reported a variation of spathe colours and vacuolar pH among tested cultivars, had screened the germplasm for lower vacuolar pH to be utilized in genetic engineering for blue anthurium. Athough the pH values of Table 1 in the current work were not similar to the previous study (Avila- Rostant *et al*., 2010), the effect of colour groups such as purple, red and white were consistent with the variation of vacuolar pH. Furthermore, the red cultivars with high chroma values had more anthocyanin saturation as mentioned in the above section. Based on CIE L*a*b* system, the negative values for a* indicated the green cultivars as previously reported by Gopaulchan *et al*. (2015). The red and purple cultivars were of higher pH over 4.77 (Table 1). Therefore, it is suggested that spathe colour and anthocyanin saturation has a relationship with higher vacuolar pH. To confirm that purple colour spathes were associated with higher pH, 10 M NaOH was added to the pigment extracts of red and orange cultivars to increase the pH *in vivo*. The pigment extracts turned purple at a pH of around 4.8 (Figure 5). According to a previous study, the vacuolar pH adjustment to a higher pH level of 5.7 - 6 had given rise to more purplish and bluish flowers in soy bean (Sundaramoorthy *et al*., 2020). The above reports are consistent with our current results suggesting that dark colours appear at higher pH.

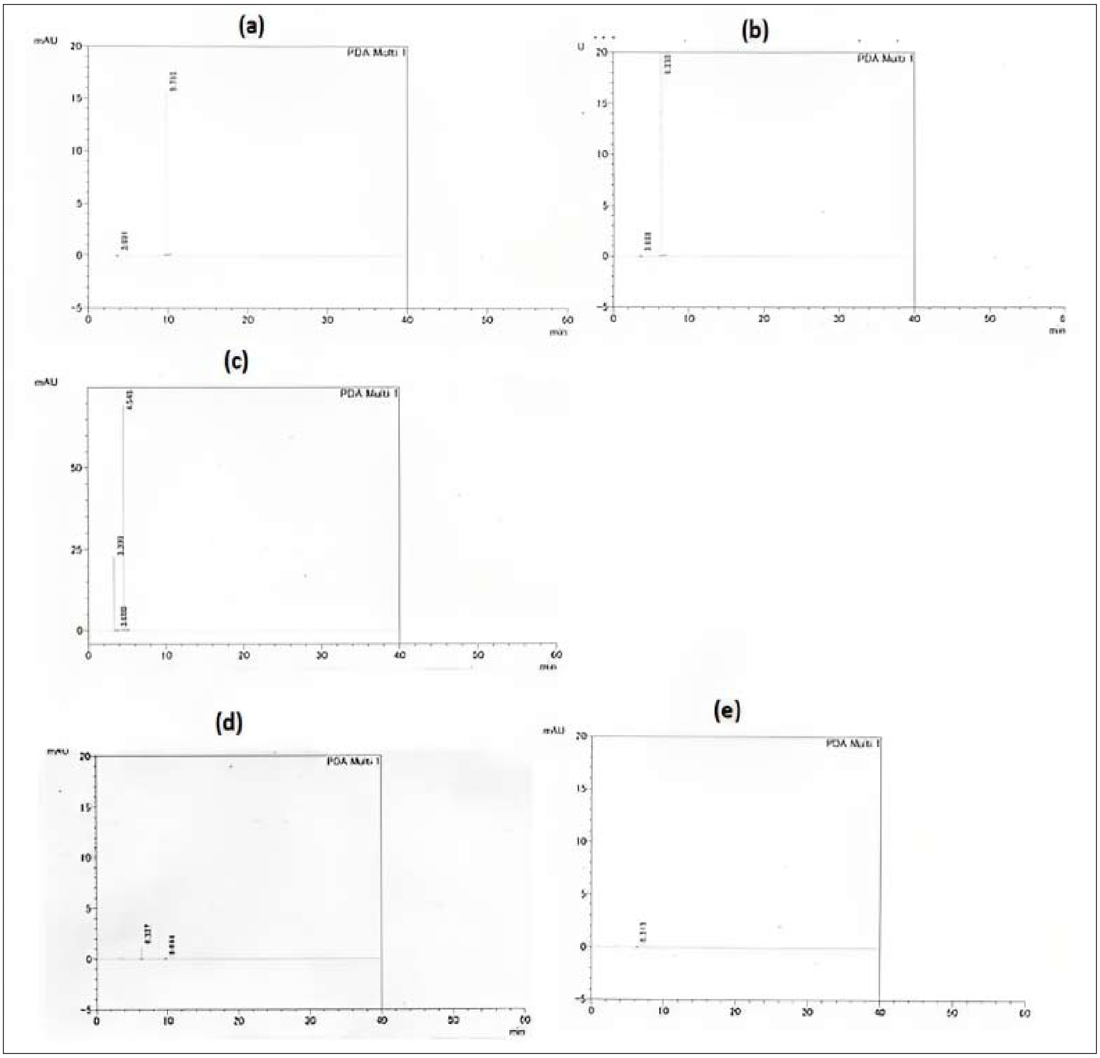

Figure 2: HPLC chromatograms for standard anthocyanidins, (a) Pelargonidins, (b) Cyanidins, (c) Delphinidins; For tested cultivars, (d) Maxima with cyanidins and pelargonidins, (e) T. Arura Pink with cyanidins

The fate of dihydrokaempferol in the anthocyanin biosynthesis pathway is crucial for the production of blue colour. Dihydrokaempferol is converted to dihydromyricetin through the *flavonoid-3',5'-hydroxylase* (*F3'5'H)* gene. Higher pH in the vacuole is favourable for this reaction. Noman *et al*. (2017) had reviewed the procedures of transgenic blue rose and chrysanthemum production, where the introduction of *F3'5'H* gene is highlighted for accumulation of delphinidin for blue colour.

Table 2a: The standards of anthocyanidins used in HPLC

Retention time (min)	Anthocyanidin type
6.350	Cyanidin (Cy)
9.790	Pelargonidin (Pg)
4.546	Delphinidin (Dp)

Higher values for vacuolar pH had been recorded for selected blue flowers in a previous study of ours (Jayaprada & Geekiyanage, 2016). The increase of pH in pigment extract of above selected blue flowers with 0.1 M NaOH had resulted a darker blue colour. However, the pigment extracts of current work must not contain the required genetic pathway including *F3'5'H* gene for the reaction. Therefore, identification of anthurium cultivars with higher vacuolar pH is important in future breeding for blue anthurium with an introduced *F3'5'H* gene.

Table 2b: The anthocyanidins of cultivars detected through HPLC

Anthurium cultivar	Peak number	Retention time (min)	Anthocyanidin type
Paradise	1	6.341	Cyanidin
Maxima	1	6.327	Cyanidin
Maxima	2	9.694	Pelargonidin
Tulip Summer	1	6.347	Cyanidin
Sharren	1	6.338	Cyanidin
Sharren	2	9.697	Pelargonidin
Maxima Erigancia	1	6.331	Cyanidin
Flabia	1	6.330	Cyanidin
Losa green	1	6.324	Cyanidin
Eternum	1	6.321	Cyanidin
Torenda(l)	1	6.326	Cyanidin
Maxima(m)	1	6.322	Cyanidin
Sabia	1	6.314	Cyanidin
T. Sopink	1	6.311	Cyanidin
Karishth	1	6.323	Cyanidin
T. Arura Pink	1	6.313	Cyanidin
Tropic Night	1	6.314	Cyanidin

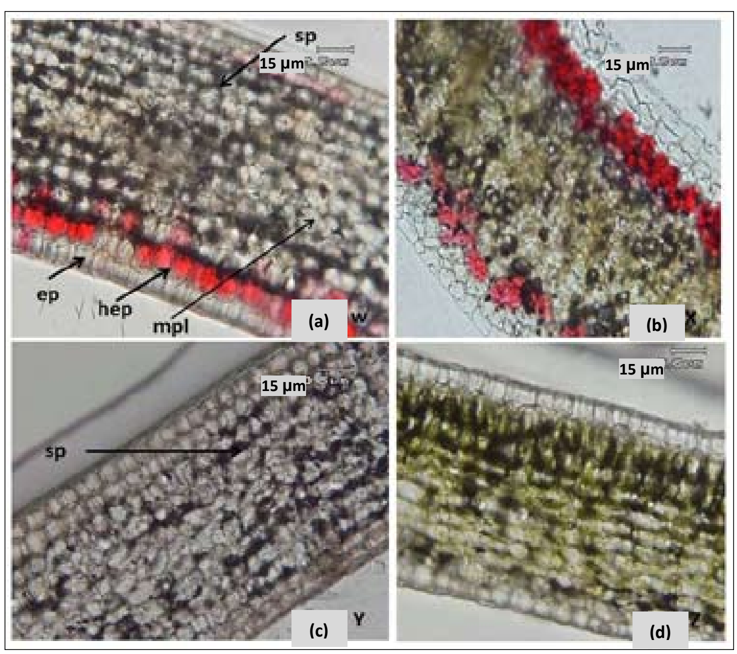

Figure 3: Localization of anthocyanin. (a) in lower epidermal layers, (b) in outermost mesophyll layer and chlorophyll in inner mesophyll cells, (c) (purple cultivar Flabia) in mesophyll cells, (d) chlorophyll in inner mesophyll cells, ep epidermal Layer, hep lower Epidermal layer, mpl mesophyll cells. (Enhanced light Microscope, Olympus, Japan; ×100)

Figure 4: Location diversity of pigments of selected different anthurium cultivars of (a) Wind, (b) Paradise, (c) Sharren, (d) Flabia, (e) Eternum, (f) Torenda, (g) Tropic Night, (h) Kisstouche, (i) Maxima Berdin, (j) Sabia and (k) Maxima Berdin, (l) Middle part of Losa Green, (m) Lobes of Losa Green. (Enhanced light Microscope, Olympus, Japan; ×10)

The location of the pigment was restricted to mesophyll and epidermis. Based on the fact that cyanidin pigment was present in all tested anthurium cultivars, the anthocyanidin type did not determine the colour variation in them. Our findings led us to investigate the genetic basis behind anthocyanidin transport and vacuolar pH, along with anthocyanin biosynthesis towards anthurium spathe colour variation.

Association between factors determining colour variation and anthocyanin regulatory pathways

Mostly the anthurium colour variation is influenced by the expression changes in structural genes such as *CHI, F3H, F3'5'H, F3'H, ANS,* and *CHS* in the anthocyanin biosynthesis pathway (Spelt *et al*., 2002; Collette *et al*., 2004; Avila-Rostant *et al*., 2010; Gopaulchan *et al*., 2014; Osorio-Guarín *et al*., 2021). According to the gene network analysis, spathe colour in anthurium was determined by three major pathways, namely, anthocyanin biosynthesis, anthocyanidin vacuolar transport, and vacuole pH/H^+ pumps in plants (Figure 6). The proposed coordinated mechanism is explained hereafter.

After biosynthesis, the anthocyanidin is transported and stored in vacuoles (Shitan & Yazaki, 2020). Fluctuations in vacuolar pH led to structural changes in the stored anthocyanidins, which result in colour changes. Furthermore, network analysis identified that all these three pathways were regulated by an R2R3-MYB transcription factor. The R2R3-MYB transcription factor fine-tunes the vacuolar pH by regulating the Vacuole-type ATPase (*V-ATPase*) which is the main H^+ concentration controller in the cell vacuole (Sundaramoorthy *et al*., 2020). The different spathe colours in tested cultivars are the result of a combination of cyanidin, which is the end product of anthocyanin biosynthesis, and the R2R3-MYB transcription factor regulating different pH values. R2R3-MYB transcription factors from chrysanthemum are reported to be inducing key structural genes in the anthocyanin pathway (Hong *et al*., 2019).

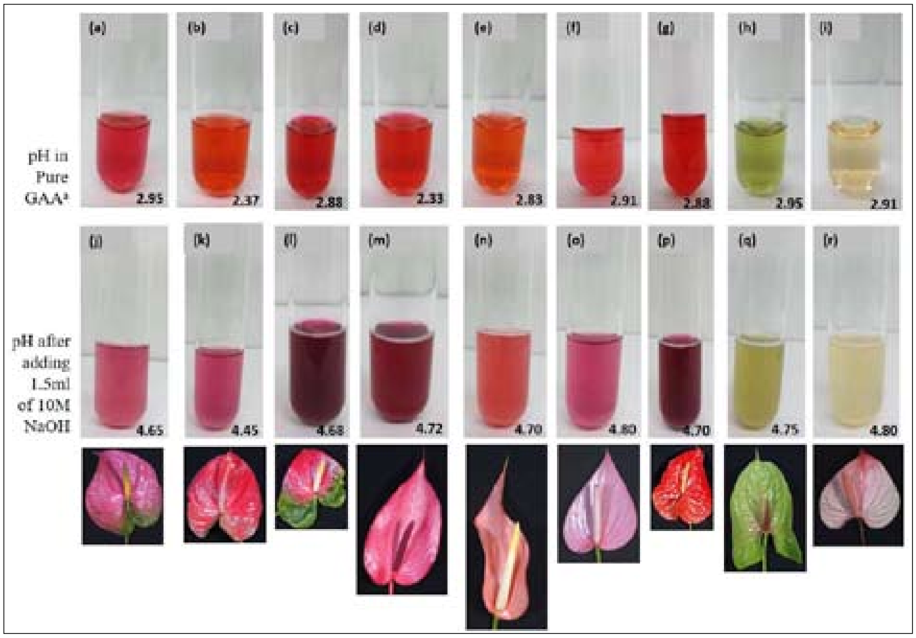

Figure 5: The effect of external change in pH on colour. (a)-(i) Colours of the glacial acetic acid extracts of the cultivars. (a) Losa Green, (b) Eternum, (c) Torenda, (d) Sabia, (e) Tulip Summer, (f) T. Sopink, (g) Karishth, (h) Kisstouche and (i) Maxima, (j)-(r) Colours of the glacial acetic acid extracts after adding 10 M NaOH. (j) Flabia, (k) Eternum, (l) Torenda, (m) Sabia, (n) Tulip Summer, (o) T. Sopink, (p) Karishth, (q) Kisstouche and (r) Maxima. [a]The pH of pure GAA was obtained as 2.73.

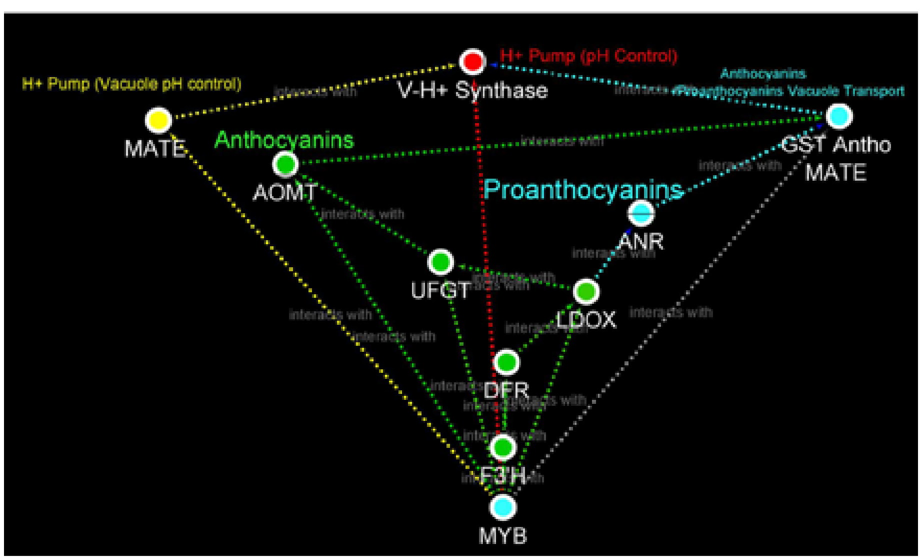

Figure 6: Proposed generalized gene biosynthesis pathway of anthocyanins using Cytoscape 3.8. The *R2R3-MYB* transcription factor gene (*MYB*), Flavanone-3-hydroxylase (*F3H*), Anthocyanidin-3-O-glucosyltransferase (*UFGT*), Leucoanthocyanidin dioxygenase (*LDOX*), Anthocyanin O-methyltransferase (*AOMT*), glutathione S-transferase anthocyanin multidrug and toxic compound extrusion family protein (*GST Antho MATE*), Multidrug and toxic compound extrusion family protein (*MATE*), anthocyanidin reductase (*ANR*), Vacuolar H^+ synthase (*V-H^+ Synthase*), are involved. Each dotted line represents one enzymatic step. Circles represent the Enzyme genes.

The effect of temperature and light on anthocyanin accumulation is regulated by *MYB* genes in the anthocyanin pathway (Azuma *et al.,* 2012). Meanwhile, Wang *et al.* (2022), reported about indirect repressors of anthocyanin biosynthesis from the MYB transcription factor family. The corresponding transcription factors are reported to be unable to bind to the promoters of the target genes and compete with the R2R3-MYB transcription activators by interacting with bHLH transcription factors in MBW complexes (Li *et al*., 2019a). Chen *et al*., 2019 had reported about R2R3-MYB transcription factors with repressive motifs as well, which directly repress the flavonoid biosynthetic genes.

There are previous reports on mutations affecting vacuolar pH regulation leading to bluish flower colour and increased pH of petal homogenates of petunia (Verweij *et al*., 2008; Faraco *et al*., 2014). According to the above study, wild-type (WT) petunia petals carrying cyanidins, displayed red colour at a vacuolar pH of 5.5 when all pH genes were functional (Faraco *et al*., 2014). However, mutations in any of the above genes had increased the vacuolar pH of petals, up to 6.0, resulting in a blue colour (Spelt *et al*., 2002; Faraco *et al*., 2014). Avila-Rostant *et al.,* 2010 had reported the relationship between spathe colour variation and vacuolar pH in anthurium, as green and white cultivars had the highest pH (5.65), while coral, (5.38), red (5.10) and orange (4.5) followed a descending order. However, there are no reports on downstream structural genes that control vacuolar pH in anthurium. Different spathe colours of anthurium were observed from spathes that had cyanidin as the only pigment. According to the pathway analysis an MYB transcription factor is involved with vacuolar pH controlling genes, which opens a new avenue for *MYB* gene function in addition to transcription activation of structural genes of the anthocyanin pathway. Therefore, we would indicate the possibility that different spathe colours resulted due to vacuolar pH manipulation through the MYB transcription factor. Although there are no reports on the identification of downstream structural genes that control vacuolar pH in anthurium, this is one possible scenario that justifies different anthurium spathe colours with cyanidin as the major dominating anthocyanidin type.

R2R3-MYB transcription factors are considered as a key determinant controlling distinct pigmentation patterns throughout the plant (Albert *et al*., 2011). The *R2R3-MYB* genes *AaMYB2* and *AaMYB3* from *Anthurium andraeanum* (Hort.) had positively regulated the anthocyanin biosynthesis genes of *AaF3H*, *AaANS*, *AaDFR,* and *AaCHS* in the spathes and leaves (Li *et al*., 2016; 2019b). In fact, there are reports on increased flower colour expression in transgenic tobacco via ectopic expression of these two R2R3-MYB transcription factors (Li *et al*., 2019). However, there are rare insights on the influence of these R2R3-MYB transcription factors on other influential pathways such as pH manipulation pathways, which affect expression of anthurium spathe colour genes.

Sundaramoorthy *et al*. (2020) had detected that R2R3-MYB was the main transcription factor in controlling vacuole acidification for flower colour changes. Three SNP mutations in an R2R3-MYB transcription factor in soy bean flower had caused fluctuations in vacuolar pH between 5.0-6.1 converting purple petals to blue petals (Sundaramoorthy *et al*., 2020). This is another possibility that explains the colour variations in selected anthurium cultivars.

Generated network models further explained that the R2R3-MYB transcription factor also regulates cyanidin transport genes like *GST Antho MATE* and *MATE*. Cutanda-Perez *et al*. (2009) reported that *VlmybA1* in grapevine is involved in anthocyanin synthesis and transport in transgenic plants. Further, the MdMYB1/10 transcription factor was reported to be affecting the cellular pH and anthocyanin accumulation by regulating different H^+ -pumping and anthocyanidin transport genes in transgenic apples resulting in colour variation in apple calli (Ling-Wang *et al.*, 2010; Hu *et al*., 2016; Li *et al.*, 2019b). In our study, we identified *Antho MATE* as the main anthocyanidin transport gene which is being regulated by R2R3-MYB transcription factor. Differential localization of cyanidin into mesophyll or epidermis in tested cultivars is suggested through the above method of transport regulation. R2R3-MYB transcription factor regulates *V-ATPase* and *MATE* genes*,* which mainly determine spathe colour variation in terms of vacuolar pH and pigment location respectively. Based on the above interpretations, R2R3-MYB transcription factors are among the key regulators of anthurium spathe colour. Therefore, the R2R3-MYB transcription factor will be an effective candidate over structural genes for genetic manipulation of spathe colour. The above assumption could be validated through a genetic transformation of homologous R2R3-MYB transcription factors from other species for novel anthurium colours.

CONCLUSIONS

Selected anthurium cultivars were variable in spathe colour, anthocyanin location, and vacuolar pH, while the main identified anthocyanidin type was cyanidin.

According to the Gene Network Model analysis, the spathe colour, anthocyanin location, and vacuolar pH were controlled by anthocyanin transport, biosynthesis, and vacuolar pH regulatory pathways respectively. An *R2R3-MYB* transcription factor gene was identified as the main regulator of vacuolar pH in the spathe leading to the higher vacuolar pH variation. Therefore, we suggest that different spathe colours resulted due to vacuolar pH manipulation through an R2R3-MYB transcription factor. The R2R3-MYB transcription factor gene could be a potential candidate in colour manipulation via genetic engineering.

Acknowledgements

The authors acknowledge the research grant by the Sri Lanka Council for Agricultural Research Policy (SLCARP). The National Science Foundation (NSF), Sri Lanka awarded a grant through the Overseas Special Training Programme (OSTP) to conduct a part of the research at Kagawa University, Japan. Further, the authors thank Prof. Takejiro Takamura of the Department of Horticulture, Faculty of Agriculture, Kagawa University, Japan for his assistance.

REFERENCES

Albert N.W., Davies K.M., Lewis D.H., Zhang H., Montefifiori M., Brendolise C., Boase M.R., Ngo H., Jameson P.E. & Schwinn K.E. (2014). A conserved network of transcriptional activators and repressors regulates anthocyanin pigmentation in eudicots. *The Plant Cell* **26**: 962–980.
DOI: https://doi.org/10.1105/tpc.113.122069

Albert N.W., Lewis D.H., Zhang H., Schwinn K.E., Jameson P.E. & Davies K.M. (2011). Members of an R2R3-MYB transcription factor family in *Petunia* are developmentally and environmentally regulated to control complex floral and vegetative pigmentation patterning. *The Plant Journal* **65**: 771–784.
DOI: https://doi.org/10.1111/j.1365-313X.2010.04465.x

Avila-Rostant O., Lennon A.M. & Umaharan P. (2010). Spathe color variation in *Anthurium andraeanum* Hort. and its relationship to vacuolar pH. *HortScience* **45**(12): 1768–1772.
DOI: https://doi.org/10.21273/HORTSCI.45.12.1768

Azuma A., Yakushiji H., Koshita Y. & Kobayashi S. (2012). Flavonoid biosynthesis-related genes in grape skin are differentially regulated by temperature and light conditions. *Planta* **236**(4): 1067–1080.
DOI: https://doi.org/10.1007/s00425-012-1650-x

Berardi A.E., Esfeld K., Jäggi L., Mandel T., Cannarozzi G.M. & Kuhlemeier C. (2021). Complex evolution of novel red floral color in Petunia. *The Plant Cell* **33**(7): 2273–2295.
DOI: https://doi.org/10.1093/plcell/koab114

Chen K., Du L., Liu H. & Liu Y. (2019). A novel R2R3-MYB from grape hyacinth, MaMybA, which is different from MaAN2, confers intense and magenta anthocyanin pigmentation in tobacco. *BMC Plant Biology* **19**(1): 1–15.
DOI: https://doi.org/10.1186/s12870-019-1999-0

Collette V.E., Jameson P.E., Schwinn K.E., Umaharan P. & Davies K.M. (2004). Temporal and spatial expression of flavonoid biosynthetic genes in flowers of *Anthurium andraeanum*. *Physiologia Plantarum* **122**(3): 297–304.
DOI: https://doi.org/10.1111/j.1399-3054.2004.00402.x

Cutanda-Perez M.C., Ageorges A., Gomez C., Vialet S., Terrier N., Romieu C. & Torregrosa L. (2009). Ectopic expression of VlmybA1 in grapevine activates a narrow set of genes involved in anthocyanin synthesis and transport. *Plant Molecular Biology* **69**: 633–648
DOI: https://doi.org/10.1007/s11103-008-9446-x

Elibox W. & Umaharan P. (2008). Inheritance of major spathe colors in *Anthurium andraeanum* Hort. is determined by three major genes. *HortScience* **43**(3): 787–791.
DOI: https://doi.org/10.21273/JASHS.115.1.169

Faraco M. *et al*. (13 authors) (2014). Hyper acidification of vacuoles by the combined action of two different P-ATPases in the tonoplast determines flower colour. *Cell Reports* **6**: 32–43.
DOI: https://doi.org/10.1016/j.celrep.2013.12.009

Geekiyanage S., Takase T., Ogura Y. & Kiyosue T. (2007). Anthocyanin production by over-expression of grape transcription factor gene VlmybA2 in transgenic tobacco and Arabidopsis. *Plant Biotechnology Reports* **1**: 11–18.
DOI: https://doi.org/10.1007/s11816-006-0001-4

Geekiyanage S. (2010). Potential of VlmybA1-2 as a candidate marker for visual identification of transgenic plants: induced anthocyanin production in arabidopsis and tobacco. *Tropical Agricultural Research and Extension* **12**(1): 35–41.
DOI: https://doi.org/10.4038/tare.v12i1.1982

Gonzalez A., Zhao M., Leavitt J.M. & Lloyd A.M. (2008). Regulation of the anthocyanin biosynthetic pathway by the TTG1/bHLH/Myb transcriptional complex in *Arabidopsis* seedlings. *The Plant Journal* **53**: 814–827.
DOI: https://doi.org/10.1111/j.1365-313X.2007.03373.x

Gopaulchan D., Umaharan P. & Lennon A. M. (2014). A molecular assessment of the genetic model of spathe color inheritance in *Anthurium andraeanum (Hort.). Planta* **239**(3): 695–705.
DOI: https://doi.org/10.1007/s00425-013-2007-9

Gopaulchan D., Lennon A.M. & Umaharan P. (2015). Expression analysis of the anthocyanin genes in pink spathes of anthurium with different color intensities. *Journal of the American Society for Horticultural Science* **140**(5): 480–489.
DOI: https://doi.org/10.21273/JASHS.140.5.480

Henny R.J. (1999). 'Red Hot' Anthurium. *HortScience* **34**(1): 153–154.
DOI: https://doi.org/10.21273/HORTSCI.34.1.153

Holton T.A. & Cornish E.C. (1995). Genetics and biochemistry of anthocyanin biosynthesis. *Plant Cell* **7**: 1071–1083.
DOI: https://doi.org/10.1105/tpc.7.7.1071

Hong Y., Li M. & Dai S. (2019). Ectopic expression of multiple chrysanthemum (*Chrysanthemum* × *morifolium*) R2R3-MYB transcription factor genes regulates anthocyanin accumulation in tobacco. *Genes (Basel)* **4**(10): 777. DOI: https://doi.org/10.3390/genes10100777

Hu D.G., Sun C.H., Ma Q.J., You C.X., Cheng L. & Hao Y.J. (2016). MdMYB1 regulates anthocyanin and malate accumulation by directly facilitating their transport into vacuoles in apples. *Plant Physiology* **170**(3): 1315–1330. DOI: https://doi.org/10.1104/pp.15.01333

Jayaprada N.V.T. & Geekiyanage S. (2016). Analysis of morphological and physiological aspects of the flowers of selected Sri Lankan blue flower species. *International Journal of Minor Fruits and Medicinal and Aromatic Plants* **2**(2): 1–5.

Jayaprada N.V.T. & Geekiyanage S. (2017). Analysis of morphological variation of Anthurium from Southern Sri Lanka. *Bangladesh Journal of Botany* **46**(2): 799–804.

Kamemoto H. & Sheffer R.D. (1978). A new species hybrid, *Anthurium scherzerianum Anthurium wendlingerii*1. *HortScience* **13**(2): 177–179. DOI: https://doi.org/10.21273/HORTSCI.13.2.177

Kamemoto H. & Kuehnle A.R. (1997). *Breeding anthuriums in Hawaii*. University of Hawaii Press, Hawaii.

Kobayashi S., Ishimaru M., Hiraoka K. & Honda C. (2002). Myb-related genes of the Kyoho grape (*Vitis labruscana*) regulate anthocyanin biosynthesis. *Planta* **215**: 924–933.

Li C., Qiu J., Yang G., Huang S. & Yin J. (2016). Isolation and characterization of a R2R3-MYB transcription factor gene related to anthocyanin biosynthesis in the spathes of *Anthurium andraeanum* (Hort.). *Plant Cell Reports* **35**: 2151–2165. DOI: https://doi.org/10.1007/s00299-016-2025-8

Li C., Qiu J., Huang S., Yin J. & Yang G. (2019a). AaMYB3 interacts with AabHLH1 to regulate proanthocyanidin accumulation in *Anthurium andraeanum* (Hort.)—another strategy to modulate pigmentation. *Horticulture Research* **6**. DOI: https://doi.org/10.1038/s41438-018-0102-6

Li C., Qiu J., Yang G., Huang S. & Yin J. (2019b). Ectopic expression of the *Anthurium andraeanum* (Hort.) R2R3-MYB genes AaMYB4 and AaMYB5 enhance the flower color in transgenic tobacco. *Plant Cell, Tissue and Organ Culture (PCTOC)* **139**: 105–117. DOI: https://doi.org/10.1007/s11240-019-01667-7

Li Y., Shan X., Zhou L., Gao R., Yang S., Wang S., Wang L. & Gao X. (2019). The R2R3-MYB factor FhMYB5 from Freesia hybrida contributes to the regulation of anthocyanin and proanthocyanidin biosynthesis. *Frontiers in Plant Science* **9**: 1935. DOI: https://doi.org/10.3389/fpls.2018.01935

Lin-Wang K., Bolitho K., Grafton K., Kortstee A., Karunairetnam S., McGhie T.K., Espley R.V., Hellens R.P. & Allan A.C. (2010). An R2R3 MYB transcription factor associated with regulation of the anthocyanin biosynthetic pathway in Rosaceae. *BMC Plant Biology* **10**(1): 1–17. DOI: https://doi.org/10.1186/1471-2229-10-50

Morita Y. & Hoshino A. (2018). Recent advances in flower color variation and patterning of Japanese morning glory and petunia. *Breeding Science* **68**: 128–138. DOI: https://doi.org/10.1270/jsbbs.17107

Noda N. (2018). Recent advances in the research and development of blue flowers. *Breeding Science* **68**: 79–87. DOI: https://doi.org/10.1270/jsbbs.17132

Noman A., Aqeel M., Deng J., Khalid N., Sanaullah T. & Shuilin H. (2017). Biotechnological advancements for improving floral attributes in ornamental plants. *Frontiers in Plant Science* **8**: 530. DOI: https://doi.org/10.3389/fpls.2017.00530

Okitsu N., Noda N., Chandler S. & Tanaka Y. (2018). Flower color and its engineering by genetic modification. In: *Ornamental Crops*, pp. 29–62. Springer, USA. DOI: https://doi.org/10.1007/978-3-319-90698-0_3

Osorio-Guarín J.A., Gopaulchan D., Quanckenbush C., Lennon A.M., Umaharan P. & Cornejo O.E. (2021). Comparative transcriptomic analysis reveals key components controlling spathe color in *Anthurium andraeanum* (Hort.). *Plos One* **16**(12): e0261364. DOI: https://doi.org/10.1371/journal.pone.0261364

Puchooa D. (2005). *In vitro* mutation breeding of Anthurium by gamma radiation. *International Journal of Agriculture and Biology* **7**(1): 11–20.

Rodríguez H.G., Maiti R. & Kumari C.A. (2020). Influence of pH on coloration of anthocyanin and betalaine. In *Experimental Ecophysiology and Biochemistry of Trees and Shrubs*, pp. 81–88. Apple Academic Press, Florida, USA. DOI: https://doi.org/10.2307/4448451

Saigo T., Wang T., Watanabe M. & Tohge T. (2020). Diversity of anthocyanin and proanthocyanin biosynthesis in land plants. *Current Opinion in Plant Biology* **55**: 93–99. DOI: https://doi.org/10.1016/j.pbi.2020.04.001

Sangeetha Priya S., Bhatt S., Bhatt T. & Chawla L. (2020). Approaches for modification of flower colour–a review. *Journal of Emerging Technologies and Innovative Research* **7**(4): 1337–1343. DOI: https://www.jetir.org/view?paper=JETIR2004379

Shitan N. & Yazaki K. (2020). Dynamism of vacuoles toward survival strategy in plants. *Biochimica et Biophysica Acta (BBA)-Biomembranes* **1862**(12): 183127. DOI: https://doi.org/10.1016/j.bbamem.2019.183127

Spelt C., Quattrocchio F., Mol J. & Koes R. (2002). ANTHOCYANIN1 of petunia controls pigment synthesis, vacuolar pH, and seed coat development by genetically distinct mechanisms. *Plant Cell* **14**: 2121–2135. DOI: https://doi.org/10.1105/tpc.003772

Sundaramoorthy J., Park G.T., Lee J.D., Kim J.H., Seo H.S. & Song J.T. (2020). A P3A-type ATPase and an R2R3-MYB transcription factor are involved in vacuolar acidification and flower coloration in soybean. *Frontiers in Plant Science* **11**: 1880. DOI: https://doi.org/10.1105/tpc.003772

Verweij W., Spelt C., Di Sansebastiano G.P., Vermeer J., Reale L., Ferranti F., Koes R. & Quattrocchio F. (2008). An H^+ P-ATPase on the tonoplast determines vacuolar pH and flower colour. *Nature Cell Biology* **10**: 1456–1462. DOI: https://doi.org/10.1038/ncb1805

Wang Y., Zhou L.J., Wang Y., Geng Z., Ding B., Jiang J., Chen S. & Chen F. (2022). An R2R3-MYB transcription factor CmMYB21 represses anthocyanin biosynthesis in color fading petals of chrysanthemum. *Scientia Horticulturae* **293**: 110674. DOI: https://doi.org/10.1016/j.scienta.2021.110674

Yan H., Pei X., Zhang H., Li X., Zhang X., Zhao M., Chiang V.L., Sederoff R.R. & Zhao X. (2021). MYB-mediated regulation of anthocyanin biosynthesis. *International Journal of Molecular Science* **22**(6): 3103. DOI: https://doi.org/10.3390/ijms22063103

Zhang G.T., Qi H., Yang S.N., Chu Z.Y., Tian T., Yuan S.X. & Liu C. (2021). Research progress of floral organ vacuole pH regulating flower color formation. *Biotechnology Bulletin* **37**(4): 204. DOI: https://doi.org/10.13560/j.cnki.biotech.bull.1985.2020-0615

J.Natn.Sci.Foundation Sri Lanka 2023 51 (4): 643 - 650
DOI: http://dx.doi.org/10.4038/jnsfsr.v51i4.11256

RESEARCH ARTICLE

Moleculalar Pathology

Whole exome sequencing coupled with *in silico* functional analysis identified *NID1* as a novel candidate gene causing neuro-psychiatric disorder in a Pakistani family

M Muzammal[1], S Ahmad[1], MZ Ali[1], S Fatima[1], S Abbas[1], J Khan[2], H Ullah[1], W Shah[3], L Duan[4*] and MA Khan[1*]

[1] *Gomal Centre of Biochemistry and Biotechnology, Gomal University Dera Ismail Khan, KP, Pakistan.*
[2] *Institute of Biological Sciences, Gomal University Dera Ismail Khan, KP, Pakistan.*
[3] *University of Science and Technology of China, Hefei, Anhui, China.*
[4] *Department of Reproduction Andrology, Sichuan Jinxin Xinan Woman & Childern Hospital, Chengdu, Sichuan, China.*

Submitted: 23 June 2022; Revised: 6 June 2023; Accepted: 27 June 2023

Abstract: Intellectual disability (ID) is a neuro-developmental condition that affects a person's cognitive ability and results in a learning defect. It affects 1–3% of the general population; however, the ratio may be expected to be more in a consanguineous population. Herein in the present study, we identified a nuclear family from Dera Ismail Khan City in Pakistan. Whole exome sequencing was performed to map the pathogenic variant. Protein structural modeling and interaction studies were carried out to validate the variant with disease-association. Molecular modeling of normal and mutated proteins was performed through I-TASSER and Chimera tools, while docking and interaction analysis was carried out using Cluspro. Clinical analysis of the patient determined mild intellectual disability and gait problem. Candidate gene analysis in this family found a homozygous missense mutation NM_002508:c.C2512T (p.Arg838Cys) in the 12th exon of *NID1* gene. Molecular modeling of wild-type and mutant NID1 proteins determined a significant effect on the protein's secondary and tertiary structure. Hence, based on the exome sequence analysis, *NID1* is proposed to be a strong novel candidate ID gene in this family. The genetic mapping of the present family led us to determine a novel candidate gene to be associated with intellectual disability. Linkage of additional ID families with genes would confirm its validity and strengthen our notion. Furthermore, expression studies and pathway analysis will help in exploring the biological mechanism of learning and memory.

Keywords: Exome sequencing, ID, NID1, novel candidate gene, Pakistani family.

INTRODUCTION

Intellectual disability (ID) is a neurological defect that occurred due to anomalies of the brain. Previously, ID was also known as mental retardation, learning defect or developmental delay (Ropers, 2010). Intellectual defect results in loss of social adaptive skills and usually occurs before the age of 18 (WHO, 1992). The worldwide prevalence of ID ranges from 1 to 3% (APA, 2013). Precisely, its prevalence is 1 to 2% in developed countries and 2 to 3% in less developed countries like Pakistan (Durkin, 2002; Maulik *et al*., 2011). However, its incidence is speculated to be high in those countries where the rate of cousin marriages is high (Salvador-Carulla *et al*., 2008). Based on the intelligence quotient (IQ) value, ID is characterized into mild (IQ range 55> - >69), moderate (IQ range 35> - >54), severe (IQ range 20> - >34) and profound (IQ range below 19) (Ahmed *et al*., 2021). Phenotypically, ID is categorized as syndromic and non-syndromic intellectual disability (NS-ID). In syndromic ID, the individual suffers from additional biological anomalies, while in NS-ID, the individual is merely suffering from

* Corresponding authors (675068375@qq.com; m.ahmad@gu.edu.pk; https://orcid.org/0009-0000-1105-2154; https://orcid.org/0000-0001-8591-0377)

learning defect, as in the case of autosomal recessive non-syndromic intellectual disability (ARNSID) (Bittles & Black, 2010). Much research has documented that approximately 10% of marriages worldwide are between blood relatives (*https://www.ncbi.nlm.nih.gov/omim/*), but its frequency is much higher in Central Asian regions especially Pakistan, India, and Iran. In Pakistan, the exact number of intellectually disabled children is still unknown due to unavailability of any proper survey. According to the census of 1998, Pakistan has 2.5% of people suffering from different kinds of disabilities. Until now, 75 genes/loci are enlisted in the Online Mendelian Inheritance in Man (OMIM) database (*https://www.ncbi.nlm.nih.gov/omim/*) involved in NS-ARID.

Almost 560 genes have been associated with intellectual disability (*https://www.omim.org*). All the modes of Mendelian heredity (*i.e.*, autosomal recessive, autosomal dominant, or X-linked) are associated with intellectual disabilities. Physiologically, these reported genes are involved in various cellular signaling cascades, inter-neuronal connectivity, neuronal proliferation, neuronal migration, and the extensive guideline of genetic/epigenetic transcription and translation (Muzammal *et al.*, 2022). Improvement in identifying genes accountable for the worldwide developmental delays and intellectual impairment has expanded our knowledge of the molecular mechanism in learning and memory, which is essential for understanding cognition and intelligence from a neurological perspective. Growing awareness of molecular pathology will assist in finding new pharmacological methodologies (Muzammal *et al.*, 2022).

The current genetic study reported a Pakistani family to have the causative genetic factors of ARID. The current ID family was recruited from Dera Ismail Khan City of Pakistan. Exome sequence analysis in this family found a novel missense mutation NM_002508:c.C2512T (p.Arg838Cys) in the *NID1* gene.

MATERIALS AND METHODS

The current study was approved by the institutional Ethical Review Board of Gomal University, D.I. Khan, Pakistan, and supported by the Higher Education Commission (HEC) of Pakistan through an NPRU grant (project #5564/KPK/NRPU/R&D/HEC/2016). Venous blood samples were obtained from patients and normal individuals (including parents) of the affected family as per the standard protocols, and kept at 4^0C in EDTA tubes. and DNA was extracted using DNeasy Blood Kit (Qiagen).

Genetic analysis

The positional cloning approach was adopted for gene mapping, which involved whole exome sequencing (WES), homozygosity mapping (based on SNP data of WES), and candidate gene and/or variant prioritization. The detailed description of gene mapping and mutation analysis is outlined as follows.

Whole exome sequencing

Whole exome sequencing was done on NextSeq500 platform, using Nextera rapid capture exome kit for library construction, following the manufacturer's protocol (Illumina, San Diego, USA).

For candidate gene analyses, several online tools were employed, *e.g.*, Exomiser (*https://monarch-exomiser-web dev.monarchinitiative.org*), PhenIX (*http://compbio.charite.de/PhenIX/*), ENDEVOUR (*https://endeavour.esat.kuleuven.be*), and ToppGene (*https://www.toppgene.cchmc.org*).

Protein Secondary structure prediction

The secondary structure of the protein was predicted through PSI-blast based secondary structure Prediction (PSIPRED) tool (McGuffin *et al.*, 2000). This method is used to examine the folding pattern of protein secondary structure.

Protein 3D Modeling and docking

I-TASSER online (Yang & Zhang, 2015) tool was used to design the 3D models of normal and mutant NID1 protein and its close interactor. Model with top confidence score (C-Score) was selected for further investigation (Muzammal *et al.*, 2022). Chimera 1.13.1 (Goddard *et al.*, 2007) was used to visualized the designed 3D models (Ali *et al.*, 2022). Protein-protein docking was carried out with its close functional interactors through an online tool called Cluspro server (Kozakov *et al.*, 2017).

RESULTS AND DISCUSSION

The current genetic study was conducted on a Saraiki origin consanguineous Pakistani family suffering from NS-ID, and *NID1* was identified as novel candidate gene involved in NS-ID.

The family was recruited from Dera Ismail Khan City. The nuclear family consisted of an affected father

(I:1), normal mother, and six children with one affected daughter (II: 3). The pedigree analysis apparently determined autosomal recessive mode of disease inheritance (Figure 1a). The patients were suffering from mild intellectual impairment with low IQ. The affected father also had some psychiatric problems and had attention deficit. The female patient (II: 3) had Gait issue, attention deficits, and kidney issues. The general phenotypes of patients were consistent with AR-NSID. Whole exome sequencing was selectively performed on patient II:3. The rest of the clinical details are described in Table 1.

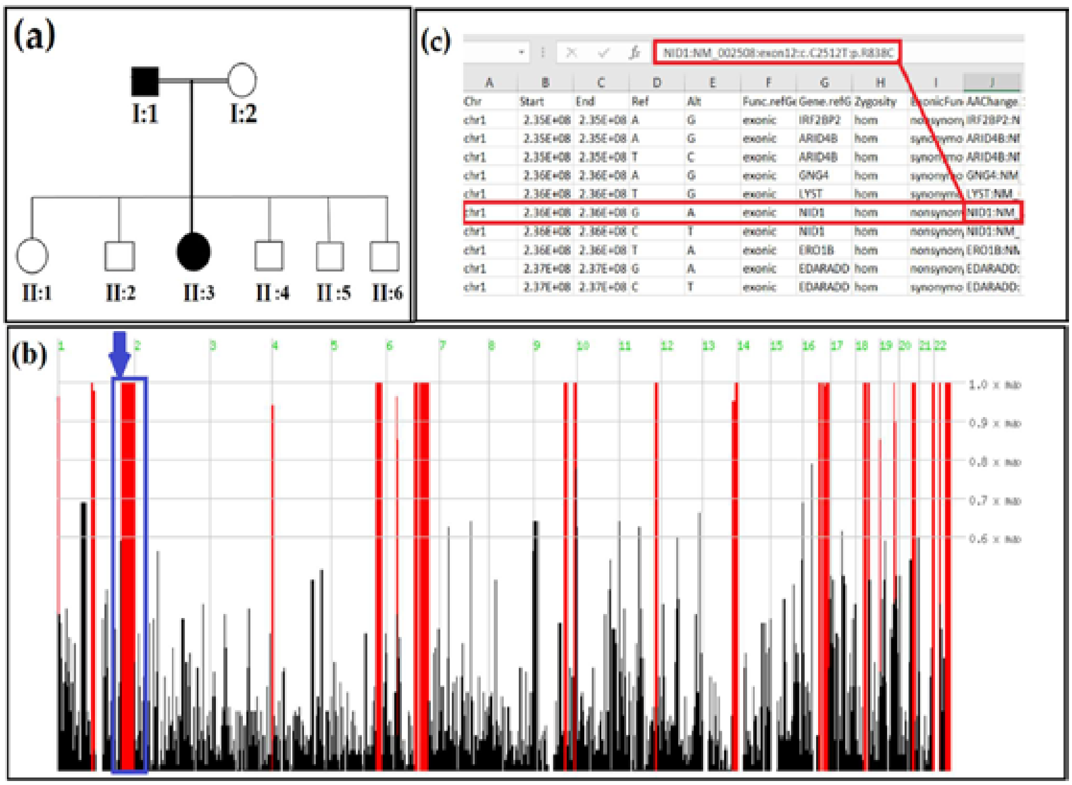

Figure 1: a) Pedigree of the family showing autosomal recessive mode of inheritance, (b) screenshot homozygosity mapper showing the homozygous region, largest region on chromosome is highlighted in the blue box. (c) Presence of candidate gene NID1 variant in the exome file.

Genetic analysis

Candidate gene analysis

Whole exome analysis found a total of 23,600 variants. Through homozygosity mapper, HBD analysis found a large significant homozygous region on chromosome 1 (chr1:206579936-240371106), spanning a 33.7 Mb region on DNA. The subsequent exome analysis, with primary target on the large homozygous region coupled with screening of the top 10 candidate genes identified through different candidate gene analysis tools, identified homozygous single nucleotide substitution in NM_002508: c.C2512T:(p.Arg838Cys) in the 12th exon of the *NID1* gene (Figure 1 b & 1c). The identified variant (rs763658641) has a minor allele frequency of 0.000003 in ExAC and 0.000015 in the gnomAD exomes databases.

However, the clinical significance of this variant is not reported in the Clinvar database. ACMG-AMP classification categorized this variant as VUS (variant of unknown significance).

Table 1: Clinical features of patients (I:1 and II:3)

Phenotypes	II:3	I:1
Gender	Female	Male
Level of intellectual disability	Mild	Mild
Kidney stone	Yes	No
Muscular degeneration	Yes	No
Gait problem	Yes	No
Epileptic fits	No	No
Hearing problem	No	No
Dermal lesion	No	No
Psychiatric phenotypes	Late responsive, *i.e.*, attention deficit	Late responsive, *i.e.*, attention deficit
Jerking of limbs	Yes	No
Self-feeding	Yes	Yes
Microcephaly features	No	No
Macrocephaly features	No	No
Digit anomaly	No	No
Facial dysmorphism	No	No
Obesity	No	No
Shape and length of digits	Normal	Normal
Ophthalmic issues	No	No

In silico analysis

Secondary structure prediction of wild-type and mutant NID1 proteins

Secondary structure comparison of normal and mutant NID1 protein revealed different changes in the folding pattern (highlighted in red boxes). These changes were detected both in upstream and downstream regions from the site of mutation (highlighted in the purple box). These changes were present on the mutant protein's strand, helix, and coil. Changes observed in the mutant protein can be clearly seen in the Figure 2b.

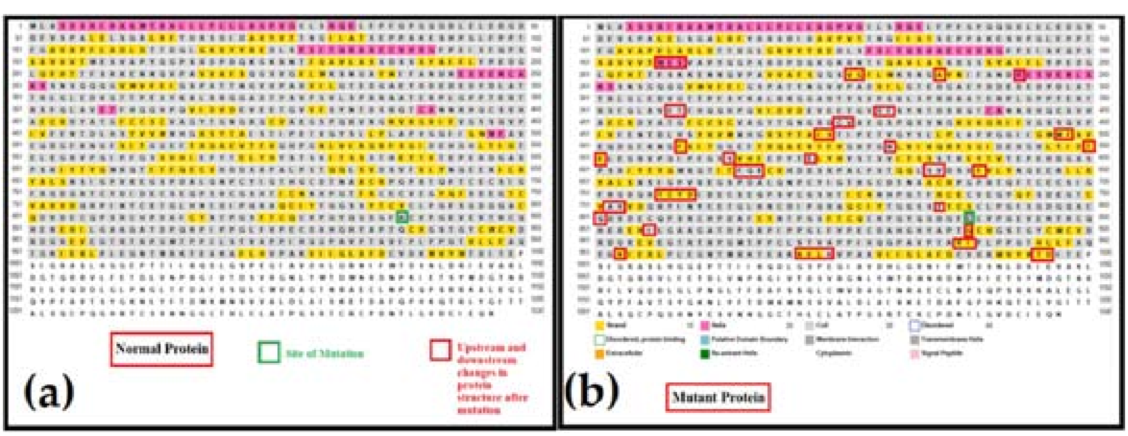

Figure 2: Secondary structure wild-type (a) and mutant NID1 protein (b) predicted through PSIPRED tools. Showing the site of mutation in green box, upstream and downstream changes after mutation are highlighted in red boxes.

Protein tertiary structure and interaction analysis

Superimposed 3D models of NID1 wild-type and mutant proteins determined a similarity index of 77.15% and different changes in folding of the 3D structure were observed (Figure 3). Protein-protein interaction of wild-type and mutant NID1 protein were done with their close functional interactor LAMC1 protein, which showed great changes in the interacting residues of all the wild-type and mutant proteins with their interactors (Figure 4). The mutant NID1 protein showed less interaction with its close interactor LAMC1 protein, *i.e.*, via 4 hydrogen bonds and 1 salt bridge only, while in the case of wild-type NID1 protein, its interaction with LAMC1 protein was through 17 hydrogen bonds and 2 salt bridges. Complete details of all the interacting residues of wild-type and mutant NID1 proteins with their close interactor are shown in Table 2.

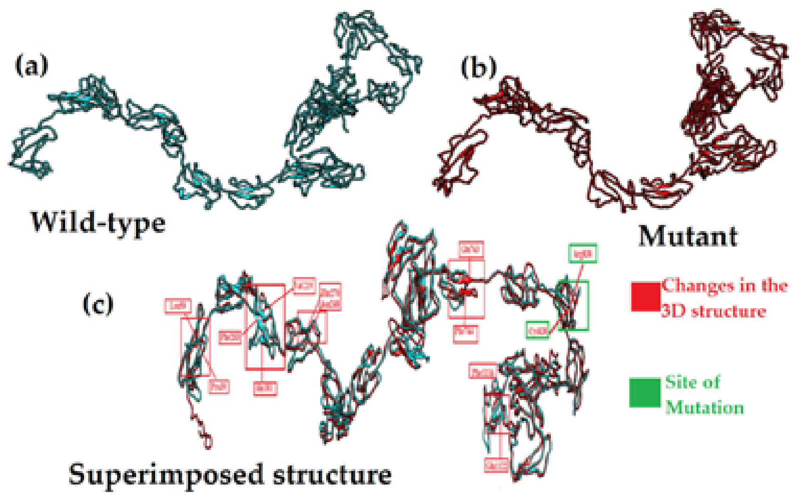

Figure 3: (a) 3D structure of wild-type NID1 protein; (b) 3D structure of mutant NID1 protein; (c) superimposed structure of wild-type and mutant NID1 protein.

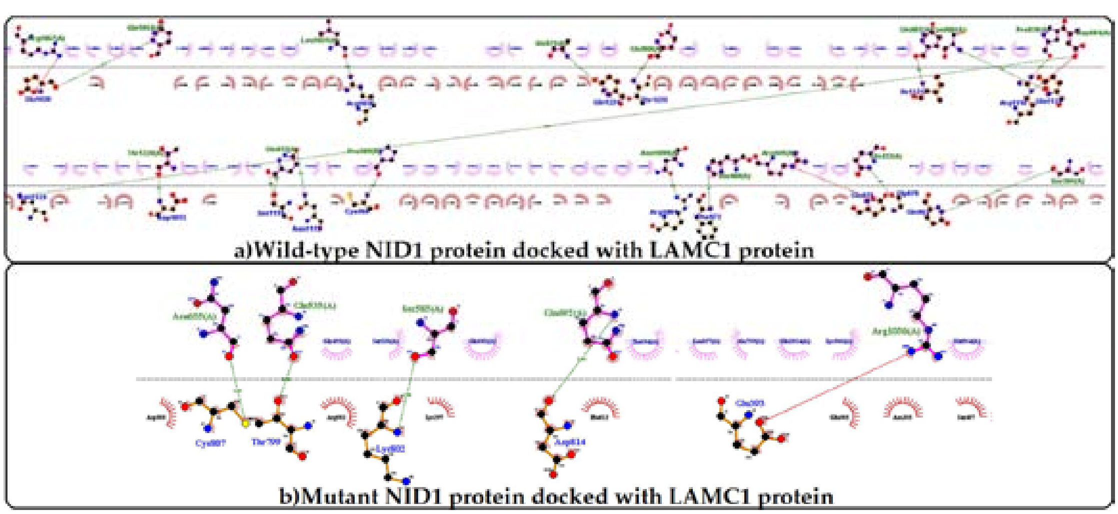

Figure 4: (a) Protein-protein interaction of wild-type NID1 and its close interactor LAMC1 protein; (b) protein-protein interaction of mutant NID1 and its close interactor LAMC1 protein

Table 2: Protein-Protein interaction of wild-type and Mutant NID1 proteins with LAMC1 protein

Protein	Interacting resides with LAMC1 protein	No and type of bonds
Wild-type NID1 protein	Glu1030, Arg1036, Gln1224, Thr1225, Ile1124, Arg1116, Glu1125, Asn1129, Asp1013, Ser1115, Asn119, Cys968, Arg1004, Phe973, Glu978, Gly979, Gln963	17 hydrogen bonds and 2 salt bridges
Mutant NID1 protein	Cys807, Thr799, Lys802, Asp814 and Glu393, and Tyr116	4 hydrogen bonds and 1 salt bridge

Discussion

The present family was recruited from Dera Ismail Khan city and ethnically it belonged to a Saraiki origin population. This family had 2 affected individuals, *i.e.*, an affected father (I: 1) and his daughter (II: 3). Both the patients were suffering from mild intellectual disability. The patient (II: 3) had some additional anomalies like attention deficits, a walking problem, and a kidney problem (Table 1). Molecular investigation in this family found a homozygous missense variant NM_002508: c.C2512T:(p.Arg838Cys) in the 12^{th} exon of the *NID1* gene. Allele frequency of this variant in multiple population databases was found to be very low. The additional convincing evidence for *NID1* gene involvement included the presence of the variant in a large stretch of homozygous regions (Figure 1c), high expression of *NID1* gene in the brain, and strong evolutionary conservation of the substituted amino acid (p.Arg838) due to missense mutation (Figure 5). Not only p.Arg838 was conserved but the entire region was highly conserved throughout different species (Figure 5).

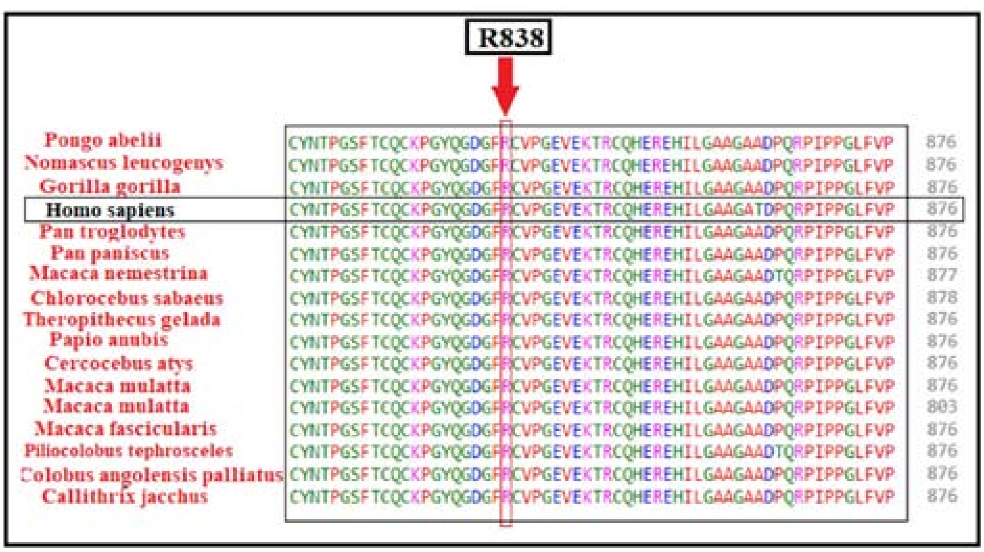

Figure 5: Conserved sequence alignment of substituted amino-acid. Position of substituted amino acid (R838) is given in red box.

Mattei *et al.* (1989) localized the human *NID1* gene to chromosome 1. Later in 1995, Zimmermann *et al.* (1995) described the *NID1* and documented that it consists of 20 exons with a genomic size of about 90kb. The NID1 protein consists of 1247 amino acids. Each exon encodes individual protein subdomains. The *NID1* gene codes a member of the nidogen family of basement membrane glycoproteins. The protein interacts with several other components of basement membranes, and may play a role in cell interactions with the extracellular matrix (Zimmermann *et al*., 1995). Jenkins *et al.* (1991) mapped the nidogen gene (Nid) to mouse chromosome 13 and found a linkage to the beige (bg) mutation. The bg mutation is supposed to be the mouse homologue of the Chediak-Higashi syndrome (CHS). Major phenotypes of CHS comprise muscle stiffness, developmental delay, mental deficiency, and skin problems etc. (Jenkins *et al*., 1991).

Murshed *et al.* (2000) produced Nid1-deficient mice and noted that homozygous mice produced neither mRNA nor protein. Astonishingly, the homozygous mice were fertile and their basement membranes appeared normal, though Nid2 expression was much greater in certain basement membranes (Murshed *et al*., 2000). Darbo *et al.* (2013) described a large Vietnamese family with Dandy-Walker malformation with occipital cephalocele. They found a heterozygous mutation c.C1162T (p.Gln388*) in the *NID1* gene, which probably results in the complete truncation of the G2 and G3 regions of NID1 (Darbo *et al*., 2013).

Dong and his co-workers in 2002 targeted the disruption of the *NID1* in the mouse presented in their study and found a duplication of the entacin-1 locus. Homozygous mutants for the functional locus lacked NID1 mRNA and protein and often displayed seizure-like symptoms and loss of muscle control in the back legs (similar features were present in patient II:3) (Dong *et al*., 2002; Alazami *et al*., 2015). The behavior patterns suggested the presence of neurologic deficits in the CNS, thus providing genetic evidence linking entactin-1 to proper neuromuscular system functions. In homozygous mutants, structural alterations in the basement membranes were found only in selected tissues, *i.e.*, brain capillaries and the lens capsule. The structure of the basement membranes in other tissues were observed to be normal. These findings showed that the lost functions of NID1 protein results in pathologic alterations that are extremely tissue specific.

Based on the expression and animal studies, it can be showed that NID1 has significant linkage with intellectual functioning and cognition. Our patients did not disclose previously documented features, except ID, due to *NID1* gene mutation. Hence, to the best of our knowledge, *NID1* is a novel candidate gene to be involved in a new phenotype of non-syndromic ID.

CONCLUSION

The present genetic study reported a novel candidate *NID1* (c.C2512T; p.Arg838Cys) responsible for causing non-syndromic ID. Mutagenesis and cellular based expression studies on the novel identified *NID1* gene will further explore the molecular function of this gene. Linkage of additional ID families with this gene will strengthen the power of this study and assist in molecular diagnostics.

Acknowledgements

The authors are grateful to all intellectual disability family members for their voluntary participation in the present study, and the Higher Education Commission of Pakistan for supporting the present study through an NPRU grant (5564/KPK/NRPU/R&D/HEC/2016).

Data availability

The computational data are available upon request.

REFERENCES

Ahmed I., Muzammal M., Abbasi S.W., Khan M.A. & Mir A. (2021). Whole exome analysis in consanguineous Pakistani families determined ROR2 and RPTN as novel candidate genes to be involved in autosomal recessive non-syndromic intellectual disability. *International Journal of Computational Intelligence in Control* **13**(2): 163–171.

Alazami A.M., Patel N., Shamseldin H.E., Anazi S., Al-Dosari M.S., Alzahrani F. & Alkuraya F. S. (2015). Accelerating novel candidate gene discovery in neurogenetic disorders via whole-exome sequencing of prescreened multiplex consanguineous families. *Cell Reports* **10**(2): 148–161. DOI: https://doi.org/10.1016/j.celrep.2014.12.015

Ali M.Z. *et al.* (12 authors) (2022). In silico analysis identified putative pathogenic missense nsSNPs in human SLITRK1 gene. *Genes* **13**: 672. DOI: https://doi.org/10.3390/genes13040672

American Psychiatric Association (APA)(2013). *Diagnostic and Statistical Manual of Mental Disorders (DSM-5®)*. American Psychiatric Association, Washington DC, USA. DOI: https://doi.org/10.1176/appi.books.9780890425596

Bittles A.H. & Black M.L. (2010). Consanguinity, human evolution, and complex diseases. *Proceedings of the National Academy of Sciences* **107**(suppl 1): 1779–1786. DOI: https://doi.org/10.1073/pnas.0906079106

Darbro B.W., Mahajan V.B., Gakhar L., Skeie J.M., Campbell E., Wu S. & Bassuk A.G. (2013). Mutations in extracellular matrix genes NID1 and LAMC1 cause autosomal dominant D andy-Walker malformation and occipital cephaloceles. *Human Mutation* **34**(8): 1075–1079. DOI: https://doi.org/10.1002/humu.22351

Dong L., Chen Y., Lewis M., Hsieh J.C., Reing J., Chaillet J.R. & Chung A.E. (2002). Neurologic defects and selective disruption of basement membranes in mice lacking entactin-1/nidogen-1. *Laboratory Investigation* **82**(12): 1617–1630. DOI: https://doi.org/10.1097/01.LAB.0000042240.52093.0F

Durkin M. (2002). The epidemiology of developmental disabilities in low income countries. *Mental Retardation and Developmental Disabilities Research Reviews* **8**(3): 206–211.
DOI: https://doi.org/10.1002/mrdd.10039

Goddard T.D., Huang C.C. & Ferrin T.E. (2007). Visualizing density maps with UCSF Chimera. *Journal of Structural Biology* **1**(157): 281–287.
DOI: https://doi.org/10.1016/j.jsb.2006.06.010

http://compbio.charite.de/PhenIX/, accessed at 25 Jan 2021.

https://endeavour.esat.kuleuven.be, accessed at 20 Jan 2021.

https://monarch-exomiser-webdev.monarchinitiative.org, accessed at 16th Jan 2021.

https://www.ncbi.nlm.nih.gov/omim/, a Accessed at 16 May 2022.

https://www.toppgene.cchmc.org, a Accessed at 30 Jan 2021.

Jenkins N.A., Justice M.J., Gilbert D.J., Chu M.L. & Copeland N.G. (1991). Nidogen/entactin (Nid) maps to the proximal end of mouse chromosome 13 linked to beige (bg) and identifies a new region of homology between mouse and human chromosomes. *Genomics* **9**(2): 401–403.
DOI: https://doi.org/10.1016/0888-7543(91)90275-J

Kozakov D., Hall D.R., Xia B., Porter K.A., Padhorny D., Yueh C. & Vajda S. (2017). The ClusPro web server for protein–protein docking. *Nature Protocols* **12**(2): 255–278.
DOI: https://doi.org/10.1038/nprot.2016.169

Mattei M.G., Passage E., Weil D., Nagayoshi T., Knowlton R.G., Chu M.L. & Uitto J. (1989). Chromosomal mapping of human basement-membrane zone genes-laminin a chain At Locus 18p11. 31 and Nidogen At Locus 1q43. *In Cytogenetics and Cell Genetics* **51**(4): 1041–1041.

Maulik P.K., Mascarenhas M.N., Mathers C.D., Dua T. & Saxena S. (2011). Prevalence of intellectual disability: a meta-analysis of population-based studies. *Research in Developmental Disabilities* **32**(2): 419–436.
DOI: https://doi.org/10.1016/j.ridd.2010.12.018

McGuffin L.J., Bryson K. & Jones D.T. (2000). The PSIPRED protein structure prediction server. *Bioinformatics* **16**(4): 404–405.
DOI: https://doi.org/10.1093/bioinformatics/16.4.404

Murshed M., Smyth N., Miosge N., Karolat J., Krieg T., Paulsson M. & Nischt R. (2000). The absence of nidogen 1 does not affect murine basement membrane formation. *Molecular and Cellular Biology* **20**(18): 7007–7012.
DOI: https://doi.org/10.1128/MCB.20.18.7007-7012.2000

Muzammal M. *et al.* (11 authors) (2022). In silico analysis of the L-2-hydroxyglutarate dehydrogenase gene mutations and their biological impact on disease etiology. *Genes* **13**: 698.
DOI: https://doi.org/10.3390/genes13040698

Ropers H.H. (2010). Genetics of early onset cognitive impairment. *Annual Review of Genomics and Human Genetics* **11**: 161–187.
DOI: https://doi.org/10.1146/annurev-genom-082509-141640

Salvador-Carulla L., Rodríguez-Blázquez C. & Martorell A. (2008). Intellectual disability: an approach from the health sciences perspective. *Salud Pública de México* **50**(S2): 142–150.
DOI: https://doi.org/10.1590/S0036-36342008000800006

World Health Organization (WHO) (1992). The ICD-10 classification of mental and behavioural disorders: clinical descriptions and diagnostic guidelines, volume 1. World Health Organization, Geneva, Switzerland.

Yang J. & Zhang Y. (2015). I-TASSER server: new development for protein structure and function predictions. *Nucleic Acids Research* **1**(43): 174–181.
DOI: https://doi.org/10.1093/nar/gkv342

Zimmermann K., Hoischen S., Hafner M. & Nischt R. (1995). Genomic sequences and structural organization of the human nidogen gene (NID). *Genomics* **27**(2): 245–250.
DOI: https://doi.org/10.1006/geno.1995.1038

J.Natn.Sci.Foundation Sri Lanka 2023 51 (4): 651 - 659
DOI: http://dx.doi.org/10.4038/jnsfsr.v51i4.11483

RESEARCH ARTICLE

Bioremediation

Biodegradation of the cyanotoxin cylindrospermopsin by *Bacillus cereus*, *Micrococcus luteus* and *Alcaligenes faecalis*

HT Peduruarachchi [1], GY Liyanage [1,2], FS Idroos [1], EMMS Ekanayake [1,3] and PM Manage [1]

[1] *Centre for Water Quality and Algae Research, Department of Zoology, Faculty of Applied Sciences, University of Sri Jayewardenepura, Nugegoda, Sri Lanka.*

[2] *Department of Aquatic Bioresources, Faculty of Urban and Aquatic Bioresources, University of Sri Jayewardenepura, Wijerama Ln, Nugegoda, Sri Lanka.*

[3] *Department of Aquaculture and Fisheries, Faculty of Livestock, Fisheries and Nutrition, Wayamba University of Sri Lanka, Makandura, Gonawila (NWP), Sri Lanka.*

Submitted: 23 November 2022; Revised: 27 June 2023; Accepted: 22 September 2023

Abstract: Cylindrospermopsin (CYN) is a cyanotoxin found in natural waters, with potential risk to human health through the inhibition of protein synthesis. Despite the implementation of conventional water treatment procedures, complete removal of CYN remains a question due to its heat-stable nature. Hence, contamination of water sources with CYN is a challenge in providing safe drinking water throughout the world. The present study was conducted to test the ability to degrade CYN at 28^{0}C and pH 7, of four bacterial strains: *Bacillus cereus*-Y, *Bacillus cereus*-S (*B. cereus*-S), *Micrococcus luteus*, and *Alcaligenes faecalis*, which were previously isolated from different water sources as different hydrocarbon degraders. The CYN degradation kinetics of each bacterial species were studied using High Performance Liquid Chromatography. The greatest CYN degradation (28.22 ± 0.24%) was shown by the bacterium *B. cereus*-S in 5.0 mg/L CYN within 14 days. The CYN degradation by the other strains was lower than 10% under the same conditions. Further studies employing different initial concentrations of CYN revealed that *B. cereus*-S could degrade lower CYN concentrations at a higher percentage (1.0 mg/L, 2.5 mg/L, and 5.0 mg/L of CYN removal percentages were 36.83 ± 2.43%, 32.25 ± 1.25%, and 24.72 ± 0.40%, respectively, after 14 days of incubation at 28^{0}C and pH 7). The maximum average degradation rates were recorded for 1.0 mg/L, 2.5 mg/L, and 5.0 mg/L CYN on the 6th (0.05 ± 0.00 mg/L/day), 8th (0.04 ± 0.01 mg/L/day), and 12th (0.02 ± 0.01 mg/L/day) days of incubation, respectively. The study showed the potentiality of the bacterium *B. cereus*-S on the application for degrading CYN among the tested bacteria species.

Keywords: *Bacillus cereus*-S, biodegradation, cyanotoxin, cylindrospermopsin, hepatotoxic.

INTRODUCTION

Cyanobacteria are a group of prokaryotic microorganisms, which belong to the kingdom Bacteria. They produce cyanotoxins which are secondary metabolites, and these cyanotoxins are found in a range of chemical groups. Cylindrospermopsins (CYNs), a specific group of cyanotoxins, were initially isolated from the cyanobacterium, *Raphidiopsis raciborskii* (previously known as *Cylindrospermopsis raciborskii*). CYNs have since been detected in surface water bodies worldwide, with different cyanobacterial producers. CYN is an alkaloid with three distinct groups of tricyclic guanidine, uracil, and sulphate. It posse a molecular weight of 415.2 g/mol and is soluble in water and organic solvents (Adamski *et al*., 2014). Furthermore, the toxin shows stability at room temperature (21 ± 1°C) and in a wide pH range (3, 5, 7) (Adamski *et al*., 2016).

CYNs enter the human body via different pathways, such as dermal contact during bathing, swimming, and other recreational activities and ingestion of water or food that are contaminated with CYN (Pichardo *et al*., 2017). In most cases of CYN toxicity, the environmental concentrations of CYN have been recorded within the range of 1–10 µg/L, while exceptional values have been reported from aquaculture farms and farm dams in Australia (Pichardo *et al*., 2017). CYN has been detected in mollusks, crustaceans, and fish with the maximum

* Corresponding author (hirushitp@gmail.com; https://orcid.org/0000-0003-4971-1172)

detection range of 0.00007–4.3 µg/g in Redclaw crayfish (*Cherax quadricarinatus*) in Australia. Certain studies suggest that CYN has a bioaccumulation factor (BAF) of 4–171, indicating the potential to bioaccumulate in aquatic species (Scarlett *et al*., 2020). During chronic toxicity, it acts as a hepatotoxin, resulting in severe liver necrosis (Abeysiri *et al*., 2021b). Further, it affects kidneys (Abeysiri *et al*., 2021c) and has the potential to cause cytotoxicity (Poniedziałek *et al*., 2014; Abeysiri *et al*., 2021a; Chichova *et al*., 2021). It has been reported that CYN has the potential to inhibit the synthesis of proteins such as globin and antioxidants such as glutathione, leading to oxidative stress (López-Alonso *et al*., 2013). Moreover, prolonged exposure to CYNs could result in genotoxicity, immunotoxicity, and tumour initiations (Pichardo *et al*., 2017).

Numerous studies have confirmed the presence of CYN producing cyanobacteria, including *Raphidiopsis* sp., in water bodies of Sri Lanka. It is evident from these reports that *Raphidiopsis* sp. was not significantly dominant prior to the 20th century in Sri Lanka. The species has spread widely during 20th century, which might be due to increased human habitation that led to an increased number of point and non-point sources of aquatic pollution (Jayatissa *et al*., 2006; Kulasooriya, 2017). Furthermore, *Raphidiopsis* sp. has been observed to be prevalent in a majority of water bodies located in the North Central Province of Sri Lanka, as compared to other regions of the country (Sethunge & Manage, 2010).

During the study of Abeysiri *et al*. (2018b), a positive correlation ($p < 0.05$) between the CYN-producing cyanobacterial cell density and the CYN concentrations was observed in the surface and groundwater sources of CKDu (chronic kidney disease of unknown aetiology) strike areas in Sri Lanka. Additionally, Abeysiri *et al*. (2018a) recorded the presence of CYN in well water samples of CKDu endemic areas in the Anuradhapura district. Further, Arachchi & Liyanage (2012) have detected CYN in an average concentration of 0.137 ng/mL in the Kala Wewa, Nuwara Wewa, and Tissa Wewa of the Anuradhapura District, where CKDu is highly prevalent. In addition to the aforementioned facts, Piyathilaka *et al*. (2015) reported that CYN has the potential to cause severe damage to livers and kidneys due to chronic exposure. Consequently, the presence of CYN in drinking water sources in Sri Lanka is alarming.

Various studies have been carried out worldwide on physicochemical methods of removing toxic CYN through the drinking water treatment process. UV irradiation catalyzed by titanium dioxide (TiO_2) (Chen *et al*., 2015; Camacho-Muñoz *et al*., 2020), ozonation (Yan *et al*., 2016), catalytic wet peroxide oxidation (Munoz *et al*., 2019), non-thermal plasma approaches (Schneider *et al*., 2020) and electrolysis approaches (Bakheet *et al*., 2018) have been tested as effective in removing CYN. Although such physicochemical methods have proven to be effective in removing CYN, their high operational and maintenance costs have become a significant constraint in their application, specially in local drinking water treatment processes in developing countries.

Therefore, biodegradation is now accepted as the most efficient, cost-effective, and environmentally friendly method of removing cyanotoxins. Even so, there is limited information available on CYN biodegradation. Wormer *et al.* (2008) showed that biodegradation of CYN produced by *Aphanizomenon ovalisporum* is not achieved by the co-occurring natural bacterial community within 40 days, and concluded that previous exposure of bacteria to CYN has no effect on their ability to degrade the toxin. In contrast, several successful degradation studies have been reported lately. During the study of Ho *et al*. (2012a) the biodegradability of five cyanobacterial metabolites was tested and the ease of biodegradation was achieved in the order of MC-LR (Microcystin-LR) ≥ CYN > saxitoxins > geosmin ≥ 2- methylisoborneol. Maghsoudi *et al*. (2015) studied the simultaneous biodegradation of MC-LR, MC-YR, MC-LY, MC-LW, MC-LF, and CYN using particulate attached bacteria and phycocyanin in clarifier sludge of a drinking water treatment plant and a drinking water source in Canada. In this study, CYN was degraded with a half-life of 6.0 days in the sludge, but it was not degraded in the lake water samples. In contrast, Ho *et al*. (2012b) found that CYN was biodegradable in a tested source water in Australia, along with MC-LR, saxitoxins, and geosmin and the order of ease of biodegradability was reported as MC-LR > CYN > geosmin > saxitoxins. This study has supported the fact that the biodegradation of CYN occurs in waters with historical exposure to blooms of CYN producing cyanobacteria.

Besides, Mohamed & Alamri (2012) reported successful biodegradation of CYN using a *Bacillus* strain (AMRI-03) isolated from cyanobacterial blooms, which was previously reported as an MC degrader. Growth of the bacteria is observed in the presence of CYN, and the development has increased with an increasing initial concentration of CYN. Consequently, the researchers concluded that complete degradation of CYN depends on the initial toxin concentration. Complete degradation in this experiment occurred after six days at the highest concentration (300 μg/L) compared to 7 and 8 days at lower concentrations (10 and 100 μg/L) and the highest rate of degradation (50 μg/L/day) was reported for the highest initial concentration. Moreover, Dziga *et al*. (2016) reported a 25% removal of CYN within 6 days of incubation with *Aeromonas* sp. isolated from Lake Rusałka, Poland. The effects of pH and temperature were studied too here, and CYN removal was reported as 47 and 49% at 20 and 30^{0}C, respectively, and 48.9 and 41.5% at pH 6.5 and 8.0, respectively. Based on such literature, it is clear that the majority of the studies on CYN biodegradation have utilized microorganisms which previously showed the ability to degrade MCs and nodularin (Mohamed & Alamri, 2012). Nonetheless, the inadequate CYN degradation rates of these bacterial strains make them inappropriate for environmental applications. Therefore, it is important for researchers to focus more on CYN biodegradation, since this might become a huge environmental issue in the upcoming years without proper management.

The objective of the present study is to determine the efficacy of degrading CYN by four bacterial strains namely, *Bacillus cereus*-S (BC-S), *Bacillus cereus*-Y (BC-Y), *Micrococcus luteus* (ML-M), and *Alcaligenes faecalis* (AF-M) which were previously proven to degrade several other environmental pollutants including pesticides (Geed *et al.*, 2017), dyes (Thakur *et al.*, 2014; Ekanayake & Manage, 2017), polycyclic aromatic hydrocarbons (Liyanage & Manage, 2016; Dharmadasa *et al*., 2017; Idroos & Manage, 2017) and antibiotics (Idroos & Manage, 2014). The BC-S strain employed in this study was isolated from the surface water of the Giradurukotte reservoir in Sri Lanka during a previous study and has been proven to degrade MC-LR completely within 8 days (Idroos & Manage, 2018). The other *Bacillus* strain used in this study, BC-Y, was previously isolated from crude oil contaminated surface water and identified as a hydrocarbon degrader (Liyanage & Manage, 2016). ML-M and AF-M, the two other bacteria employed in this study, were isolated from water and soil samples from textile wastewater in Sri Lanka (Ekanayake & Manage, 2020). *Micrococcus luteus* has been reported to have the ability to degrade environmental pollutants such as arsenic (Sher *et al.*, 2020) and biphenyl (Su *et al.*, 2015). In contrast, *Alcaligenes faecalis* has been studied for its biodegradation ability on plastics (Caruso, 2015) and has been used in the treatment of hospital wastewater (Rashid *et al.*, 2020).

MATERIALS AND METHODS

Screening of CYN degradation using *Bacillus cereus*-Y, *Bacillus cereus*-S, *Micrococcus luteus*, and *Alcaligenes faecalis*

Four bacterial strains—two strains of *Bacillus cereus* named *B. cereus*-S (BC-S) and *B. cereus*-Y (BC-Y), *M. luteus* (ML-M), and *A. faecalis* (AF-M)—which have been isolated from previous studies (Liyanage & Manage, 2016; 2018; Idroos & Manage, 2018; Ekanayake & Manage, 2020) were tested to evaluate their ability to degrade CYN, following the method described by Manage *et al*., (2016) and Manage *et al*., (2009). A loop-full of each bacterial isolate was inoculated in 5 mL of sterile Lurial Broth (LB) and incubated overnight at 28^{0}C and at pH 7. The bacteria grown overnight were washed 03 times by adding equal volumes of 0.01 M phosphate-buffered saline (PBS), followed by centrifugation at 6000 rpm for 20 min. The resulting pellet was re-suspended in 0.01 M PBS and kept overnight to remove residual carbon, if any. The cell suspensions were centrifuged at 6000 rpm for 20 min, and the resulting pellet was washed three times using PBS (Manage, 2009). Then the optical densities of all bacterial suspensions were equalized (A_{590} = 0.35) using the UV-Vis spectrophotometer. Approximately 0.5 mL of the equalized bacterial suspension (approximately 10^{5} cells/mL) were inoculated into pure CYN purchased from Sigma Aldrich in sterile distilled water at a final concentration of 5 μg/mL. Triplicate samples were prepared for each bacterial strain and incubated at 28°C for 14 days. Sample aliquots (1000 μL) were removed at intervals of two days for 14 days, and the samples were frozen immediately at -20^{0}C. For the analysis of CYN, the samples were freeze-dried, reconstituted in 1 mL of 80% (v/v) HPLC grade methanol followed by centrifugation at 6000 rpm for 20 min and the supernatant was removed, filtered through a 0.2 μm nylon syringe filter and 50 μL of the sample were subjected to PDA-HPLC analysis (Idroos & Manage, 2018).

Detection of CYN using the high-performance liquid chromatography (HPLC) method

The remaining CYN in sub-samples were quantified using Agilent 1200 series High-Performance Liquid chromatography (HPLC) which was equipped with a diode array and fluorescence detector, following the method of Manage *et al*. (2018), with minor modifications. The detection limit of the HPLC was 0.5 mg/L The injected volume was 20 µL, and chromatography was performed at 30^{0}C. The mobile phase consisted of a mixture of HPLC grade methanol (Component A) and Water (Component B), 0:100 (v/v) was pumped at the beginning at a flow rate of 0.3 mL/min for CYN, followed by linear gradient elution of solvent B from 100% to 0%. The run time was set as 15 min, and the detector was set at the range of 200-300 nm to monitor the column effluent. The standard retention time for the CYN peak is 2 min, and the concentration calculation was made using the equation given below.

$Y = 43.433X + 11.945$

where,

Y = Peak area (mAU) and X = CYN concentration (mg/L)

The relevant HPLC standard CYN (5 mg/L) peak is given in Figure 1.

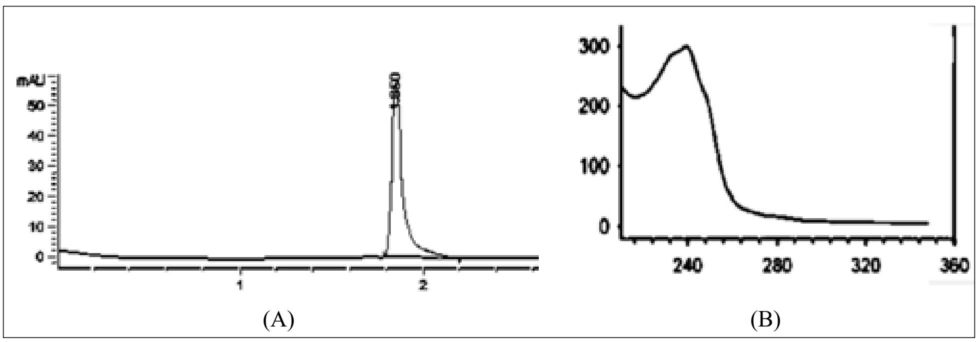

Figure 1: (A) UV chromatogram for 5 mg/L standard CYN toxin; (B) UV spectrum for 5 mg/L standard CYN toxin

Determination of CYN removal percentage

The remaining CYN concentrations of subsamples were quantified, and the CYN removal percentages were calculated following the equation given below (Manage *et al*., 2009).

CYN removal percentage = $[(a-b)/a] \times 100$

where,

a = Initial CYN concentration
b = CYN concentration on sampling day

The average degradation rates at which each bacterial strain degraded CYN for different time periods of incubation were calculated using the following equation.

$h = [(C_0 - C_t)]/t$

where,
h = Average Rate of degradation (mg/L/day)
C_0 = Concentration of CYN at the beginning (mg/L)
C_t = Concentration of CYN at the end (mg/L)
t = Time interval

The bacterial strain which showed the highest degradation was selected and the procedure was repeated for the selected bacterial strain under three different concentrations of CYN (5.0 mg/L, 2.5 mg/L and 1.0 mg/L).

Determination of adsorbance of CYN on the bacterial cells

The potential adsorbance of CYN onto the bacterial cells were determined at the end of the 14 days of the incubation period. The remaining samples were filtered using a 0.45 µm filter to obtain the bacterial cells. Then the filter paper was cut into pieces and washed with distilled water to extract any cell bound CYN. The washing was repeated three times by periodic centrifugation and letting cell-bound CYN be dragged into it. The obtained samples were then subjected to Solid Phase Extraction (SPE). SPE was carried out using C18 ENV cartridge. The cartridges were attached to the vacuum manifold system and conditioned by passing 10 mL methanol and 10 mL water through each. Then the samples were passed through the cartridges and eluted with 3 mL of 80% methanol. The eluted samples were collected in sample tubes and analyzed for the presence of CYN, using the HPLC. The control samples of the three experimental concentrations containing CYN without bacteria were also subjected to this procedure.

Statistical analysis

One-way ANOVA was performed using Minitab 17 software, during the initial study to select the suitable bacterial strain which would efficiently degrade CYN and during the latter study to find if there is a significant relationship between the initial concentration and the rate of degradation for the selected bacterial strain.

RESULTS AND DISCUSSION

Selection of potential bacterial strain which degrades CYN

Starting with a value of 5.0 mg/mL, bacterial strains had different CYN degradation percentages. After 14 days, the percentage degradations for *B. cereus*-S (BC-S), *M. luteus* (ML-M), *A. faecalis* (AF-M), and *B. cereus*-Y (BC-Y) were reported to be 29.67 ± 0.24, 10.94 ± 0.28, 9.09 ± 0.16, and 7.58 ± 0.14%, respectively. The control sample, which did not contain bacteria, only revealed a 1.45 ± 0.05% decrease in CYN, which could be attributed to natural degradation of the toxin due to the temperature. Considering this fact, the exact bacterial degradation was calculated by deducting natural degradation from the values obtained for each sample set. Accordingly, the real bacterial degradation values are 28.22, 9.49, 7.64 and 6.13% for BC-S, ML-M, AF-M and BC-Y respectively. The bacterial strains AF-M, ML-M and BC-Y showed significantly lower degradations compared to the degradation of BC-S. This lack of CYN degradation by rest of the bacteria could be due to the inhibition of their growth by CYN, or because they might be possessing enzymes with low reaction kinetics. According to the results of one-way ANOVA, there are significant differences ($p < 0.05$) between the percentage degradations of all the bacterial strains and the highest mean value of percentage degradation was obtained for BC-S. As a result, BC-S was chosen as a potential bacterial candidate for degrading CYN. Figure 2 illustrates the reduction of the toxin by the four bacterial strains throughout 14 days of degradation study.

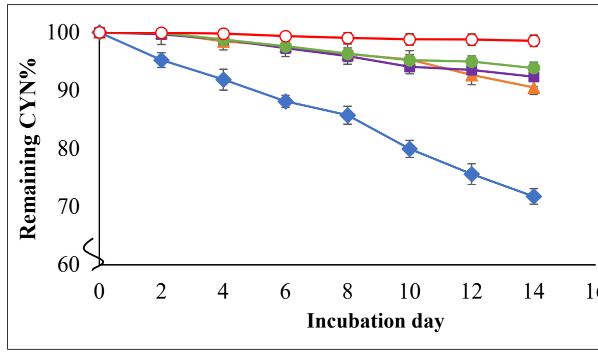

Figure 2: Remaining CYN after incubating the four bacterial strains under 28°C for 14 days with 5.0 mg/L CYN. When error bars are not shown, the standard deviation is less than the width of the symbol. (Closed diamond; *Bacillus cereus*-S, closed circle; *Bacillus cereus*-Y, closed triangle; *Micrococcus luteus*, closed square; *Alcaligenes faecalis* and open circle; Sterile control).

Degradation of different CYN concentrations by the bacterium *B. cereus*-S (BC-S)

Under three different initial concentrations of CYN, the degradation kinetics of the selected bacterial strain, BC-S, were studied (5.0, 2.5, and 1.0 mg/L). For a 14-day incubation period, the degradation kinetics were calculated every two days. At the end of the 14-day incubation period, different amounts of CYN were detected in each sample (5.0, 2.5, and 1.0 mg/L). BC-S degraded 39.06 ± 2.43% of 1.0 mg/L CYN after 14 days of incubation at 28°C, while 34.22 ± 1.25% and 26.35 ± 0.40% of CYN were degraded in the 2.5 mg/L and 5.0 mg/L samples, respectively. In all three samples, CYN concentrations were gradually declining at different rates. The removal patterns of CYN by BC-S at different concentrations suggest that high initial concentrations of CYN will result in comparatively low degradation rates. During the incubation period, there was no significant loss of CYN in the sterile controls, and only 2.23 ± 0.15, 1.97 ± 0.15, and 1.63 ± 0.08% decreases were found in the 1.0, 2.5, and 5.0 mg/L control samples, respectively. Accordingly, the natural degradations were deducted from the obtained values in order to determine the exact bacterial degradation. After the reduction the obtained values were 24.72, 32.25 and 36.83% for 5.0, 2.5 and 1.0 mg/L samples respectively. The remaining CYN percentages of the three samples, 5.0, 2.5, and 1.0 mg/L, and the relevant control samples, are displayed against the incubation day in Figure 3. The graphs show a clearly declining CYN trend as the incubation day advances.

The average degradation rates were also calculated every two days, and it was found that the average rates changed throughout the incubation period. This variation in rates of degradation could be attributed to fluctuations in enzyme activity during different phases of bacterial growth. The highest average rates were recorded for the 5.0 mg/L (0.02 ± 0.01 mg/L/day), 2.5 mg/L (0.04 ± 0.01 mg/L/day), and 1.0 mg/L (0.05 ± 0.00 mg/L/day) samples on the 12th, 8th, and 6th days of incubation, respectively. The average degradation rates determined for the three CYN concentrations are illustrated in Figure 4.

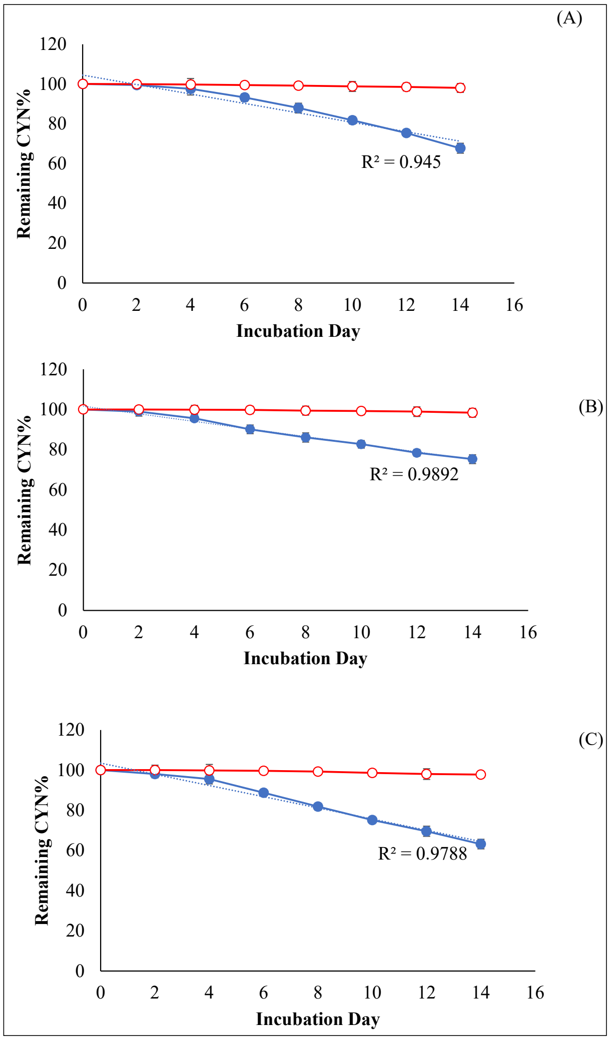

Figure 3: Remaining CYN percentages after degradation by the bacterial strain *Bacillus cereus*-S under (A) 5.0 mg/L, (B) 2.5 mg/L, and (C) 1.0 mg/L initial CYN concentrations after incubating at 28°C for 14 days. When error bars are not shown, the standard deviation is less than the width of the symbol. (closed circle -sample treated with bacteria, open circle – control sample).

Based on the results of the one-way ANOVA analysis of the initial CYN concentrations (1.0, 2.5, and 5.0 mg/L) (all the P values were less than 0.05) there is a relationship between the initial CYN concentrations (1.0, 2.5, and 5.0 mg/L) and the average rates of degradation. According to the results, the highest mean degradation rate (0.05 mg/L/day) was obtained for a 1.0 mg/L initial concentration, whereas the lowest (0.02 mg/L/day) was obtained for a 5.0 mg/L initial concentration. As a result, the degradation rate at lower initial CYN concentrations has become significant.

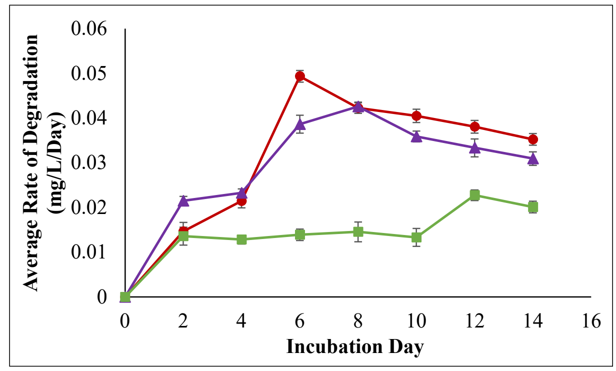

Figure 4: Average rates of CYN degradation under different concentrations of by the bacterial strain *Bacillus cereus*-S after incubating at 28°C for 14 days. When error bars are not shown, the standard deviation is less than the width of the symbol. (closed circle; 1.0 mg/L CYN, closed triangle; 2.5 mg/L CYN, closed square; 5.0 mg/L CYN)

The reason for this result can be attributed to several external and internal factors. The availability of the substrate is a main factor for any enzymatic bacterial degradation. The enzyme-substrate reaction might be limited due to the availability of limited number of active sites in the enzyme. It can be hypothesized that once the enzyme is saturated with the substrate, the rate of reaction might reduce. It is important to note that the specific mechanisms underlying the degradation of CYN by *Bacillus cereus* may involve factors such as the presence of co-metabolites, genetic variations among bacterial strains, and environmental conditions. Further research is necessary to gain a more comprehensive understanding of the exact reasons for the observed pattern in degradation rates.

During the study of Mohamed & Alamri (2012) using *Bacillus* strain (AMRI-03) for degrading three different CYN concentrations (300, 100, and 10 µg/L), it was found that the average rate of degradation increases with increasing initial concentration. In contrast, the present study indicates an increase in average degradation rate with decreasing initial concentration. Both studies conclude that the average degradation rate depends on the toxin's initial concentration, although the observations between the two studies are contradictory. Furthermore, both Mohamed & Alamri (2012), and the present study also used *Bacillus* sp. and reported significant CYN degradation rates. This reveals an important fact: *Bacillus* sp. can be exploited as a promising CYN degrader.

Furthermore, in the present study, the maximum average degradation rate employing BC– S was 47.9 µg/L/day for 1000 µg/L (1 mg/L) CYN concentration. Yet, Mohamed & Alamri (2012), found the highest average rate of CYN degradation by *Bacillus* sp. to be 50 µg/L/day for 300 µg/L CYN concentration. The present study achieved a noticeably higher average degradation rate of CYN toxin, even under a higher CYN concentration compared to the previous studies. This finding offers valuable insight into developing an effective means of degrading CYN toxin through method optimization.

Although the HPLC analysis reported a reduction of the toxin during 14 days of incubation, it was uncertain whether this reduction was actually a degradation or due to the toxin's adsorbance on the bacterial cells. Therefore, a further study was conducted to determine the potential adsorbance of CYN on bacterial cells. No adsorbance was reported here, and it can be concluded that the toxin reduction was solely due to a degradation process occurring within the bacterial cells.

CONCLUSION AND RECOMMENDATIONS

The study aimed to develop a viable method for degrading the CYN toxin by employing native bacteria. It was found that *Bacillus cereus*-S is an excellent degrader of CYN, with the greatest degradation rate of 0.05 ± 0.00 mg/L/day on the 6th day when CYN was introduced in 1.0 mg/L concentration, per the biodegradation study. The degradation rates reported in the present study are greater than previously documented values, despite the high initial CYN concentrations used. Therefore, it is concluded that *Bacillus cereus*-S is a promising candidate for the degradation of CYN toxin in water sources during the water treatment process, ensuring that consumers receive safe drinking water.

The reported bacterial degradation could be improved by optimizing environmental parameters, particularly those that affect the growth and activity of bacteria, such as temperature, pH, light, and nutrients. Additionally, providing a suitable substrate for the bacteria to attach to, such as biochar, would impact its degradation efficiency. According to literature, such bacterial degradations are enzyme-driven mechanisms, with enzymes that can function within or outside the cell. Hence, further research is necessary to identify the enzymatic activity of this bacteria, which will pave the way for enzymes to be isolated from the bacteria and applied in the field. This could minimize the adverse effects of introducing bacteria itself, as it would have other consequences, such as competition with native species. Furthermore, it is necessary to identify other factors which specially affect the rate of degradation of the toxin by the selected bacteria and their limitations. Moreover, the intermediate products of this biodegradation route must be researched, as the intermediate compounds can sometimes be beneficial or harmful.

Conflict of interest

The authors declare that they have no known competing financial interest or personal relationships that could have appeared to influence the work reported in this paper.

Acknowledgement

The authors wish to thank the Centre for Water Quality and Algal Research, Department of Zoology, University of Sri Jayewardenepura, for providing the financial support.

REFERENCES

Abeysiri H.A.S.N., Dilrukshi K.T., Wanigasuriya K., Perera C.T. & Manage P.M. (2021a). Cytotoxic effect of Microcystin-LR, Microcystin-RR, Nodularin and cylindrospermopsin on (Vero-89) kidney cell line. *26th International Forestry and Environment Symposium*, University of Sri Jayewardenepura, p. 30.

Abeysiri H.A.S.N., Wanigasuriya K., Suresh T. S., Benaragama D.H. & Manage P.M. (2021b). Hepatotoxicity of cylindrospermopsin in wistar rats. *8th International Conference on Multidisciplinary Approaches*, University of Sri Jayewardenepura, Sri Lanka.

Abeysiri H.A.S.N., Wanigasuriya K., Suresh T. S., Benaragama D.H. & Manage P.M. (2021c). Renal-toxicity of cylindrospermopsin in wistar rats, University of Peredeniya, Sri Lanka.

Abeysiri H.A.S.N., Wanigasuriya K. & Manage P.M. (2018a). Detection of cylindrospermopsin from well water in CKDu endemic Padaviya, Medawachciya and Kebithigollewa area in Anuradhapura District, Sri Lanka. *5th International Symposium on Water Quality and Human Health: Challenges Ahead*. University of Peradeniya, Sri Lanka, p. 32.

Abeysiri H.A.S.N., Wanigasuriya K. & Manage P.M. (2018b). Cyanobacterial cyanotoxins and water quality in well water at CKDU endemic Girandurukotte and Dehiaththakandiya, Sri Lanka. *5th International Conference on Multidisciplinary*

Approaches. University of Sri Jayewardenepura, Sri Lanka.

Adamski M., Chrapusta E., Bober B., Kamiński A. & Białczyk J. (2014). Cylindrospermopsin: cyanobacterial secondary metabolite. Biological aspects and potential risk for human health and life. *Oceanological and Hydrobiological Studies* **43**(4): 442–449.
DOI: https://doi.org/10.2478/s13545-014-0148-5

Adamski M., Żmudzki P., Chrapusta E., Bober B., Kaminski A., Zabaglo K., Latkowska E. & Bialczyk J. (2016). Effect of pH and temperature on the stability of cylindrospermopsin. Characterization of decomposition products. *Algal Research* **15**: 129–134.
DOI: https://doi.org/10.1016/j.algal.201602.020.

Arachchi D.M. & Liyanage H.M. (2012). Determining the presence of cyanotoxins in water reservoirs of Anuradhapura, using molecular and bioassay methods. *Journal of the National Science Foundation of Sri Lanka* **40**(2): 157–167.
DOI: http://doi.org/10.4038/jnsfsr.v40i2.4443

Bakheet B., Islam M.A., Beardall J., Zhang X. & McCarthy D. (2018). Electrochemical inactivation of *Cylindrospermopsis raciborskii* and removal of the cyanotoxin cylindrospermopsin. *Journal of Hazardous Materials* **344**: 241–248.
DOI: https://doi.org/10.1016/j.jhazmat.2017.10.024

Camacho-Muñoz D., Fervers A.S., Pestana C.J., Edwards C. & Lawton L.A. (2020). Degradation of microcystin-LR and cylindrospermopsin by continuous flow UV-A photocatalysis over immobilized TiO_2. *Journal of Environmental Management* **276**: 111368.
DOI: https://doi.org/10.1016/j.jenvman.2020.111368.

Caruso G. (2015). Plastic degrading microorganisms as a tool for bioremediation of plastic contamination in aquatic environments. *Journal of Pollution Effects and Control* **3**(3): 1–2.
DOI: https://doi.org/10.4172/2375-4397.1000e112

Chen L., Zhao C., Dionysiou D.D. & O'Shea K.E. (2015). TiO_2 photocatalytic degradation and detoxification of cylindrospermopsin. *Journal of Photochemistry and Photobiology A: Chemistry* **420–307**: 115–122.
DOI: https://doi.org/10.1016/j.jphotochem.2015.03.013

Chichova M. *et al*. (11 authors) (2021). New data on cylindrospermopsin toxicity. *Toxins* **13**(1): 41.
DOI: https://doi.org/10.3390/toxins13010041

Dharmadasa P.S., Liyanage G.Y. & Manage P.M. (2017). Degradation of microcystin LR, oxytetracycline and amphicillin by four native bacteria species **7**(2).

Dziga D., Kokocinski M., Maksylewicz A., Czaja-Prokop U. & Barylski J. (2016). Cylindrospermopsin biodegradation abilities of *Aeromonas* sp. isolated from Rusałka Lake. *Toxins* **8**(3): 55.
DOI: https://doi.org/10.3390/toxins8030055

Ekanayake E.M.M.S. & Manage P.M. (2020). Green approach for decolorization and detoxification of textile dye-CI direct blue 201 using native bacterial strains. *Environment and Natural Resources Journal* **18**(1): 1–8.

Ekanayake E.M.M.S. & Manage P.M. (2017). Decolorization of CI Direct Blue 201 textile dye by native bacteria. *International Journal of Multidisciplinary Studies* **4**(1): 49–58.
DOI: https://doi.org/10.31357/ijms.v4i1.3329

Geed S.R., Shrirame B.S., Singh R.S. & Rai B.N. (2017). Assessment of pesticides removal using two-stage Integrated Aerobic Treatment Plant (IATP) by *Bacillus* sp. isolated from agricultural field. *Bioresource Technology* **242**: 45–54.
DOI: https://doi.org/10.1016/j.biortech.2017.03.080

Ho L., Tang T., Hoefel D. & Vigneswaran B. (2012a). Determination of rate constants and half-lives for the simultaneous biodegradation of several cyanobacterial metabolites in Australian source waters. *Water Research* **46**(17): 5735–5746.
DOI: https://doi.org/10.1016/j.watres.2012.08.003.

Ho L., Tang T., Monis P.T. & Hoefel D. (2012b). Biodegradation of multiple cyanobacterial metabolites in drinking water supplies. *Chemosphere* **87**(10): 1149–1154.
DOI: https://doi.org/10.1016/j.chemosphere.2012.02.020

Idroos F.S. & Manage P.M. (2014). Evaluation of antibiotic degradation feasibility of *Bacillus cereus* and *Rahnella aquatilis*. *Journal of Environment and Natural Resources* **1**(1): 189–194.

Idroos F.S. & Manage P.M. (2017). Removal of microcystins by cellular extracts of *Bacillus Cereus*. *KDU Journal of Multidisciplinary Studies* **1**(1): 5–9.

Idroos F.S. & Manage P.M. (2018). Bioremediation of microcystins by two native bacteria; *Bacillus Cereus* and *Rahnella Aquatilis*. *Asian Journal of Microbiology, Biotechnology and Environmental Sciences* **20**(3): 24–32.

Jayatissa L.P., Silva E.I.L., McElhiney J. & Lawton L.A. (2006). Occurrence of toxigenic cyanobacterial blooms in freshwaters of Sri Lanka. *Systematic and Applied Microbiology* **29**(2): 156–164.
DOI: https://doi.org/10.1016/j.syapm.2005.07.007

Kulasooriya S.A. (2017). Toxin producing freshwater cyanobacteria of Sri Lanka. *Ceylon Journal of Science* **46**(1): 3–16.
DOI: http://doi.org/10.4038/cjs.v46i1.7413

Liyanage G.Y. & Manage P.M. (2016). Isolation and characterization of oil degrading bacteria from coastal waters and sediments from three locations in Sri Lanka. *Journal of the National Science Foundation of Sri Lanka* **44**(4): 351–358.
DOI: http://doi.org/10.4038/jnsfsr.v44i4.8017

Liyanage G.Y. & Manage P.M. (2018). Removal of Ciprofloxacin (CIP) by bacteria isolated from hospital effluent water and identification of degradation pathways. *International Journal of Medical, Pharmacy and Drug Research* **2**(3): 37–47.
DOI: https://dx.doi.org/10.22161/ijmpd.2.3.1

López-Alonso H., Rubiolo J.A., Vega F., Vieytes M.R. & Botana L.M. (2013). Protein synthesis inhibition and oxidative stress induced by cylindrospermopsin elicit apoptosis in primary rat hepatocytes. *Chemical Research in Toxicology* **26**(2): 203–212.
DOI: https://doi.org/10.1021/tx3003438

Maghsoudi E., Fortin N., Greer C., Duy S.V., Fayad P., Sauvé S., Prévost M. & Dorner S. (2015). Biodegradation of multiple microcystins and cylindrospermopsin in clarifier sludge and a drinking water source: effects of particulate attached bacteria and phycocyanin. *Ecotoxicology and Environmental Safety* **120**: 409–417.
DOI: https://doi.org/10.1016/j.ecoenv.2015.06.001

Manage P.M., Abeysiri H.A.S.N., Levine K., Redmon J.H., Edwards C., Lawton L.A. & Wanigasuriya K. (2018). Cyanotoxins: a hidden cause of chronic kidney disease of uncertain etiology in Sri Lanka? International CKDu Conference on Costa Rica. (author)

Manage P.M., Edwards C. & Lawton L.A. (2016). Biodegradation of microcystin-LR by natural bacterial populations. In: *Interdisciplinary Studies on Environmental Chemistry — Environmental Research in Asia* (eds. Y. Obayashi, T. Isobe, A. Subramanian, S. Suzuki & S. Tanabe), pp. 277–285.

Manage P.M., Edwards C., Singh B.K. & Lawton L.A. (2009). Isolation and identification of novel microcystin-degrading bacteria. *Applied Environmental Microbiology* **75**(21): 6924–6928.
DOI: https://doi.org/10.1128/AEM.01928-09

Mohamed Z.A. & Alamri S.A. (2012). Biodegradation of cylindrospermopsin 507 toxin by microcystin-degrading bacteria isolated from cyanobacterial blooms. *Toxicon* **60**(8): 1390–1395.
DOI: https://doi.org/10.1016/j.toxicon.2012.10.004.

Munoz M., Nieto-Sandoval J., Cirés S., de Pedro Z.M., Quesada A. & Casas J.A. (2019). Degradation of widespread cyanotoxins with high impact in drinking water (microcystins, cylindrospermopsin, anatoxin-a and saxitoxin) by CWPO. *Water Research* **163**: 114853.
DOI: https://doi.org/10.1016/j.watres.2019.114853.

Pichardo S., Cameán A.M. & Jos A. (2017). *In vitro* toxicological assessment of cylindrospermopsin: A review. *Toxins* **9**(12): 402.
DOI: https://doi.org/10.3390/toxins9120402

Piyathilaka M.A.P.C., Manage P.M., Tennekoon K.H., De Silva B.G.D.N.K., Samarakoon S.R. & Chanthirika S. (2015). Microcystin-LR-induced cytotoxicity and apoptosis in human embryonic kidney and human kidney adenocarcinoma cell lines. *Microbiology* **161**: 819–828.
DOI: https://doi.org/10.1099/mic.0.000046

Poniedziałek B., Rzymski P. & Wiktorowicz K. (2014). Toxicity of cylindrospermopsin in human lymphocytes: Proliferation, viability and cell cycle studies. *Toxicology in vitro* **28**(5): 968–974.
DOI: https://doi.org/10.1016/j.tiv.2014.04.015.

Rashid A., Mirza S.A., Keating C., Ali S. & Campos L.C. (2020). Indigenous 537 *Bacillus paramycoides* spp. & *Alcaligenes faecalis*: sustainable solution for bioremediation of hospital wastewater. *Environmental Technology* **43**(12): 1903–1916.
DOI: https://doi.org/10.101610.1080/09593330.2020.1858180

Scarlett K.R., Kim S., Lovin L.M., Chatterjee S., Scott J.T. & Brooks B.W. (2020). Global scanning of cylindrospermopsin: Critical review and analysis of aquatic occurrence, bioaccumulation, toxicity and health hazards. *Science of the Total Environment* **738**: 139807.

Schneider M., Rataj R., Kolb J.F. & Bláha L. (2020). Cylindrospermopsin is effectively degraded in water by pulsed corona-like and dielectric barrier discharges. *Environmental Pollution* **266**: 115423.
DOI: https://doi.org/10.1016/j.envpol.2020.115423

Sethunge S. & Manage P.M. (2010). Nuisance algae in water supply projects in Sri Lanka. Available at *http://dl.lib.mrt.ac.lk/handle/123/9147*

Sher S., Hussain S.Z. & Rehman A. (2020). Phenotypic and genomic analysis of multiple heavy metal–resistant *Micrococcus luteus* strain AS2 isolated from industrial waste water and its potential use in arsenic bioremediation. *Applied Microbiology and Biotechnology* **104**(5): 2243–2254.
DOI: https://doi.org/10.1007/s00253-020-10351-2

Su X., Zhang Q., Hu J., Hashmi M.Z., Ding L. & Shen C. (2015). Enhanced degradation of biphenyl from PCB-contaminated sediments: the impact of extracellular organic matter from Micrococcus luteus. *Applied Microbiology and Biotechnology* **99**(4): 1989–2000.
DOI: https://doi.org/10.1007/s00253-014-6108-6

Thakur J.K., Paul S., Dureja P., Annapurna K., Padaria J.C. & Gopal M. (2014). Degradation of sulphonated azo dye red HE7B by *Bacillus* sp. and elucidation of degradative pathways. *Current Microbiology* **69**(2): 183–191.
DOI: https://doi.org/10.1007/s00284-014-0571-2

Wormer L., Cirés S., Carrasco D. & Quesada A. (2008). Cylindrospermopsin is not degraded by co-occurring natural bacterial communities during a 40-day study. *Harmful Algae* **7**(2): 206–213.
DOI: https://doi.org/10.1016/j.hal.2007.07.004

Yan S., Jia A., Merel S., Snyder S.A., O'Shea K.E., Dionysiou D.D. & Song W. (2016). Ozonation of cylindrospermopsin (cyanotoxin): degradation mechanisms and cytotoxicity assessments. *Environmental Science and Technology* **50**(3): 1437–1446.
DOI: https://doi.org/10.1021/acs.est.5b04540.

J.Natn.Sci.Foundation Sri Lanka 2023 51 (4): 661 - 674
DOI: http://dx.doi.org/10.4038/jnsfsr.v51i4.11429

RESEARCH ARTICLE

Tree Cover Assessment

Assessment of tree cover density of Sri Lanka using visual interpretation of open-source high-resolution imagery and geographic information system interface mapping

KT Premakantha[1], RPDS Chandani[2], GGJR Silva[2], RPSIK Gunatilaka[2] and DKNG Pushpakumara[3*]
[1] *Department of National Zoological Gardens, Anagarika Dharmapala Mawatha, Dehiwala, Sri Lanka.*
[2] *Forest Department, 82, Rajamalwatta Road, Battarmulla, Sri Lanka.*
[3] *Department of Crop Science, Faculty of Agriculture, University of Peradeniya, Peradeniya, Sri Lanka.*

Submitted: 23 November 2022; Revised: 27 June 2023; Accepted: 22 September 2023

Abstract: Trees are found in various formations, ranging from individual trees to randomly occurring tree clusters and systematically established tree plantations, as well as natural forests. Accurate information about trees, their distribution and density is crucial for the development of national policies, strategies, and management decisions related to tree planting, and environmental management. While some organizations and individuals have mapped forests, home gardens, and trees outside forests at different scales, the lack of comprehensive and systematic spatial distribution data on trees and tree cover density in Sri Lanka has been a significant challenge for policymakers. To address this issue, this study utilized the tree cover mapping (TCM) tool developed by U.S. Geological Survey. High-resolution images were visually interpreted within a geographic information system interface to map tree cover. The TCM tool employed a systematic sample grid, with a sampling interval of 200 m. The study encompassed 1.64 million sampling units, and mapping and interpretation were conducted at a scale of 1:3000. The resulting tree density map had a resolution of 200 m. Results show that 78% of the country's land area has a tree cover density exceeding 10%, resembling open and sparse forests, while 64% of the country exhibits a tree cover density exceeding 40%, comparable to dense forest areas. The study found that although forest cover was limited in districts such as Colombo, Gampaha, and Jaffna, these areas still displayed a significant level of tree cover density, offering services and functions similar to those provided by forests.

Keywords: Canopy density, Sri Lanka, tree cover, tree density.

INTRODUCTION

The world's forests have undergone significant modifications due to human activities, resulting in the conversion of large forest areas into smaller, fragmented patches (Haddad *et al*., 2015). This transformation is primarily driven by population growth (FAO, 2015), leading to the creation of diverse landscapes where trees can be found in various situations and spatial patterns (de Foresta *et al*., 2013). They comprise tree formations ranging from individual trees in various places to systematically managed tree plantations and natural forest areas (Kleinn, 2000; de Foresta *et al*., 2013). In this context, Sri Lanka is not an exceptional country as the country's forest cover has been depleted to 29.2% (Premakantha *et al*., 2021), and exhibits fragmented forests interspaced within agricultural, urban, and built-up areas. This trend of diminishing forest extent and increasing tree presence in non-forest areas is observed throughout the tropics (FAO, 2005). A 'tree' can be defined as a woody perennial with a single self-supporting

* Corresponding author (ngpkumara@pdn.ac.lk; https://orcid.org/0000-0002-6371-1972)

main stem, with a minimum height of 5 m (Nicholson & Clapham, 1975; Thomas, 2000). Trees, including bamboo and palms, provide various environmental services categorized as provisioning, regulating, cultural, and supporting services (MEA, 2005). The products and services offered by trees are generally consistent across different land use types, although their abundance and intensity can vary depending on the specific land use (de Foresta *et al.*, 2013). Hence, while conserving the existing limited extent of natural forests in the country, it is essential to obtain products and services which are provided by forests from trees outside forests also.

Tree canopy cover density is a primary structural characteristic (Coulston *et al*., 2012) that is important for forest landscapes including forest plantations as well as non-forest landscapes such as urban lands, home gardens, tea (*Camellia sinensis*), rubber (*Hevea brasiliensis*), coconut (*Cocos nucifera*), and other agricultural lands. Tree cover density, referred to as tree canopy coverage or crown cover, is defined as the proportion of the forest or land-use floor covered by the vertical projection of the tree crowns, which is a critical aspect of forest management activities (Jennings *et al*., 1999). Tree cover density products represent the level of tree canopy density coverage on a scale of 0 (no trees) to 100% (full canopy coverage) (EARSC, 2015; Cotillon & Mathis, 2016). The amount of tree cover is a fundamental component of the landscape, which is directly related to environmental services provided, including carbon sequestration (Kellndorfer *et al*., 2006; Suganuma *et al*., 2006), atmospheric cooling (Shashua-Bar & Hoffman, 2000; Shashua-Bar *et al*., 2011), maintaining stream water temperatures (Webb & Crisp, 2006), stormwater mitigation and erosion control (Bartens *et al*., 2009), air pollution mitigation (Nowak *et al*., 2008; 2018; John *et al*., 2012), reduced energy use (Hsieh *et al*., 2018), habitat provision (Burghardt *et al*., 2009), increased property values (Escobedo *et al*., 2015), and reduced mental fatigue (Houlden *et al*., 2018).

Despite the significance of trees and their products and services, comprehensive global documentation of their spatial distribution, volume, and value remains inadequate in official statistics (Warner, 2000; Thomas *et al*., 2021). However, obtaining reliable information on the spatial distribution, density, species composition, quality, and temporal changes of trees is essential for developing national policies, strategies, and management decisions, as well as monitoring their impacts (Bradshaw, 2012; Hansen *et al*., 2013; Thomas *et al*., 2021).

Accurately mapping and monitoring tree cover across extensive areas poses a significant challenge (Fisher *et al*., 2016). While ground surveying provides the most precise method, its use is limited due to cost and time constraints (Kleinn, 2000). Even though several remote sensing-based methodologies have been developed to generate information on tree cover across large spatial extents, most data are based on satellite sensors with resolutions too coarse to observe isolated trees or regeneration of trees, or both (Cotillon & Mathis, 2016).

For instance, in dry land regions like the Sahel in Africa, where trees are scarce, traditional satellite-derived methods struggle to accurately map tree cover (Cotillon & Mathis, 2016). However, the application of the Support Vector Machine (SVM) approach using Sentinel-2 satellite images has shown great promise in accurately mapping tree cover and assessing their potential, achieving over 96% accuracy (Mirończuk & Hościło, 2017). Comparative studies have demonstrated SVM's superiority over other classifiers, such as conventional k-Nearest Neighbour (kNN) and radial basis neural network (Melgani & Bruzzone, 2004).

Although Sri Lanka has produced land use maps that include forest cover and home garden areas (LUPPD, 2020; Premakantha *et al*., 2021; Gunawardena & Fernando, 2022), as well as certain systems of trees outside forests (Premakantha *et al*., 2008), comprehensive information on tree cover density and its distribution across different land use types and the stream network is currently unavailable. This knowledge gap is a fundamental requirement for sustainable planning, implementation, and monitoring of tree planting programmes to maximize ecological, economic, and social benefits. Therefore, the objective of this study is to estimate the extent and spatial distribution of tree cover density in Sri Lanka, considering forest cover, various land use types, and the stream network. High-resolution satellite imagery will be utilized to map tree cover density and identify potential areas for tree planting and management beyond forest areas.

MATERIALS AND METHODS

Accurately mapping the extent of tree cover in large areas presents challenges due to the limitations of satellite-derived data with coarse resolutions. However, the Tree Cover Mapping (TCM) tool (Figure 1), developed by the U.S. Geological Survey Earth Resources Observation and Science Centre (Cotillon & Mathis, 2016), offers the facility to estimate tree cover. The TCM tool usually (1) facilitates the process of panning and zooming into each sample; (2) facilitates estimation of the amount of tree cover within a specific sampling frame by placing a grid of calibration points on each sample; (3) makes it compatible with Google Earth, and (4) generates a map based on the sample points (Cotillon & Mathis, 2016). This ArcGIS add-on utilizes high-resolution imagery and visual interpretation to facilitate large-scale tree cover mapping. The TCM tool enables the estimation of tree cover within a defined sampling frame by placing a grid of calibration points on each sample. It also integrates with Google Earth to synchronize location and extent information for mapping purposes.

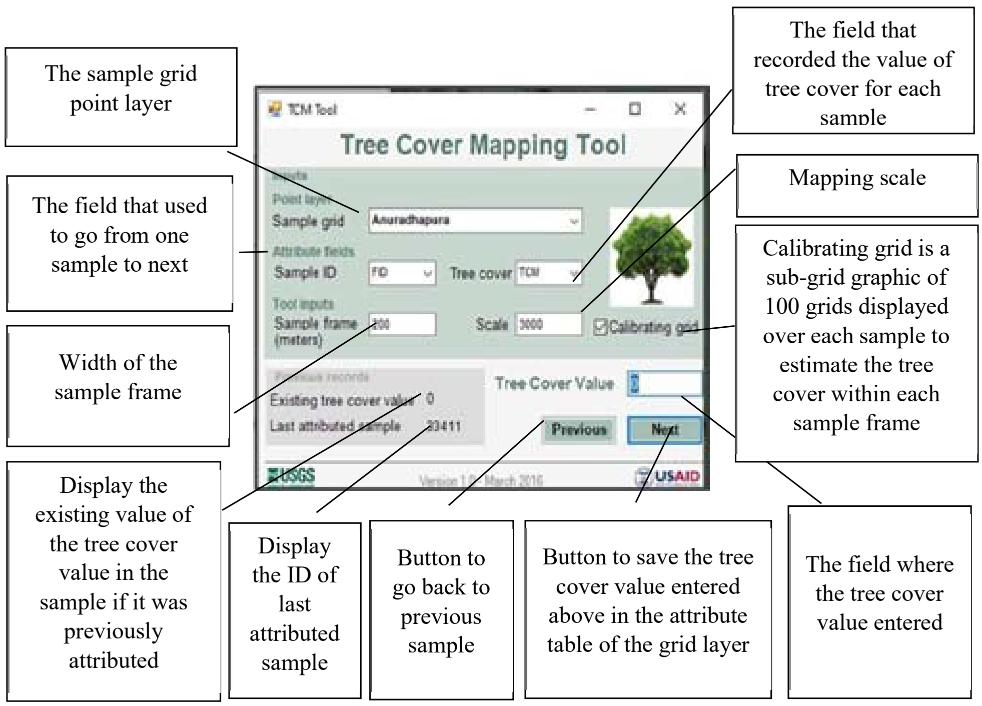

Figure 1: Tree cover density mapping parameters in Tree Cover Mapping Tool

To map tree cover using the TCM tool, a systematic sampling grid was established over the study area. This grid, created using the 'Create Fishnet' Arc Toolbox, consists of regularly spaced intervals and defines the resolution and precision of the output map. The two layers were created over the study area: a point layer, which was the sample grid, and a polygon or polyline layer that can be deleted. The sample frame's area is 4 ha and its width is 200 m. Hence, the resolution of the tree density map is 200 m. High-resolution imagery is used for tree cover mapping, typically at a scale ranging from 1:6000 to 1:2000, depending on the desired level of precision, confidence, and effort dedicated to the mapping exercise.

In this study, a sample grid layer comprising more than 1.6 million grids covering the entire island of Sri Lanka was visually interpreted to estimate tree cover density. Skilled remote sensing technicians conducted this interpretation. A Tree Cover field was created in the attribute table of the sample grid layer to record the tree cover value for each sample. The value was estimated based on the number of dots touching the canopy of a tree within the sample frame as shown in Figure 2.

Once all the sample grid points were attributed, the systematic sample grid was converted to a raster format. This conversion allows for further analysis using geographic information system (GIS) techniques such as Zonal Statistics and Heatmaps using Kernel Density or Point Density functions. The accuracy of mapping was assessed through manual validation using Google Earth Street view images for ground truthing purposes, resulting in an accuracy rate exceeding 90%.

Figure 2: The method of assessing percent of tree canopy cover within each sample frame

To create tree cover density maps for different land use types, widely used categories that include significant tree components were selected. These categories were based on the land use classifications of the Survey Department of Sri Lanka and the Land Use Policy Planning Department (LUPPD). The selected land use categories included tea, coconut, and rubber plantations, agricultural areas, grasslands, home gardens, forests, and built-up areas, each contributing varying tree cover densities that support different ecosystem functions.

RESULTS AND DISCUSSION

The tree cover density map of Sri Lanka produced using the Tree Cover Mapping Tool based on administrative districts of the country is given in Figure 3. As of the assessment, 78% of the land area of the country has more than 10% tree cover density, which is similar to the open and sparse forests category, while 64% of the country has more than 40% tree cover density, which is similar to the dense forest category. This study reveals that the tree cover density in Sri Lanka is high (64%) compared to Nepal (44.9% in 2016; Fox *et al*., 2019), India (36.18% in 2021; ISFR, 2021), Bangladesh (21% in 2014; Potapov *et al*., 2017) and New South Wales, Australia (27.11% in 2016; Fisher *et al*., 2016). The spatial distribution of the tree cover density map indicates that it is well-distributed throughout Sri Lanka, and may be offering goods and services spreading equally through the entire country, especially in areas with limited natural forest cover (Figures 3).

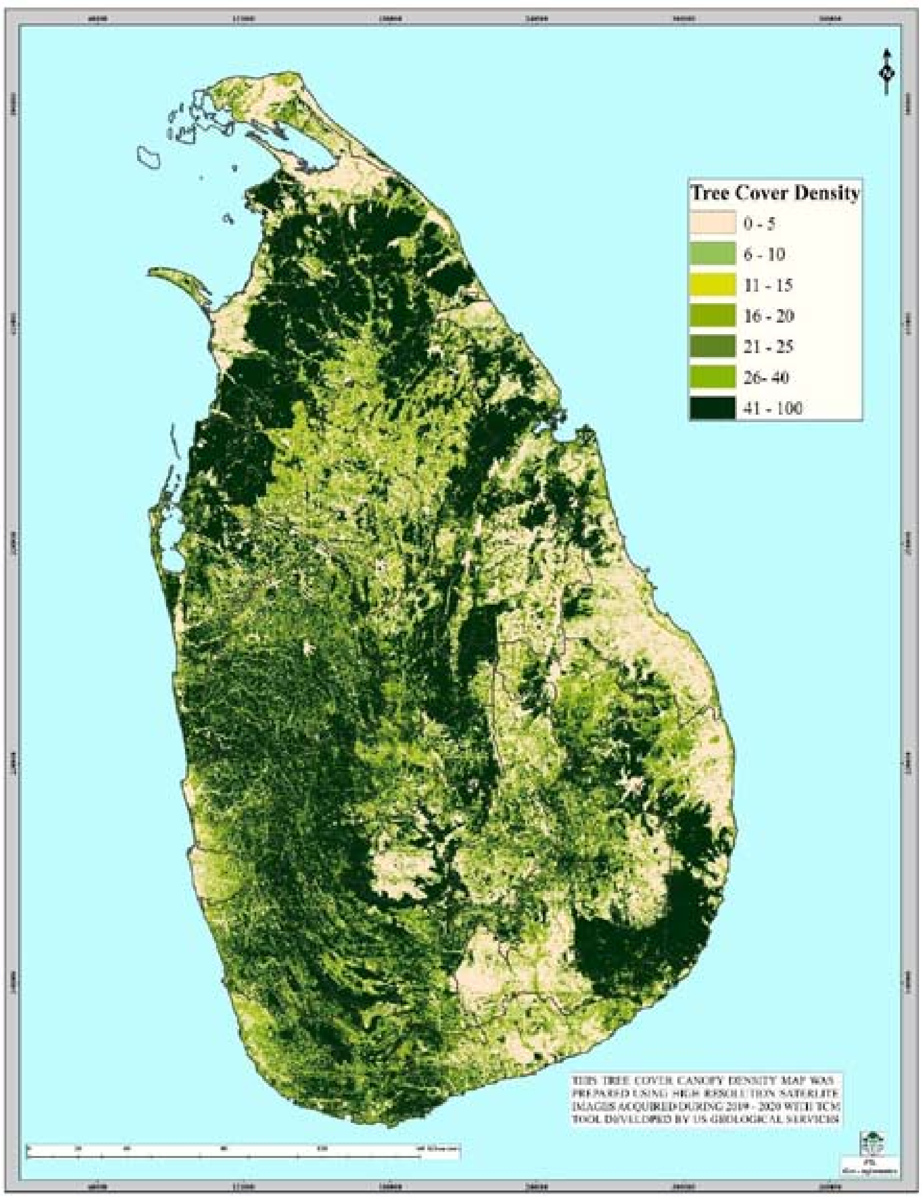

Figure 3: Tree cover density map based on administrative districts of Sri Lanka

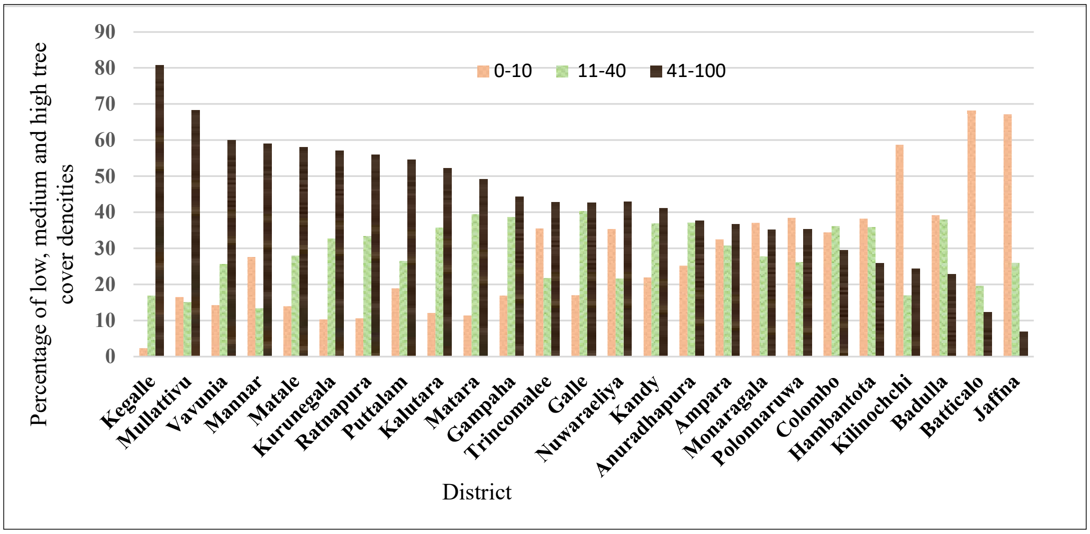

Figure 4: District level distribution of low (0-10%), medium (11-40%) and high tree cover densities (41-100%) of Sri Lanka

Figure 4 illustrates the distribution of areas with tree density similar to non- or low forest areas (0–10%) and those similar to forests (11–40% and 41–100%) in each district, as of FAO (2012) definition used to define a forest. This information highlights the significant roles of tree cover in providing ecosystem services comparable to forests in districts where natural forest cover is limited. For example, in Gampaha, Colombo, Kurunegala, and Jaffna, the natural forest cover is limited to 1.6%, 2.9%, 4.5%, and 4.7%, respectively (Premakantha *et al.*, 2021), but tree cover density is substantial (Figure 4). Additionally, Kegalle (97%), Kurunegala (90%), Matara (89%), and Ratnapura (89%) districts have larger areas with relatively high tree cover densities (11–100%), while Batticaloa (68%), Jaffna (66%), and Kilinochchi (59%) districts have relatively large areas with low tree cover density (0–10%) (Figure 4). These data emphasize the importance of assessing different land use categories and their tree utilization in each district and province for effective planning of tree planting and environmental conservation proposals.

Figure 5 provides the spatial distribution of tree densities in different land-use systems that include trees as a major component. The results of the study revealed that the tree cover density varies significantly among land-use systems. Areas where rubber is grown on a commercial scale exhibit high tree cover density (41–100%) similar to that of forests, justifying the inclusion of it into forest cover in the FAO definition (FAO, 2005). Similarly, coconut plantations too have a higher tree density. Agricultural areas, grasslands, and built-up areas have over 50% their land area with low tree densities (0-10%). As indicated by MEA (2005), Premakantha (2015), and Tassera *et al.* (2020), different land use type performs different functions at varying magnitudes that are important for human well-being and environmental conservation. Therefore, all land use types have a certain value in terms of provisioning ecosystem services and goods under the current land use system of the country. By changing the special composition and structure of the tree components, their capacity can be greatly improved. Hence, correct interventions should be chosen or else they might hinder the performance of any land use type in terms of environmental services.

The Food and Agriculture Organization (FAO) defines 'forest' as a portion of land bigger than 0.5 ha with trees higher than 5 m and a tree canopy cover of more than 10%, or with trees that will be able to meet these criteria. It does not include land that is predominantly under agricultural or urban land use. However, Trees Outside the Forests (TOFs) which includes agricultural (tea, coconut and rubber plantations, home gardens, and other agroforestry systems) and urban lands play a major role in providing ecosystem services under the present land use system of the country. This is important for the districts such as Kurunegala, Gampaha, Kalutara, and Colombo, where natural forest cover is limited and tree cover is high in performing major functions similar to forests.

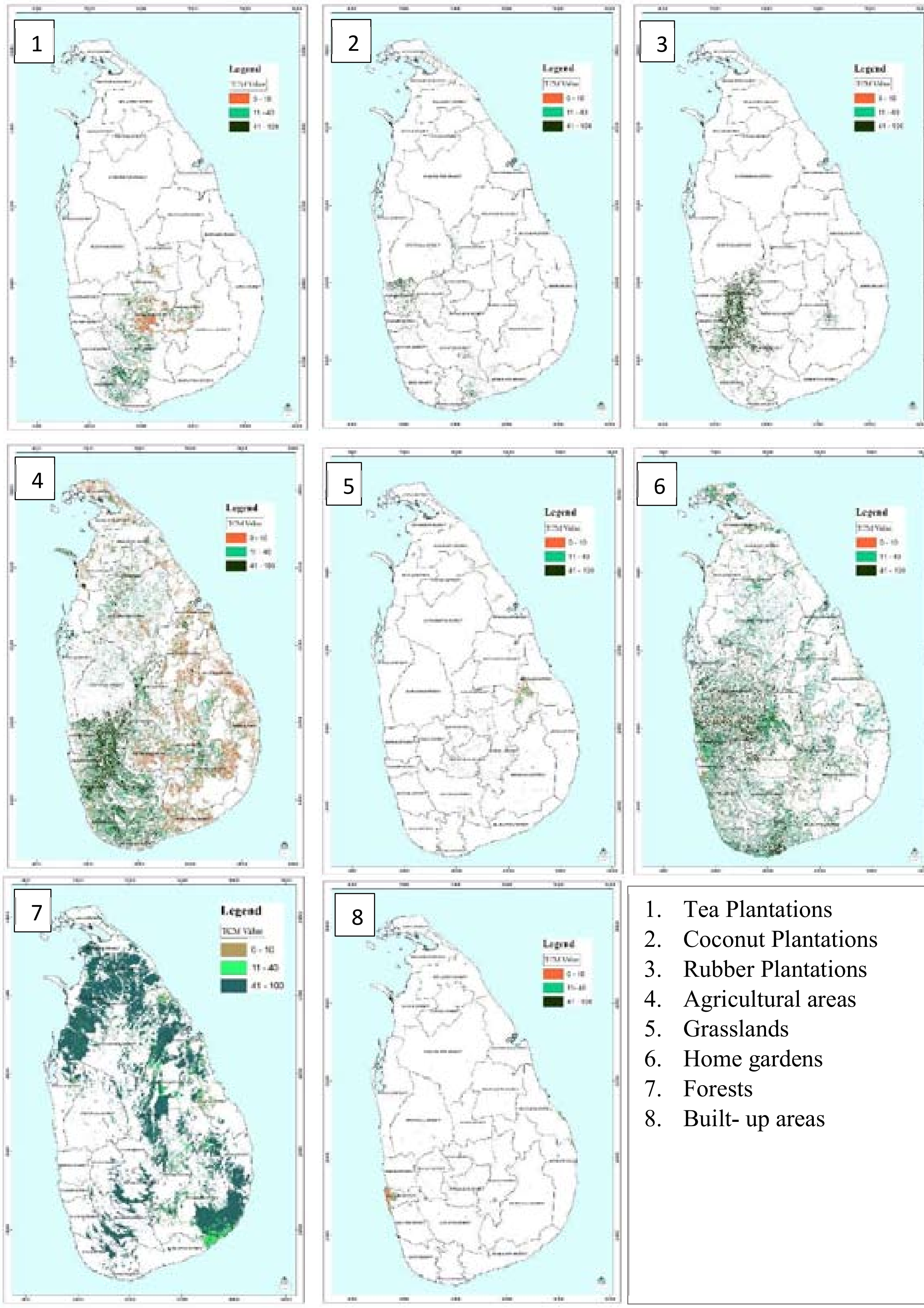

Figure 5: Distribution of tree cover densities in main land use classes in Sri Lanka.
Note: Scale of an A4 size map is 1:1,800,000

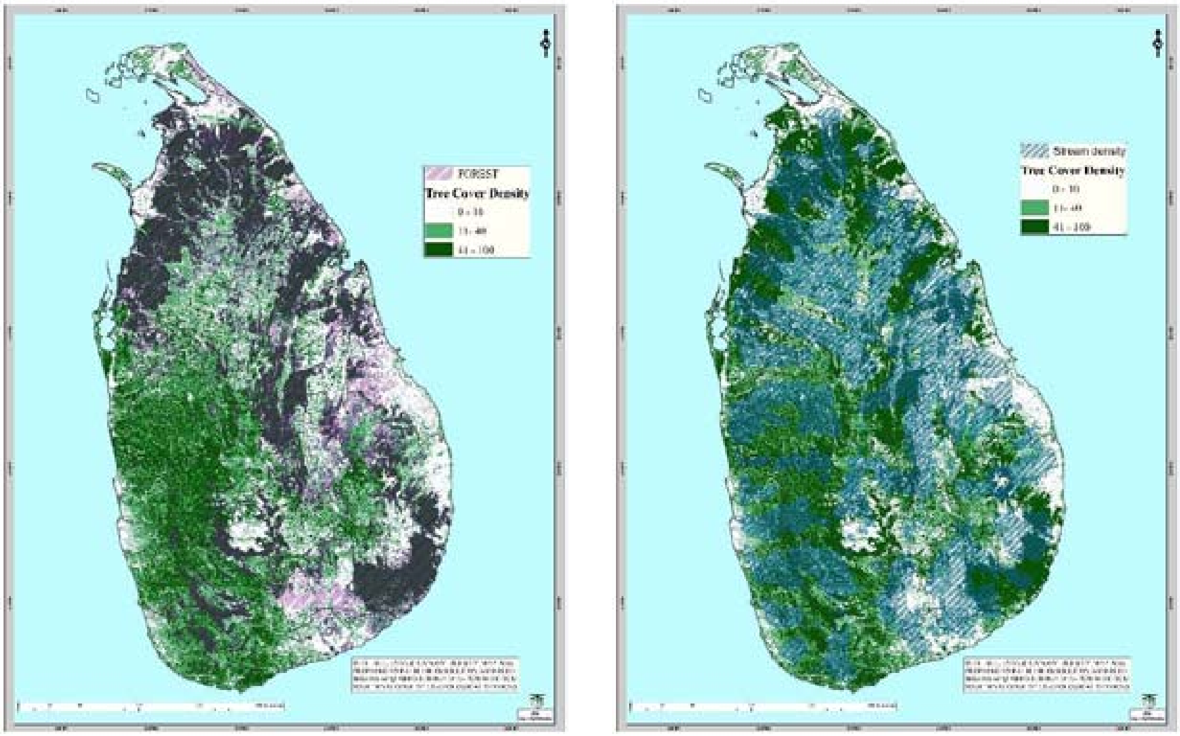

Figure 6: The maps of forest cover overlaid on tree cover density (left) and stream densities overlaid on tree cover density map (right) of Sri Lanka

Figure 6 displays the forest cover map overlaid on the tree cover density map, as well as the stream density map overlaid on the tree cover density map in Sri Lanka. The forest cover map shows that the forest area is only 29.2% (Premakantha *et al*., 2021). However, there are other types of land use with tree cover densities greater than 10%, but they do not qualify as forests because they do not meet the other criteria of the FAO. Deforestation due to various drivers takes place continuously leading to the fragmentation of forests in Sri Lanka and elsewhere. In this regard, the tree cover density map helps to determine the best suitable area for connecting fragmented forests taking into account the proximity and type of land use and their tree cover density. The stream network map shows high tree cover density in most areas but low density in certain areas that require interventions to increase tree cover (Figure 6). Hence, attention should be given to such areas in tree planting campaigns. Sri Lanka is blessed with a network of over 100 streams, which is distributed across all land use categories. Stream bank vegetation, called riparian, is an ecosystem situated between aquatic and terrestrial environments, and is a relatively narrow strip of land along the bank of a river. The riparian systems along the river/stream banks function to reduce soil erosion by trapping sediments and minimizing bank erosion, to filter nutrients and pollutants, to stabilize surrounding ecosystems by shading, reducing temperature, and adding organic matter, to recharge groundwater and reduce floods (Debano & Schmidt, 1990; Naiman & Decamps, 1997; Pusey & Arthington, 2003). Further, healthy riparian vegetation can also provide significant habitats for flora and fauna and aesthetic value to the environment. Thus, proper planning and implementation of tree planting with suitable species for a given environment can be facilitated and monitored with maps of tree density along the stream network of Sri Lanka.

Planting trees in forests as well as outside forests is a major topic of discussion today as the impact of climate change can be seen and felt around the world. Historically, numerous tree-planting programmes by various organizations have been implemented, but their success is questionable. Planting trees without a clear objective, lack of proper planning and coordination among institutions, use of unsuitable species, and lack of follow-up activities and maintenance programmes have been identified as the main reasons for the failure of tree-planting programmes in Sri Lanka. Thus, increasing tree cover and tree density has to be planned and implemented wisely, otherwise resources could be wasted without achieving expected targets. Therefore, the tree component of each land use type needs to be identified, before deciding on interventions to change species composition, structure, density, and tree management, hence functions. Such kinds of planning and intervention will enhance the tree cover further, achieving ecological, economic, and social benefits. As demonstrated by examples from various locations, such as the successful case in Nepal (Fox *et al*., 2019), proper planning and implementation of tree planting campaigns can result in a doubling of tree cover within a period of 24 years.

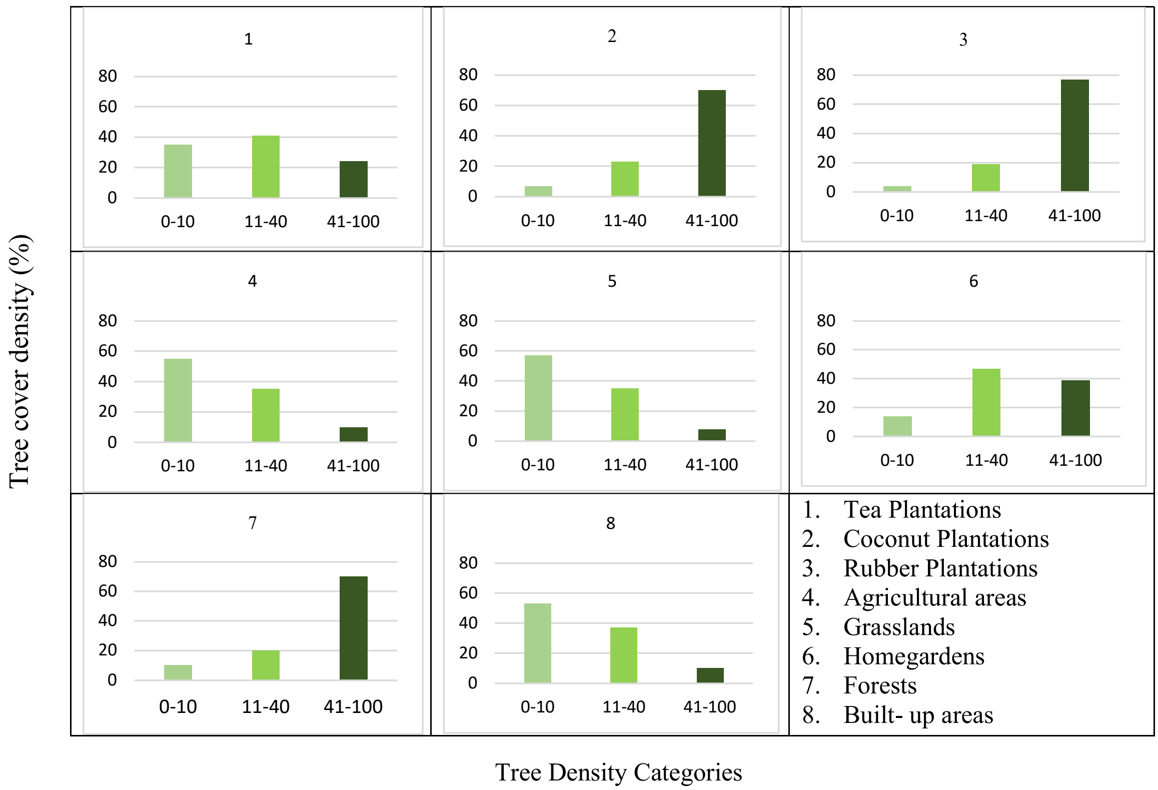

Figure 7: Distribution of tree cover density categories of major land use types in Sri Lanka

Tree cover density and its implication on land use planning and policy decisions

Different land use types have several tree components and their functionality varies greatly depending on their location, composition, and management (Premakantha, 2015). The tree cover density of major land use types used in this study is presented in Figure 7. To maximize the ecological, economic, and social benefits of trees and land use types, it is crucial to investigate the spatial distribution of each land-use type along with tree density distribution, social structure, and strategies for increasing tree presence in the system. This may involve adding more trees to the system, replacing or substituting trees based on community or national goals, and providing appropriate guidelines to align with the existing system. Moreover, the perception of tree resources outside forests varies among stakeholders representing agriculture, forestry, irrigation, urban, and suburban land uses. Consequently, planning tree inventories outside forests poses several challenges compared to forest inventories (Schnell *et al*., 2015). As suggested by Crowther *et al*. (2015), establishing tree planting targets and assessing the proportionate contribution of such projects require a solid baseline understanding of current and potential tree populations at sub national, national, regional, and global scales. In Sri Lanka, this baseline assessment based on different land use categories, where objectives of tree planting and stakeholders' interest align closely, is yet to be determined.

Tea plantations

The tea-growing districts of Sri Lanka include Nuwara Eliya, Kandy, Badulla, Matale, Kegalle, Galle, Matara, and Ratnapura. Figure 5 illustrates the distribution of tree cover density in these tea plantation areas. Within tea plantations, various tree components serve different purposes: shade trees within tea cultivation, riparian vegetation along streams, natural forest patches, forest plantations, and trees planted along roadsides and around offices and resident areas of workers. This study reveals that the tree cover density in tea plantations is lower compared to other major plantation crops such as coconut and rubber (Figure 7), despite the presence of visible tree components in certain areas of tea plantations. However, incorporating multi-purpose trees and fruit trees like apples (*Malus domestica*) and pears (*Pyrus communis*) in the upcountry region and jackfruit (*Artocarpus heterophyllus*) in low country areas, as shade trees or planted along borders, offices, and residential areas can contribute to food and environmental securities. In some cases, tea plantations also contain isolated forest patches, requiring a forest management plans for the Regional Plantation Companies when natural forest patches or forest plantations coexist within tea plantations. Selecting suitable areas and seed sources for establishing forest plantations, along with appropriate silvicultural practices, can enhance timber production and carbon sequestrating. Additionally, degraded areas can be utilized for establishing fuelwood or biomass blocks, as tea plantations heavily rely on fuelwood for tea drying and cooking by the plantation community. Furthermore, in tea plantations where riparian or stream banks directly adjoin tea fields without a buffer strip, incorporating appropriate shrubs, trees and other species such as wild sugarcane as a buffer strip can prevent stream bank erosion and washing of nutrients, conserving biodiversity while supporting tea production.

Coconut plantations

Currently, coconuts are grown in the coconut triangle, which comprises Colombo, Puttalam, and Kurunegala but spatially extends beyond these districts and also in the dry zone of Sri Lanka. Figure 5 illustrates the distribution of tree cover density of these coconut plantation areas. Although coconut cultivations generally have a high tree density, their function as a habitat is limited due to monoculture practices. Nonetheless, certain areas within coconut plantations exhibit visible tree components, including intercropped perennial trees, patches of natural forests, forest plantations, roadside plantings, and trees surrounding office premises and residential areas for workers. Increasing tree density is crucial to optimize the lands under coconut more efficiently in a way that creates more economic, social, and environmental benefits. Kurunegala Plantation Limited has successfully demonstrated the feasibility of incorporating additional tree species into coconut cultivation. They have introduced trees such as durian (*Durio zebethensis*), jackfruit, rambutan (*Nephelium lappaceum*), mango (*Mangifera indica*), and gliricidia (*Gliricidia sepium*), with pepper (*Piper nigrum*), cloves (*Syzygium aromaticum*), cinnamon (*Cinamomum zeylanicum*), and annuals such as turmeric (*Curcuma longa*) in various mixtures. This approach, including roadside plantations, has proven to be successful, resulting in increased revenue for the company and generating additional employment opportunities (Samarakoon *et al*., 2023). The company plans to further expand the agroforestry area by incorporating more tree species into coconut plantations. Augmenting tree cover density in coconut plantations will not only contribute to increased agricultural productivity but also yield environmental benefits. These include carbon sequestration and establishment of biological corridors to connect fragmented forests.

Rubber plantations

The districts where rubber is grown in Sri Lanka are Colombo, Galle, Gampaha, Kalutara, Kandy, Kegalle, Matale, Matara and Ratnapura, and recently in Moneragala (Figure 5). Although rubber plantations are not officially classified as forests in Sri Lanka, they meet the definition of forest according to the FAO (FAO, 2005) because their structure is similar to forests, albeit cultivated as monoculture stands. Consequently, they fulfil most functions of forests. Rubber cultivation plays a significant role in the Sri Lankan economy, contributing to foreign exchange earnings, employment generation, and environmental protection. However, there are limited opportunities to increase the tree cover in rubber plantations, except during the early years when intercropping with certain tree crop species is possible. Nevertheless, opportunities exist to enhance tree density along stream banks, around office premises, residential areas of workers, forest plantations, and natural forest patches (Figure 7).

Home gardens

The expansion of home gardens in Sri Lanka has been driven by population growth, resulting in approximately 18% of the country's coverage being occupied by home gardens (Figure 5; Pushpakumara *et al*., 2012; LUPPD, 2020). Home gardens are a crucial element of the rural community, offering functions similar to forests. In home gardens, variations in species composition of trees and their structure can be observed based on their location, including the front yard, back yard, fence, and around the water sources. Increasing tree density in home gardens can be achieved through scientific approaches, such as adding more trees to the system. Additionally, management of existing trees involves pruning unwanted and diseased branches, while thinning helps remove weak trees (those that are dying, diseased, decayed, damaged, or have broken tops), allowing healthier trees to grow faster and reducing competition for growth. When timber volume ceases to increase due to maturity or death, replacement of trees with the same species can be carried out, especially for economically valuable trees. Furthermore, non-economic trees can be removed and replaced with high-yielding tree species. In areas with low tree density, tree introduction can also be practiced (Pushpakumara *et al*., 2012). Increasing trees in home gardens contributes to improved food security, dietary diversity, micro-climate, and income for rural communities while enhancing environmental security and resilience in the region (Pushpakumara *et al*., 2012; Weerahewa *et al*., 2012; Lowe *et al*., 2021). There is significant potential to expand tree density in home gardens, as recent assessments indicate that approximately 52% of home gardens in the country are underutilized (LUPPD, 2020). By analyzing the total number of home gardens and identifying those with available space for tree crops in each district or AGA division, it becomes possible to address issues related to food and nutritional security. Suitable species such as jackfruit, coconut, leafy vegetable species, fruit trees, etc. can be included in the system or dedicated tree crop villages (*e.g.*, jackfruit village, durian village) can be established for commercial production, as previously practiced by the Department of Agriculture. Due to its extensive high-canopy home gardens and its high biodiversity per unit area, Sri Lanka is exceptional in South Asia concerning tree cover density.

Grasslands

There are several types of grasslands, including *patana* (montane), savannah, and lowland grasslands. The composition of trees in these grassland types varies significantly based on the climate zone and the presence of biotic and abiotic disturbances (Figure 5; Figure 7). When increasing tree cover density in grasslands, careful planning is essential. Naturally occurring grasslands serve as habitats for birds and small animal species, as well as crucial feeding grounds for migratory birds and large animals such as elephants, deer, and buffaloes. Therefore, before preparing a plan to enhance tree density in the grassland system, it is crucial to identify the underlying causes that have led to concerns regarding the grasslands. In some cases, increasing tree density may require no interventions beyond addressing the driving forces that impact the grasslands. The Forest Department of Sri Lanka implements interventions such as assisting natural regeneration and planting trees where they are absent, or a combination of both, to increase the tree density in grasslands. Additionally, it is also possible to protect stream banks in grasslands by planting appropriate trees.

Agricultural areas

The agricultural sector plays a vital role in the economy of Sri Lanka, as over 70% of the rural population relies on agriculture for their livelihoods. Being an agricultural country, the cultivation of trees and crops is prevalent in almost all districts of Sri Lanka (Figure 5). Trees grown on agricultural lands serve important purposes such as facilitating nutrient recycling, controlling soil erosion, enhancing the micro-climate, and providing agricultural inputs such as green manure. In agricultural lands, it is essential to increase tree density in a manner that does not lead to competition with crops for vital resources such as sunlight, water, and nutrients. To achieve the optimal level of agricultural production and tree-based products, it is necessary to test various tree-crop models and introduce new species. Increasing tree density in agricultural areas is critical as it helps to connect isolated forest patches, thereby expanding the habitat range of numerous plant and animal species. This requires a comprehensive analysis of different agricultural systems, such as paddy-based systems, maize and other field crop-based systems, fruit orchards, chena system, including their spatial distribution and the level of underutilization of lands (Figure 7). Additionally, planting trees along stream banks, tanks, and water bodies can offer further benefits. This holds particular significance in the village tank systems of Sri Lanka, where the traditional system operates with various tree-dominated sub-ecosystems such as catchment forests, tree belts, interceptors, and homesteads. Originally, human settlement was restricted to designated areas within these systems, but currently, settlements have expanded to multiple areas. Consequently, trees must play a crucial role in these expanded settlements.

Built-up areas

Built-up areas cover permanent buildings in urban and semi-urban regions, trees along streets, roads, and canals, as well as isolated trees within urban areas and a few forest patches left for recreation activities or as urban parks (Figure 5), and are exposed to a high level of CO_2 emissions. Trees play a crucial role in urban areas by improving the micro-climate, mitigating the urban heat island effect, reducing dust particles and alleviating noise pollution. Increasing tree density in urban areas may pose challenges beyond certain levels. However, through proper planning, areas such as urban parks, city roadsides, vehicle parking lots, sidewalks, street tree planting and space around water bodies have been identified as suitable for increasing tree density. It is important to emphasize that proper planning, including selection of the right trees for the right locations, and effective management practices such as the removal of weak and dead branches, and pruning of excess branches are essential for sustainability. These measures also help to minimize potential damage caused by trees during strong winds and heavy rain events.

Forests

As of 2021, Sri Lanka's natural forest cover is at 29.2%, and although the rate of depletion and degradation has slowed compared to previous periods, it continues to decrease. Sri Lanka's natural forest cover comprises a range of ecosystems, including savanna, mangroves, and forests of varying openness and density. This natural vegetation types exhibit diversity and are dispersed across the wet, dry and intermediate climate zones of the country. However, forest cover is predominantly concentrated in the Northern and Eastern provinces and the central hills (Figure 5). In order to fulfill its Nationally Determined Contribution (NDC) to the United Nations Framework Convention on Climate Change (UNFCCC), Sri Lanka places great importance on planned and organized activities within its forest landscape. One of the targets outlined in the NDC is to increase the national forest cover from the current level to 32% by 2030 (MoE, 2023). To achieve this target, several key areas of focus have been identified, including sustainable management of natural forests, improving the quality of growing stocks in natural forests, demarcating forest boundaries, establishing protected areas and environmentally sensitive zones, restoring and rehabilitating degraded forests (including mangrove vegetation), enhancing catchment protection for major rivers and cascade systems, and establishing plantation forests (MoE, 2023). Additionally, reforestation efforts on non-forest lands, accompanied by proper land use planning, as well as restoration and reforestation of degraded and marginal agricultural lands, are essential for increasing the country's forest cover. To effectively carry out these activities, it is crucial to have an understanding of the current level of tree density and anticipate future changes resulting from proposed interventions. This information can be obtained from tree cover density maps specifically designed for identified forests and non-forest lands.

We have developed the first country-scale map depicting tree canopy cover density in Sri Lanka by utilizing high-resolution imagery within a geographic information system interface mapping. This map also incorporates the distribution of tree cover density across different land use categories, along with forest cover and stream density. Despite the country's forest cover being 29.2%, the tree cover density of 64% indicates that more than half of the total tree cover in Sri Lanka originates from trees outside forests. In some areas, these trees outside forests represent the sole available resource for local populations. They encompass various types of trees, which the Sri Lankan government, Forest Department, Department of Agriculture, and Department of Export Agriculture have actively promoted through initiatives such as home garden improvement programmes, participatory forestry, social and community forestry, urban woodlots and parks, and agroforestry among others. These trees outside forests serve as the second-best options for natural forests, highlighting their significance.

The information presented in this paper serves as baseline information for monitoring tree cover density in the future, as well as tracking tree-planting programmes across different land use types. These monitoring efforts can be implemented at various administrative levels, including *Grama Niladari* (GN) division, Assistant Government Agents (AGA) division, district, provincial, and national levels, to achieve respective environmental, food, and nutritional security goals.

CONCLUSIONS

The tree cover density map of Sri Lanka provides valuable insights into the distribution and density of trees across different land-use categories in the country, hence providing valuable information for land-use planning and policy decisions. The findings reveal that a significant portion of the land area, approximately 78%, has more than 10% tree cover density, similar to the open and sparse forests, while 64% of the country has more than 40% tree cover density, similar to the dense forests. These findings also highlight the important role of tree cover in providing ecosystem services, particularly in districts with low forest cover. The map also highlights the variation in tree cover density across different land-use systems and the potential for increasing tree cover in such land-use systems. However, there are challenges and shortcomings in tree-planting programmes in Sri Lanka in different land use systems. Hence, proper planning and implementation is needed to maximize the benefits of tree cover within each land-use type and enhance their environmental performance.

REFERENCES

Bartens J., Day S.D., Harris J.R., Wynn T.M. & Dove J.E. (2009). Transpiration and root development of urban trees in structural soil storm water reservoirs. *Environmental Management* **44**: 646–657.
DOI: https://doi.org/10.1007/s00267-009-9366-9

Burghardt K.T., Tallamy D.W. & Gregory Shriver W. (2009). Impact of native plants on bird and butterfly biodiversity in suburban landscapes. *Conservation Biology* **23**: 219–224.
DOI: https://doi.org/10.1111/j.1523-1739.2008.01076.x

Bradshaw C.J.A. (2012). Little left to lose: deforestation and forest degradation in Australia since European colonization. *Journal of Plant Ecology* **5**: 109–120.
DOI: https://doi.org/10.1093/jpe/rtr038

Cotillon S. & Mathis M. (2016). *Tree Cover Mapping Tool - Documentation and User Manual (ver. 1.0, March 2016)*, pp. 11. Open-File Report 2016–1067, U.S. Geological Survey, USA.
DOI: https://doi.org/10.3133/ofr20161067

Coulston J.W., Moisen G.G., Wilson B.T., Finco M.V., Cohen W.B. & Brewer C.K. (2012). Modeling percent tree canopy cover: a pilot study. *Photogrammetric Engineering and Remote Sensing* **78**(7): 715–727.
DOI: https://doi.org/10.14358/PERS.78.7.715

Crowther T.W. *et al*. (38 authors) (2015). Mapping tree density at a global scale. *Nature* **525**: 201–205.
DOI: https://doi.org/10.1038/nature14967

Debano L.F. & Schmidt L.J. (1990). Potential for enhancing riparian habitats in the Southwestern United States with watershed practices. *Forest Ecology and Management* **33**: 385–403.
DOI: https://doi.org/10.1016/0378-1127(90)90205-P

De Foresta H., Somarriba E., Temu A., Boulanger D., Feuilly H. & Gauthier M. (2013). *Towards the Assessment of Trees Outside Forests: Resources Assessment Working Paper 183*. FAO, Rome, Italy. Available at *http://www.fao.org/docrep/017/aq071e/aq071e00.pdf*

EARSC (2015). *Product sheet: Tree cover dens*ity. European Association of Remote Sensing, Available at *https://earsc-portal.eu/display/EOSTAN/Product+Sheet%3A+Tree+Cover+Density*

Escobedo F.J., Adams D.C. & Timilsina N. (2015). Urban forest structure effects on property value. *Ecosystem Services* **12**: 209–217.
DOI: https://doi.org/10.1016/j.ecoser.2014.05.002

FAO (2015). *Global Forest Resources Assessment*. Food and Agriculture Organization of the United Nations, Rome, Italy.

FAO (2012). *FRA 2015 Terms and Definitions, Forest Resources Assessment Working Paper 180*. Food and Agriculture Organization of The United Nations, Rome, Italy.

FAO (2005). *Trees Outside the Forests: Towards a Better Awareness*. FAO Conservation Guide 35, FAO, Rome, Italy.

Fisher A., Day M., Gill T., Roff A., Danaher T. & Flood N. (2016). Large-area, high-resolution tree cover mapping with multi-temporal SPOT5 imagery, New South Wales, Australia. *Remote Sensing* **8**(515).
DOI: https://doi.org/10.3390/rs8060515

Fox J., Saksena S., Hurni K., Van Den Hoek J., Smith A.C., Chhetri R. & Sharma P. (2019). Mapping and understanding changes in tree cover in Nepal: 1992 to 2016. *Journal of Forest and Livelihood* **18**(1): 1–11.

Gunawardena A.R. & Fernando T.T. (2022). The Kandyan home gardens: Sustainable agricultural ecosystem in Sri Lanka. In: *Remote Sensing of Agriculture and Land Use Cover/Land Use Changes in South and Southeast Asian Countries* (eds. K.P. Vadrevu, T.L. Toan, S. Shankar & C. Justice), pp. 471–485. Springer Nature, Switzerland.
DOI: https://doi.org/10.1007/978-3-030-92365-5_27

Haddad N.M. *et al*. (24 authors) (2015). Habitat fragmentation and its lasting impact on Earth's ecosystems. *Science Advance* **1**(2):
DOI: https://doi.org/10.1126/sciadv.1500052

Hansen M.C. (15 authors) (2013). High-resolution global maps of 21st-century forest cover change. *Science* **342**: 850–853.
DOI: https://doi.org/10.1126/science.1244693

Houlden V., Weich S., de Albuquerque J.P., Jarvis S. & Rees K. (2018). The relationship between greenspace and the mental wellbeing of adults: a systematic review. *PLoS One* **13**: e0203000
DOI: https://doi.org/10.1371/journal.pone.0203000

Hsieh C.-M., Li J.-J., Zhang L. & Schwegler B. (2018). Effects of tree shading and transpiration on building cooling energy use. *Energy and Buildings* **159**: 382–397.
DOI: https://doi.org/10.1016/j.enbuild.2017.10.045

ISFR (2021). *India State of Forest Report - 2021*. Forest Survey of India. Ministry of Environment Forest and Climate Change. Dehradun, India

Jennings S.B., Brown N.D. & Sheil D. (1999). Assessing forest canopies and understory illumination: canopy closure, canopy cover and other measures. *Forestry* **72**(1): 59–73.
DOI: https://doi.org/10.1093/forestry/72.1.59

Kellndorfer J.M., Walker W., LaPoint E., Hoppus M. & Westfall J. (2006). Modeling height, biomass, and carbon in US forests from FIA, SRTM, and ancillary national scale datasets. *Proceedings of the IEEE International Symposium on Geoscience and Remote Sensing (IGARSS)*, 31 July–04 August 2006, Denver, Colorado, pp. 3591–3594.
DOI: https://doi.org/10.1109/IGARSS.2006.920

Kleinn C. (2000). On large-area inventory and assessment of trees outside forest. *Unasylva* **51**: 3–10.

Lowe A.M., Sinniah J., Jeyavanan K., Silva G.L.L.P. & Pushpakumara D.K.N.G. (2021). Can home gardens

assist in enhancing the domestic food security? A study in Jaffna Peninsula, Sri Lanka. *Agroforestry Systems* **95**: 1205–1216.
DOI: https://doi.org/10.1007/s10457-021-00647-1

LUPPD (2020). *Data and Information of Home Gardens in Sri Lanka: the Main Report*. Land Use Policy Planning Department, Colombo, Sri Lanka.

MEA (2005). *Ecosystems and Human Well-Being: Synthesis. Millennium Ecosystem Assessment*. Island Press, Washington DC, USA.

MoE (2023). *NDC Implementation Plan*. Climate Change Secretariat, Ministry of Environment. Battaramulla, Sri Lanka.

Melgani F. & Bruzzone L. (2004). Classification of hyperspectral remote sensing images with support vector machines. *IEEE Transactions on Geoscience and Remote Sensing* **42**(8): 1778–1790.
DOI: https://doi.org/10.1109/TGRS.2004.831865

Mirończuk A. & Hościło A. (2017). Mapping tree cover with Sentinel-2 data using the Support Vector Machine (SVM). *Geoinformation Issues* **9**1(9): 27–38.

Nicholson B.E. & Clapham A.R. (1975). *The Oxford Book of Trees*. Oxford University Press, London, UK.

Naiman R.J. & Decamps H. (1997). The ecology of interfaces: Riparian zones. *Annual Review of Ecology and Systematics* **28**: 621–658.
DOI: https://doi.org/10.1146/annurev.ecolsys.28.1.621

Nowak D. J., Hirabayashi S., Doyle M., McGovern M. & Pasher J. (2018). Air pollution removal by urban forests in Canada and its effect on air quality and human health. *Urban Forestry and Urban Greening* **29**: 40–48.
DOI: https://doi.org/10.1016/j.ufug.2017.10.019

Nowak D.J., Crane D.E., Stevens J.C., Hoehn R.E., Walton J.T. & Bond J. (2008). A ground-based method of assessing urban forest structure and ecosystem services. *Arboriculture and Urban Forestry* **34**(6): 347–358.
DOI: https://doi.org/10.48044/jauf.2008.048

Premakantha K.T. (2015). Large area inventory of tree resources outside forests. Unpublished PhD Thesis. Postgraduate Institute of Agriculture, University of Peradeniya, Peradeniya, Sri Lanka.

Potapov P., Siddiqui B.N., Iqbal Z., Aziz T., Zzaman B., Islam A., Pickens A., Talero Y., Tyukavina A., Turubanova S. & Hansen M.C. (2017). Comprehensive monitoring of Bangladesh tree cover inside and outside of forests, 2000–2014. *Environmental Research Letters* **12**: 104015.
DOI: https://doi.org/10.1088/1748-9326/aa84bb

Premakantha K.T., Chandani R.P.D.S., Kingsly S.A.D., Dias H.U. & Kekulandara N.S.B. (2021). Forest cover assessment in Sri Lanka using high resolution satellite images. *The Sri Lanka Forester* **40**: 1–16.

Premakantha K.T., Pushpakumara D.K.N.G. & Dayawansa N.K.D. (2008). Identification of tree resources outside forests in the upcountry of Sri Lanka using medium resolution satellite imagery. *Tropical Agricultural Research* **20**: 354–365.

Pusey B.J. & Arthington A.H. (2003). Importance of the riparian zone to the conservation and management of freshwater fish: a review. *Marine and Freshwater Research* **54**: 1–16.
DOI: https://doi.org/10.1071/MF02041

Pushpakumara D.K.NG., Marambe B., Silva G.L.L.P., Weerahewa J. & Punyawardena B.V.R. (2012). A review of research on home gardens in Sri Lanka: the status, importance and future perspective. *Tropical Agriculturists* **160**: 55–118.

Samarakoon S.M.M., Weerahewa H.L.J., Pushpakumara D.K.N.G. & Gunarathne L.H.P. (2023). Financial and economic sustainability and risk resiliency of coconut-based agroforestry systems in Sri Lanka. *Cocos* **24**(1): 23–42.

Schnell S., Kleinn C. & Ståhl G. (2015). Monitoring trees outside forests: a review. *Environment Monitoring and Assessment* **187**: 600.
DOI: https://doi.org/10.1007/s10661-015-4817-7

Shashua-Bar L. & Hoffman M. (2000). Vegetation as a climatic component in the design of an urban street: an empherical model providing the cooling effect of urban green areas with trees. *Energy and Buildings* **31**: 221–235.
DOI: https://doi.org/10.1016/S0378-7788(99)00018-3

Shashua-Bar L., Pearlmutter D. & Erell E. (2011). The influence of trees and grass on outdoor thermal comfort in a hot-arid environment. *International Journal of Climatology* **31**: 1498–1506.
DOI: https://doi.org/10.1002/joc.2177

Suganuma H., Abe Y., Taniguchi M., Tanouchi H., Utsugi H., Kojima T. & Yamada K. (2006). Stand biomass estimation method by canopy cover for application to remote sensing in an arid area of Western Australia. *Forest Ecology and Management* **222**(1-3): 75–87.
DOI: https://doi.org/10.1016/j.foreco.2005.10.014

Tassera E., Schirpkea U., Zodererb B.M. & Tappeinera U. (2020). Towards an integrative assessment of land-use type values from the perspective of ecosystem services. *Ecosystem Services* **42**: 101082.
DOI: https://doi.org/10.1016/j.ecoser.2020.101082

Thomas P. (2000). *Trees: their Natural History*. Cambridge University Press, Cambridge, UK.

Thomas N., Baltezar P., Lagomasino D., Stovall A., Iqbal Z. & Fatoyinb L. (2021). Trees outside forests are an underestimated resource in a country with low forest cover. *Scientific Reports* **11**: 7919.
DOI: https://doi.org/10.1038/s41598-021-86944-2

Warner K. (2000). Forestry and sustainable livelihoods. *Unasylva* **202**(51): 3–12.

Webb B.W. & Crisp D.T. (2006). Afforestation and stream temperature in a temperate maritime environment. *Hydrological Processes* **20**(1): 51–66.
DOI: https://doi.org/10.1002/hyp.5898

Weerahewa J., Pushpakumara G., Silva P., Daulagala, C. Punyawardena R., Premalal S., Miah G., Roy J., Jana S. & Marambe B. (2012). Are home garden ecosystems resilient to climate change? an analysis of the adaptation strategies of home gardeners in Sri Lanka. *APN Science Bulletin* **2**: 22–27.
DOI: https://doi.org/10.30852/sb.2012.22

J.Natn.Sci.Foundation Sri Lanka 2023 51 (4): 675 - 688
DOI: http://dx.doi.org/10.4038/jnsfsr.v51i4.11548

RESEARCH ARTICLE

Remote Sensing

Multiscale analysis of land use and land cover changes in Sri Lanka by remote sensing: the impacts of post-war infrastructure development in the last 20 Years (2002-2022)

J Andrieu[1,2*], K Anupama[1], N Bautes[1,3], S Benabou[1,4], O-J Crook[1,2], V Gunasekera[5], T Jayasingam[6], C Jayathilaka[7], KAS Kodikara[8], F Lombard[2], SK Madarasinghe[8], T Mathiventhan[6], G Muthusankar[1], R Premathilake[9], C Proisy[1,10], N Vanniasinkam[5], N Weeratunge[5], N Wickramaarachchi[7] and R Mathevet[1,11]

[1] *French Institute of Pondicherry, CNRS – MEAE, 11 Saint Louis Street, 605001 Pondicherry, India.*
[2] *ESPACE, Université Cote d'Azur - CNRS, 98 Boulevard E. Herriot, 06205 Nice, France.*
[3] *ESO, CNRS, Université de Caen, Esplanade de la paix, 14032 Caen, France.*
[4] *PALOC, IRD - MNHN, 57 rue Cuvier - CP 51, 75231 Paris Cedex 05, France.*
[5] *International Centre for Ethnic Studies, 02, Kynsey Terrace, Colombo 8, Sri Lanka.*
[6] *Department of Botany, Faculty of Science, Eastern University, Vantharumoolai, Chenkalady, Sri Lanka.*
[7] *Department of Geography, Faculty of Arts, University of Peradeniya, Peradeniya, Sri Lanka.*
[8] *Department of Botany, Faculty of Science, University of Ruhuna, Matara, Sri Lanka.*
[9] *Postgraduate Institute of Archaeology, University of Kelaniya, No. 407, Bauddhaloka Mawata, Colombo 7, Sri Lanka.*
[10] *AMAP, IRD, University Montpellier, CNRS, INRAE, CIRAD - TA A51/PS2, 34398 Montpellier cedex 5 – France*
[11] *CEFE, Univ Montpellier – CNRS – EPHE - PSL University - IRD, 1919, Route de Mende, 34293 Montpellier cedex 5, France.*

Submitted: 03 January 2023; Revised: 11 July 2023; Accepted: 22 September 2023

Abstract: On a worldwide scale, land use and land cover changes (LULCC) is a major driver of global change and biodiversity erosion. This study aims to monitor at the scale of Sri Lanka, LULCC and vegetation dynamics, to identify the main changes and their drivers. It places emphasis on multiscale geospatial monitoring with satellite data but also mobilises the interdisciplinary knowledge of a research programme. First, national scale data allows the identification of major changes with the MODIS NDVI dataset using Mann-Kendall tests and time profile analysis. A second local scale was mobilised with a systematic diachronic visual interpretation of high-resolution images on Google Earth. The third step, a macro-regional scale focus on the South and East coasts, used LANDSAT imagery (Stacked K-means) verified by field studies (botanical and vegetation analysis, and interviews). About 92.5% of the island of Sri Lanka is stable or presents no significant trends in the vegetation cover. 5% show a significant positive (greening) trend between 2000 and 2020 around the Puttalam lagoon, west of the Samanalawewa Reservoir, in the Udawalawe National Park, east and north of Ella, and the Nuwaragala Forest Reserve. Only about 2.5% (165,000 ha) of the Island shows a negative significant trend mainly in the periphery of Colombo and Trincomalee. The first driver is a set of national planning decisions in terms of infrastructure development (including urban growth, housing programmes and agricultural fields, and the management of protected areas). The second driver comes under rural dynamics with increasing tree density in rural landscapes over the Uva Province. Infrastructure development initiated by the state, creates both underlying conditions for other activities and negative impacts on coastal ecosystems, such as degradation of wetlands (including protected areas).

Keywords: Infrastructure development, LULCC, NDVI, South and East Coast.

INTRODUCTION

Changes in land cover and land use largely contribute to a global environmental crisis, combining the threats of climate change (IPCC, 2021) with biodiversity loss (IPBES, 2019). Land use and land cover changes (LULCC) mainly include deforestation and urbanization (Hu *et al*., 2021). These dynamics, are however often poorly explained (Lambin *et al*., 2001). Rapidly

* Corresponding author (julien.andrieu@ifpindia.org; https://orcid.org/0000-0002-0031-1672)

developing countries are environmental hotspots because of the inherent relationship between economic growth and resource exploitation (Andrée *et al*., 2019); additionally, many are located in the tropical zone, characterised by high genetic, specific, and ecological biodiversity (Myers *et al*., 2000).

Despite decelerated growth due to civil war (Ganegodage & Rambaldi, 2011), Sri Lanka initially experienced a boost to growth in the immediate post-war period (2009-2012) but with a sharp decline thereafter (Weerakoon, 2018), followed by the worldwide economic downturn caused by the COVID-19 pandemic (Rishandani, 2021). This growth was mainly sustained by infrastructure development, based on multilateral, bilateral, and private-sector loans (Weerakoon, 2018). The external debt incurred by the country became largely unsustainable, as the share of non-concessional loans grew from a mere 7% in 2006 to 53% in 2016 (Weerakoon, 2018).

Sri Lanka has also undergone considerable population growth from 18.7 to 21.8 million between 2001 and 2019 (CBSL, 2020). Population growth has been accompanied by urban growth and urban sprawling in both the capital (Antalyn & Weerasinghe, 2020) and small sized cities (Manesha *et al*., 2021). During the last 20 years, in particular since the armistice of 2009, Sri Lanka embarked on large-scale, planned development programmes. Major infrastructure development has been implemented on the South and East coasts (Perera, 2014). A good example is the region of Hambantota, on the South coast where a lagoon has been converted to a port associated with a chemical industry complex, an international airport and some urban development projects, including housing, administrative complexes, conference hall, stadium, and hospital. Resettlement programmes for those displaced by war were implemented in territories in the North and East, of which the government regained full control after 2009.

Sri Lanka is placed in the main list of Biodiversity Hotpots (Myers *et al*., 2000) because of species richness and endemism rates (*e.g.*, birds and plants), particularly in the southwestern part of the country (*e.g.*, Gabadage *et al*. 2015; Wikramanayake *et al*., 2022). Trade-offs between the environment and development are unavoidable (Dasanayaka *et al*., 2022). However, the state of the environment in Sri Lanka is far from being exhaustively studied and very little systematic assessment on LULCC is available. Based on a multiscalar approach, this paper therefore aims to first map the main LULCC on national scale, and then focus on the South and East coasts of Sri Lanka, to identify the main drivers of these changes on a macro-regional scale. Such knowledge might later be used to better plan infrastructure development with regard to past environmental impacts of planning. Remote sensing is an efficient and well recognized method to monitor LULCC and vegetation dynamics (Alqurashi & Kumar, 2013). However, it is still rarely used in Sri Lanka. It has been applied to monitor urban growth (Subasinghe *et al*., 2016; Antalyn & Weerasinghe, 2020; Manesha *et al*., 2021) and its links with urban heat and vegetation (Senanayake *et al*., 2013, Dissanayake *et al*., 2019), to carry out studies focusing on one type of LULCC, such as deforestation for planting of rubber (Cho *et al*., 2022) or locally specific interventions, such as a protected area (Perera & Tsuchyia, 2009; Lindstöm *et al*., 2012; Wickramaarachchi *et al*., 2013; Perera *et al*., 2021). Changes at the national level, using LANDSAT data processed with the LandTrendr algorithm (Kennedy *et al*., 2015), have been monitored (Rathnayake *et al*., 2020), detecting changes for 13.5% of the Island surface between 1993 and 2018.

Moderate Resolution Imaging Spectroradiometer (MODIS) has been mobilized either in a local land cover study (Perera & Tsuchyia, 2009) or with a focus on agricultural phenology (Jayawardhana & Chathurange, 2016). Sri Lanka has also been included in studies on the macro-regional scale (Mondal *et al*., 2020; Fu *et al*., 2022) delivering, however, little precision on the country *per se*.

The present study basically aims to monitor, on a national scale, a large spectrum of changes, including LULCC and vegetation dynamics, in order to identify the main changes and when possible, identify the drivers and the processes of change. More precisely, three questions are targeted: a) What are the main land cover and vegetation trends in Sri Lanka? b) What drivers underlying these changes and processes, can be identified by a multiscalar remote sensing approach? c) What do changes along the South and East coasts reveal of the environment/development nexus in Sri Lanka?

MATERIALS AND METHODS

Study areas within a multiscale framework

To assess social-ecological changes on the South and East coasts of Sri Lanka, a multiscale approach was chosen (Figure 1). First, small (national) scale (Figure 2) data allows the identification of major changes with the MODIS Normalized Difference Vegetation Index (NDVI) dataset. However, this dataset, because of its coarse spatial resolution, does not easily reveal the drivers of the detected changes and requires further analyses. A second large (local) scale was mobilised with a systematic diachronic visual interpretation of high-resolution images on Google Earth. The third step, a medium scale (macro-regional) one, focuses on the South and East coasts, with the same MODIS Time series, allowing environmental and social processes to be put in synergy. The fourth step was a local focus on a few sites studied with LANDSAT imagery with diachronic land cover mapping (micro-regional), verified by field study (botanical and vegetation analysis, and interviews).

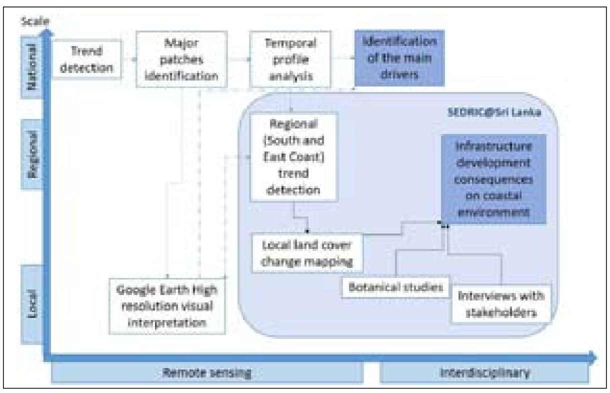

Figure 1: Multiscale and interdisciplinary flow chart

Mapping LULCC is a synthetic and transversal way of approaching the issue of social-ecological changes (Rogan & Chen, 2004). Indeed, without being able to reveal certain fine, discrete or complex ecological (fauna, flora) or social (economic, demographic dynamics) changes, they nonetheless reveal the main changes through the transformation of landscapes (deforestation, reforestation, urban growth, changes in the coastline, etc.). In addition, these transformations can then be associated with more complex dynamics that can be the causes of these changes (demographic growth or rural exodus explaining urban growth) or their consequences (deforestation causing soil erosion and destabilising the watercourse regime) (Mondal *et al*., 2020).

Remote sensing

Remote sensing allows the combining of various scales and resolutions (Mondal *et al*., 2020). The multiscale approach has a lot of advantages. First, the consistent observation of phenomena at two scales enables its validation. Next, it might bring different knowledge about the change itself. If the local scale brings more precision and possible identification of drivers, the broad scale enables it to be placed in relation to general trends, and indicates if a studied change corresponds to a general trend or is a unique process. The present work is the first one mobilizing 3 different types of remotely sensed imagery at 4 different scales even if there have been many earlier studies with remote sensing in Sri Lanka (Perera & Tsuchyia, 2009; Lindstöm *et al*., 2012; Wickramaarachchi *et al*., 2013; Alqurashi & Kumar, 2013; Senanayake *et al*., 2013; Subasinghe *et al*., 2016; Dissanayake *et al*., 2019; Antalyn & Weerasinghe, 2020; Rathnayake *et al*., 2020; Manesha *et al*., 2021; Perera *et al*., 2021; Cho *et al*., 2022).

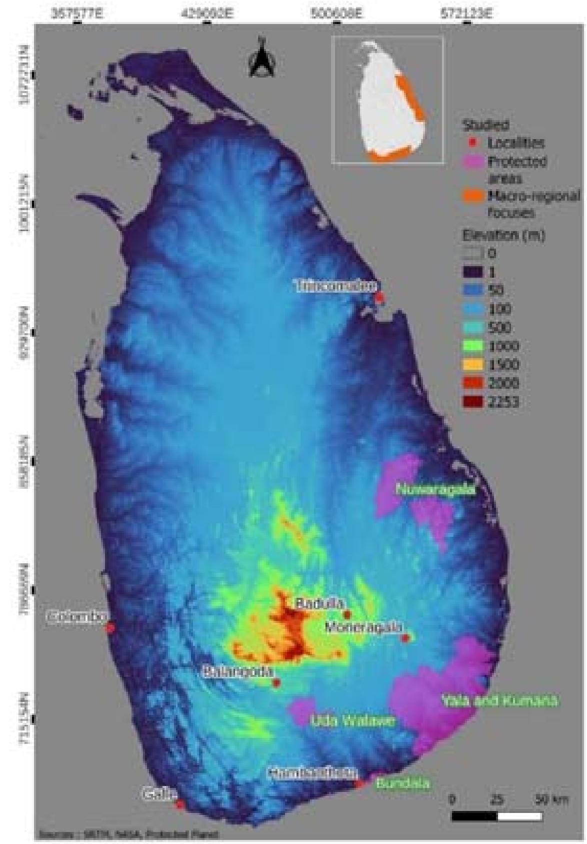

Figure 2: Elevation map of Sri Lanka showing the study areas and locations of case studies on the South and East coasts

MODIS time series analysis

MODIS satellites are a set of two satellite-based sensors used for earth and climate measurements in Earth orbit, mostly used for data accessible as pre-processed time series. Of the 6th version of the NDVI from MOD13Q1 downloaded, two tiles (V8H25; V8H26) were necessary to cover Sri Lanka. Images are a synthesis covering a 16-day period (23 images per year) with a spatial resolution of 230 meters. The time series starts in February 2000 and runs until December 2021. Further details on this well-known dataset can be found in Didan *et al*. (2015).

The dataset has been filtered with a Fourier inverse filter (Cochran *et al*., 1967). The Kendall correlation, or Kendall's Tau (Kendall, 1938), is regularly used to identify data, especially with the NDVI time series (De Jong *et al*., 2011). The Kendall correlation is associated with a P value test set up, here, at 0.0001. Even tested by the P value, the Kendall test is known to be very sensitive to the first and last years of the time series (Dardel *et al*., 2014). The same analysis was computed after removing the first year, the two first years, the last year and the two last years. Only the trends that are robust (P-value under 0.0001 and not sensitive to changes in the first and last years) were considered in this analysis. Then the South and East coasts studied as part of the interdisciplinary research programme were isolated. Similar trends in NDVI can result from various processes. Therefore, at the first level of analysis these trends are only named as 'greening' and 'browning' until further analysis enable more precise understanding and description.

In order to get a finer understanding of the detected changes, the main patches of changes (a group of adjacent pixels with the same trend in NDVI values) were isolated: five main patches of negative significant trends in NDVI 'browning' (larger than 1600 ha) and five main patches of positive significant trends in NDVI 'greening' (larger than 9300 ha). For each, two temporal profiles of the NDVI were produced and studied. The first is a profile at raw temporal resolution (16 days) over the whole time series. It enables calculation of a trend for a group of pixels but also tests like binary segmentation (Killick & Eckley, 2014). The second kind of profile is based on the division of the time series into two periods (2000–2010; 2011–2021), and for each period, the mean of the NDVI for every 16 days of the MODIS year division. This enables a comparison of the mean annual profiles of two decades in order to interpret the changes (Andrieu, 2017).

Unlike the LandTrendr algorithm, the trend detection is not based on a 'year-to-year comparison'. Therefore, it is less accurate for identifying in space and time a precise landcover but it will be more reliable for detecting a regular change in vegetation, which the LandTrendr might not detect as it is based on break-out. The trends in NDVI are, in this paper, used as a wide change detection tool bringing one stratum of information in a multiscalar approach, but are not built to provide either classified land cover maps or a statistical view of LULCC. Hence, it is associated with both the Google Earth visual interpretation and some local field-verified LULLC maps based on classification.

Visual control and interpretation of the changes in MODIS time series based on Google Earth high spatial resolution image excerpts

Trends in NDVI values can be explained by a large spectrum of changes as LULCC (deforestation, reforestation) but also changes within the same land use or land cover category, either agricultural (change in irrigation system resulting in a change in agricultural rhythms and biomass) or natural (phenological or biomass reaction to climate change). Therefore, for the main patches of change at the national scale and on the South and East coasts, visual interpretation of high-resolution (varying from a few meters to submeter level) image excerpts on Google Earth was carried out (Cha & Park, 2007). These image excerpts are RGB colour composites of very high spatial resolution satellite images, *i.e.*, images with sub-metric or metric pixel sizes. The whole process was accomplished in a double-blind interpretation between different remote sensing specialists, and only consistent results were validated. Visual interpretation was based on a set of criteria, mobilizing colour(s), structure, and texture (Figure 3, C&D). When possible, the interpretation was validated using different images of the same year but different seasons. The differences observed and interpreted between the beginning of the 2000's decade and the most recent images were double-checked by images with intermediate dates. The combined results of temporal profiles and visual interpretation are synthetized in Tables 2 and 3 with full details provided in Supplementary Material 1 (Figures SM1.1 to SM1.30).

LANDSAT applied to LULCC mapping

At the micro-regional scale, the National Aeronautics and Space Administration (NASA) LANDSAT program was chosen for two technical characteristics that make it superior to other satellite imagery programs: the availability of images since the mid-1980s and the spectral resolution (at least 7 bands from blue to thermal infrared images come from Landsat 5 and Landsat 8). Four images are required to cover the areas studied at this scale (Table 1).

Table 1: Information on the LANDSAT Images used for the study

	Path	Row	Date 1	Intermediate date	Date 2
Batticaloa & Arugam bay	140	55	1994	2005	2019
Hambanthota	140	56	1991	-	2019
Galle	141	56	1988	-	2020
Trincomalee	141	54	1994	2000	2020

Our method consisted of a series of interlocked unsupervised classifications (K-means algorithm) followed, for each classification, by an interpretation of the mean radiometric curves of each class (Andrieu, 2018). A first classification was made with an ample number of classes to increase the probability of perceiving nuances in the wavelength variations of some similar land cover types. The interpretation then consisted of grouping them into a small number of classes, corresponding to a basic nomenclature of land cover (water, woodland, croplands, and, when present, mangroves, bare soils, sand and rocks, and built-up areas). The interlocked classifications then enabled the subdivision of each class into a small number of sub-classes (same algorithm, same interpretation of the curves) to search for possible classification errors and, if necessary, correct them (Andrieu *et al*., 2019). In the sites where field visits were possible, field verification led to assess accuracy between 81 and 83% (see supplementary material 3, Tables SM3.1 and SM3.2).

Pluridisciplinary approach

This paper mobilised data gathered during a two-year interdisciplinary monitoring of the environmental changes of coastal ecosystems and infrastructure development to better discuss the results from remote sensing. Some field studies in botany and interviews with stakeholders on various sites of the study areas were used for analysis at the local scale.

Vegetation dynamics in two wetlands on the South Coast of Sri Lanka

A field survey was conducted from 2018 to 2020 in Garanduwa and Kalametiya. In the first site, five plots of 30 m × 30 m were randomly studied, and six plots were covered in the second site. All trees and mature shrubs were counted and identified to the species level. In addition, the girth at a height of 130 cm of tree species was measured and the seedling bank was studied.

In February 2022, in addition to assessing the accuracy of the recent maps, a set of regions of interest were selected on the temporary maps of land cover changes in order to try to check the dynamics when possible, with simple landscape observation (*e.g.*, old trees, testifying to the presence of woodland in the 1980's or 1990's; new buildings testifying that urban sprawl had recently expanded), as well as some elementary interviews on the memory of land cover few decades before.

Interviews with stakeholders on the East Coast

To provide an analysis of the evolution of key social, economic, and environmental issues related to both infrastructure development and nature conservation, a literature review on the historical context and semi-structured qualitative interviews with stakeholders were conducted in case study sites. The stakeholders included national and district level key informants, as well as residents of coastal communities, using remote/virtual or face-to-face methods, depending on the changing COVID context during the fieldwork period. Altogether 27 semi-structured key informant interviews with government officers and representatives of civil society organizations (CSOs) in sectors relevant to the study, such as planning, tourism, industry, fisheries, wildlife conservation, forestry, local administration, community development, and women's empowerment were conducted at the national level and in the two study districts of Trincomalee and Batticaloa. Based on these interviews, five coastal Grama Niladhari (GN) divisions (three in Trincomalee, two in Batticaloa) which had experienced infrastructure development were identified and 50 semi-structured, open-ended household interviews with purposive samples of women and men, affected and unaffected by infrastructure development and indicative of different types of livelihoods within coastal communities, were conducted.

The social study was based on the conceptual approaches of political ecology and social wellbeing. The political ecology lens used here was influenced by Bennett (2019), who emphasizes the role of power in the ocean and coastal environment, and the marginalisation of small-scale fishing/indigenous/coastal communities, and Fabinyi *et al*. (2015), who addresses local inequalities and perceived marginalities in fisheries governance in the Pacific. The analysis of the society-environment interface was also informed by Frerks *et al*. (2014) and

Bavinck & Gupta (2014), who have challenged earlier mono-causal theories of conflict over natural resources centred on scarcity, greed, or grievance, arguing that such conflicts are multi-causal, multi-level, and involving multiple actors. Within this broader and more nuanced approach, environmental factors are combined with socio-political factors to explain conflict or contestation. In this study, overt conflict over resources has not been encountered, but, in several instances, contestation of access to resources did take place. The political-ecological perspective supported the analysis of contestation among different groups for natural resources, coastal land, and the sea, where they occurred, the differential benefits and costs of development to groups, the space for participation by local communities in decision-making in relation to coastal governance and transformations, as well as factors for the presence or absence of collective action and social movements. The social wellbeing approach (McGregor, 2008) was used to assess the impacts of infrastructure development on the lives of women and men in coastal communities, especially to understand the extent to which wellbeing outcomes were material (economic), relational (social) or subjective (emotional).

RESULTS AND DISCUSSION

Loss in vegetation cover on the coasts and the greening process in the Uva Province

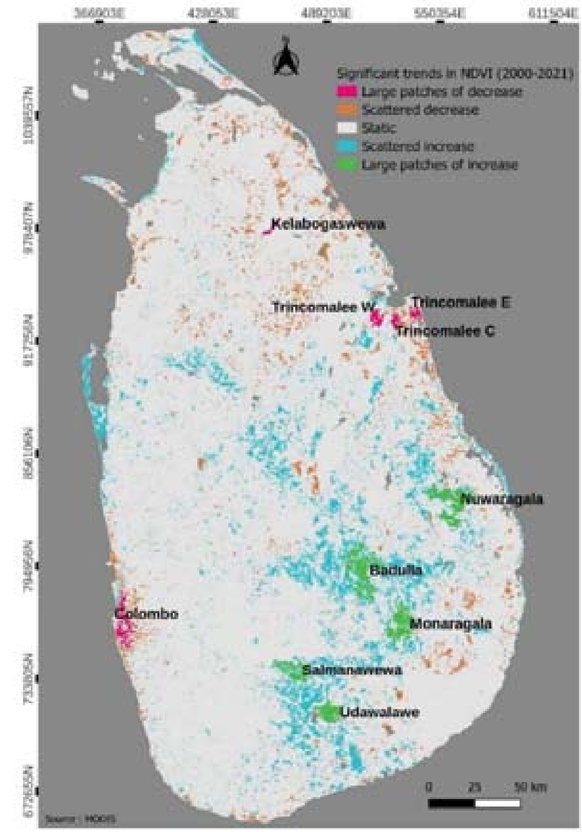

Figure 3: Trends in NDVI from 2000 to 2021

About 92.5% (*i.e.*, 6,046,000 ha) of the Sri Lanka Island is stable or presents no significant trends in the vegetation cover. Further, 5% (*i.e.*, 327,000 ha) of the territory shows a significant positive (greening) trend between 2000 and 2020. Only half of it (2.9%) keeps a significant positive trend if one or two (first or last) years are not taken into account. The greening appears in areas located in the following places: around the Puttalam lagoon, west of the Samanalawewa Reservoir, in the Udawalawe National Park, east and north of Ella, or the Nuwaragala Forest Reserve (Figure 3).

A significant negative trend is shown in 2.5% (165,000 ha) of the Island. Only two-thirds of it (1.8%) retain a significant positive trend if one or two (first or last) years are not taken into account. The main patch of decreasing values (browning) is situated in the periphery of Colombo, the capital of Sri Lanka, experiencing significant urban sprawl in the last 20 years. Three important patches can be observed south of Trincomalee (further identified as E, C, and W for East, Centre and West). Then small patches are scattered over the east of the island. Detailed graphs of NDVI temporal profiles are presented in the Supplementary material 1, while only two synthesis tables are given here.

The five main patches of significant negative Kendall correlation (Table 2) present different comportments revealed by the profile analysis. The patch in the suburb of Colombo shows a gradual decrease in NDVI values in the 21-year profile, while a comparison of the NDVI mean annual profiles of the two decades shows parallel profiles with a moderate difference between them. This is consistent with the visual interpretation of Google Earth's high-resolution imagery: progressive densification of buildings replacing trees.

The four other curves show a long stable period and a neat breakout in the time series followed in some cases by another stable period or an unstable one. This is consistent with the visual interpretation of Google Earth's high-resolution imagery: sudden deforestation and conversion to cropland.

Table 2: Interpretation of the five main patches of decreasing NDVI values.

Locality	Change in NDVI regime 2000–2010 / 2011–2021	Trend and breakout	Land cover 2000's	Land cover 2020's
Kelabogaswewa	Same seasonal profile with lower values	Clear breakout in 2013	Forest	Scattered buildings in fields
Trincomalee E	Same seasonal profile with lower values	Breakout in 2009	Open woodland	Rice fields
Trincomalee W	Sempervirent becomes unimodal (max November)	Breakout in 2009	Forest	Rice fields
Trincomalee C	Sempervirent becomes unimodal (max May)	Breakout in 2009	Mangrove	Rice fields
Colombo	Same seasonal profile with lower values	Regular negative slope	Scattered buildings	Dense urban

The five biggest patches with significant positive trends in NDVI (Table 3) reveal in common a series of minor breakouts in the time series, with the first breakout quite early on. The three patches in the northeast show fewer changes than the two located more toward the south. Some of the sites have changed seasonal regimes, revealing a dry season with low NDVI values in the first decade, followed by an evergreen regime in the second decade. We hypothesize that irrigation and perennial cultivation could be responsible but a change in rainfall regime is also possible as a trigger of the greening of vegetation during the driest season.

Table 3: Interpretation of the five main patches of decreasing NDVI values.

Locality	Change in NDVI regime 2000-2010 / 2011-2021	Trend and breakout	Land cover 2000's	Land cover 2020's
Nuwaragala	Bimodal (max Mars) becomes Unimodal (max October).	Regular increase	Open woodland	Dense woodland
Badulla	Same seasonal profile with higher values	Regular increase	Cropland mosaic	Cropland mosaic
Monaragala	Same seasonal profile with higer values	Regular increase	Cropland mosaic	Cropland mosaic
Salmanawewa	Unimodal (max Mars) becomes Sempervirent	Regular increase	Cropland mosaic	Cropland mosaic
Udawalawe	Unimodal (max Mars) becomes Sempervirent	Regular increase	Open woodland	Dense woodland

Therefore, on this scale, the main LULCC in Sri Lanka revealed by the trends analysis of MODIS and Google Earth visual interpretations can be explained by different factors imposing their own dynamics. The first one is urban growth. On a national scale, the growth of Colombo appears first but various patches reveal subaltern urbanization as well. The second driver of change detected is a set of national planning decisions in terms of infrastructure development. This driver covers the planned settlement of houses and agricultural fields, and the management of protected areas (creation, replantation). The third driver comes under rural dynamics (apart from settlement programmes). Interestingly, the only rural dynamic revealed by this method is an increase in tree density in rural landscapes over the Uva Province, constituting a general increase in tree cover replacing seasonal cropland.

Detection of trends along the South and East coasts

By isolating the South and East coasts, a similar series of LULCC directly or closely linked with rapid development, and in particular, infrastructure development driven by political interests, especially in tourism development, is observed. Various examples of the first two dynamics can be found and studied at a finer scale on the South Coast (Figure 4). Several patches of urban growth have been mapped (Galle, Matara) (see Supplementary Material 2, Figure SM2.1). Infrastructure development can be perceived as patches of deforestation at the sites of the Mattala International Airport and the industrial complex adjacent to the port of Hambantota (Figure SM2.2). Settlement programmes are detected in the northeast of Hambantota (Wediwewa), along with urban growth in the form of wooded 'home gardens' in newly built-up areas (Figure SM4.4). Two patches of increase of vegetation cover and biomass appear in protected areas of the South Coast, Kalametiya Lagoon and Bundala National Park (Figure SM4.2). These dynamics were further studied based on high resolution remote sensing, field observation and interviews.

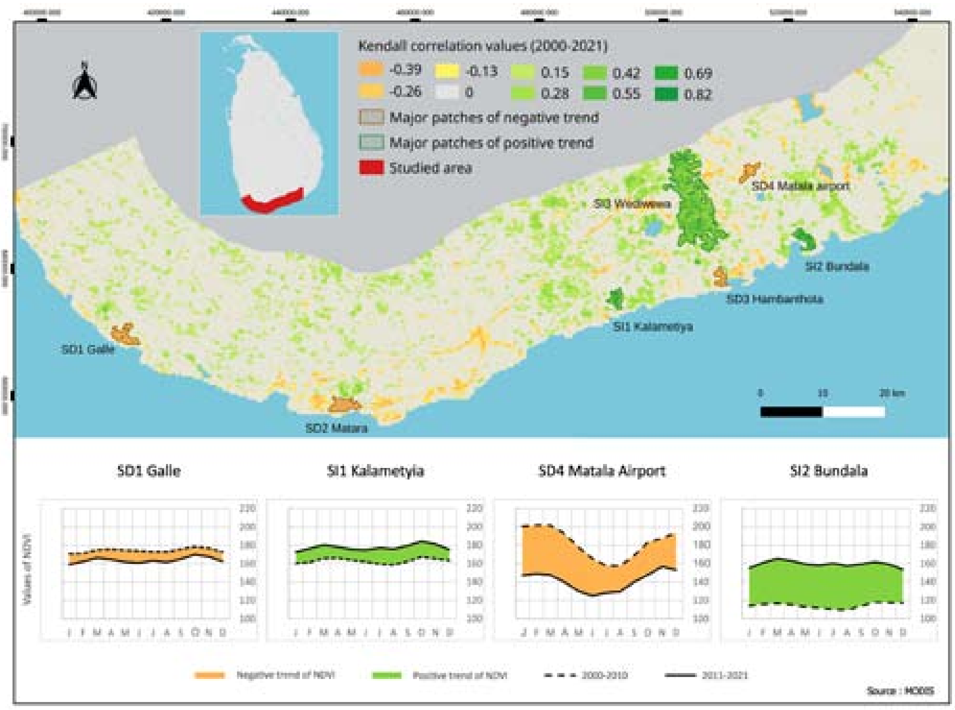

Figure 4: Changes in NDVI values from 2000 to 2021 on the South Coast

The coastal stretch presents a series of lagoons where mangroves develop. Since the Tsunami of 2004 and the 'Reducing emissions from deforestation and forest degradation in developing countries' (REDD+) programme, the restoration of mangroves is an important concern in Sri Lanka. Mangroves in Galle have shown a moderate (17.3 ha) increase from 1988 to 2020; in particular, 30.7 ha which constituted water downstream of the lagoon in 1988 became mangrove in 2020, in the main patch, east of the city. In the same period, 13.4 ha of mangroves disappeared into many small scattered patches (Figure SM 2.1).

Further east on the south coast, the Kalametiya lagoon appears as one of the significant patches of increase in vegetation cover and biomass. Sedimentation, botanical changes, and water pollution were studied during the research programme. The rate of area increase in the Kalametiya mangrove cover was 5.82 ha in year 1. With a total percentage increase of 1451% (Figure SM4.3). from 1956 to 2021, the vegetation was also made of mixed stands of four true mangrove species. After 2000, due to cryptic ecological degradation, only *Sonneratia caseolaris* has increased in cover. This took place with a drastic decrease in salinity and bulk sedimentation. Excess freshwater generated from the Udawalawa irrigation project which came into operation in 1967 happened to bring a large amount of sediment/silt (Madarasinghe *et al*., 2020; Kodikara *et al*., 2022). Due to this ill-planned project, lagoon salinity has drastically dropped (nearly freshwater condition) and a low saline mangrove species (*e.g.*, *S. caseolaris)* has dramatically increased. However, the measured heavy metal pollution (brought by inland freshwater and sediments) remains under the thresholds of concern for public health (Kodikara *et al*., 2022). A similar trend could be observed at the Bundala lagoon.

On the East Coast (Figure 5), some patches of the significant decrease in NDVI values occur in the Muttur area (c.f. supra), south of Trincomalee, corresponding to post-war settlement programmes, corroborated by stakeholder interviews in three communities in the case study area, outlined below (Figure SM2.3). On the other hand, a significant increase in NDVI values occurs on the East Coast. Many forest reserves have been declared, especially in Eastern Province around 2013 by the Forest Department. On the Batticaloa coastline, the greening results from the combination of three dynamics all converging toward more tree cover. First, this coastline has been the object of replanting, especially of *Casuarina equisetifolia* especially after the 2004 Asian tsunami (Mathiventhan & Jayasingam 2014). Second, cashew orchards (*Anacardium occidentale*) have increased in this region along with the agricultural crops in certain coastal areas. Third, touristic and wooded urbanization also occurred. Stakeholder interviews in study sites in coastal Batticaloa did not indicate the destruction of forests or mangroves during the last decade. Destructive environmental activities reported were mostly limited to instances of sand mining (Mathiventhan, 2013) and some very local degradation of mangroves (Dahdouh-Guebas

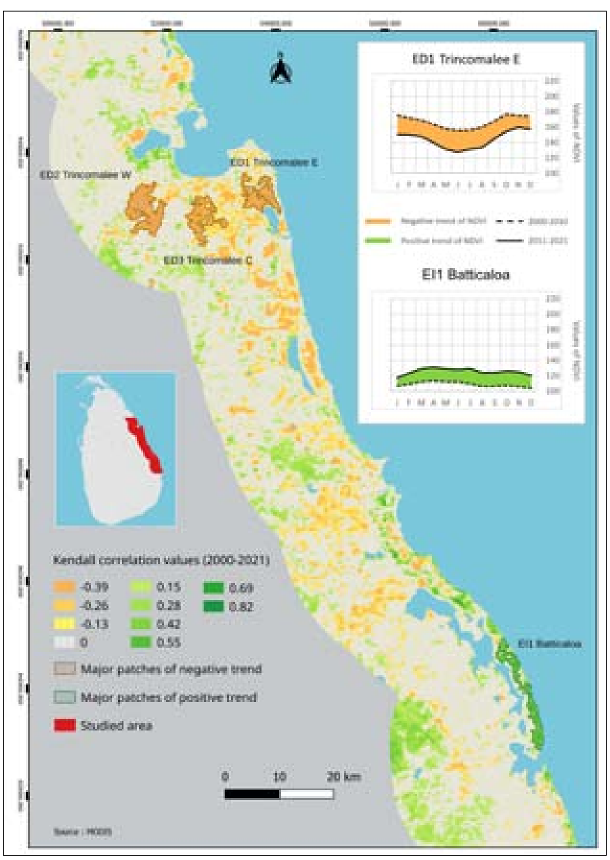

Figure 5: Trends in NDVI on the East Coast (2000–2021)

et al., 2021). Mangrove destruction had also been noticed before 2009, for security reasons, along both sides of the main driveway during the armed conflict (Mathiventhan, 2007).

Discussion

This paper is aimed at linking national scale trends detected in NDVI values with interdisciplinary research generated by local case studies, based on MODIS and Landsat satellite data.

Accuracy, robustness of change detection and analysis

Results from MODIS on a national scale have been tested for significance, and appear consistent with the other data. It is an example of very robust but simple results.

At larger scales (coastal regions and local case studies) the same trends have been observed and confirmed by all the other data sets (visual interpretation from Google Earth images, land cover changes from LANDSAT with precision around 80–85%) and field observation, when this has been possible. These integrated results can therefore be considered trustworthy in relation to the main interpretations:

- Sri Lanka is mostly stable in its vegetation cover and in the case of changes analysed, greening is more important than browning. This encompasses a variety of processes (tree densification in agricultural landscape, biomass increase in protected areas), not all corresponding to a 'healthier' environment (biomass increase explained by invasive species).
- The main driver of change is national scale infrastructure development (direct and indirect changes), based on political interests. Urban growth (including the sprawl of home gardens, which appears as greening), rural settlement, and port and airport construction are the main changes observed.

However, limitations need to be considered. The first is that each scale of observation (and for imagery each resolution) reveals its scale of changes. The visual interpretation of metric resolution Google Earth enables us to see individual trees grow or being cut. The Landsat 30 meters resolution enables a fine scale mapping by classification methods where a change between 2 land cover types (*i.e.*, forest cleared for crops) can be detected if larger than a few hectares. MODIS, at 230 meters of resolution might smooth changes of very fine grain. Some minor changes might, therefore, not have been detected. That might give a first explanation of the smaller proportion of changes detected, in comparison to Rathnayake *et al*. (2020). Changes of surfaces of the size of a LANDSAT Pixel (900 m²) surrounded by a stable land cover of the size of a MODIS pixel (53 000 m²) would have been detected by their method but not by ours. Another explanation might be given by two steps of our method dedicated to filtering significant changes from insignificant ones: with the P-value test set at 0.0001 the removal of changes sensitive to the 2 first and or the 2 last years of the time series. It is normal that a method filtering only significant changes shows fewer changes than a method listing all detected changes. With similar data (LANDSAT) focussed on the LULCC Hotspot on the South and East coast, we found high LULCC rates ranging from 23% for Hambantota-Bundala to 31% for Trincomalee and 48% for Galle.

Therefore, in addition to the previous state of the art describing 13.5% of LULCC in the Island, the present multiscale approach brings a more contrasted estimation. First, by revealing only changes appearing on a large scale (250 m), only 7.5 % of the Island appears with significant (p value 0.0001) changes. Then, by focusing on hotpots of coastal changes at a higher resolution, changes locally appear as much more important.

Coastal environment and infrastructure development on South and East coasts

Infrastructure development emerged as the main driver of LULCC in the case study areas on the south and east coasts when the results of remote sensing were compared with social analysis, based on a literature review and stakeholder interviews, as previously stated by Rathnayake *et al*. (2020). For nearly half a century, Sri Lanka has undergone a major move towards development of infrastructure of different sizes and types (Perera, 2014). From major industrial port projects, the expansion of irrigated areas (*e.g.*, Mahaweli Development Programme) and tourism resorts, the spectrum of this infrastructure is wide, as is its consequences on physical spaces and social dynamics already impacted by a post-conflict (civil war) and post-disaster (tsunami of 2004) context. The main thrust of the state's economic strategy in both the Southern and Eastern Provinces of Sri Lanka in the post-war period (since 2009) has been on such infrastructure development (Perera, 2014). In the Eastern Province, this strategy has been particularly focused on increasing connectivity and trade with the rest of the island by developing roads, railways, transport, electricity and water supply, hotels and tourism, as well as improving the economic and living conditions of the population (Perera, 2014). National poverty reduction programmes were implemented alongside infrastructure for livelihood development through micro-small enterprise promotion and micro-credit services, targeted at the large numbers of returning internally displaced persons (IDPs), who needed to be resettled. The government also supported private sector investment in establishing manufacturing industries, as well as tourism facilities. However, the dominant approach to infrastructure development has been accompanied by a heavy military presence (Buthpitiya, 2013; Perera, 2014), exclusion of local communities in decision-making and/or access to employment in these development programmes (Buthpitiya, 2013), inadequate power-sharing between central and provincial government (Perera, 2014), and lack of attention to political and socio-economic grievances, peace building and reconciliation (Perera, 2014). In the Southern Province, infrastructure development (in the form of roads, port, airport, industrial zone, hospital, conference centre, stadium), has also been accompanied by livelihood development in agriculture, micro-small enterprises and industries, as well as expansion of human settlements. However, as this province was not directly affected by war, negative political, economic, and social impacts might not have been as severe as in the Eastern Province.

While population growth, expansion of human settlements, and agricultural activities have contributed to LULCC in Sri Lanka, these processes also appear to be largely driven by infrastructure development initiated by the state, creating underlying conditions for the expansion of other activities. In the desired trade-off between development and environment conservation, Sri Lanka thus appears to emerge in a median position where recent strategies have neglected neither the economy nor biodiversity. However, stakeholder interviews revealed that projects implemented by the state in the last decades have targeted material wellbeing of coastal communities, without adequately addressing relational and subjective wellbeing, which were perceived as important by coastal communities. Moreover, negative impacts of infrastructure development on coastal ecosystems, such as sand mining, degradation and filling of wetlands and lagoons were reported by research participants in these communities on the east coast. Similar impacts also emerged on the south coast, where Hundlani (2019) referring to the port of Hambantota, wrote that 'Tourism and industries as well as the construction of new infrastructures (dams, power plants, roads, ports), aiming to foster and sustain development, are causing displacement, pollution, land degradation and water shortage, particularly affecting the communities of farmers and fishermen whose livelihoods are based on such natural resources. To do so, 40,000 m³ of material was dredged from the nearby Karagan Levava Lagoon, which essentially destroyed the entire ecosystem of the lagoon and surrounding habitats.' Weerasekara *et al*. (2015) studied the impacts of pollution (solid waste and untreated industrial effluents) while Senevirathna *et al*. (2018) mentioned coastal erosion in this area.

Thus, infrastructure development has had negative impacts on both the coastal environment and well-being of communities on the South and East coasts of Sri Lanka.

CONCLUSION

Overall, the remote sensing results of this study reveal stability in Sri Lanka's vegetation indexes, therefore in its vegetation cover and activity. It also reveals that greening, rather than browning in vegetation cover, is the more prominent trend in Sri Lanka. Regionally, this increase in tree density in agricultural landscapes is most visible in the Uva Province, as well as several locations in the Sabaragamuwa and Northwestern provinces. The Local Hotspot of LULCC studies with LANDSAT revealed 30% (Hambantota-Bundala) to 50% (Galle) of land cover change. However, infrastructure development in coastal areas, more specifically in the Southern and Eastern provinces, chosen as case study sites in this research, has resulted in a decrease in vegetation cover, especially in the Hambantota and Trincomalee districts. The changes in LULC are confirmed by stakeholder interviews on the ground. In coastal areas of both districts, the decrease in vegetation cover is a consequence of the implantation of major infrastructure such as ports, industrial zones, roads, and irrigation devices, as well as the expansion of social infrastructure, such as displacements followed by new settlements.

Stakeholder interviews revealed that the state's attention to the impacts of infrastructure development on coastal ecosystems was inadequate as revealed by sand mining or degradation of wetlands. A better focus on preventing environmental destruction, pollution, and waste, and increased awareness among all stakeholders on conservation of the coastal environment is necessary. Moreover, the main development thrust of the state in implementing infrastructure development has been the material well-being of coastal communities without adequate consultation of these communities. A broader and inclusive policy approach to wellbeing would improve benefit-sharing with communities affected by infrastructure development, and sustain better the coastal environment, upon which they depend.

With remote sensing results as a proxy for environmental assessment, no major environmental degradation is observed on the South and East coasts. Some landscapes have been transformed during the last decades, but without a major negative trend (*e.g.*, deforestation). Protected areas seem to play an important role in preserving stable landscapes on the coast. However, some major infrastructure seems to have seriously impacted the environment on a local scale, such as the area surrounding the port of Hambantota, constructed around a coastal lagoon. Protected areas seem to be more affected by external threats (*e.g.*, construction of major infrastructure, upstream pollution, encroachment) than by activities of the local population (*e.g.*, pasture) but the regulation of protected areas focuses overwhelmingly on social and economic activities, rather than the impacts of infrastructure. The development and conservation of coastal areas in Sri Lanka come under the Coast Conservation Act No 57 of 1981 and Amendment No 49 of 2011. However, a multitude of other acts and regulations pertaining to wildlife, forestry, fisheries, and marine environment also apply. There is often a lack of coordination, sometimes duplication, by the institutions mandated to regulate development activities that impinge on coastal protected areas. Thus, there is a need for integrated area-based management to prevail over sectorial policies so that conflicts between the conservation of protected areas and the implementation of industrial hubs are avoided.

Acknowledgement

This paper mobilizes the knowledge of a two-years interdisciplinary and international research programme entitled SEDRIC. This interdisciplinary and international research programme is granted by a Fund of Solidarity for Innovative Projects (FSPI), placed under the umbrella of the French Embassy of Colombo, Sri Lanka (2019–2021). Its main objective is to address the social-ecological change and its impacts in southern and eastern Sri Lanka's coastal regions.

REFERENCES

Alqurashi A.F. & Kumar L. (2013). Investigating the use of remote sensing and GIS techniques to detect land use and land cover change: a review. *Advances in Remote Sensing* **2**: 193–204.
DOI: https://doi.org/10.4236/ars.2013.22022

Andrée B.P.J., Chamorro A., Spencer P., Koomen E. & Dogo H. (2019). Revisiting the relation between economic growth and the environment; a global assessment of deforestation, pollution and carbon emission. *Renewable and Sustainable*

Energy Reviews **114**: 109221.
DOI: https://doi.org/10.1016/j.rser.2019.06.028

Andrieu J. (2017). Phenological analysis of the savanna-forest transition from 1981 to 2006 from Côte d'Ivoire to Benin with NDVI NOAA time series. *European Journal of Remote Sensing* **50**(1): 588–600.
DOI: https://doi.org/10.1080/22797254.2017.1377051

Andrieu J. (2018). Land cover changes on the West-African coastline from the Saloum Delta (Senegal) to Rio Geba (Guinea-Bissau) between 1979 and 2015. *European Journal of Remote Sensing* **51**(1): 314–325.
DOI: https://doi.org/10.1080/22797254.2018.1432295

Andrieu J., Cormier-Salem M.C., Descroix L., Sané T., Dièye E.H.B. & Ndour N. (2019). Correctly assessing forest change in a priority West African mangrove ecosystem: 1986–2010 An answer to Carney *et al*., 2014 paper 'Assessing Forest change in a priority West African mangrove ecosystem: 1986–2010'. *Remote Sensing Applications: Society and Environment* **13**: 337–347.
DOI: https://doi.org/10.1016/j.rsase.2018.12.001

Antalyn B. & Weerasinghe V.P.A. (2020). Assessment of urban sprawl and its impacts on rural landmasses of Colombo District: a study based on remote sensing and GIS techniques. *Asia-Pacific Journal of Rural Development* **30**(1-2): 139–154.
DOI: https://doi.org/10.1177/1018529120946245

Bavinck M. & Gupta J. (2014). Pluralism in freshwater and marine governance: A challenge for earth system governance architecture. *Current Opinion in Environmental Sustainability* **11**: 78–85.

Bennett J. (2019). In political seas: engaging with political ecology in the ocean and coastal environment. *Coastal Management* **47**(1) :67–87.
DOI: https://doi.org/10.1080/08920753.2019.1540905

Buthpitiya V. (2013). *Reconciling Rights, Responsibilities and Disjunctures: An Assessment of Sri Lanka's Post-War Development Drive*. Law and Society Trust, 3, Kynsey Terrace, Colombo 08, Sri Lanka.

CBSL (2020). *Economic & Social Statistics of Sri Lanka*. Central Bank of Sri Lanka, PO Box 590, Colombo 01, Sri Lanka. Available at *https://www.cbsl.gov.lk/en/publications/other-publications/statistical-publications/economic-and-social-statistics-of-sri-lanka*

Cha S.Y. & Park C.H. (2007). The utilization of google earth images as reference data for the multitemporal land cover classification with MODIS data of North Korea. *Korean Journal of Remote Sensing* **23**(5): 483–491.
DOI: https://doi.org/10.7780/kjrs.2007.23.5.483

Cho K., Goldstein B., Gounaridis D. & Newell J.P. (2022). Hidden risks of deforestation in global supply chains: a study of natural rubber flows from Sri Lanka to the United States. *Journal of Cleaner Production* **349**: 131275.
DOI: https://doi.org/10.1016/j.jclepro.2022.131275

Cochran W.T., Cooley J.W., Favin D.L., Helms H.D., Kaenel R.A., Lang W.W., Maling G.C., Nelson D.E., Rader C.M. & Welch P.D. (1967). What is the fast Fourier transform? *Proceedings of the IEEE* **55**(10): 1664–1674.
DOI: https://doi.org/10.1109/PROC.1967.5957

Dahdouh-Guebas F. *et al*. (17 authors) (2021). Reconciling nature, people and policy in the mangrove social-ecological system through the adaptive cycle heuristic. *Estuarine, Coastal and Shelf Science* **248**: 106942.
DOI: https://doi.org/10.1016/j.ecss.2020.106942

Dardel C., Kergoat L., Hiernaux P., Mougin E., Grippa M. & Tucker C.J. (2014). Re-greening Sahel: 30 years of remote sensing data and field observations (Mali, Niger). *Remote Sensing of Environment* **140**: 350–364.
DOI: https://doi.org/10.1016/j.rse.2013.09.011

Dasanayaka C.H., Perera Y.S. & Abeykoon C. (2022). Investigating the effects of renewable energy utilization towards the economic growth of Sri Lanka: a structural equation modelling approach. *Cleaner Engineering and Technology* **6**: 100377.
DOI: https://doi.org/10.1016/j.clet.2021.100377

De Jong R., de Bruin S., de Wit A., Schaepman M.E. & Dent D.L. (2011). Analysis of monotonic greening and browning trends from Global NDVI Time-Series. *Remote Sensing of Environment* **115**(2): 692–702.
DOI: https://doi.org/10.1016/j.rse.2010.10.011

Didan K., Munoz A.B., Solano R. & Huete A. (2015). *MODIS Vegetation Index User's Guide (MOD13 Series)*, pp. 1–38. Vegetation Index and Phenology Lab, The University of Arizona: Tucson, USA.

Dissanayake D.M.S.L.B., Morimoto T., Ranagalage M. & Murayama Y. (2019). Land-use/land-cover changes and their impact on surface urban heat islands: case study of Kandy City, Sri Lanka. *Climate* **7**(8): 99.
DOI: https://doi.org/10.3390/cli7080099

Fabinyi M., Foale S. & Macintyre M. (2015). Managing inequality or managing stocks? An ethnographic perspective on the governance of small-scale fisheries. *Fish and Fisheries* **16**(3): 471–485.
DOI: https://doi.org/10.1111/faf.12069

Frerks G.E., Dietz T. & van der Zaag P. (2014). Conflict and cooperation on natural resources: justifying the CoCooN Programme. In: *Conflict Over Natural Resources in the Global South*. *Conceptual Approaches*, pp. 13–43. CRC Press, USA.

Fu T., Zhang L., Chen B. & Yan M. (2022). Human disturbance on the land surface environment in tropical islands: a remote sensing perspective. *Remote Sensing* **14**(9): 2100.
DOI: https://doi.org/10.3390/rs14092100

Gabadage D.E., Botejue W.M.S., Surasinghe T.D., Bahir M.M., Madawala M.B., Dayananda B., Weeratunga V.U. & Karunarathna D.M.S.S. (2015). Avifaunal diversity in the peripheral areas of the Maduruoya National Park in Sri Lanka: with conservation and management implications. *Journal of Asia-Pacific Biodiversity* **8**(2): 121–132.
DOI: https://doi.org/10.1016/j.japb.2015.04.005

Ganegodage K.R. & Rambaldi A.N. (2011). The Impact of education investment on Sri Lankan economic growth. *Economics of Education Review* **30**(6): 1491–1502.
DOI: https://doi.org/10.1016/j.econedurev.2011.08.001

Hu X., Næss J.S., Iordan C.M., Huang B., Zhao W. &

Cherubini F. (2021). Recent global land cover dynamics and implications for soil erosion and carbon losses from deforestation. *Anthropocene* **34**: 100291.
DOI: https://doi.org/10.1016/j.ancene.2021.100291

Hundlani D. (2019). Navigating a green BRI in Sri Lanka. In: *Silk Road to Belt Road* (ed. M.N. Islam), pp. 215–233. Springer, Singapore.
DOI: https://doi.org/10.1007/978-981-13-2998-2_13

IPCC (2021). *Climate Change 2021: The physical Science Basis. Contribution of Working Group I to the Sixth Assessment Report of the Intergovernmental Panel on Climate Change*. Cambridge University Press, Cambridge, United Kingdom and New York, USA.
DOI: https://doi.org/10.1017/9781009157896

IPBES (2019). Global assessment report on biodiversity and ecosystem services of the Intergovernmental Science-Policy Platform on Biodiversity and Ecosystem Services (eds. E.S. Brondizio, J. Settele, S. Díaz & H.T. Ngo), pp. 1148. IPBES Secretariat, Bonn, Germany.
DOI: https://doi.org/10.5281/zenodo.3831673

Jayawardhana W.G.N.N. & Chathurange V.M.I. (2016). Extraction of agricultural phenological parameters of Sri Lanka using MODIS, NDVI time series data. *Procedia Food Science, International Conference of Sabaragamuwa University of Sri Lanka*, pp. 235–241.
DOI: https://doi.org/10.1016/j.profoo.2016.02.027

Kendall M.G. (1938). A new measure of rank correlation. *Biometrika* **30**(1–2): 81–93.
DOI: https://doi.org/10.1093/biomet/30.1-2.81

Kennedy R.E., Yang Z., Braaten J., Copass C., Antonova N., Jordan C. & Nelson P. (2015). Attribution of disturbance change agent from Landsat time-series in support of habitat monitoring in the Puget Sound region, USA. *Remote Sensing of Environment* **166**: 271–285.
DOI: https://doi.org/10.1016/j.rse.2015.05.005

Killick R. & Eckley I.A. (2014). Changepoint: An R package for changepoint analysis. *Journal of Statistical Software* **58**(3): 1–19.
DOI: https://doi.org/10.18637/jss.v058.i03

Kodikara K.A.S., Lewandowski S., de Silva P.M.C.S., Gunarathna S.D., Madarasinghe S.K., Ranasinghe P., Jayatissa L.P. & Dahdouh-Guebas F. (2022). Heavy metal pollution in selected upland tributaries of Sri Lanka: comprehension towards the localization of sources of pollution. *Journal of Water and Health* **20**(3): 505–517.
DOI: https://doi.org/10.2166/wh.2022.250

Lambin E.F. *et al*. (26 authors) (2001). The causes of land-use and land-cover change: moving beyond the myths. *Global Environmental Change* **11**(4): 261–269.
DOI: https://doi.org/10.1016/S0959-3780(01)00007-3

Lindström S., Mattsson E. & Nissanka S.P. (2012). Forest cover change in Sri Lanka: The role of small-scale farmers. *Applied Geography* **34**: 680–692.

Madarasinghe S.K., Yapa K.K.A.S. & Jayatissa L.P. (2020). Google Earth imagery coupled with on-screen digitization for urban land-use mapping: Case study of Hambantota, Sri Lanka. *Journal of the National Science Foundation of Sri Lanka* **48**(4): 357–366.
DOI: http://doi.org/10.4038/jnsfsr.v48i4.9795

Manesha E.P.P., Jayasinghe A. & Kalpana H.N. (2021). Measuring urban sprawl of small and medium towns using GIS and remote sensing techniques: a case study of Sri Lanka. *The Egyptian Journal of Remote Sensing and Space Science* **24**(3) Part 2: 1051–160.
DOI: https://doi.org/10.1016/j.ejrs.2021.11.001

Mathiventhan T. (2007). Ecological and social resiliencies of mangroves of Batticaloa, Sri Lanka, in the face of human activities, conflicts and natural hazards. *MSc thesis*, Norwegian University of Life Sciences, Norway.

Mathiventhan T. (2013). Post Tsunami status of selected coastal ecosystems and its relevance to coastal environment and communities in Batticaloa district, Sri Lanka. *PhD thesis*, Eastern University, Sri Lanka.

Mathiventhan T. & Jayasingam T. (2014). Coastal greenbelt in Batticaloa district: Is Casuarina a success? *International Journal of Marine Sciences* **4**(55): 1–5
DOI: http://doi:10.5376/ijms.2014.04.0055

Mathiventhan T. & Jayasingam T. (2018). Geomorphological changes along the east coast of Sri Lanka. *International Journal of Research Studies in Biosciences* **6**(7): 2349–2365.
DOI: http://dx.doi.org/10.20431/2349-0365.0607002

McGregor A. (2008). *Well-Being, Poverty and Conflict*. Briefing Paper 1/08, ESRC Research Group on Well-being in Developing Countries. University of Bath, Bath, UK.

Mondal P., McDermid S.S. & Qadir A. (2020). A reporting framework for sustainable development goal 15: multi-scale monitoring of forest degradation using MODIS, landsat and sentinel data. *Remote Sensing of Environment* **237**: 111592.
DOI: http://doi.org/10.1016/j.rse.2019.111592

Myers N., Mittermeier R.A., Mittermeier C.G., da Fonseca G.A.B. & Kent J. (2000). Biodiversity hotspots for conservation priorities. *Nature* **403**: 853–858.
DOI: https://doi.org/10.1038/35002501

Perera P. (2014). The political economy of post war economic development in Sri Lanka. *International Journal of Business and Social Research* **4**(12): 43–62.

Perera W.P.T.A., Prematilaka P.H.K.L.A., Haseena M.H.A., Athapaththu A.H.L.C.M. & Wijesinghe M.R. (2021). Changes in habitat coverage from 2005 to 2019 in the Udawalawe National Park, Sri Lanka. *Ceylon Journal of Science* **50**(4): 467–474.
DOI: https://doi.org/10.4038/cjs.v50i4.7945

Perera K. & Tsuchiya K. (2009). Experiment for mapping land cover and it's change in South-eastern Sri Lanka utilizing 250m resolution MODIS imageries. *Advances in Space Research* **43**(9): 1349–1355.
DOI: https://doi.org/10.1016/j.asr.2008.12.016

Rathnayake C.W., Jones S. & Soto-Berelov M. (2020). Mapping land cover change over a 25-year period (1993–2018) in Sri Lanka using Landsat time-series. *Land* **9**(1): 27.
DOI: https://doi.org/10.3390/land9010027

Rishandani D. (2021). *COVID-19 and Its Impact of Sri Lanka Economy*. SSRN Scholarly Paper. Rochester, USA.
DOI: https://doi.org/10.2139/ssrn.3914025

Senanayake I.P., Welivitiya W.D.D.P. & Nadeeka P.M. (2013). Remote sensing based analysis of urban heat islands with vegetation cover in Colombo City, Sri Lanka using Landsat-7 ETM+ Data. *Urban Climate* **5**: 19–35.
DOI: https://doi.org/10.1016/j.uclim.2013.07.004

Senevirathna E.M.T.K., Edirisooriya K.V.D., Uluwaduge S.P. & Wijerathna K.B.C.A. (2018). Analysis of causes and effects of coastal erosion and environmental degradation in southern coastal belt of Sri Lanka special reference to Unawatuna coastal area. Procedia Engineering, *7th International Conference on Building Resilience: Using Scientific Knowledge to Inform Policy and Practice in Disaster Risk Reduction* **212**: 1010–1017.
DOI: https://doi.org/10.1016/j.proeng.2018.01.130

Subasinghe S., Estoque R.C. & Murayama Y. (2016). Spatiotemporal analysis of urban growth using GIS and remote sensing: A case study of the Colombo Metropolitan Area, Sri Lanka. *ISPRS International Journal of Geo-Information* **5**(11): 197.
DOI: https://doi.org/10.3390/ijgi5110197

Weerakoon D. (2018). Sri Lanka: Post-war economic development in a changing global landscape. *12th ISAS International Conference on South Asia, Emerging South Asia: Politics, Economy and International Relations*, 6 April 2018, ISAS, National University of Singapore, Singapore.

Weerasekara K.A.W.S. *et al*. (11 authors) (2015). Assessment of water pollution status of selected fishery harbours located in the southern province of Sri Lanka. *Journal of Environmental Professionals Sri Lanka* **4**(2): 36–46.
DOI: http://doi.org/10.4038/jepsl.v4i2.7861

Wickramaarachchi T.N., Ishidaira H. & Wijayaratna T.M.N. (2013). Projecting land use transitions in the Gin Catchment, Sri Lanka. *Research Journal of Environmental and Earth Sciences* **5**(8): 473–480.
DOI: http://dx.doi.org/10.19026/rjees.5.5677

Wikramanayake E., Fernando S., Wickramaratne C., Akbarally Z. & Wikramanayake S. (2022). Sri Lankan moist forests ecoregion: an imperiled island rainforest. In: *Imperiled: The Encyclopedia of Conservation* (ed. D.A. DellaSala & M.I. Goldstein), pp. 37–52. Elsevier, Oxford, UK.
DOI: https://doi.org/10.1016/B978-0-12-821139-7.00004-0

J.Natn.Sci.Foundation Sri Lanka 2023 51 (4): 689 - 701
DOI: http://dx.doi.org/10.4038/jnsfsr.v51i4.11558

RESEARCH ARTICLE

Advanced Modelling

Socio-demographic and behavioural factors associated with prominent misconceptions of HIV/AIDS transmission among ever married women in Sri Lanka: An application of modelling correlated binary outcomes using a bridge distribution function

NM De Alwis[1*], N Withanage[1], CL Jayasinghe[1] and S Ananda[2]
[1] *Department of Statistics, Faculty of Applied Sciences, University of Sri Jayewardenepura, Gangodawila, Nugegoda, Sri Lanka.*
[2] *Department of Social Sciences, Faculty of Social Sciences and Languages, Sabaragamuwa University of Sri Lanka, Belihuloya, Sri Lanka.*

Submitted: 09 January 2023; Revised: 19 June 2023; Accepted: 28 July 2023

Abstract: Human Immunodeficiency Virus (HIV) case reporting usually represents only the trending pattern of HIV infected people in Sri Lanka. Having a decent level of knowledge about HIV largely contributes to preventing HIV prevalence in the country. People with HIV are not hazardous to the public who live together with them and with whom they have ordinary, non-sexual contact. However, suffering from HIV in a culture like Sri Lanka generates an extreme level of stigmatizing by people living with HIV and many psychological and social effects. This study aims to identify the factors that are associated with possessing knowledge, among ever married women in the reproductive age in Sri Lanka, regarding two prominent misbeliefs on HIV/AIDS transmission. This will be useful to identify various socio-economic, geographic subgroups who are lacking knowledge on HIV/AIDS spread. Secondary data from 2016 Sri Lanka Demographic and Health Survey was used in the analysis. Joint modelling was considered since it was found that two outcome variables are highly associated and hence the ever-married woman who believes one misconception is more likely to believe the second misconception too. To capture the association between two outcomes, we incorporated a shared random effect and assumed the bridge distribution for the random effect. Respondent's province, highest level of education, access to mass media, religion, age and wealth index were found to have a significant effect on prominent misconceptions on HIV/AIDS transmission.

Keywords: Bridge distribution, correlated binary responses, HIV/AIDS transmission, logistic regression, misconceptions on disease transmission.

INTRODUCTION

Human immunodeficiency virus (HIV) gives rise to acquired immune deficiency syndrome (AIDS), which is known as an incurable disease of human beings ultimately leading to death. According to UNAIDS in 2022 there were 37.7 million (30.2 million–45.1 million) people globally living with HIV. Among them, 36.0 million (28.9 million–43.2 million) were adults and 1.7 million (1.2 million–2.2 million) were children (<15 years old). Approximately 84% [67–>98%] of people with HIV globally knew their HIV status in 2020. The remaining people about 6.1 million (4.9 million–7.3 million) still need access to HIV testing services to test their HIV status. HIV testing is an essential gateway to HIV prevention, treatment, care and support services. Most people with HIV are living in low- and middle-income countries. By 2021, new HIV infections have been reduced by 54% since the peak in 1996. In 2021, around 1.5 million (1.1 million–2.0 million) people

* Corresponding author (madumalidealwis@gmail.com; https://orcid.org/0009-0002-2266-3908)

were newly infected with HIV, compared to 3.2 million (2.4 million–4.3 million) people in 1996. According to UNAIDS, women and girls accounted for 49% of all new infections in 2021 (UNAIDS Fact Sheet, 2022).

Consistent with the final report of the Sri Lanka Demographic and Health Survey (SLDHS) in 2016, since the identification of the first HIV infected Sri Lankan in 1987, a cumulative total of 4,245 HIV positive cases has been reported up to the end of 2022. In 2021, 410 HIV cases have been reported to the National STD/AIDS control programme (NSACP) which is responsible for coordinating, planning, and implementing the HIV National Strategic Plan and the AIDS Policy in the country. However, the reported numbers represent only a fraction of HIV infected people in the country, as many infected people may perhaps not be aware of their HIV status and in addition, stigma and discrimination towards HIV infected people adversely affect voluntary testing for HIV (Annual Report NSACP, 2021). An estimated 3638 (3250 – 4000) people were living with HIV in Sri Lanka at the end of 2021. During 2021, 411 people living with HIV were newly diagnosed. This is a 13% increase from the previous year. Further, an increase in the incidence rate of HIV cases has also been observed in the Island during the recent past (Figure 1).

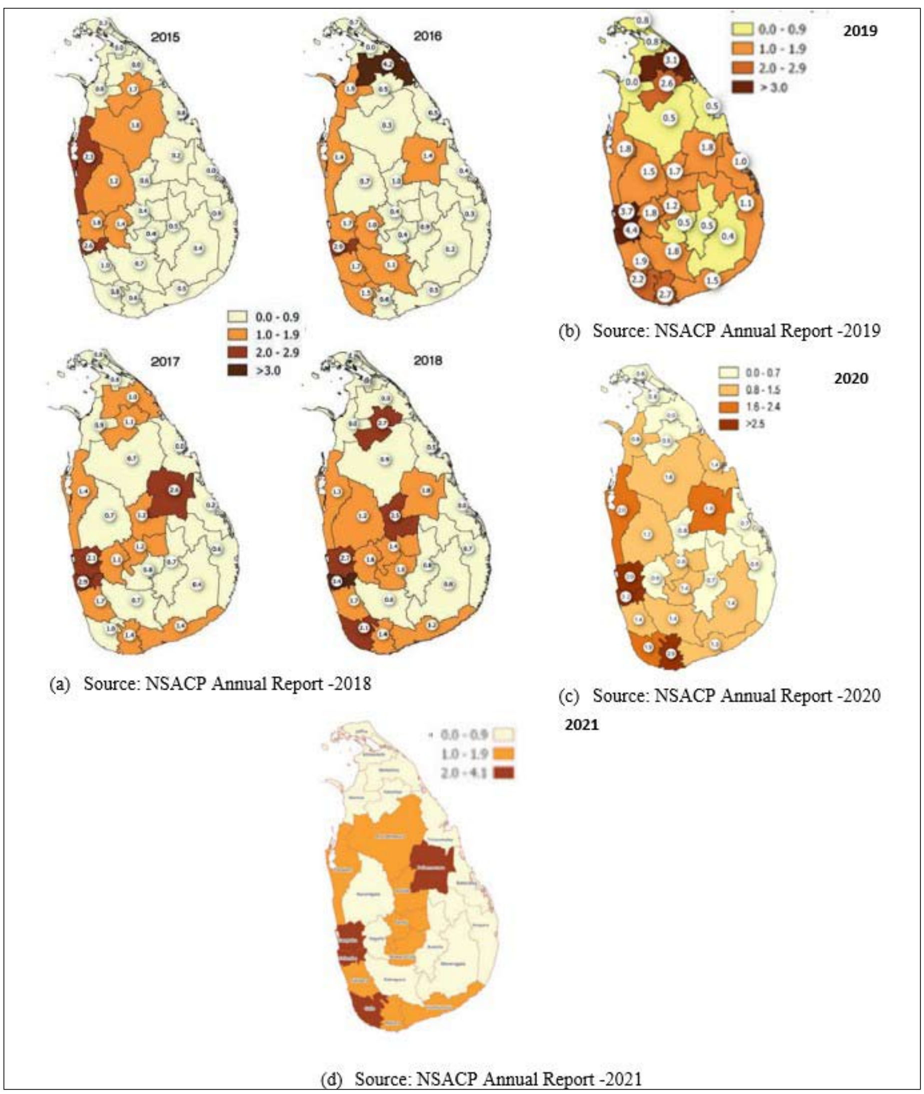

Figure 1: Rate of newly reported HIV cases per 100,000 population as reported in NSACP Annual reports 2018 – 2021.

People living with HIV are not a public hazard to those who coexist with them in the community and engage in ordinary, non-sexual contact. However, in the cultural context of Sri Lankan society, individuals living with HIV experience a significant degree of stigmatization, resulting in various psychological and social consequences. An HIV infected individual also loses his/her social recognition, respect and acceptance (Samarakoon *et al*., 2020). In conservative societies that still exist in most countries in the South Asian region, including Sri Lanka, the treatment that Society accords an HIV infected person seems to depend on the social status of that individual. As Thakuri and Thapa (2018) claim regarding the case of India, 'those whose characters are unblemished enjoy a high position in the society and the extreme opposite creates serious issues like social marginalization.' Saki *et al.* (2015) point out how the AIDS patients suffer from different dimensions of stigma, rejection, and insult that affect the individual him- or herself, family, others, and finally the society. The majority of people who live with HIV are in the African Continent, more than any other region of the world, and numerous misconceptions are prevalent about HIV and AIDS (Niehaus & Jonsson, 2005). Most of these false ideas prevail when the people are unable to comprehend the scientific basis behind them. Hence, they tend to formulate different ideas based on norms, values, public opinion, and speculation. Such beliefs are prominent in third world countries such as Ethiopia, Bangladesh, Iran, and India, which tend to possess similar cultural characteristics (Niehaus & Jonsson *et al*., 2005; Saki *et al.*, 2015; Thakuri & Thapa, 2018; Agegnehu & Tesema, 2020). Even at present, many rural communities with less educated people and even the educated, urban younger generation who do not have access to the latest knowledge of the sciences tend to live in their own traditional, gloomy spheres. Current misconceptions include genocidal beliefs such as 'HIV/AIDS was developed by White people in the West to control Black African population' and superstitious beliefs such as 'AIDS is caused by supernatural forces or witchcraft' (Niehaus & Jonsson, 2005). Some African men believe that condoms were infected with 'AIDS worms' and that HIV was created by racist Whites and that HIV is put into the lubricant in condoms exported and distributed in Africa. Hence, these HIV/AIDS misconceptions are also obstructing HIV prevention efforts since they were associated with decreased condom use among African men (Bogart & Thorburn, 2005).

There also exist several misconceptions about HIV transmission that are common in most communities: HIV infection can be acquired by swimming, sharing meals, shaking hands, casual touch, speaking face-to-face with an infected person, and transmission through mosquito bites (Choudhary *et al*., 2015; Thakuri & Thapa, 2018). Qian *et al.* (2007) have identified that the gender of the respondent is not significantly associated with the misconceptions of HIV transmission in rural Chinese communities, while Bogart *et al.* (2011) observed that some misconceptions are gender specific among African Americans aged 15 to 44 years and living in the contiguous United States. As aforesaid, these beliefs prevail when people are unable to comprehend the scientific basis behind them. For example, there is a biological reason why HIV cannot be transmitted through a mosquito bite; this is because HIV cannot replicate inside the mosquito due to the lack of a T4 antigen on the cell surface (Iqbal, 1999). It has also been found that among young Sri Lankan adults the knowledge of HIV prevention and misconceptions of HIV transmission is not at a sufficient level (Bogart *et al.*, 2011; Karthijekan, 2017).

Asaduzzaman *et al.* (2016) found that awareness and knowledge of HIV/AIDS among married women in rural Bangladesh are associated with exposure to mass media. Extracted data of 11,570 rural married women aged 15–49 years old from the sixth Bangladesh Demographic Health Survey in 2011 was utilized and through logistic regression analysis it was found that exposure to each type of media (listening to the radio, reading newspapers/magazines, watching television) was significantly associated with awareness of HIV/AIDS. Authors suggested that television can be utilized to increase awareness and comprehensive knowledge of HIV/AIDS through effective TV programmes. Furthermore, Haque *et al.* (2018) found that apart from exposure to mass media access, respondents' education status, place of living, and working status played a significant role on the attention of HIV/AIDS among married women in Bangladesh by performing a logistic regression analysis.

Many authors have addressed the knowledge of HIV prevention among adults in Sri Lanka (Kanda *et al.*, 2010; de Silva *et al.*, 2014; Karthijekan, 2017; Madurapperuma *et al.*, 2018) but have not sufficiently addressed knowledge about the misconceptions of HIV/AIDS. Samarakoon *et al.* (2020) through a generalized linear mixed model approach found that among tertiary and vocational education trainees in Sri Lanka, possessing knowledge on these prominent misconceptions is associated with their level of education, having a sound knowledge on sexual and reproductive health, and having attended workshops on sexually transmitted diseases.

According to the 2016 Sri Lanka Demographic and Health Survey, comprehensive knowledge of HIV/AIDS among 18,302 ever-married women is defined as understanding the following:

1) Consistent use of condoms during sexual relationships can reduce the chance of contracting HIV.
2) Having just one uninfected faithful partner can reduce the chance of contracting HIV.
3) It is possible for a healthy-looking person to have HIV.
4) It is a misconception that people can get the HIV virus from mosquito bites.
5) It is a misconception that someone can contract the HIV virus by sharing food with an HIV-infected person.

The most common fallacies about HIV transmission in Sri Lanka are that 'people can get the HIV virus from mosquito bites' and 'someone can get the HIV virus by sharing food with an HIV-infected person,' as stated in the final report of the 2016 SLDHS.

In this paper we made an in-depth investigation on these two common misconceptions on HIV transmission using the data gathered through the most recent SLDHS conducted by the Department of Census and Statistics (DCS) in 2016. The main objective of the current study was to identify the awareness of ever-married women about these two misconceptions about HIV transmission and to investigate how their awareness varies with their socio-demographic and behavioural factors. This was achieved by jointly modelling the outcome variables considering the correlation between outcomes.

It is obvious that two responses regarding the misconceptions of spreading HIV observed from the same respondent are likely to be correlated since a single person who believes one misconception is more likely to believe the second misconception too and awareness of two delusions are related to individual characteristics. Failure to account for such correlations by treating responses from the same respondents as independent may consequently yield incorrect inferences. Standard errors calculated by incorrectly assuming correlated observations to be independent tend to underestimate the true sampling variability, consequently yielding a type I error of significance tests (Withanage *et al*., 2014). Hence, joint modelling of two outcomes provides better control over type I error rates in multiple tests and gains efficiency in the parameter estimates.

MATERIALS AND METHODS

The survey and data source

The data used for this study were obtained from the Sri Lanka Demographic and Health Survey (SLDHS) 2016 conducted by the Department of Census and Statistics (DCS) of Sri Lanka. Demographic and health surveys, also known as DHS programmes, are national representative population-based household surveys, which provide accurate and internationally comparable data on health indicators in developing countries. They collect and disseminate data on areas such as fertility, family planning, maternal and child health, gender, HIV/AIDS, malaria, and nutrition. DHS surveys are part of the world-wide DHS project, intending to observe and improve population health (The DHS programme, 2016).

Computer-Assisted Personal Interviewing (CAPI), coupled with the use of mobile and wireless technology, was the method of data collection used in the SLDHS 2016. In CAPI, the data entry and validation of DHS 2016 was also done on-site using the digital questionnaire on tablet computers for the first time in DCS history. A total of 28,720 housing units were selected as the sample, from which 27,455 were occupied at the time of the survey and out of those existing households 27,210 were successfully interviewed. Moreover, there were 18,302 ever married women who were interviewed during the research. However, for the current study, all respondents who satisfy the criteria given below were selected: (1) ever married women in the age group 15 – 49 years in Sri Lanka, (2) who have ever heard about HIV/AIDS, and (3) have given 'Right' or 'Wrong' as answers for the two response variables which were identified as the two most prominent local misconceptions about HIV transmission, in the SLDHS in 2016. This resulted in a sample of size 11,808 women. Note that the whole population of ever married women in the reproductive age group (15 – 49) who have heard about HIV/AIDS was the target population of the study.

Response variables and predictors

In the SLDHS 2016, respondents were asked a couple of questions regarding misconceptions about HIV/AIDS. Among these questions, two prominent misconceptions were analysed: the belief that 'people can get the HIV virus from mosquito bites (Y1)' and the belief that 'someone can get the HIV virus by sharing food with an HIV-infected person (Y2)' (Table 1). Both questions were close-ended, allowing for responses of 'Right,' 'Wrong,' or 'Don't know.' However, for the analysis, we focused on individuals who answered either 'Right' or 'Wrong' as these options provide clear information about the respondents' awareness regarding these misconceptions. It is important to note that both statements, Y1 and Y2, are false.

Table 1: Response variable statements considered

Response variables	Percentage of responses	
	Wrong (%)	Right (%)
People can get HIV virus from mosquito bites (Y1)	76.2	23.8
Someone can get the HIV virus by sharing food with a HIV infected person (Y2)	79.1	20.9

Since the SLDHS 2016 aimed to measure various aspects of households and their members, the questionnaire comprised a substantial number of questions and variables. Through a meticulous review and consideration of existing literature, relevant predictors related to misconceptions about the spread of HIV/AIDS were carefully filtered and selected for examination. The association between these predictors and response variables was determined using a Chi-squared test. Predictors that exhibited a significant association with responses at a 10 % level of significance were chosen to model the responses in conjunction with the predictions.

Statistical analysis

As the first step, a descriptive analysis followed by a Chi-squared analysis was conducted to understand the composition of the sample and investigate for the possible existence of associations between various categorical variables and each response variable. Binary logistic regression models were fitted for each response variable separately as the next step to identify the factors influencing the awareness of Y1 and Y2 among ever married women in the reproductive age range (15–49 years) in Sri Lanka. The final logistic regression models were selected based on forward conditional procedure. Predictors that showed significance (at 10% level of significance) for at least one of the response variables were included in the joint model. A higher level of significance (10%) was chosen for individual logistic models to ensure that all important predictors would be included in the joint model.

Only significant predictors identified for at least one response model were included in the joint model. Non-significant predictors were removed from the model using the Wald test statistic. However, the results of the separate logistic regression models for Y1 and Y2, assuming independence between the two outcomes, were not included in this manuscript. Only the joint model results, which account for the correlation between Y1 and Y2, are presented. PROC NLMIXED in SAS 9.2 University edition was used to fit the joint model. The SAS codes are in the appendix.

Joint modelling (random intercept logistic regression model)

Random effects logistic regression models are often used to model clustered binary response data assuming normal distribution for the random effects. Regression parameters in these models have a conditional, subject-specific interpretation in that they quantify regression effects for each cluster/unit. Hence, these parameter estimates are not directly comparable with the parameter estimates of the binary logistic regression models. In this study, joint modelling of two outcomes is appropriate since it was found that the two outcome variables are highly associated. In this joint modelling approach, following Wang and Louis (2003), a shared random effect was incorporated to capture the correlation between the two outcomes and a bridge distribution was assumed for the random effect. Under this assumption, the marginal functional shape is logistic and regression parameters have an explicit marginal interpretation. In addition, with a simple transformation, likelihood inference can be obtained for either marginal or conditional regression inference within a single model framework. A brief description of the joint model formulation is as follows:

The model conditional on random intercept has the following form:

$$logit\{Pr\left(Y_{ij}=1|b_i,\boldsymbol{X}_{ij}\right)\}=b_i+\boldsymbol{\alpha}_j^T\boldsymbol{X}_{ij} \quad ...(01)$$

where the Y_{ij} is the j^{th} outcome for the i^{th} individual (i = 1, 2, ..., n, j = 1 or 2), $\boldsymbol{X}_{ij}$ are the vectors of covariates associated with j^{th} outcome and $\boldsymbol{\alpha}_j$ are the corresponding vectors of regression coefficients. The marginal probability has the form,

$$Pr\left(Y_{ij}=1\right)=\int\frac{exp\left(b_i+\boldsymbol{\alpha}_j^T\boldsymbol{X}_{ij}\right)}{1+exp\left(b_i+\boldsymbol{\alpha}_j^T\boldsymbol{X}_{ij}\right)}dF(b_i) \quad ...(02)$$

where, $F(.)$ is the bridge distribution function. The bridge density function for the logit link is,

$$f(b_i)=\frac{1}{2\pi}\frac{sin\ (\phi\pi)}{cosh\ (\phi b_i)+cos\ (\phi\pi)}$$
$$(0<\phi<1,-\infty<b_i<\infty) \quad ...(03)$$

with $\phi=\left(1+\frac{3}{\pi^2}d\right)^{-1/2}$ and d the random-intercept variance (Wang & Louis, 2003).

With the above bridge distribution for the random effects, the marginal distribution can be modelled directly by,

$$logit\{Pr\left(Y_{ij}=1\right)\}=\boldsymbol{\alpha}_{mj}^T\boldsymbol{X}_{ij} \quad ...(04)$$

where $\boldsymbol{\alpha}_{mj}$ measures a marginal regression effect associated with the covariate X_{ij} for the j^{th} outcome. The relationships of regression parameters between conditional and marginal regression models are given by

$$\boldsymbol{\alpha}_{mj}=\frac{\boldsymbol{\alpha}_j}{\sqrt{(1+3d/\pi^2)}} \quad ...(05)$$

RESULTS AND DISCUSSION

Descriptive statistics

Around 76% of the respondents indicated that the Y1 statement is false, while approximately 79% of the respondents stated that the Y2 statement is false (Table 1). This indicates that the majority of ever married women were aware about two prominent HIV/AIDS transmission misconceptions. Table 2 presents a summary of the composition of the sample of women considered by the study with respect to residential sector, region

Table 2: Composition of the sample considering respondents' Residence, Region, Religion, Age, Current marital status, Highest educational qualification, Have given birth, Working status, and Wealth index.

Variable	Count	Percent (%)
Residence		
Estate	334	2.83
Rural	9467	80.17
Urban	2007	17.00
Region		
Central	1177	9.97
Eastern	1076	9.11
North Central	847	7.17
North Eastern	1363	11.54
Northern	1335	11.31
Sabaragamuwa	1276	10.81
Southern	1465	12.41
Uva	794	6.72
Western	2475	20.96
Religion		
Buddhist	8150	69.02
Hindu	1606	13.60
Islam	1001	8.48
Other	167	1.41
Roman Catholic	884	7.49
Age group (years)		
15-19	112	0.95
20-24	838	7.10
25-29	1761	14.91
30-34	2487	21.06
35-39	2619	22.18
40-44	2096	17.75
45-49	1895	16.05
Current marital state		
Currently married	10760	91.12
Living with a man	450	3.18
Other	598	5.06
Highest education qualification		
Degree and above	744	6.30
Passed G.C.E.(A/L) or equivalent	2910	24.64
Passed G.C.E.(O/L) or equivalent	2917	24.70
Passed Grade 6-10	4711	39.90
Passed Grade 1-5	460	3.90
No Schooling	66	0.56
Have you ever given birth		
No	1193	10.10
Yes	10615	89.90
Working status		
No	7885	66.78
Yes	3923	33.22
Wealth Index		
Lowest	2049	17.35
Second	2258	19.12
Middle	2428	20.56
Fourth	2532	21.44
Highest	2541	21.52

of the residence, current marital status, religion of the respondent, wealth index group, current working status, age, highest educational qualification and whether the respondent has given birth before. In the sample, of respondents, around 80% were from rural sector and 3% were from estate sector. In terms of the province where respondents resided, a majority were from Western province (21%) and the smallest number of respondents were from Uva province (7%). More than 91% of the ever-married women were currently married and around 5% of the ever-married women in the sample were not in the union, or were widowed, divorced, or separated. Around 90% of the respondents had given birth. Considering the religiosity of the respondents, the majority were Buddhist (69%), and among the others 14% and 9% of the respondents were Hindu and Islamic devotees, respectively. Out of the ever-married women in the sample, 33% were engaged in jobs. Considering the age of the respondents, 8% belonged to the age group of 15–24 years and 34% were 40 years or above. Regarding the highest educational level of the respondents, 25% have successfully passed G.C.E.(O/L) examination, 25% have successfully passed G.C.E.(A/L) examination and 6% have attained a degree or higher qualification. It is worth mentioning that approximately 4% of the respondents had received education only up to grade 5.

It has been observed in previous studies, *e.g.*, by Agegnehu and Tesema (2020), that exposure to mass media is significantly associated with awareness of misconceptions of HIV/AIDS and also the comprehensive knowledge of HIV/AIDS. The reason for this observation is obvious since mass media (radio, television, and newspaper) is the main source of information, and the most powerful way of addressing a large group of people to change the community awareness, attitude, and practice towards HIV/AIDS. In the SLDHS 2016, exposure to mass media of ever married women was measured by three questions: (1) Frequency of reading newspapers (at least once a week, less than once a week, and not at all) (2) Frequency of watching television (at least once a week, less than once a week, and not at all) and (3) Frequency of listening to radio (at least once a week, less than once a week, and not at all). Table 3 illustrates the cross tabulation of exposure to mass media and two misconceptions Y1 and Y2. The awareness of two misconceptions of transmission of HIV/AIDS were higher among the ever-married women who read newspapers, who watched television and who listened radio, than among the ones who did not perform those activities at all.

Analysis based on two independent binary logistic regression models

The significant predictors for Y1 or Y2, identified using Chi squared test, included the following categorical variables: age group (15–19, 20–24, 25–29, 30–34, 35–39, 40–44, 45–49), place of residence (estate, rural, and urban), province (Central, Eastern, Northern, North Central, North Eastern, Sabaragamuwa, Southern, Uva, and Western), respondent's education (never schooled, passed grade 1–5, passed grade 6–10, passed G.C.E. (O/L), passed G.C.E. (A/L), degree and above), wealth index (lowest, second, middle, fourth, and highest),

Table 3: Distribution of frequency of reading newspapers, watching television and listening to radio for the two response variables (Y1 and Y2).

Variable	Total (column %)	Y1 (row %)		Y2 (row %)	
		Right	Wrong	Right	Wrong
Frequency of reading newspapers					
At least once a week	5553 (47.00%)	1185 (21.3%)	4368 (78.7%)	920 (16.6%)	4633 (83.4%)
Less than once a week	3807 (32.30%)	881 (23.1%)	2926 (76.8%)	820 (21.5%)	2987 (78.5%)
Not at all	2448 (20.70%)	746 (30.5%)	1702 (69.5%)	732 (29.9%)	1716 (70.1%)
Frequency of watching television					
At least once a week	9691 (82.00%)	2270 (23.4%)	7421 (76.6%)	1857 (19.2%)	7834 (80.8%)
Less than once a week	1291 (11.00%)	290 (22.5%)	1001 (77.5%)	337 (26.1%)	954 (73.9%)
Not at all	826 (7.00%)	252 (30.5%)	574 (69.5%)	278 (33.7%)	548 (66.3%)
Frequency of listening to radio					
At least once a week	6092 (51.60%)	1475 (24.2%)	4617 (75.8%)	1200 (19.7%)	4892 (80.3%)
Less than once a week	2686 (22.70%)	559 (20.8%)	2127 (79.2%)	538 (20.0%)	2148 (80.0%)
Not at all	3030 (25.70%)	778 (25.7%)	2252 (74.3%)	734 (24.7%)	2296 (75.8%)

religion (Buddhist, Hindu, Islam, Roman Catholic, and other), working status (yes, no), exposure to mass media and current marital status (currently married, living with man, not in union) and ever given birth (yes, no).

The correct answer for each statement, Y1 and Y2, was considered a 'success' outcome, while giving the wrong answer was considered a 'failure' outcome. Logistic models were utilized to estimate the probability of success for each statement, Y1 and Y2, separately. Table 4 provides a summary of the significant explanatory variables (at a 10% level of significance) for each response variable, indicating their significant impact on the knowledge of HIV spread among ever-married women in the reproductive age group in Sri Lanka.

Results of the joint model

All predictors mentioned in Table 4 were included into the joint model as discussed. However, it was noted that the three predictors related to the exposure to mass media of ever married women were highly associated with each other, and hence the joint model including these three predictors (after adjusting for other predictors stated in Table 4) led to unrealistic conclusions due to problem of multicollinearity. To avoid high collinearity among these three predictors, the predictor variable of frequency of listening to radio was dropped from the model.

Table 4: Significant explanatory variables in the fitted binary logistic models.

Response variables	Significant explanatory variables (under 10% level of significance)
People can get HIV virus from mosquito bites (Y1)	Province Highest education qualification Frequency of reading newspaper Frequency of listening to radio Religion Wealth index
Someone can get the HIV virus by sharing food with a HIV infected person (Y2)	Residence Province Current marital state Highest education qualification Frequency of watching television Frequency of reading newspaper Religion Age group Wealth index

Interestingly, in the joint model, the predictors 'age' and 'residence' became significant for the response variable Y1 which was not significant individually (Table 4). It was stimulating to find out that when the two responses (Y1 and Y2) were jointly modelled, still current marital status no longer appeared as significant for Y1 at the 5% level of significance, but it is momentous at the 10% level of significance (p value = 0.068); therefore, we decided to keep it in the model. According to the fitted joint model, ever married woman's residence area, province, age group, level of education, religion, current marital status, wealth index, frequency of reading newspapers and frequency of watching television were statistically associated with the knowledge of two prominent misconceptions of HIV/AIDS. The regression coefficients (standard errors) of the joint model for two outcomes alone with odds ratios are presented in Table 5.

Women residing in urban areas had 1.3 times higher odds of possessing knowledge regarding the statement 'people can get HIV from mosquito bites,' and 1.4 times higher odds of knowledge regarding the statement 'HIV can be transmitted by sharing food with an infected person', compared to women residing in the estate sector. On the other hand, women in the Central province, which is relatively more ethnically diverse, had lower odds (0.811 and 0.801) of providing the correct answer for the statements regarding 'HIV transmission through mosquito bites' and 'sharing food with an infected person', respectively, compared to women in the Sabaragamuwa province, which is relatively less ethnically varied. When considering the age of the respondents, it was observed that women belonging to the 25–29 and 30–34 age groups exhibited decreased odds of giving the correct answer for the statement 'people can get HIV from mosquito bites' by 24% and 17%, respectively, compared to women in the 45–49 age group. However, for the second statement 'someone can get HIV by sharing food with an HIV-infected person,' it was observed that women belonging to the 35–39 and 40–44 age groups had an increased odds of giving the right answer by 23% and 18%, respectively, compared to women in the 45–49 age group. When considering the highest education level, women who had never been schooled had 77.6% lower odds of giving the correct answer for the statement 'people may get infected with HIV virus from mosquito bites' compared to women with a degree or above educational qualifications. Similarly, compared to the highest education level, women who had never been schooled had 59.5% lower odds of giving the correct answer for the statement 'HIV can be transmitted by sharing food with an HIV-

Table 5: Parameter estimates (standard errors) and odds ratios (95% confidence interval) with respect to the reference category for the joint model of Y1 and Y2.

Variable (Reference category)	Y1 (People can get HIV virus from mosquito bites)		Y2 (Someone can get HIV virus by sharing food with HIV infected person)	
	Regression coefficient (standard error)	Odds ratio (95% confidence interval)	Regression coefficient (standard error)	Odds ratio (95% confidence interval)
Residence (Estate)				
Urban	0.262 (0.121)*	1.300 (1.025, 1.647)	0.346 (0.156)*	1.413 (1.041, 1.919)
Rural	0.274 (0.139)*	1.315 (1.002, 1.727)	0.337 (0.143)*	1.401 (1.058, 1.854)
Province (Sabaragamuwa province)				
Western	0.012 (0.087)	1.012 (0.853, 1.200)	-0.034 (0.098)	0.967 (0.798, 1.171)
Central	-0.210 (0.094)*	0.811 (0.674, 0.975)	-0.222 (0.105)*	0.801 (0.652, 0.984)
Southern	0.150 (0.094)	1.162 (0.966, 1.397)	0.387 (0.112)*	1.473 (1.182, 1.834)
Northern	0.390 (0.119)*	1.477 (1.17, 1.865)	-0.299 (0.121)*	0.742 (0.585, 0.94)
Eastern	0.052 (0.108)	1.053 (0.852, 1.302)	-0.352 (0.113)*	0.703 (0.564, 0.878)
North Eastern	0.047 (0.094)	1.048 (0.872, 1.260)	0.016 (0.105)	1.016 (0.827, 1.248)
North Central	0.925 (0.125)*	2.522 (1.974, 3.222)	0.593 (0.132)*	1.809 (1.397, 2.344)
Uva	0.043 (0.107)	1.044 (0.846, 1.288)	-0.073 (0.117)	0.93 (0.739, 1.169)
Age group (45-49 years)				
15-19	-0.382 (0.219)	0.682 (0.444, 1.048)	-0.155 (0.128)	0.856 (0.666, 1.101)
20-24	-0.119 (0.102)	0.888 (0.727, 1.084)	-0.065 (0.103)	0.937 (0.766, 1.147)
25-29	-0.275 (0.082)*	0.76 (0.647, 0.892)	0.129 (0.088)	1.138 (0.958, 1.352)
30-34	-0.182 (0.076)*	0.834 (0.718, 0.968)	0.147 (0.081)	1.158 (0.988, 1.358)
35-39	-0.138 (0.075)	0.871 (0.752, 1.009)	0.204 (0.079)*	1.226 (1.050, 1.432)
40-44	-0.114 (0.077)	0.892 (0.767, 1.038)	0.164 (0.082)*	1.178 (1.003, 1.384)
Religion (Buddhist)				
Roman Catholic	0.029 (0.095)	1.029 (0.855, 1.240)	-0.272 (0.099)*	0.762 (0.628, 0.925)
Islam	-0.312 (0.085)*	0.732 (0.62, 0.865)	-0.719 (0.087)*	0.487 (0.411, 0.578)
Hindu	-0.325 (0.093)*	0.723 (0.602, 0.867)	-0.669 (0.093)*	0.512 (0.427, 0.615)
Other	-0.122 (0.188)	0.885 (0.612, 1.28)	-0.385 (0.191)*	0.684 (0.468, 0.989)
Highest education qualification (Degree and above)				
Never schooled	-1.494 (0.287)*	0.224 (0.128, 0.394)	-0.903 (0.307)*	0.405 (0.222, 0.74)
Passed Grade 1-5	-1.335 (0.154)*	0.263 (0.195, 0.356)	-1.455 (0.173)*	0.233 (0.166, 0.328)
Passed Grade 6-10	-0.608 (0.115)*	0.544 (0.435, 0.682)	-0.969 (0.137)*	0.379 (0.290, 0.496)
Passed G.C.E.(O/L)	-0.438 (0.115)*	0.645 (0.515, 0.809)	-0.552 (0.139)*	0.576 (0.439, 0.756)
Passed G.C.E.(A/L)	-0.152 (0.114)	0.859 (0.687, 1.074)	-0.203 (0.140)	0.816 (0.620, 1.074)
Current marital state (Not in union/Husband died/Divorced/Separated				
Currently married	0.031 (0.099)	1.031 (0.85, 1.252)	-0.113 (0.105)	0.893 (0.727, 1.097)
Living with a man	0.321 (0.155)	1.379 (1.017, 1.868)	0.317 (0.174)	1.373 (0.976, 1.931)
Wealth Index (Highest)				
Lowest	-0.290 (0.093)*	0.748 (0.624, 0.898)	-0.514 (0.101)*	0.598 (0.491, 0.729)
Second	-0.212 (0.081)*	0.809 (0.690, 0.948)	-0.481 (0.091)*	0.618 (0.517, 0.739)
Middle	-0.148 (0.078)	0.862 (0.740, 1.005)	-0.113 (0.098)	0.893 (0.737, 1.082)
Fourth	-0.160 (0.074)*	0.852 (0.737, 0.985)	-0.178 (0.087)*	0.837 (0.706, 0.993)
Frequency of reading newspaper (Not at all)				
At least once a week	0.189 (0.063)*	1.208 (1.068, 1.367)	0.261 (0.067)*	1.298 (1.139, 1.480)
Less than once a week	0.162 (0.064)*	1.176 (1.037, 1.333)	0.061 (0.067)	1.063 (0.9321, 1.212)
Frequency of watching TV (Not at all)				
At least once a week	0.342 (0.087)*	1.408 (1.187, 1.67)	0.371 (0.089)*	1.449 (1.217, 1.725)
Less than once a week	0.233 (0.108)*	1.262 (1.022, 1.56)	0.178 (0.109)	1.195 (0.965, 1.479)
Constant	1.341 (0.240)		1.751 (0.261	
Standard deviation of the random effect $\sqrt{d}$			1.377 (0.049)	

* Refers to significance at 5% level of significance

infected person. It is interesting to note that the odds of providing a correct response for both misconceptions tends to decrease as the level of education decreases. When considering the frequency of reading newspapers, women who read newspapers at least once a week had increased odds of giving the correct answers for both statements, ‘people can get HIV virus from mosquito bites’ and ‘HIV can be transmitted by sharing food,’ by 21% and 30%, respectively, compared to women who never read newspapers or cannot read. Similarly, women who watched television at least once a week had increased odds of giving the correct answers for both statements, by 41% and 45%, respectively, compared to women who never read newspapers or are illiterate. The odds of giving correct answers for both misconceptions tended to increase with the wealth index of ever-married women. In terms of religion, Hindu and Islamic followers had lower odds of giving the right answers for both misconceptions compared to Buddhist followers. Ever-married women who were living with a partner were more likely to have knowledge about both misconceptions compared to women who were divorced, separated, or widowed.

Related literature also supports these findings. Asaduzzaman *et al.* (2016) found that exposure to different types of media (radio, newspapers/magazines, television) was significantly associated with awareness of HIV/AIDS. Similarly, Haque *et al.* (2018) found that education status, mass media access, place of residence, and working status played significant roles in the perception of HIV/AIDS among married women in Bangladesh. A study conducted by Kanda *et al.* (2010) among the general population in Kandy, Sri Lanka, revealed significant associations between knowledge of HIV/AIDS and gender, marital status, education, religion, and residence. The SLDHS 2016 report also indicated that urban and rural ever-married women had very high awareness about HIV/AIDS (94% for both groups), while only 60% of their counterparts living in estate areas were aware of HIV/AIDS. Furthermore, the report stated that knowledge of HIV prevention and transmission was higher among currently married women compared to those who were divorced, separated, or widowed.

In this study, we proposed a joint model to model two binary outcomes under the generalized linear mixed model (GLMM) framework. We incorporated the shared random effect to capture the correlation between two responses and assumed bridge distribution for the random effect, which in turn has the flexibility of marginal interpretation of regression coefficients. Modelling two misconceptions about HIV/AIDS jointly is more appropriate than separate fitting of models that ignore the dependence between two outcomes. The Pearson Chi-squared test of independence between two responses Y1 and Y2 was statistically significant, thereby indicating that the women who believe Y1 are more likely to believe Y2 as well (Chi-Squared value = 677.476, p-value < 0.0001). This was concluded by our model since the variance of the random intercept was different from zero ($\sqrt{d}$ = 1.377, p value < 0.0001).

The study has also several strengths compared to previous studies. First, the correlation between two misconceptions about HIV/AIDS was taken into consideration in our analytic approach. Second, following Wang and Louis (2003), our model parameters have marginal interpretations and hence, marginal odds ratios. A similar study has been conducted by Samarakoon *et al.* (2020) for the awareness of misconceptions of HIV/AIDS among trainees in vocational centres in Sri Lanka, but their model parameters originally do not have marginal interpretation. Third, our study covered a large population-based study, enhancing its generality to all married women in Sri Lanka.

CONCLUSIONS

In this study, we focused on investigating the factors associated with two prominent misconceptions about HIV/AIDS among ever-married women in the reproductive age (15–49) who have heard about HIV/AIDS. The data used for the analysis were collected through the SLDHS 2016 conducted by DCS. The two misconceptions under scrutiny were: 1) the belief that people can acquire the HIV virus from mosquito bites, and 2) the belief that someone can contract the HIV virus by sharing food with an HIV-infected person. The study aimed to explore the correlation between these two misconceptions while jointly modelling them by incorporating a shared random intercept into the logistic regression model. To interpret the parameter estimates, a bridge distribution was assumed for the random intercept, allowing for marginal interpretation. The joint model analysis revealed that a woman’s residence area, province, age group, level of education, religion, current marital status, wealth index, frequency of reading newspapers, and frequency of watching television are significantly related to the awareness of the above two prominent misconceptions among ever-married women.

Limitations

The main limitation of this study is restraining measurement of women's awareness on HIV/AIDS into selected variables of which most are relevant to only the woman's residence area, province, age group, level of education, religion, current marital status, wealth index, frequency of reading newspapers and frequency of watching television. However, the education level and work experience of the husband too may be vital regarding awareness of disease or infection. The kinship, friendship, and neighbourhood relationships have been identified as crucial regarding determinants of disease spread in Sri Lanka. This research also could have been more successful if there were data provisions to comprehend women's knowledge on HIV/AIDS with regard to other aspects such as all supplementary types of STDs and maternity healthcare. Therefore, future researchers can consider these aspects too when designing the study, which will consequently allow them to arrive at more valid and applicable conclusions.

Acknowledgement

The authors would like to express their gratitude to the Department of Census and Statistics, Sri Lanka for giving permission to use data gathered through the Demographic and Health Survey, 2016.

Data availability

Demographic and Health Survey, 2016 dataset is not in the public domain and is the property of the Department of Census and Statistics, Sri Lanka. However, data can be obtained through a written request to the Department of Census and Statistics, Sri Lanka.

Ethical approval

The Sri Lanka Demographic and Health Survey obtained written informed consent from all the participants during the data collection. The survey secured ethical clearance from the Sri Lanka Medical Association - Ethics review committee. All methods were performed in accordance with the relevant guidelines and regulations (Declaration of Helsinki). Permission was obtained to analyse this data from the Department of Census and Statistics in Sri Lanka.

Conflict of interest

No potential conflict of interest was reported by the author(s).

REFERENCES

Agegnehu C.D. & Tesema G.A. (2020). Effect of mass media on comprehensive knowledge of HIV/AIDS and its spatial distribution among reproductive-age women in Ethiopia: a spatial and multilevel analysis. *BMC Public Health* **20**(1): 1–12.
DOI: https://doi.org/10.1186/s12889-020-09536-1

Asaduzzaman M., Higuchi M., Sarker M.A.B. & Hamajima N. (2016). Awareness and knowledge of HIV/AIDS among married women in rural Bangladesh and exposure to media: a secondary data analysis of the 2011 Bangladesh Demographic and Health Survey. *Nagoya Journal of Medical Science* **78**(1): 109.

Bogart L.M., Skinner D., Weinhardt L.S., Glasman L., Sitzler C., Toefy Y. & Kalichman S.C. (2011). HIV/AIDS misconceptions may be associated with condom use among black South Africans: an exploratory analysis. *African Journal of AIDS Research* **10**(2): 181–187.
DOI: https://doi.org/10.2989/16085906.2011.593384

Bogart L.M. & Thorburn S. (2005). Are HIV/AIDS conspiracy beliefs a barrier to HIV prevention among African Americans? *JAIDS Journal of Acquired Immune Deficiency Syndromes* **38**(2): 213–218.
DOI: https://doi.org/10.1097/00126334-200502010-00014

Choudhary H.A., Ali R.A. & Altaf S. (2015). Knowledge, behaviour and attitudes regarding HIV/AIDS among undergraduate students in an Irish university. *International Journal of Surgery and Medicine* **1**(2): 58–66.
DOI: https://doi.org/10.5455/ijsm.20150814034728

De Silva A.H.W., Rizwaan M.S.A., Ramanayake R.P.J.C., Perera D.P. & Sumanasekara R.D.N. (2014). Knowledge on HIV prevention amongst a group of post war re-settlers in Sri Lanka.
DOI: http://doi.org/10.4038/sljv.v5i1.7348

Department of Census and Statistics (2016). *Sri Lanka Demographic and Health Survey Final Report.* Department of Census and Statistics, Sri Lanka. Available at *http://www.statistics.gov.lk/Health/StaticalInformation/DemographicAndHealthSurvey-2016FullReport,* accessed 10 May 2022.

Haque M.A., Hossain M.S.N., Chowdhury M.A.B. & Uddin M.J. (2018). Factors associated with knowledge and awareness of HIV/AIDS among married women in Bangladesh: evidence from a nationally representative survey. *SAHARA-J: Journal of Social Aspects of HIV/AIDS* **15**(1): 121–127.
DOI: https://doi.org/10.1080/17290376.2018.1523022

Iqbal M.M. (1999). Can we get aids from mosquito bites? *Journal of the Louisiana State Medical Society* **151**(8): 429–433.

Kanda K., Obayashi Y., Jayasinghe A., Silva K.T., Lee R.B. & Tamashiro H. (2010). Current HIV/AIDS knowledge, perceptions and practices among the general population in Kandy, Sri Lanka: program implications. *Kokusai Hoken Iryo (Journal of International Health)* **25**(1): 11–19.
DOI: https://doi.org/10.11197/jaih.25.11

Karthijekan K. (2017). Undergraduate students' knowledge on AIDS/HIV and its associated factors in Eastern University, Sri Lanka. *International Journal of Scientific and Research Publication* **7**(10): 198–203.

Madurapperuma B.D., Nishad A.A.N., Borges J.S., Solangaarachchi D.I.K., Kangath R.V. & Hewage S.A. (2018). A preliminary assessment of sexual transmitted infections (STIs) in Sri Lanka: District-wise overview. *Sri Lanka Journal of Obstetrics and Gynaecology* **40**(2). DOI: http://doi.org/10.4038/sljog.v40i2.7844

National STD/AIDS control programme-Sri Lanka (2019). *Annual report 2018* (Pdf). Available at *http://www.aidscontrol.gov.lk/images/publications/NSACP_Annual-report_-2018_updated-PDF-8.8.2019.pdf*, accessed 01 June 2023.

National STD/AIDS control programme-Sri Lanka (2020). *Annual report 2019* (Pdf). Available at *http://www.aidscontrol.gov.lk/images/publications/NSACP_Annual-Report_2019.pdf*, accessed 01 June 2023.

National STD/AIDS control programme-Sri Lanka (2021). *Annual report 2020* (Pdf). Available at *http://www.aidscontrol.gov.lk/images/publications/annual_reports/Annual_Report-2020.pdf*, accessed 01 June 2023.

National STD/AIDS control programme-Sri Lanka (2022). *Annual report 2021* (Pdf). *Available at http://www.aidscontrol.gov.lk/images/publications/annual_reports/2021/Anual_report_2021_online_version_final.pdf*, accessed 01 June 2023.

Niehaus I. & Jonsson G. (2005). Dr. Wouter Basson, Americans, and wild beasts: men's conspiracy theories of HIV/AIDS in the South African Lowveld. *Medical Anthropology* **24**(2): 179–208. DOI: https://doi.org/10.1080/01459740590933911

Qian H.Z., Wang N., Dong S., Chen H., Zhang Y., Chamot E., Shi X., Gao J., Vermund S.H. & Shao Y. (2007). Association of misconceptions about HIV transmission and discriminatory attitudes in rural China. *AIDS care* **19**(10): 1283–1287. DOI: https://doi.org/10.1080%2F09540120701402814

RStudio Team (2020). RStudio: Integrated Development for R. RStudio, PBC, Boston, MA. Available at *http://www.rstudio.com/*, accessed 12 May 2022.

Saki M., Kermanshahi S. M. K., Mohammadi E. & Mohraz M. (2015). Perception of patients with HIV/AIDS from stigma and discrimination. *Iranian Red Crescent Medical Journal* **17**(6). DOI: https://doi.org/10.5812/ircmj.23638v2

Samarakoon T., Withanage N., Samarakoon N., Lekamge U. & De Silva N. (2020). Joint modelling of correlated binary outcomes regarding the misconceptions of HIV transmission: a study with reference to the tertiary and vocational education trainees in Sri Lanka. *International Journal of Community Medicine and Public Health* **7**(8): 2950. DOI: https://dx.doi.org/10.18203/2394-6040.ijcmph20203368

SAS Institute Inc. (2015). SAS/IML® 14.1 User's Guide. Cary, NC: SAS Institute Inc.

Thakuri D.S. & Thapa C.B. (2018). Knowledge, attitude and perception regarding HIV/AIDS among postgraduate students of university of Pune. *International Journal of Community Medicine and Public Health* **5**(5): 1750. DOI: https://dx.doi.org/10.18203/2394-6040.ijcmph20181681

UNAIDS (2022). Available at *https://www.unaids.org/sites/default/files/media_asset/UNAIDS_FactSheet_en.pdf*, accessed 01 June 2023.

Wang Z. & Louis T.A. (2003). Matching conditional and marginal shapes in binary random intercept models using a bridge distribution function. *Biometrika* **90**(4): 765–775.

Withanage N., de Leon A.R. & Rudnisky C.J. (2014). Joint estimation of disease-specific sensitivities and specificities in reader-based multi-disease diagnostic studies of paired organs. *Journal of Applied Statistics* **41**(10): 2282–2297. DOI: https://doi.org/10.1080/02664763.2014.909790

Appendix

SAS Code used for the analysis of data:

```
proc nlmixed data=sample3;
pi=3.1415926535897931;
parms beta10=1.348 beta11=0.256 beta12=0.278 beta13=-0.009 beta14=-0.219 beta15=0.140 beta16=0.373
beta17=0.022 beta18=0.034 beta19=0.889 beta110=0.028 beta111=-0.115 beta112=0.018 beta113=-0.324 beta114=-
0.319 beta115=-0.389 beta116=-0.107 beta117=-0.278 beta118=-0.171 beta119=-0.135 beta120=-0.124 beta121=0.035
beta122=0.341 beta123=-1.482 beta124=-1.337 beta125=-0.616 beta126=-0.436 beta127=-0.151 beta128=0.191
beta129=0.166 beta130=0.141 beta131=0.250 beta132=-0.079 beta133=0.145 beta134=-0.219 beta135=-0.295
beta136=-0.153 beta137=-0.163 beta20=1.754 beta21=0.366 beta22=0.343 beta23=-0.051 beta24=-0.229 beta25=0.385
beta26=-0.310 beta27=-0.375 beta28=0.008 beta29=0.552 beta210=-0.087 beta211=-0.387 beta212=-0.294 beta213=-
0.733 beta214=-0.668 beta215=-0.155 beta216=-0.054 beta217=0.126 beta218=0.157 beta219=0.206 beta220=0.151
beta221=-0.105 beta222=0.355 beta223=-0.885 beta224=-1.443 beta225=-0.964 beta226=-0.535 beta227=-0.189
beta228=0.260 beta229=0.063 beta230=0.371 beta231=0.193 beta232=-0.053 beta233=0.059 beta234=-0.529
beta235=-0.495 beta236=-0.124 beta237=-0.184 s1=2;
uni = probnorm(b/s1);
phi = 1.0/sqrt(1+3/pi/pi*s1*s1);
B1 = 1/phi*log(sin(pi*uni*phi)/sin(phi*pi*(1-uni)));


if Y=”Y1” then do;
tmp1 = beta10 + beta11*resurb + beta12*resrur + beta13*prov1 + beta14*prov2 + beta15*prov3 + beta16*prov4
+ beta17*prov5 + beta18*prov6 + beta19*prov7 + beta110*prov8 + beta111*reli1 + beta112*reli2 + beta113*reli3
+ beta114*reli4 + beta115*age1 + beta116*age2 + beta117*age3 + beta118*age4 + beta119*age5 + beta120*age6
+ beta121*currmari1 + beta122*currmari2 + beta123*highedu1 + beta124*highedu2 + beta125*highedu3
+ beta126*highedu4 + beta127*highedu5 + beta128*rednews1 + beta129*rednews2 + beta130*watchtel1 +
beta131*watchtel2 + beta132*lisradio1 + beta133*lisradio2 + beta134*wi1 + beta135*wi2 + beta136*wi3 +
beta137*wi4;
expeta1 = exp(B1+tmp1);
p1 = expeta1/(1+expeta1);
ll = response*log(p1) + (1-response)*log(1-p1);
end;

if Y=”Y2” then do;
tmp2 = beta20 + beta21*resurb + beta22*resrur + beta23*prov1 + beta24*prov2 + beta25*prov3 + beta26*prov4 +
beta27*prov5 + beta28*prov6 + beta29*prov7 + beta210*prov8 + beta211*reli1 + beta212*reli2 + beta213*reli3
+ beta214*reli4 + beta215*age1 + beta216*age2 + beta217*age3 + beta218*age4 + beta219*age5 + beta220*age6
+ beta221*currmari1 + beta222*currmari2 + beta223*highedu1 + beta224*highedu2 + beta225*highedu3
+ beta226*highedu4 + beta227*highedu5 + beta228*rednews1 + beta229*rednews2 + beta230*watchtel1 +
beta231*watchtel2 + beta232*lisradio1 + beta233*lisradio2 + beta234*wi1 + beta235*wi2 + beta236*wi3 +
beta237*wi4;
expeta2 = exp(B1+tmp2);
p2 = expeta2/(1+expeta2);
ll = response*log(p2) + (1-response)*log(1-p2);
end;

model zz ~ general(ll);
random b ~ normal(0,s1*s1) subject=woman_id;
run;
```

J.Natn.Sci.Foundation Sri Lanka 2023 51 (4): 703 - 718
DOI: http://dx.doi.org/10.4038/jnsfsr.v51i4.11286

RESEARCH ARTICLE

Remote Sensing

Land-use and land cover changes along the coastal belt of Hambantota district, southern Sri Lanka, over the period 1996-2017

SK Madarasinghe[1], KKAS Yapa[2], PMP Udayakantha[3] and B Satyanarayana[4]
[1] *Department of Botany, Faculty of Science, University of Ruhuna, Matara, Sri Lanka.*
[2] *Department of Physics, Faculty of Science, University of Ruhuna, Matara, Sri Lanka.*
[3] *Sri Lanka Survey Department, 150 Bernard Soysa Mawatha, Colombo 5, Sri Lanka.*
[4] *Institute of Oceanography and Environment, Universiti Malaysia Terengganu, Kuala Terengganu, Malaysia.*

Submitted: 21 December 2022; Revised: 21 September 2023; Accepted: 27 October 2023

Abstract: Through the years, the green cover has been substantially reduced and transformed into human development projects and settlements in many cities of Sri Lanka. Hambantota, a southern coastal district, has faced similar changes over the last two decades. Therefore, this study was aimed at the Land-Use and Land-Cover (LULC) changes which had taken place along its coastal belt during the period, 1996–2017. Comparison was done among LULC maps bearing fourteen different classes for the years 1996 and 2017. The results reveal that all LULC classes except coconut plantations and paddy lands show significant area changes ($p < 0.05$) during the period considered. Among the LULC changes, forest cover showed the highest area change (2341 ha loss ($p < 0.05$)) while 358 ha of scrubland has been cleared to establish housing schemes. The settlements have significantly increased (1318 ha) and a considerable amount is due to development projects including the Hambantota port. The survey results show that 63.9% of the residents in the study area agreed that the natural environment of the city had been affected by the development projects. Analysis of LULC changes and Normalized Difference Vegetation Index (NDVI) data suggests that Hambantota coastal area has developed significantly at the cost of forests and associated vegetation from 1996 to 2017. Rapid economic and population growths are identified as the main driving forces for the LULC changes. These results deliver an important decision-making reference for LULC planning and sustainable development in the Hambantota coastal region, which is, in broad sense, valid for any booming city in the country and the world. The urban forestry concept can be an ideal sustainable move to compensate the green cover loss.

Keywords: Development projects, green cover loss, LULC planning, sustainability, urban forestry.

INTRODUCTION

Over the past decades, socioeconomic activities have substantially increased in urban areas compared to rural areas, mainly due to the migration of large rural populations to urban areas and to the expansion of urban areas to accommodate such large numbers of people (Yu *et al*., 2011). During urban development, Land Use and Land Cover (LULC) changed remarkably and such changes are intense in developing countries (Chen & Zhang, 2017). In general, conversion of natural vegetation and agricultural lands into built-up areas such as settlements, buildings, roadways, and parking areas become common during many urban development projects (Van & Bao, 2010; Ranagalage *et al*., 2017). This trend causes numerous environmental impacts, such as decrease in green cover and agricultural lands, environmental pollution, habitat destruction, etc., at local, regional, and global levels

* Corresponding author (sandunikm89@gmail.com; https://orcid.org/0000-0002-8594-7476)

(Alphan, 2003; Shalaby & Tateishi, 2007; Rousta *et al*., 2018). The situation in Sri Lanka is not very different from world trends (Suthakar & Bui, 2008; Dissanayake *et al*., 2019; Ranagalage *et al*., 2019).

In the Sri Lankan context, many development projects came into practice after the tsunami in 2004 and the end of the war in 2009. The coastal district of Hambantota in the Southern Province, in particular, had received quite a high number of development projects. Geographically, Hambantota is the largest district in the southern province of Sri Lanka, where both dry and arid climatic conditions are found. It is situated from 5°58'16"N to 6°34'45"N and 80°36'28"E to 81°42'24"E, and is 261,915 ha in extent, representing 4% of the whole land area of the country.

Hambantota bears a high economic importance, particularly due to salt and fishing industries. It provides 60% of the country's salt production and about 13% of national fish catch (UDA, 2019). Additionally, it is a major tourist attraction due to sites such as the Bundala Bird Sanctuary, Yala National Wildlife Park, Ridiyagama Safari Park, and Dry Zone Botanical Garden. This district inherits a long history from the ancient Rohana Kingdom. People belonging to different races and religions, with Sinhalese forming the majority of the population, live in harmony (Department of Census & Statistics, 2012). It had a total population of 599,903 in 2012, according to the last census carried out, living in both urban and rural areas of the district (Department of Census & statistics, 2012).

Hambantota district borders the Indian Ocean from its southern and eastern directions, having a long coastal belt, which includes important coastal ecosystems such as scrub forests, mangrove forests, sandy beaches, and sand dunes. The two major national parks, Yala and Bundala, are the major tourist attractions in the Hambantota district. Yala was designated as a national park in 1938, and Bundala, in 1992. Bundala was declared as a Ramsar site in Sri Lanka in 1990 and as a biosphere reserve by UNESCO in 2005 (CEA/Euroconsult, 1993). Hambantota town, the district capital, and a few other urban cities are located along the coastal belt. A fragmented land-use pattern depicted by man-made constructions and cultivations could be observed in these urban areas.

Many changes in land-use practices have taken place in the Hambantota urban area in the recent past. Major development projects had been initiated after the tsunami in 2004 as well as after the eradication of civil war in 2009. Establishment of the Hambantota port and the Mattala airport have resulted an unprecedented change in land-use architecture in the area, and the living condition of the residents has been severely affected (Mariyathas *et al*., 2016; Madarasinghe *et al*., 2018). Construction of the port commenced in 2008 and was opened in 2010 after completion of the first phase. The port plays a vital role in international shipping routes between Asia and Europe (Kotelawala, 2017).

The tsunami had destroyed 2754 houses in the Hambantota district, which included 157 houses from the Tissamaharama Divisional Secretariat Division (DSD), 299 from the Ambalantota DSD, 1167 from the Hambantota DSD, and 1131 from the Tangalle DSD (source: Hambantota District Secretary's office). Therefore the LULC of the Hambantota coast has considerably changed after the tsunami in 2004. Madarasinghe *et al*. (2018) recorded an increase of settlements by about 15%, replacing scrubland, chena, and dry forests (~21%) in the Hambantota urban area during 1996–2016. This directly indicated a rapid economic growth, but with simultaneous green cover loss.

Although several studies had been conducted to study the LULC architecture and dynamics in other parts of the country (Lindström *et al.*, 2012; Dissanayaka, 2020; Rathnayake *et al.*, 2022), the booming city of Hambantota remained understudied. Despite the fast infrastructure development, little attention had been paid to study LULC dynamics of this booming city, associated impacts on the environment, and the living status of the residents. The available literature only focused on limited areas (one Divisional Secretariat Division (DSD), the Hambantota DSD, and one housing scheme, Siribopura) in the Hambantota district. Edirisooriya *et al.* (2021) have reported LULC changes in the Hambantota DSD from 2008 to 2019, and reveal a significant loss of total forest cover in the area from 41.95% in 2008 to 23.07% in 2019, while the built-up area has significantly increased. Furthermore, Perera *et al.* (2012) has evaluated the Siribopura Resettlement Housing Program, which was one of the resettlement programmes developed to relocate the communities affected by the tsunami in 2004 and communities displaced due to development projects in Hambantota. Even though population growth and urbanization have been taking place to a great extent in the coastal zone of the island, literature on the LULC changes of the coastal zone of Hambantota district and the effects of rapid urbanization on the coastal zone are scanty.

This study, therefore, was aimed at investigating the LULC changes occurred in the coastal belt of the Hambantota district over a period of two decades (1996–2017) and their effect on the environment and the social status of the residents. The following questions were addressed in the study: a) What were the LULC changes that have taken place during the study period? b) Were the LULC changes environmentally sustainable? c) If the LULC changes were not sustainable, what possible managerial actions could be taken to restore environmental sustainability? d) How did development-oriented changes affect the social status of the residents? The main working hypothesis of the study was that the LULC changes that took place during the past two decades were not environmentally sustainable.

MATERIALS AND METHODS

Study area

Hambantota is the largest of the three districts in the Southern Province with a total area of 261,915 ha and a 151 km long shoreline. The coastal belt of a minimum of 2 km width from the shoreline (adapting to the definition of 'coastal zone' in the Coast Conservation Act No. 57 of 1981, Sri Lanka) was taken into consideration in this study. All Grama Niladhari Divisions (GNDs) located within this 2 km width of the coastal belt of Hambantota district were considered and the landward margin of the belt was taken as GND boundaries so the belt always contains whole GNDs. Thus, the belt extends beyond the 2 km limit in some instances, and the widest is, for example, about 20 km where the Yala national park is located. This total inclusion of GNDs was necessary to use available data from GNDs. The total study area under this case study consists of seventy-four GNDs covering a total area of 79,683 ha. A digital map of the GND boundaries of Sri Lanka made in 2013 was obtained from the Sri Lanka Survey Department [Figure 1(a)] and the GNDs that are located within a 2 km distance from the shoreline were extracted and it was used as the study area vector [highlighted area in Figure 1(a)] in image processing and analysis in the present study.

LULC change analysis

Digital LULC maps of the coastal belt of the Hambantota district for 2017 and 1996 were used in this study. Details of the maps used are given in Table 1(a). The extraction of the area was done using ArcMap *v.*10.3 software using the study area vector mentioned earlier (Figure 1).

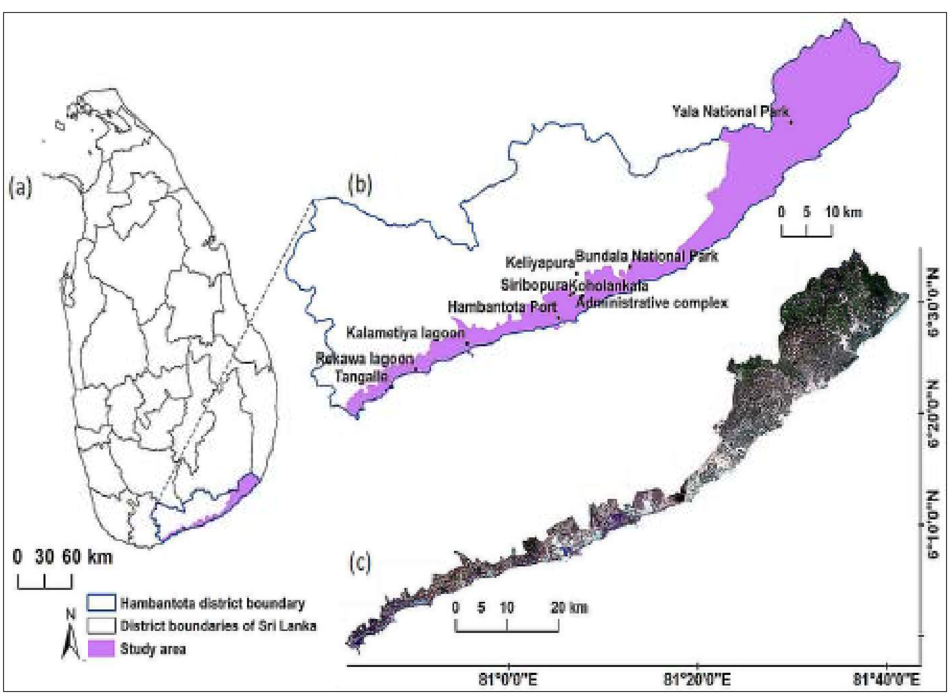

Figure 1: (a) Map of Sri Lanka showing the district boundaries and the coastal belt of Hambantota district taken into consideration in this study; (b) map of Hambantota district with some important locations along the study area; (c) Landsat 8 (2017) mosaicked satellite image showing the study area.

Thereby, fourteen LULC classes—bare lands, coconut plantations, forest, grassland and marsh, homesteads, mangroves, paddy lands, other cultivations, saltpan, sandy areas, scrubland and chena, settlements, water, and other land-uses—were identified to be studied in the LULC map of the Hambantota coastal belt in 2017. LULC maps of 1996 were bearing a classification system as reported in the Topographic Database Specifications and Data Dictionary (TDSDD), Sri Lanka Survey Department. Thus, digital maps were then reclassified into the 14-class classification system of the study through merging necessary LULC classes. For example, all the water bodies such as streams, rivers, ponds, canals, channels, reservoirs, and waterholes were merged to generate the LULC class 'water'. Subsequently, the area of each LULC class was estimated for both 1996 and 2017 through area statistics using ArcMap software. This was followed by an area loss and gain analysis (to determine area change from 1996 to 2017), carried out using the overlay analysis method in ArcMap software. Two-sample proportion test was applied using R statistical software (R *v*. 4.0.3) to test the significance of the area changes which occurred from 1996 to 2017 on the Hambantota coastal belt. Area statistics for the conversion of each LULC class from 1996 to another class by 2017 were derived by intersecting each overlay output separately with each LULC class in the two years, 1996 and 2017. For example, the area gain map of 'settlements', obtained as an overlay output, was again subjected to overlay analysis (intersecting) with the 'saltpan' LULC layer in 1996 to obtain the area of saltpan that was sacrificed for settlements by 2017. A transition matrix was generated using the area statistics obtained after overlay analysis to show all the area changes from one LULC to another during the 1996-2017 period.

Estimation of normalized difference vegetation index (NDVI)

NDVI's of the study area in 1997 and 2017 were estimated and compared in order to track the changes in greenness and vegetation health of the area over the two-decade period. This procedure was carried out merely to display the changes in vegetation of the area and to confirm

Table 1: Details of the image data used in the study.

1. Image data used for LULC change analysis

Map	Area covered	Year	Scale	Details
Digital LULC map	Coastal belt of Hambantota district	2017	1:17,500	©S.K. Madarasinghe. (Data from; Madarasinghe S.K. (2022). Investigation of land-use changes in Western and Southern coasts of Sri Lanka in the past two decades (1996-2017): A field based geo-informatics approach. PhD Thesis, University of Ruhuna, Matara, Sri Lanka. WGS 1984 UTM zone 44N coordinate system. Maps have been created applying on-screen digitization techniques for Google earth satellite images (Madarasinghe *et al*., 2020a).
Digital LULC map	Coastal belt of Hambantota district	1996	1:50,000	©Sri Lanka Survey Department- SLSD. WGS 1984 UTM zone 44N coordinate system. Maps have been created applying on-screen digitization techniques for Google earth satellite images (Madarasinghe *et al*., 2020a).

2. Image data used for NDVI analysis

Satellite name	Sensor	Resolution	Path/ row	Coordinate system	Imagery date/s	Downloaded platform
Landsat 8	OLI	30m	140/056 and 141/056	WGS 84 UTM zone 44N	13th January and 28th April 2017	United States Geological Survey (USGS) Earth Explorer
Landsat 7	ETM+	30m	140/056 and 141/056	WGS 84 UTM zone 44N	23rd February and 16th February 1997	United States Geological Survey (USGS) Earth Explorer

the area changes obtained from the overlay analysis. Landsat 8 Operational Land Imager (OLI) and Landsat 7 Enhanced Thematic Mapper plus (ETM+) satellite data, both at a resolution of 30 m, were used for this purpose for 2017 and 1997, respectively. Cloud-free Landsat images of the area were not available for the year 1996 and thus, the closest cloud-free images from 1997 were obtained. Details of data used are given in Table 1(b).

All satellite images were obtained from the dry season of the Hambantota district to avoid seasonal variations in vegetation and to avoid misclassifications due to flooding conditions mainly in the paddy lands. ArcMap 10.3 software was used to perform image processing and image analysis. Standard colour composite images were derived using green, red, and near infrared bands and those composites were then geo-referenced using 6 to 8 ground control points obtained from GPS. Two composite images of the same year were mosaicked and the study area, the coastal belt of the Hambantota district, was clipped from the mosaic using the study area vector created using the process described in section 2.1. NDVI's for 1997 and 2017 were calculated for each mosaic image and their maximum values were compared.

NDVI outputs were overlapped with their standard colour composites and three land cover types, no-vegetation areas (*e.g.*, water, rocky areas, built-up areas, and bare lands), other vegetation (*e.g.*, grasslands, scrublands, chena, home gardens, and sparse forests), and dense forest areas, were identified through comparisons. The tool 'Identify' in ArcMap was used to select break values to be used in classifying the NDVI outputs into the three aforementioned classes. NDVI of 0.25 was selected as the break value for the classification of NDVI output to vegetated and non-vegetated areas, after comparison of the NDVI outputs with their respective standard colour composites, the classified NDVI images were generated for 1997 and 2017. Area statistics were obtained for each NDVI class in order to detect the area change of the vegetation classes over the twenty-year period. Compatibility of NDVI results with the area statistics obtained from overlay analysis were checked and the NDVI results were then presented visually as a verification of the vegetation dynamics revealed from the overlay analysis.

Questionnaire survey and population density

To study how land-use changes observed in Hambantota urban area had affected the lives of displaced families, a comprehensive questionnaire survey was carried out in 2019 in two selected GNDs, namely, Siribopura and Keliyapura, where the dislocated communities due to Hambantota port project and the tsunami in 2004 were resettled. Maps of the two GNDs obtained from the village heads (Grama Niladhari) were used to select forty households randomly, and the questionnaire survey was carried out through interviewing the heads of the households. Demographic information on the lives of respondents were gathered through a set of close-ended questions. Additionally, a series of Likert-scale questions were included in the questionnaire covering four major areas: people's perspectives (14 questions), economy (24), goods and services (13), and the environment (16). Reliability tests followed by a principal component analysis (PCA) were performed for each category to refine the most reliable and representative Likert-scale questions for each of the four areas. Refined questions included five questions from the 'people's perspectives' section, three from 'economy', four from 'goods and services' and four from the 'environment'. Subsequently, descriptive statistics, particularly, frequency data, were generated for the responses given for these selected Likert-scale questions. All statistical tests were performed using SPSS *v*.25 statistical package.

GND-wise population data in the Hambantota district in 2001, 2012, and 2017 were gathered from the Hambantota Divisional Secretariat's office and the Department of Census and Statistics, Sri Lanka. Population data of the studied GN divisions were extracted from the data sets to study the trend of population change in the Hambantota coastal belt. The population density of each GND in 2001, 2012, and 2017 was then mapped using ArcMap *v*.10.3 software.

RESULTS AND DISCUSSION

Results

LULC change analysis

The LULC architecture of the Hambantota coastal belt has changed at an unprecedented rate over the study period of the two decades from 1996 to 2017. Out of fourteen LULC classes studied for the year 2017, all the classes except coconut plantations and paddy lands showed significant area changes (positive and negative) over the considered period. Area statistics of each LULC class and the LULC changes which occurred over the two-decade period are tabulated in Table 2, whereas the overall area loss and gain of each LULC class in Hambantota coast during the period considered are illustrated in Figure 2.

Table 2: Land-use/land-cover areas in Hambantota coastal belt in 1996 and 2017 and the area changes over the twenty one years. p value indicates the significance of the area change of each LULC class at 95% confident interval. Significant area changes are marked with an asterisk. Area gains are given as positive values while area losses are shown as negative values.

Land-use class	Area (ha)		Area change (ha)	p value (at 95% level)
	In 1996	In 2017		
Bare land	14	479	465*	< 2.2e-16
Coconut plantation	999	1060	61	0.1832
Forest	44128	41389	-2739*	< 2.2e-16
Grassland and marsh	1465	3806	2341*	< 2.2e-16
Homesteads	7140	6340	-800*	6.352e-13
Mangroves	270	477	207*	4.193e-14
Other cultivations	385	552	167*	5.358e-08
Paddy lands	4053	3972	-80	0.3595
Saltpan	2346	402	-1944*	< 2.2e-16
Sandy areas	1632	2649	1018*	< 2.2e-16
Scrubland and chena	12332	11481	-851*	2.337e-09
Settlements	36	1353	1318*	< 2.2e-16
Water	3800	4339	539*	9.252e-10
Other land-uses	1083	1384	302*	1.148e-09

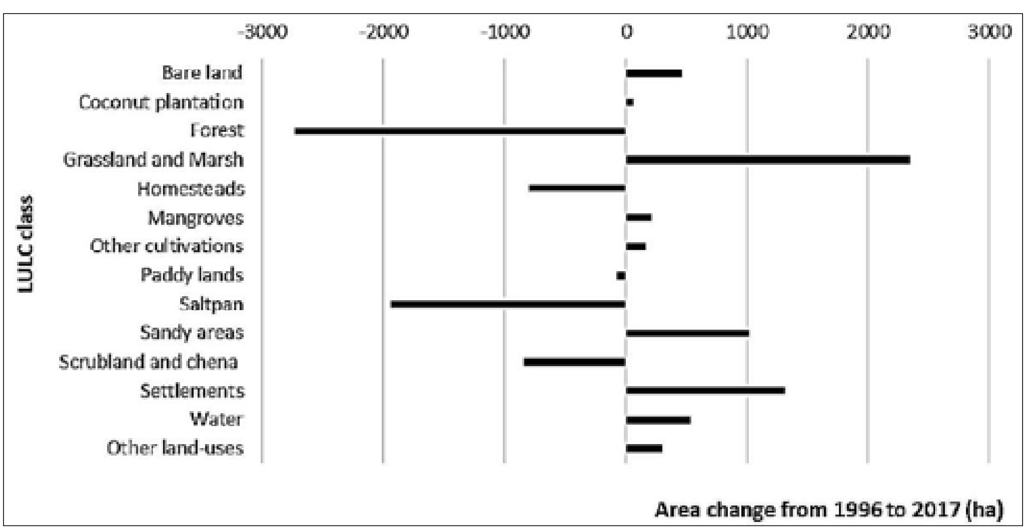

Figure 2: Area loss/gain of each land-use/cover class in the Hambantota coastal belt from 1996 to 2017. Area gains are illustrated as positive values and area losses as negative values.

The transition matrix that shows the spatial changes of LULC in Hambantota coast from 1996 to 2017 is given in Table 3. LULC maps of the Hambantota coastal belt in 2017 and 1996 are displayed in Figure 3.

Table 3: Transition matrix showing the land-use/cover changes of Hambantota coast from 1996 to 2017. The highlighted numbers on the diagonal represent unchanged land-use/cover proportions from 1996 to 2017, while the others are the areas changed from one class to another.

		1996														
		Bare land	Coconut plantation	Forest	Grassland and Marsh	Homesteads	Mangroves	Other cultivations	Paddy lands	Saltpan	Sandy areas	Scrubland and chena	Settlements	Water	Other land-uses	Total area gain (by 2017)
2017	Bare land	2	2	0	94	63	0	0	100	0	0	179	0	39	0	477
	Coconut plantation	0	493	0	23	141	2	0	202	0	0	199	0	0	0	567
	Forest	0	23	41179	0	43	0	0	0	0	82	62	0	0	0	210
	Grassland and Marsh	0	26	661	1165	126	0	0	89	147	0	631	0	941	20	2641
	Homesteads	6	74	127	0	5423	0	0	33	0	0	677	0	0	0	917
	Mangroves	0	1	0	114	0	268	0	0	0	0	8	0	86	0	209
	Other cultivations	0	13	0	0	66	0	119	52	0	0	302	0	0	0	433
	Paddy lands	0	0	0	47	52	0	129	3110	0	0	634	0	0	0	862
	Saltpan	0	0	0	0	0	0	0	0	402	0	0	0	0	0	0
	Sandy areas	0	0	0	0	0	0	0	0	0	1538	0	0	270	841	1111
	Scrubland and chena	6	197	1541	0	62	0	110	0	100	0	9465	0	0	0	2016
	Settlements	0	0	0	21	934	0	27	14	62	0	74	35	0	85	1318
	Water	0	170	0	0	0	0	0	0	1635	12	0	1	2464	57	1875
	Other land-uses	0	0	620	1	230	0	0	453	0	0	0	0	0	80	1304
	Total area loss (from 1996)	12	506	2949	300	1717	2	266	943	1944	94	2867	1	1336	1003	

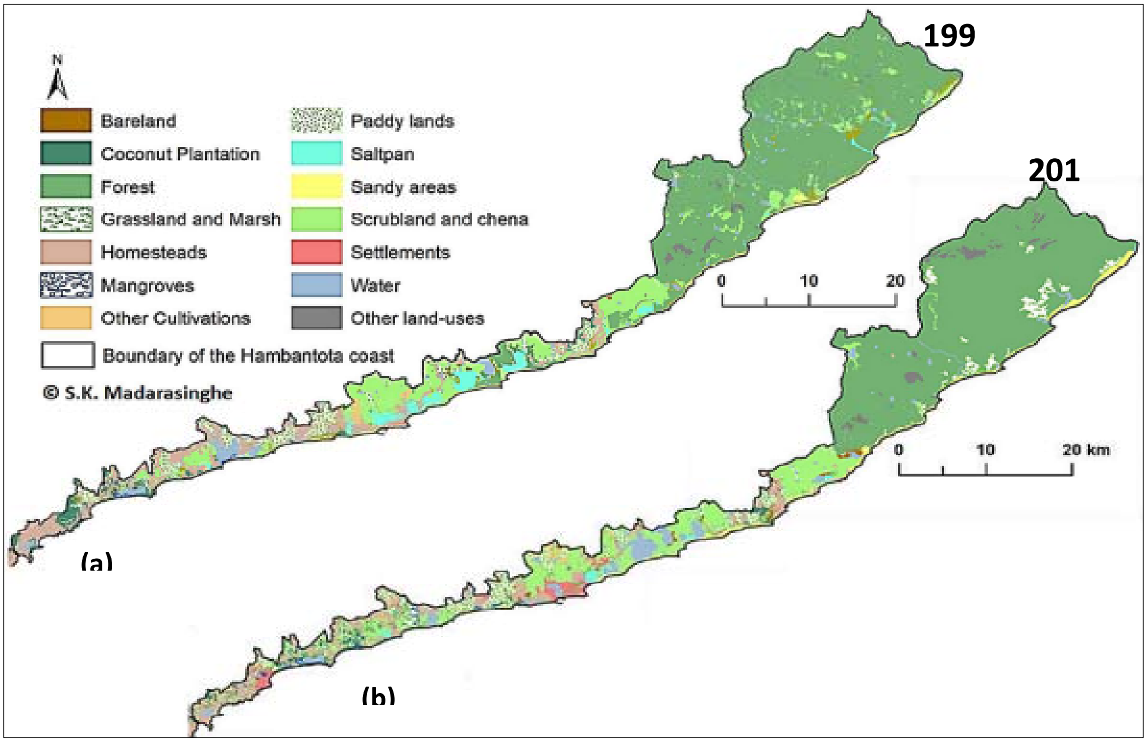

Figure 3: Land-use/land-cover maps of the coastal belt of Hambantota district in 1996 (a) and 2017 (b).

The Hambantota coastal belt includes Yala and Bundala national parks along with few other forest patches, distributed along the belt. The forest cover reduced by 2739 ha ($p < 0.05$), showing the highest area change among all the LULC changes, over the period from 1996 to 2017. Overlay analysis further revealed that most of the forest cover losses was observed in Yala and Bunadala national parks, as it had been transformed into scrubland and chena, grassland and marsh, homesteads and other land-uses by 2017 (see Table 3 for transition matrix). However, the LULC class, scrubland and chena, in the study area showed a significant overall decrease over the two decades by 851 ha. ($p < 0.05$). According to the overlay analysis, approximately 368 ha of scrubland had been cleared to establish housing schemes for relocation programme, particularly in the Keliyapura, Siribopura, and Koholankala GNDs [indicated in Figure 1 (b)], and 309 ha had been sacrificed in other GNDs of the Hambantota coast. On the other hand, the grassland and marsh LULC classes had significantly expanded, by 2341 ha, $p < 0.05$) over the period. This expansion had taken place at the expense of some areas under the LULC classes *i.e.* forests, homesteads, paddy lands, scrubland and chena, saltpan and water areas, compared to the 1996 map. Marsh vegetation and grassy plains had replaced about 153 ha of water in the Kalametiya lagoon by 2017 due to formation of land masses in the lagoon (personnel communication and field observations in September 2017).

Mangrove vegetation cover was identified in the three lagoon systems, Rekawa, Kahandamodara, and the Kalametiya-Lunama complex, as well as in Tangalle and Ambalantota. Expansion of mangrove cover had taken place in all five sites, resulting an overall increase of 207 ha ($p < 0.05$). This expansion had taken place by replacing some areas under the LULC classes coconut plantation, grassland and marsh, scrubland and chena, and water in the 1996 map. The highest expansion of mangrove cover (114 ha) has taken place by replacing grassland and marsh vegetation, and most of the replacement was observed in Kalametiya lagoon area.

Paddy remains the major crop cultivated in the Hambantota coastal belt since 1996, and covered 5% (4053 ha) of the study area. Coconut plantations covered 1.3% (999 ha) of the Hambantota coastal belt in 1996. Neither paddy nor coconut cultivated land areas show any significant change over the two decades. However, the LULC class 'other cultivations' (*e.g.*, banana, finger millet, sugarcane) had expanded its area by 167 ha ($p < 0.05$). Overlay analysis revealed that some of the areas occupied under the LULC classes, coconut plantation (13 ha), homesteads (66 ha), paddy lands (52 ha), and scrubland and chena (302 ha), in the 1996 map had been replaced with the newly established croplands, which were listed under the class 'other cultivations'.

Although the settlements in the study area had significantly increased (by 1318 ha) over the period, homestead areas had been reduced by 800 ha ($p < 0.05$). Interviews with the residents in the area revealed that many homesteads had been taken by the government to implement development projects (*e.g.*, the Hambantota port). New housing schemes were observed in several GNDs (*i.e.*, Siribopura, Keliyapura and Koholankala), within which the 'affected residents' were resettled. Establishment of new infrastructure such as the Hambantota port, new Administrative Building Complex, LAUGFS LPG Transsh6ipment Terminal, Mirijjawila cement grinding plant and oil refinery plant, International Convention Centre, and development of roads had mainly contributed to expand the area under the settlement class over the period of study. Overlay analysis revealed that fractions of areas under LULCs grassland and marsh, homesteads, other cultivations, paddy lands and scrubland and chena in the 1996 map had been replaced by these newly established settlements in the 2017 map. Similarly, scrubland and chena areas in the coastal belt had been cleared to establish homesteads and housing schemes during the period.

Another significant area reduction was observed in the LULC class 'saltpans' (1944 ha; $p < 0.05$) in the Hambantota coastal belt from 1996 to 2017. In 1996, there had been six functioning saltpans ('lewaya' in Sinhala language), namely, Kahandamodara lewaya, Karagan lewaya, Hambantota Maha lewaya, Koholankala lewaya, Bundala lewaya, and Palatupana lewaya. Although the Malala lagoon was classified as a saltpan in the 1996 LULC map obtained from the Sri Lanka Survey Department, residents living in the area for more than twenty years claimed that the lagoon had never been utilized as a saltpan (personal communication, August 2019). The Karagan lewaya, which existed in the 1996 LULC map, had been partially replaced with settlements (62 ha) by 2017 and the rest of the lewaya remains as open water and marsh.

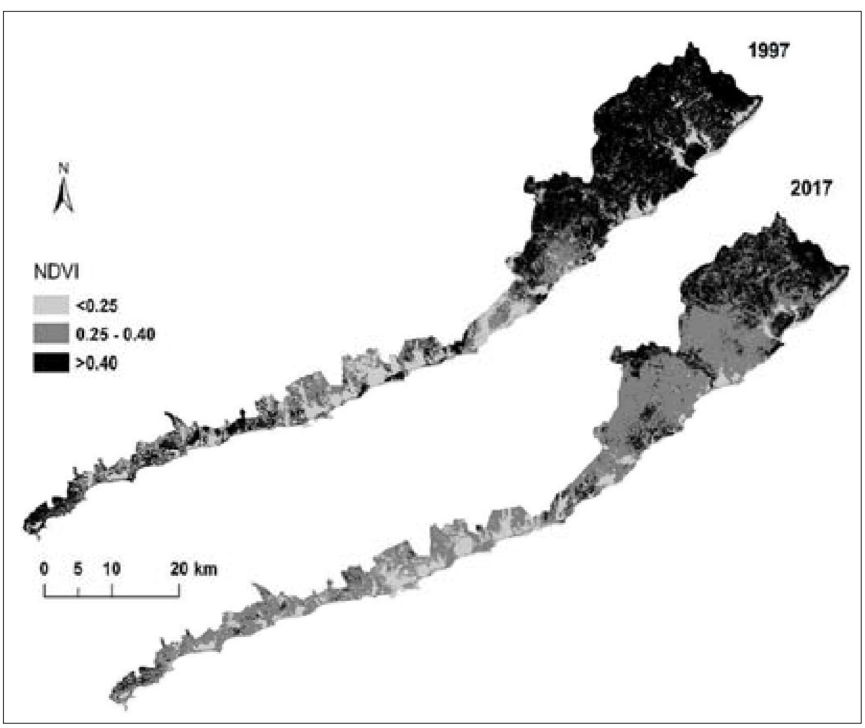

Figure 4: NDVI outputs of the coastal belt of Hambantota for 1997 and 2017. Maps are categorized into three classes (non-vegetated area: NDVI < 0.25; other vegetation: NDVI = 0.25–0.40; dense forest: NDVI > 0.40) based on the NDVI values.

The Hambantota coast bears five major lagoons, Mawalla, Rekawa, Kahandamodara, Koholankala, and Bundala, along with two lagoon complexes, Kalametiya-Lunama and Malala-Embilikanda. Two major rivers, Walawe and Menik, meet the Indian Ocean at the site of the estuaries on the Hambantota coast. Moreover, the coast bears several lakes, tanks, and reservoirs, most of which are situated inside the Bundala and Yala forest reserves. The inland water areas in the Hambantota coastal belt had significantly increased during the past twenty years (by 539 ha, $p < 0.05$).

Normalized Difference Vegetation Index (NDVI) estimation

The NDVI outputs were classified into three different classes: (1) No-vegetation area such as water, rocky areas, built-up area and bare lands (NDVI < 0.25), (2) Other Vegetation like grasslands, scrublands, chena, home gardens and sparse forests (0.25–0.40 NDVI), and (3) Dense Forest area (NDVI > 0.40). Comparison of NDVI maps of the coastal belt of Hambantota district clearly shows a decrease in dense forest cover in 2017 as compared to the status of 1997 (Figure 4 and Table 4). This dramatic reduction is significant in the Yala national forest area situated in the eastern edge of the district. The density of the forest cover has decreased since many patches of dense forest areas had been transformed into open forest areas. Also, some of the 'dense forest areas' located in the western part of the Hambantota coastal belt seen in the 1997 NDVI map are classified under 'other vegetation' areas as seen in the 2017 NDVI map.

Table 4: A summary of the NDVI results and the criterion used in classifying the map into three classes based on NDVI values.

	1997	2017
NDVI values		
Upper value	0.674074	0.540695
Lower value	-0.573034	-0.347283
Area estimations / ha		
< 0.25 (No vegetation area)	14341.7	11361.6
0.25 - 0.40 (Other vegetation)	20719.9	47976.1
> 0.40 (Dense forest area)	44346.9	20070.8

Questionnaire survey

Out of the forty households selected randomly for the survey, only 36 questionnaire forms had no missing data and thus, were considered for the analyses. All the respondents have been living in the Hambantota district for more than twenty years and that included 55.6% males and 44.4% females. Surveyed houses had utilities such as electricity, drinking water and basic sanitary facilities. All houses had grid electricity and 97.2% had direct waterlines. However, the questionnaire data revealed that only 55.6% are satisfied with their new residence in the resettlement area. Out of the dissatisfied portion, 98% of the residents claimed that the greater distance from their new home to the city area and to their working places were the main reasons for dissatisfaction.

According to the PCA results (PCA outputs are given in Figure 5), agriculture and fishery industry were the main economic sectors in the city. Moreover, goods and services were available in the city and tourism was also booming. A 94.5% portion of the respondents claimed that they did not need to go outside the town to find goods and services. According to the responses given regarding the environment, the two major components (PCA 1 & PCA 2) identified from the PCA results indicated that environment had been compromised for development projects, but the provision of services by the city to keep environment clean was satisfactory. Further, 63.8% agreed that recent development projects had affected the natural environment of the city. Verbal communication with respondents revealed that the municipal council had adopted sound managerial practices for waste management in the city. Apart from 11.1% of the respondents, others had stated that they strictly follow the guidelines that were set for the recycling programme in the city. PCA results regarding the goods and services available in the city exposed that many public and private service providers were available in the city. Moreover, the health sector provides a satisfactory service to the people including facilities for elderly care, health education, and care for disabled children, and frequency data revealed that 94.4% were satisfied with the medical facilities in the city. However, only 66.7% of the respondents were satisfied with the facilities provided for education. The survey reflects that education facilities and the public transport system need further improvement.

Many respondents complained during interviews that although there was an adequate number of schools in the city, they had a small number of well-trained teachers. When people's perspectives were taken into consideration, the PCA results indicated that people appreciate the progress that the city was making in new businesses and development projects. Moreover, it was evident that people were happy about improvements taking place in fishing industry and in agriculture sector and they were feeling good about life in town. Most importantly, they were happy about available resources in the town as 63.9% of the respondents agreed that Hambantota town was better because of new development projects while 69.5% believed that the town had enough resources to attract new businesses.

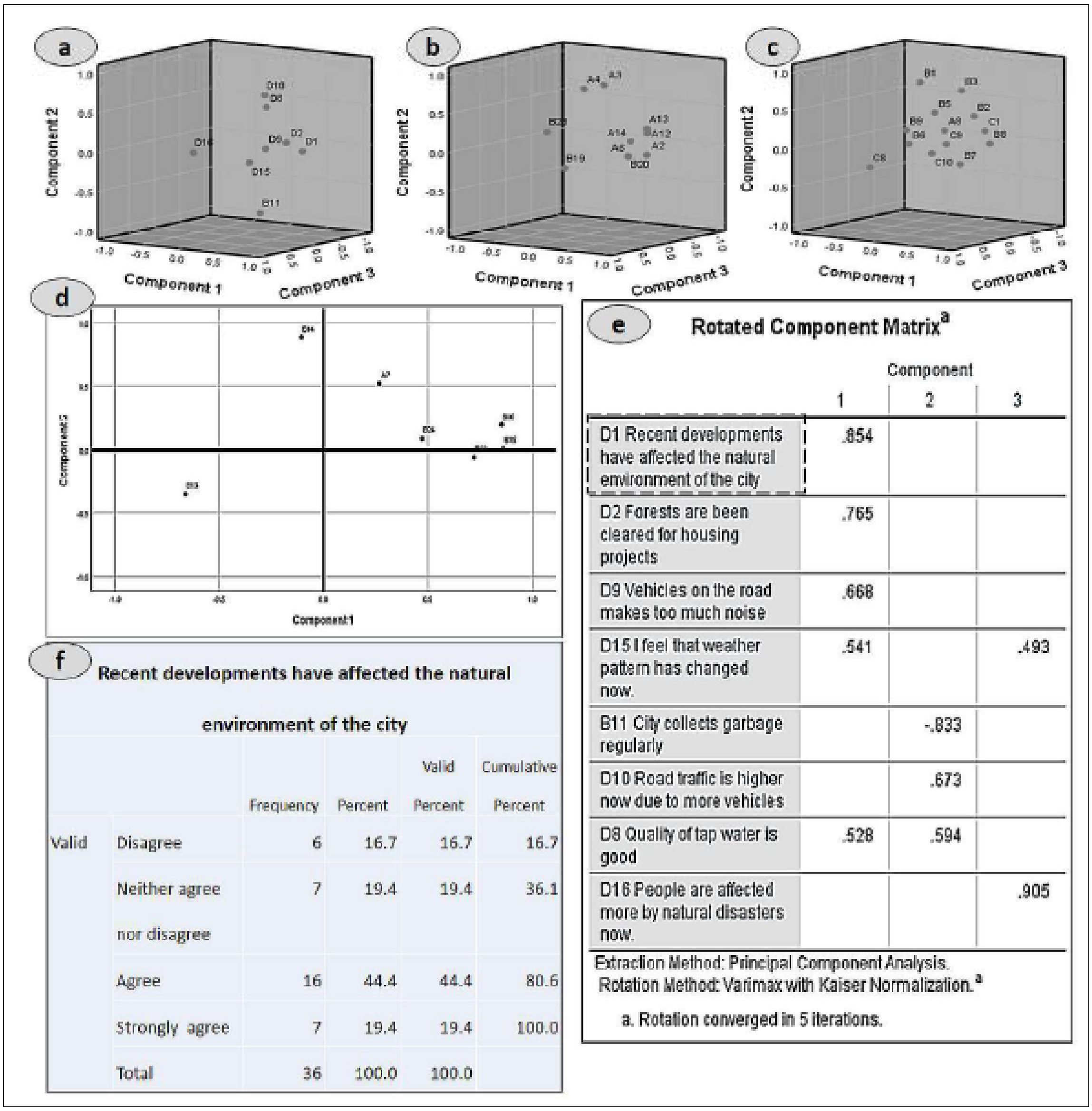

Rotated Component Matrix[a]

	Component 1	Component 2	Component 3
D1 Recent developments have affected the natural environment of the city	.854		
D2 Forests are been cleared for housing projects	.765		
D9 Vehicles on the road makes too much noise	.668		
D15 I feel that weather pattern has changed now.	.541		.493
B11 City collects garbage regularly		-.833	
D10 Road traffic is higher now due to more vehicles		.673	
D8 Quality of tap water is good	.528	.594	
D16 People are affected more by natural disasters now.			.905

Extraction Method: Principal Component Analysis.
Rotation Method: Varimax with Kaiser Normalization.[a]

a. Rotation converged in 5 iterations.

Recent developments have affected the natural environment of the city

		Frequency	Percent	Valid Percent	Cumulative Percent
Valid	Disagree	6	16.7	16.7	16.7
	Neither agree nor disagree	7	19.4	19.4	36.1
	Agree	16	44.4	44.4	80.6
	Strongly agree	7	19.4	19.4	100.0
	Total	36	100.0	100.0	

Figure 5: Image shows PCA outputs for the questions regarding (a) environment, (b) people's perspectives, (c) goods and services and (d) economy. Rotated component matrix for the questions regarding the environment is given in (e), while (f) shows an example for a frequency table generated for a question representing component-1 selected from the rotated component matrix.

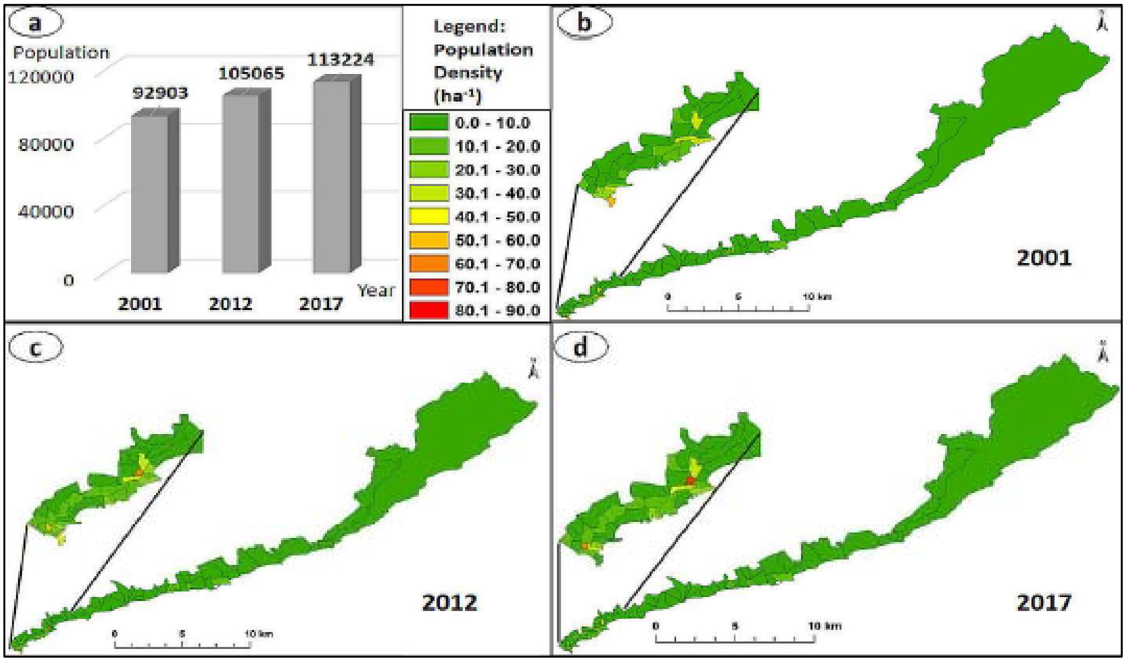

Figure 6: (a) Graph showing the population increase in Hambantota coastal belt from 2001 to 2017; Maps (b), (c), and (d) show GND-wise population densities of the study area in 2001, 2012 and 2017, respectively.

Population density

The population of the coastal belt of the Hambantota district has continuously increased from 2001 to 2017, as shown in Figure 6 (a). The population density (per ha) for the whole Hambantota coastal belt was 1.2 in 2001, 1.3 in 2012 and 1.4 in 2017. These values are low due to the fact that the Hambantota coastal belt has large non-populated forest areas such as the Yala and Bundala national parks. When the population density of each GND in 2001 was taken into consideration alone, all had values less than 30.0 ha^{-1} [Figure 6 (b)], excluding Kudawella south GND where the population density was slightly higher (33.8 ha^{-1}). In 2012, three GNDs of Tangalle DSD (divisional secretariat division) (*i.e.*, Kudawella south, Kudawella north and Indipokunagoda north) showed an increase in population density, having population densities greater than 30.0 ha^{-1}.

Discussion

Changes in LULC classes show a pattern of conversion of forest cover to other LULC types such as grassland and marsh, scrubland, and chena, indicating that the forest systems are being disturbed by human interventions. Activities that attract tourists, for example, safari tours, camping, etc., inside the Yala and Bundala national parks take place frequently, and evidently those activities also damage the forest cover disturbing the wildlife as well (Estoque & Murayama, 2017; Ranagalage *et al*., 2018). In addition, a famous Buddhist monastery, Sithulpawwa, located within the Yala national park premises, attracts large crowds of local devotees, mainly during religious activities. Increased visitor attraction could have impacted park's fauna and flora severely, due to inappropriate infrastructure developments, overcrowding, inappropriate human behaviour, and due to road accidents killing wildlife (McNeely *et al*., 1992; Ranagalage *et al*., 2018). It has been emphasized that tourism in such areas could be made sustainable, providing protection to their own unique environmental values (McKercher, 1993). The World Tourism Organization defines sustainable tourism as one that improves the quality of life of host communities, provides high quality experience for guests, and maintains the quality of the environment on which they both depend (WTO, 1993). The Department of Wildlife Conservation, which manages these national parks under the jurisdiction of the Ministry of Environment and Natral Resources (DWC, 2004) has taken some worthy actions for providing protection and freedom to the wildlife in these areas by closing the park during dry weather (from August to mid-October) due to lack of water, and also allowing animals some break from human activities during the breeding season

(Buultjens *et al*., 2005). Reduction in dense forest cover in NDVI estimations further confirms the degradation of forest quality over time. Both Yala and Bundala had been declared as national parks well before 1997, yet they had lost considerable forest cover during the two-decade period. Therefore, the government should take immediate action to prevent the illegal encroachments in the forest buffer zone and to strengthen the policies and action towards protecting these dry zone forests. In addition, forest dieback in the Bundala national park is one of the reasons for the conversion of forest cover into scrublands. Previous studies (Perera *et al*., 2007; Gunarathne & Perera, 2016) confirm the replacement of native tree species (e.g. *Manilkara hexandra*) due to invasion by *Prosopis juliflora* (Sw.) DC. and *Ganoderma* infection.

A dramatic decrease in the LULC class scrubland and chena, in the study area, was observed through the analysis. Many scrubland areas had been sacrificed to development projects which took place in the Hambantota urban area, including the establishment of the Administrative Building Complex, housing/resettlement schemes, road development/expansion and the port. Approximately 358 ha of scrubland had been cleared to establish housing schemes in the Keliyapura, Siribopura, and Koholankala GNDs for those people who were dislocated due to the port project and also due to the tsunami in 2004. How natural vegetation has been sacrificed to such establishments in the urban area is shown in Figure 7. The transformation of scrubland areas clearly indicates the degradation of natural vegetation in the Hambantota coastal belt for the development projects, even though such projects are also required during development. However, the scrubland areas located within national park territories were collectively classified under the LULC class ‘forest’ in the present study, as it was hard to demarcate when scrublands are located inside the national parks. Although the scrubland and chena class showed an overall decrease in area over the past two decades, NDVI analysis showed severe degradation of dense forest cover as well. The dense forest areas have been mostly replaced by scrub species such as *Securinega leucopyrus* (Willd.) Muell. (Katupila in Sinhala, the local language), *Prosopis juliflora* (Kalapu Andara in Sinhala) and *Mimosa pigra* L. (Yodha Nidikumba in Sinhala) with the secondary succession that had taken place after clear-felling and die-back scenarios.

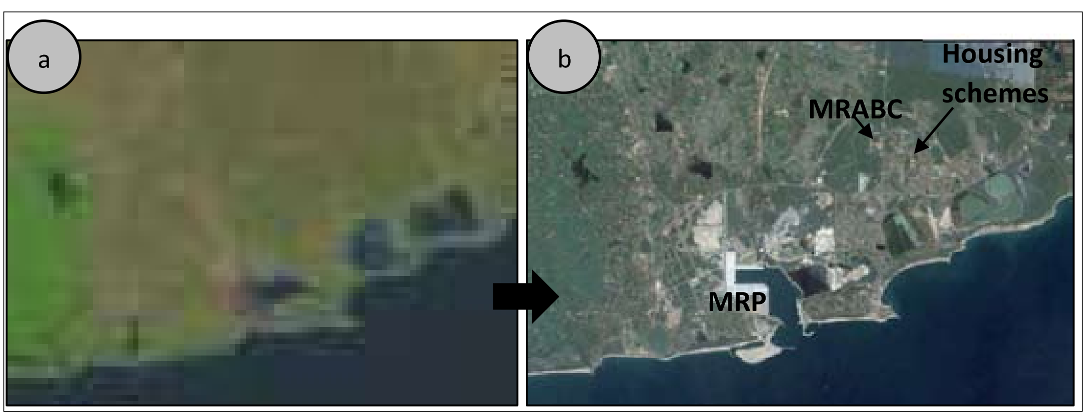

Figure 7: Satellite images showing the urbanization that has taken place during the study period of two decades in Hambantota replacing natural vegetation. (a) Landsat 5 image on 17.07.1997 and (b) Google Earth image (CNES/Air Bus) on 05.01.2017. (MRP: Magam Ruhunupura Port; MRABC: Magam Ruhunupura Administrative Building Complex; Housing schemes for tsunami affected people and communities dislocated due to development projects).

Replacement of water area by marsh vegetation in the Kalametiya lagoon, for example, had contributed to a significant increase in grassland and marsh cover from 1996 to 2017. Madarasinghe *et al*. (2020b) reported that the invasion of marshes had occurred in the newly formed landmasses in the Kalametiya lagoon due to excessive siltation. The excess of irrigated water from the Udawalawa irrigation project had been diverted to the sea through the Kalametiya lagoon, due to which siltation of the lagoon had increased, reducing the water surface area. Also, as a consequence of the construction of an artificial dyke at the lagoon mouth, the seawater influx to the lagoon had decreased, reducing the salinity of the lagoon. As a result, marsh vegetation (*i.e.*, *Typa angustifolia* L.) had invaded the newly formed landmasses in the lagoon (Madarasinghe *et al*., 2020b).

This scenario had contributed to the increased grassland and marsh cover as well as the reduction of water areas along the Hambantota coastal belt. The same scenario had contributed to the significant increase of mangrove cover as well, particularly in the Rekawa, Kahandamodara, and Kalametiya lagoons. Moreover, an increase of 282.9 ha of mangrove cover in the Kalametiya lagoon from 1982 to 2016 (Madarasinghe *et al*. 2020b), and by 1.1 ha and 19.0 ha, respectively, in the Rekawa and Kahandamodara lagoons from 1994 to 2016 (Madarasinghe *et al*., 2017) were consequences of reduction of salinity levels in the lagoons and excessive siltation resulting from irrigation projects. The overall increase of mangrove cover outshines the small-scale losses of the mangrove patches in the Rekawa and Mawella lagoons. Reclamation of lands for human settlements and agriculture as well as cutting wood for housing constructions and making fishing crafts (Katupotha, 2017; Madarasinghe *et al*., 2017) were identified as causes. Further, Jayatissa *et al*. (2002) and Madarasinghe *et al*. (2020b) showed the degradation of the quality of the mangrove forests along the Hambantota coastal belt, particularly in the Kalametiya lagoon, irrespective of the increase in total mangrove area. This scenario has been explained as 'cryptic ecological degradation' in the aforementioned research publications.

Rapid urbanization in the Hambantota coastal belt has caused abandonment of some paddy lands, especially after the tsunami in 2004. Concurrently, local people were recruited for the development projects and the newly established industries, which ultimately had indirectly forced them to abandon their traditional paddy fields. These abandoned paddy lands had then been converted to grasslands as well as to homesteads. However, the reduction of paddy land area during the study period was not so significant. Conversely, both coconut cultivation and other cultivations have increased in the area from 1996 to 2017. Abandoned paddy lands had been converted to other cultivations such as banana, and some abandoned homesteads had been utilized by the owners for coconut plantations and other cultivations such as sugarcane and finger millet, which resulted in a significant increase in the LULC class 'other cultivations' from 1996 to 2017 (personal communications and field observations in August 2019).

Karagan lewaya, which was a well-functioning saltpan, had been completely sacrificed for the establishment of the Magam Ruhunupura port, construction of which had commenced in 2008. This contributed to the reduction of the 'saltpan' area in 2017 compared to 1996. The difference in saltpan area in 1996 and 2017 includes an overestimation in area due to classification error as well, where Malala lagoon was classified as a saltpan in the 1996 LULC map, obtained from the Sri Lanka Survey Department, although it had never been used as one according to residents living in the area (*personal communication*, August 2019). A classification error in mapping Koholankala and Bundala saltpans in 2017 LULC map has led to produce an overestimation of saltpan loss from 1996 to 2017. Careful observation of Google Earth archives revealed that some large evaporation tanks filled with sea water were misclassified under the 'water' LULC class in the 2017 map, while being correctly classified under the 'saltpan' class in the 1996 map. The personal error in image interpretation can be the reason for this dissimilarity and has led to overestimating the reduction of saltpan area from 1996 to 2017.

According to the questionnaire survey, basic facilities (*i.e.*, electricity and water supply) had been provided through the resettlement programme, which was a commendable development move by the government. Greater distance from new homes to the city area and also to their working places have been identified as the main reasons for some residents' dissatisfaction about the resettlement. This indicates a shortcoming in site selection for the resettlement programme in Hambantota. Mariyathas *et al*., (2016) reports that Urban Development Authority was responsible for selecting relocation sites for the tsunami affected people. It would have been more successful if a proper need analysis of the residents were done prior to finalizing possible areas for resettlement. Due to the resettlement and major changes in the road network, the operation of many small-scale sweets shops and curd stalls, which were owned by residents living adjacent to road-side houses, had been abandoned, leaving the sellers no other option than finding jobs in construction sites (Mariyathas *et al*., 2016; personal communication with displaced residents in August 2019). Although some dissatisfaction remains in resettled communities regarding some of their life expectations, a majority is happy with the flourishing status of the city, particularly due to ongoing development programmes. This indicates that despite the shortcomings in resettling families in new areas, the government was able to make people satisfied with the development work in the town's infrastructure and facilities. It was highlighted that the green cover had been reduced due to development projects, and thus, the urban forestry concept could be an ideal sustainable move to be introduced in the urban area of Hambantota. It is also important to launch tree planting programmes and promote home gardening concepts to enhance the environmental health in the city.

CONCLUSIONS

Overlay analysis of the multi-temporal land-use/land-cover (LULC) maps of 1996 and 2017 together with a NDVI analysis and questionnaire survey to verify the results of the overlay analysis were carried out in the present study. The results reveal that the geographical areas of settlements including development projects had increased significantly (by 1318 ha compared to the area in 1996) during past two decades. In contrast, a great decline in forest cover (by 2739 ha) and scrublands and chena (by 851 ha) was seen from 1996 to 2017. NDVI results indicated a dramatic reduction of dense forest cover in the Yala national forest, which reflects a deteriorating environmental condition in the area. Thus, the study reveals that significant development along the Hambantota coastal belt has been taken place at the cost of forests and associated vegetation from 1996 to 2017. A rapid economic and population growth can be identified as the main driving forces for these LULC changes. A noteworthy increase in population has taken place in several GNDs of the coastal belt of Hambantota over the past two decades. These results deliver an important reference for authorities in proper decision-making and LULC planning for sustainable development in the Hambantota coastal belt. The urban forestry concept could be recommended as an ideal sustainable move to be introduced in the urban area of Hambantota in order to recover the greenery lost due to infrastructure development.

Acknowledgement

RU/SF/RP/2017/03 grant by the Faculty of Science, University of Ruhuna is greatly acknowledged. The authors also acknowledge the staff of Hambantota Divisional Secretariat office, Grama Niladharis of Siribopura, Keliyapura, and Koholankala GNDs, community leaders, and the residents for their support given in questionnaire surveys.

REFERENCES

Alphan H. (2003). Land-use change and urbanization of Adana, Turkey. *Land Degradation and Development* **14**(6): 575–586.
DOI: https://doi.org/10.1002/ldr.581

Buultjens J., Ratnayake I., Gnanapala A. & Aslam M. (2005). Tourism and its implications for management in Ruhuna national park (Yala), Sri Lanka. *Tourism Management* **26**(5): 733–742.
DOI: https://doi.org/10.1016/j.tourman.2004.03.014

CEA/Euroconsult (1993). *Wetland Site Report and Conservation Management Plan: Bundala National Park*. Central Environmental Authority, Sri Lanka & Euroconsult, Netherlands.

Chen X. & Zhang Y. (2017). Impacts of urban surface characteristics on spatiotemporal pattern of land surface temperature in Kunming of China. *Sustainable Cities and Society* **32**: 87–99.
DOI: https://doi.org/10.1016/j.scs.2017.03.013

Department of Census and Statistics (2012). *Census of Population and Housing of Sri Lanka*. Department of Census and Statistics, Ministry of Finance and Planning, Colombo, Sri Lanka. Available at *http://www.statistics.gov.lk*, Accessed 03 April 2017.

Dissanayake D.M.S.L.B. (2020). Land use change and its impacts on land surface temperature in Galle City, Sri Lanka. *Climate* **8**(5): 65–80.
DOI: https://doi.org/10.3390/cli8050065

Dissanayake D.M.S.L.B., Morimoto T., Ranagalage M. & Murayama Y. (2019). Land-use/land-cover changes and their impact on surface urban heat islands: Case study of Kandy City, Sri Lanka. *Climate* **7**(8): 99.
DOI: https://doi.org/10.3390/cli7080099

DWC (Department of Wildlife Conservation) (2004). *A Guide to National Parks of Sri Lanka*, 2nd Edition. Department of Wildlife Conservation, Sri Lanka, pp. 97.

Edirisooriya K.V.D., Senevirathna E.M.T.K., Dheerasinghe G.W.M.M.K. & Dauglas D.L.P.M. (2021). Analysis of land use/land cover changes in Hambantota divisional secretariat division from 2008 to 2019 using remote sensing and GIS techniques. *Vavuniya University International Research Conference (VUIRC)*, pp. 280–285.

Estoque R.C. & Murayama Y. (2017). Monitoring surface urban heat island formation in a tropical mountain city using Landsat data (1987–2015). *ISPRS Journal of Photogrammetry and Remote Sensing* **133**: 18–29.
DOI: https://doi.org/10.1016/j.isprsjprs.2017.09.008

Gunarathne R.M.U.K. & Perera G.A.D. (2016). Does the invasion of Prosopis juliflora cause the die-back of the native Manilkara hexandra in seasonally dry tropical forests of Sri Lanka. *Tropical Ecology* **57**(3): 475–488.

Jayatissa L.P., Guero M.C., Hettiarachchi S. & Koedam N. (2002). Changes in vegetation cover and socio-economic transitions in a coastal lagoon (Kalametiya, Sri Lanka), as observed by teledetection and ground truthing, can be attributed to an upstream irrigation scheme. *Environment, Development and Sustainability* **4**(2): 167–183.
DOI: https://doi.org/10.1023/A:1020831416827

Katupotha K.N.J. (2017). Mangroves in lagoon ecosystems-a neglected habitat in Sri Lanka. *WILDLANKA International Symposium on Climate Change and Conservation*, Colombo **4**(3): 79– 105.
DOI: http://dx.doi.org/10.13140/RG.2.2.13432.55049

Kotelawala H. (2017). *Everything you need to know about the Hambantota port lease*. Roar Media. 8th August 2017. Available at *https://roar.media/english/life/reports/everything-you-need-to-know-about-the-hambantota-port-lease*. Accessed 04 March 2021.

Lindström S., Mattsson E. & Nissanka S.P. (2012). Forest cover change in Sri Lanka: The role of small scale farmers. *Applied Geography* **34**: 680–692.

DOI: https://doi.org/10.1016/j.apgeog.2012.04.011

Madarasinghe S.K., Yapa K.K.A.S., Kodikara K.A.S., Satyanarayana B., Udayakantha P.M.P. & Jayatissa L.P. (2017). Spatiotemporal changes in mangrove cover of three lagoons in Southern Sri Lanka during the last two decades; A field validated GIS study. *Proceedings of 4th Ruhuna International Science and Technology Conference (RISTCON)*, University of Ruhuna, Matara, Sri Lanka, pp. 13.

Madarasinghe S.K. (2022). Investigation of land-use changes in Western and Southern coasts of Sri Lanka in the past two decades (1996-2017): A field based geo-informatics approach. *PhD Thesis*, University of Ruhuna, Matara, Sri Lanka.

Madarasinghe S.K., Yapa K.K.A.S., Satyanarayana B., Udayakantha P.M.P., Kodikara K.A.S. & Jayatissa L.P. (2018). Land-use/cover changes of city of Hambantota, Sri Lanka over past two decades – a field validated GIS study. *Proceedings of 3rd Ruhuna International Science and Technology Conference*, University of Ruhuna, Matara, Sri Lanka, pp. 87.

Madarasinghe S.K., Yapa K.K.A.S. & Jayatissa L.P. (2020a). Google Earth imagery coupled with on-screen digitization for urban land use mapping: case study of Hambantota, Sri Lanka. *Journal of the National Science Foundation of Sri Lanka* **48**(4): 357–366.
DOI: http://dx.doi.org/10.4038/jnsfsr.v48i4.9795

Madarasinghe S.K., Yapa K.K., Satyanarayana B., Udayakantha P.M.P., Kodikara S. & Jayatissa, L.P. (2020b). Inland irrigation project causes disappearance of coastal lagoon: The trajectory of Kalametiya lagoon, Sri Lanka from 1956 to 2016. *Coastal Management* **48**(3): 188–209.
DOI: https://doi.org/10.1080/08920753.2020.1747914

Mariyathas S., Perera N. & Yehiya M. (2016). What development has done to a town: Lessons from Hambantota, Sri Lanka. *Bhumi, The Planning Research Journal* **5**(1): 57–72.

McKercher B. (1993). Some fundamental truths about tourism: Understanding tourisms social and environmental impacts. *Journal of Sustainable Tourism* **1**(1): 6–16.

McNeely J., Thorsell J. & Ceballos-Lascurain H. (1992). *Guidelines: Development of Natural Parks and Protected Areas for Tourism*. Paris: World Tourism Organisation and United Nations Environment Programme. UNEP-IE/PAC technical report series; no 13, World Tourism Organization; United Nations Environment Programme, Terrestrial Ecosystems Branch, Industry and Environment Programme Activity Centre.

Perera G.A.D., Adikaram N.K.B., Senevirathna G., Nugaliyadde M., & Gunarathne R.M.U.K. (2007). Forest die-back in Bundala National Park. *Wildlife Research Symposium*, p. 2. PAM & WCP Project, Department of Wildlife Conservation. Sri Lanka.

Perera T.G.U.P., Weerasooriya I. & Karunarathne H.M.L.P. (2012). An evaluation of success and failures in Hambantota, Siribopura Resettlement Housing Program: lessons learned. *Sri Lankan Journal of Real Estate* **6**: 01–15.

Ranagalage M., Estoque R.C. & Murayama Y. (2017). An urban heat island study of the Colombo metropolitan area, Sri Lanka, based on Landsat data (1997–2017). *ISPRS International Journal of Geo-Information* **6**(7): 189.
DOI: https://doi.org/10.3390/ijgi6070189

Ranagalage M., Murayama Y., Dissanayake D.M.S.L.B. & Simwanda M. (2019). The impacts of landscape changes on annual mean land surface temperature in the tropical mountain city of Sri Lanka: A case study of Nuwara Eliya (1996–2017). *Sustainability* **11**(19): 5517.
DOI: https://doi.org/10.3390/su11195517

Ranagalage M., Dissanayake D., Murayama Y., Zhang X., Estoque R.C., Perera E. & Morimoto T. (2018). Quantifying surface urban heat island formation in the world heritage tropical mountain city of Sri Lanka. *ISPRS International Journal of Geo-Information* **7**: 341.
DOI: https://doi.org/10.3390/ijgi7090341

Rathnayake C.W., Jones S., Soto-Berelov M. & Wallace L. (2022). Human–elephant conflict and land cover change in Sri Lanka. *Applied Geography* **143**: 102685.
DOI: https://doi.org/10.1016/j.apgeog.2022.102685

Rousta I., Sarif M.O., Gupta R.D., Olafsson H., Ranagalage M., Murayama Y. & Mushore T.D. (2018). Spatiotemporal analysis of land use/land cover and its effects on surface urban heat island using Landsat data: A case study of Metropolitan City Tehran (1988–2018). *Sustainability* **10(**12): 4433.
DOI: https://doi.org/10.3390/su10124433

Shalaby A. & Tateishi R. (2007). Remote sensing and GIS for mapping and monitoring land cover and land-use changes in the Northwestern coastal zone of Egypt. *Applied Geography* **27**(1): 28–41.
DOI: https://doi.org/10.1016/j.apgeog.2006.09.004

Suthakar K. & Bui E.N. (2008). Land use/cover changes in the war-ravaged Jaffna Peninsula, Sri Lanka, 1984–early 2004. *Singapore Journal of Tropical Geography* **29**(2): 205–220.
DOI: https://doi.org/10.1111/j.1467-9493.2008.00329.x

Van T.T. & Bao H.D.X. (2010). Study of the impact of urban development on surface temperature using remote sensing in Ho Chi Minh City, Southern Vietnam. *Geographical Research* **48**(1): 86–96.
DOI: https://doi.org/10.1111/j.1745-5871.2009.00607.x

UDA (Urban Development Authority) (2019). *Hambantota Municipal Council Area Development Plan: 2019 – 2030*, Volume I. Urban Development Authority, District Office, Hambantota. Available at: *https://www.uda.gov.lk/attachments/devplan_detailed/Development%20Plans%202019-2030/Hambnthota/English.pdf.* Accessed 24 February 2021.

WTO (World Tourism Organization) (1993). *Sustainable Tourism Development: Guide for Local Planners*. Madrid: World Tourism Organisation. Tourism and the Environment Publication, Madrid, Spain.

Yu D., Jiang Y., Kang M., Tian Y. & Duan J. (2011). Integrated urban land-use planning based on improving ecosystem service: Panyu case, in a typical developed area of China. *Journal of Urban Planning and Development* **137**(4): 448–458.
DOI: https://doi.org/10.1061/(ASCE)UP.1943-5444.0000074

List of Referees - Volume 51 (2023)

Prof. Nimal Abeysingha
Dept. of Agric Engineering and Soil, Rajarata University

Dr Hemalika Abeysundara
Dept. of Statics & Computer Science
Univ. of Peradeniya

Dr Ahmad Saeed Akhter
College of Statistical Sciences
Univ. of the Punjab
Pakistan

Dr Janaka Alawatugoda
Research and Innovation Center Division, Rabdan Academy UAE

Dr Senaka Amarakeerthi
Dept. of Information & Communication Technology
Univ. of Sri Jayewardenepura

Prof. M.G.T.S. Amarasekara
Dept. of Agricultural Engineering and Soil Science
Rajarata University

Prof. Asanga Ampitiyawatta
Institute for Agro-Technology and Rural Sciences
Univ. of Colombo

Dr Thilini Ariyadasa
Dept. of Chemical and Process Engineering
Univ. of Moratuwa

Dr Navoda Atapattu
Lady Ridgeway Hospital
Borella

Dr A.B.N. Attanayake
Dept. of Earth Resources Engineering
Univ. of Moratuwa

Prof. Renuka Attanayake
Dept. of Plant & Molecular Biology, Univ. of Kelaniya

Dr Nadeesha Badanasinghe
Dept. of Microbiology
Univ. of Kelaniya

Dr C. Bamunuarachchige
Dept. of Bioprocess Technology
Rajarata University

Dr K.M.S. Bandara
Dept. of Energy & Environmental Sciences
Sabaragamuwa University

Dr Shakila Bashir
Forman Christian College
Pakistan

Dr Samitha Buddhika
Dept. of Civil Engineering
Univ. of Peradeniya

Prof. Shampa Chakraverty
Netaji Subhas University of Technology, India

Dr A.W.S. Chandana
Dept. of Sports Sciences & Physical Education
Sabaragamuwa University

Prof. Veerendra Dakulagi
Guru Nanak Dev Engineering College, India

Prof. W.B. Daundasekara
Dept. of Mathematics
Univ. of Peradeniya

Dr Kushani De Silva
Dept. of Mathematics
Univ. of Colombo

Dr Indika De Silva
Dept. of Materials Science and Engineering
Univ. of Moratuwa

Prof. Mangala De Silva
Dept. of Zoology
Univ. of Ruhuna

Prof. M.P.K.S.K. De Silva
Dept. of Zoology
Univ. of Ruhuna

Dr N.P.S. De Silva
Rice Research & Development Institute, Bombuwala

Dr Nisansa de Silva
Dept. of Computer Science & Engineering
Univ. of Moratuwa

Prof. Ranjith Premalal de Silva
Dept. of Agricultural Engineering
Univ. of Peradeniya

Dr John Dempster
Univ. of Strathclyde
Scotland

Prof. R.M.C. Deshapriya
Dept. of Animal Science
Univ. of Peradeniya

Dr C.S. Dhanapala
Dept. of Molecular Biology & Biotechnology
Univ. of Peradeniya

Prof. W.G.D. Dharmaratna
Dept. of Physics
Univ. of Ruhuna

Dr T.W.K.I.M. Dias
Dept. of Civil Engineering
General Sir John Kotelawala Defence University

Dr D.M.D.O.K. Dissanayake
Dept. of Earth Resources Engineering
Univ. of Moratuwa

Dr Shashi Prakash Dwivedi
Lloyd Institute of Engineering & Technology, India

Prof. J.P. Eeswara
Dept. of Crop Science
Univ. of Peradeniya

Dr Harinda Fernando
Faculty of Computing
SLIIT

Prof. Gayani Galhena
Dept. of Zoology & Environment Sciences
Univ. of Colombo

Prof Imalie Gamalath
Dept. of Physics
Univ. of Colombo

Dr S.R. Ganesh
Akkamahadevi Woment's
University, India

Dr Przemyslaw Glaza
Captor Therapeutics Inc.
Poland

Prof. Roshan Godaliyadda
Dept. of Electrical & Electronic
Engineering
Univ. of Peradeniya

Prof. K.B. Gunaherath
Dept. of Chemistry
The Open Univ. of Sri Lanka

Dr Jagath Gunatilake
Dept. of Geology
Univ. of Peradeniya

Dr Luminda Gunawardena
Dept. of Civil Engineering
Univ. of Moratuwa

Prof. K.T.M.U. Hemapala
Dept. of Electrical Engineering
Univ. of Moratuwa

Dr Damayanthi Herath
Dept. of Computer Engineering
Univ. of Peradeniya

Dr A.P. Hewaarachchi
Dept. of Statistics & Computer
Science, Univ. of Kelaniya

Prof. Prabhath Hewageegana
Dept. of Physics
Univ. of Kelaniya

Dr Anushka Ilangasinghe
Dept. of Chemical and Process
Engineering
Univ. of Peradeniya

Prof O.A. Ileperuma
Univ. of Peradeniya

Dr Rasheeda Imran
Univ. of the Punjab
Pakistan

Prof. Cassim Iqbal
National Institute of Fundamental
Studies

Prof. Aminul Islam
Jessore Univ. of Science and
Technology

Prof. Leslie Jayasekara
Dept. of Mathematics
Univ. of Ruhuna

Dr Anuruddhika Jayasinghe
Dept. of Civil & Environment
Engineering
Univ. of Ruhuna

Dr Upul Jayasinghe
Dep. of Computer Engineering
Univ. of Peradeniya

Prof. Gehan Jayasuriya
Dept. of Botany
Univ. of Peradeniya

Prof Mahesh Jayaweera
Dept. of Civil Engineering
Univ. of Moratuwa

Dr Viraj Jayaweera
SPD Laboratory Inc.
Japan

Dr Dimanthi Jayatilake
Dept. of Agricultural Biology
Univ. of Peradeniya

Dr Yashika Jayathunga
Dept. of Mathematics
Univ. of Colombo

Dr H.L. Jayetileke
Dept. of Mathematics
Univ. of Ruhuna

Dr B.M.S. Jinendra
Dept. of Agri Engineering Faculty
of Agriculture
Univ. of Ruhuna

Dr Bashitha Kavinga
Dept. of Statistics & Computer
Science
Univ. of Kelaniya

Dr Dharshana Kasthurirathna
Dept. of Computer Science &
Software Engineering
SLIIT

Prof. K.A.S. Kodikara
Dept. of Botany
Univ. of Ruhuna

Prof. Chaminda Konthasingha
Dept. of Civil Engineering
Univ. of Sri Jayewardenepura

Dr Shelomi Krishnaraja
National Botanic Gardens
Peradeniya

Dr Virendra Kumar
International Rice Research
Institute, Philippines

Prof. K.L. Wasantha Kumara
Dept. of Agricultural Biology
Univ. of Ruhuna

Dr Jayantha Lanel
Dept. of Mathematics
Univ. of Sri Jayewardenepura

Dr Dhammika Magana-arachchi
NIFS
Hanthana, Kandy

Prof. K.R.R. Mahanama
Dept. of Chemistry
Univ. of Colombo

Dr Anuradha Mahasinghe
Dept. of Mathematics
Univ. of Colombo

Prof. Jagath Manatunge
Dept. of Civil Engineering
Univ. of Moratuwa

Dr Inoka Manthilake
Dept. of Mechanical Engineering
Univ. of Moratuwa

Prof. K. Masakorala
Dept. of Botany
Univ. of Ruhuna

Prof. Thomas Mathews
Univ. of Maryland
USA

AUTHOR INDEX - VOL. 51 - 2023

SUBJECT INDEX - VOL 51 - 2023

JOURNAL OF THE
NATIONAL SCIENCE FOUNDATION
OF SRI LANKA

GUIDANCE TO CONTRIBUTORS

GENERAL INFORMATION

Scope

The Journal of the National Science Foundation of Sri Lanka publishes the results of research in all aspects of Science and Technology. It is open for publication of Research Articles, Reviews, Research Communications and Correspondence.

IT related and other non-empirical articles

The JNSF is a journal primarily devoted to natural sciences. It also considers for publication significant and novel contributions from formal sciences. Authors of emerging sub-disciplines of Computing and related areas such as Machine Learning, Artificial Intelligence and Data Sciences are requested to carefully adhere to the following guidelines when submitting manuscripts for this journal.

- Clear formulation of outcome-oriented **Research Objective/s** for targeted knowledge (sub)domain/s or (sub)discipline/s.
- Selection and comprehensive summarization of **appropriate Research Method/s** adopted to achieve the stated Research Objective/s.
- Reporting a sound **(Empirical) Evaluation** of the research finding/s thereby arguing reliability, validity, and generalizability of research claim/s.

Categories of manuscripts

Research Articles: Research Articles are papers that present complete descriptions of original research. Research Articles should include an Abstract, Keywords, Introduction, Methodology, Results and Discussion, Conclusion and Recommendations where relevant. References should be prepared according to the "Guidelines for the preparation of manuscripts". Maximum length of the article should be limited to 25 pages with a word count of 10,000 including references, figures and tables. Any articles above this limit will be returned.

Reviews: Reviews are critical presentations on selected topics of Science or Technology. They should be well focused and organized and avoid general "textbook" style. As reviews are intended to be critical presentations on selected topics, reviewers need to have had substantial leadership in research supported by a publication track record in the areas covered by the review. A person/s wishing to submit a Review Article should obtain prior approval from the Editorial Board by submitting a concise summary of the intended article, along with a list of the author's publications in the related area (jnsf@nsf.gov.lk). Maximum length of the article should be limited to 40 pages with a word count of 12,000 including references, figures and tables. Any articles above this limit will be returned.

Research Communications: Research Communications are intended to communicate important new findings in a specific area of limited scope that are worthy of rapid dissemination among the scientific community. Authors are required to provide a statement justifying the suitability of the submission for a Research Communication. The article should include an Abstract, Keywords, Introduction, Methodology, Results & Discussion, Conclusion and References. Maximum length of the article should be limited to 10 pages with a word count of 2,500 including references, figures and tables. Any articles above this limit will be returned.

Correspondence: Correspondence will be accepted regarding one or more articles in the preceding four issues of the Journal, as well as Letters to the Editor. Articles covering important scientific events or any other news of interest to scientists, reviews of books of scientific nature, articles presenting views on issues related to science and scientific activity will also be considered. Publication will be made at the discretion of the Editor-in Chief. Maximum length of the article should be limited to 05 pages with a word count of 1,500 including references, figures and tables. Any articles above this limit will be returned.

SUBMISSION OF MANUSCRIPT

Authors submitting articles to the JNSF should first create an account in the Sri Lanka Journals Online System (https://jnsfsl.sljol.info/). All manuscripts in MS Word format must be electronically submitted to the journal's online platform at https://jnsfsl.sljol.info/submit/start/. Submissions *via* emails are not encouraged. Please make sure that no author information is mentioned in the article submitted. The names and details of affiliations of all authors and contact information of the corresponding author must be fed into the system during the online submission process. Authors (at least the corresponding author) are required to provide their personal, validated ORCID ID (by obtaining an ORCID ID from https://orcid.org/) when submitting the manuscript. No change to the authors or order of authors will be accepted after the submission. All those who have made significant contributions should be listed as co-authors. The corresponding author should ensure that all contributing co-authors are included in the author list and have approved the final version of the paper and have agreed to its submission for publication.

All submissions should be in English. If the manuscript conforms to the guidelines specified, the date received will be the date that the manuscript was submitted to the online system.

Submissions are accepted for processing on the understanding that they will be reviewed and that they have not been submitted for publication elsewhere (including publication as a full paper or extended abstract as a part of Conference Proceedings). The JNSF does not accept manuscripts that have already been submitted to pre-print servers.

Suggesting potential reviewers by authors

The authors may suggest up to three names of referees when submitting their manuscript, in the Cover Letter space provided at the bottom of the page in the first stage of online submission. Referees should not be from the institution where the work was carried out and should not have been co-authors in previous publications. The address, institutional affiliation and e-mail of the suggested referees should be supplied. Please note that the JNSF is not bound to select all or any of the suggested referees for sending the manuscript for reviewing

Authorship
All authors designated as authors should be eligible for authorship. Those who have made a substantial contribution to the concept or design of the work; or acquisition, analysis or interpretation of data are recognized as Authors.
The corresponding author should be prompt and ensure adherence to timelines when responding to requests, queries and recommendation of reviewers conveyed by or on behalf of the Editor-in Chief and Editorial Board.

Supplementary materials
Any experimental data necessary to evaluate the claims made in the paper but not included in the paper should be provided as supplementary materials. Supplementary materials will be sent to the reviewers and published online with the manuscript if accepted. The supplementary materials should conform to Journal guidelines and should be uploaded as separate files. Authors should number Supplementary Tables and Figures as, for example, 'Supplementary Table S1'. Refer to each piece of supplementary material at the appropriate point(s) in the main article. Supplementary Materials may include description of the materials and methods, controls, or tabulated data presented in Tables or Figures, and programming codes.

Peer review
The manuscripts submitted to the JNSF will initially be screened by the Editorial Board and, if suitable, will be referred to at least two subject experts in the relevant field. The peer-review process of the JNSF is double-blind.
When revision of a manuscript has been requested, the revised manuscript should be submitted on or before the stated deadline. If the revised manuscript is not received on time, the manuscript will not be processed further. The authors' response to the comments of referees should be tabulated with the comment, response and the line number/s for reference. The decision of the Editorial Board shall be final.
Accepted papers are subject to editing. The date of acceptance will be the date when the Editorial Board has decided it to be acceptable for publication.

Article publication fee
A total of US$ 250 will be levied for each accepted manuscript for publication, except when the corresponding author is affiliated to a Sri Lankan Institute, in two stages as explained below.

- A processing fee of US$ 20 will be levied for each manuscript at peer-review stage and the remaining US$ 230 will be charged for accepted manuscripts at the time of publication.

Payments can be made online via NSF Payment Portal (http://pg.nsf.gov.lk/)

Authors' declaration
When an article is accepted for publication, the authors are required to submit the Authors' Declaration signed by all the authors.

Copyright
Articles in JNSF are published under the Creative Commons License CC-BY-ND. This license permits use, distribution and reproduction of articles for commercial and non-commercial purposes, provided that the original work is properly cited and is not changed in anyway. The copyright of the article is with the National Science Foundation of Sri Lanka. Therefore, authors are requested to check with institution's copyright and publication policy before submitting an article to the JNSF. Authors secure the right to reproduce any material that has already been published or copyrighted elsewhere. When an article is accepted for publication, the authors are required to submit the Transfer of Copyright document signed by all the authors.

Post-publication corrections
The Editorial Board reserves the right to take action on publishing an erratum or corrigendum. If serious errors are identified in a published article, the Journal may consider a retraction or publishing a correction.

STRUCTURE OF MANUSCRIPT

Manuscript
The manuscript should be free of errors and prepared in single column, using double-spaced text of Times New Roman 12 font throughout with line numbers, leaving at least 2 cm margins on both sides, and liberal spacing at the top and bottom of each page. Pages should be numbered consecutively.

a. Style
The paper should be written clearly and concisely. The style of writing should conform to scholarly writing. Slang, jargon, unauthorized abbreviations, abbreviated phrasings should not be used. In general, the impersonal form should be used. Poor usage of language will result in rejection of the manuscript during initial screening.

b. Layout
Manuscripts other than review articles should be generally organized as follows: Title, Abstract, Keywords, Introduction, Methodology, Results and Discussion, Conclusions and Recommendations (where relevant), Acknowledgements and References. Pages should be arranged in the following order:

Title page should include the title of manuscript, and no author information should be mentioned in the title page. If a major part of the research has been published as an abstract in conference proceedings, it should be cited as a footnote on the title page. Authors must also indicate the **general and specific research area** of the manuscript in the title page. In order to highlight the significance of the manuscript, authors are required to provide the following highlights in brief. (1) Why was this study conducted? (2) What are the new findings? (3) Possible applications of the findings. Please limit your answers to 25-30 words for each.

Title: Should accurately and concisely reflect the contents of the article.

Running title: Should be a shortened title (limited to a maximum of 50 characters) that could be printed at the top of every other page of the Journal article.

Abstract: Should be between 200 - 250 words for full length articles and written as a single paragraph. It should not contain any references and should be able to stand on its own. It should outline objectives and methodology together with important results and conclusions. A Review Article should carry a summary of not more than 300 words.

***Keywords*:** Include a maximum of six keywords, which may include the names of organisms (common or scientific), methods or other important words or phrases relevant to the study.

***Introduction*:** This should state the reasons for performing the work with a brief review of related research studies in the context of the work described in the paper. Objectives of the study should be clearly stated.

***Materials and Methods*:** This section should give the details of how you conducted your study. New methods may be described in detail with an indication of their limitations. Established methods can be mentioned with appropriate references. Sufficient details should be included to allow direct repetition of the work by others. Where human subjects are involved, they should be referred to by numbers or fictitious names. A paper reporting the results of investigations on human subjects or on animals must include a statement to the effect that the relevant national or other administrative and ethical guidelines have been adhered to, and a copy of the ethical clearance certificate should be submitted. Methods of statistical analyses used should be mentioned where relevant.

***Results and Discussion*:** Results: the results should be concisely and logically presented. Repetition of the same results in figures, tables or text should be avoided.
Discussion: data essential for the conclusions emerging from the study should be discussed. Long, rambling discussions should be avoided. The discussion should deal with the interpretation of results. It should logically relate new findings to earlier ones. Unqualified statements and conclusions not completely supported by data should be avoided.
Molecular sequence data, such as gene or rDNA sequences, genome sequences, metagenomic sequences etc. must be deposited in a public molecular sequence repository, such as GenBank, that is part of the International Nucleotide Sequence Database Collaboration (INSDC). The accession numbers obtained must be cited in the text, Table or on Figures of phylogenetic trees of the manuscript.

***Conclusion*:** The conclusion should be brief, highlight the outcomes of the study and should be aligned with the objectives of the study. It should not contain references.

***Conflict of interest statement*:** All authors should include a statement on conflict of interest disclosing any financial or other substantive conflicts of interest that may be construed to influence the results or interpretation of their research. All sources of financial support for the project should be disclosed.

***Acknowledgement*:** Should be brief and made for specific scientific, financial and technical assistance only. If a significant part of the research was performed in an institution other than in those indicated by the authors' affiliations given in the title page, this fact should be acknowledged. All those who have made substantial contribution to the research but do not qualify to be authors should be acknowledged.

***References* :**
All research work of other authors, when used or referred to or cited, should be correctly acknowledged in the text and in the References.

Citing references in the text:

- References to the literature must be indicated in the text and tables as per the Author-Year System, by the author's last name and year, inparenthesis (i.e. Able, 1997) or (Able & Thompson, 1998).
- Citation to work by more than two authors should be abbreviated with the use of *et al*. (i.e. Able *et al*., 1997).
- Multiple publications by the same first author in the same year should be coded by letters, (i.e. Thompson, 1991a; b).
- Multiple citations should be made in chronological order and separated by a semi-colon, (i.e. Zimmerman *et al*., 1986; Able *et al*., 1997).
- Reference to unpublished work, work in preparation or work under review should be cited in italics as (*unpublished data*) or, with the author'sinitials and surname given; such works should not be included in the Reference section.
- Personal communications may be mentioned in the text with the date of communication as (*Personal communication, 2 June 2000*).

List of references:

- The list of References should be arranged in alphabetical order based on the last name of the first author.
- Names of all the authors should be given except when there are more than 10 authors. When there are more than 10 authors, only the name of
  the first author can be given followed by *et al*.
- All the initials of the author must be given after the last name and the year of publication should follow in parentheses.
- This should be followed by the full title of the referred publication.
- When journal articles are listed, the journal name should be given in full and in italics and followed by the volume number in bold type, issue number in parentheses and then the inclusive pages.
- Where there are several publications by the same author(s) and published in the same year they should be differentiated by adding a lower-case letter after the year. When books are listed, the order should be: author(s), year, book title, volume number, edition, pagination/ inclusive pages, publisher and place of publication. The book title should be in italics. When sections of a book are listed, the order should be: author(s) of chapter, year, title of the section, title of the book, edition, inclusive pages, publisher and place of publication.
- Digital object identifiers (DOIs) should be included for all references where available.
- References should only be cited as 'in press' if the paper has been accepted for publication.

Examples of correct forms of references are given below.

Journal Articles
Boutin C. & Harper J.L. (1991). A comparative study of the population dynamics of five species of *Veronica* in natural habitats. *Journal of Ecology* **79**(01): 199 – 221.
DOI: https://doi.org/10.2307/2260793

Books
Burnham K.P. & Anderson D.R. (2002). *Model Selection and Multimodal Inference*, 2nd edition, pp. 488. Springer Science and Business Media,Inc., New York, USA.

Book Chapters
Hinrichsen R.A. & Holmes E.E. (2009). Using multivariate state-space models to study spatial structure and dynamics. In: *Spatial Ecology* (eds. R.S. Cantrell, C. Cosner & S. Ruan), pp. 145 – 166. CRC/ Chapman Hall, Florida, USA.
DOI: https://doi.org/10.1201/9781420059861.ch8

Edited Books

KimatI H., Amorim L., Rezende J.A.M., Bergamin Filho A. & Camargo L.E.A. (eds.) (2005). *Manual de Fitopatologia*, volume 2. Doenças das Plantas Cultivadas, 4th edition. Ceres, São Paulo, Brazil.

Conference Papers

Weaver D. (2002). Implementation of a learning management system using an integrated approach to professional development. In: Winds of change in the sea of learning. *Proceedings of the 19th Annual Conference of the Australasian Society for Computers in Learning and Tertiary Education (ASCILITE)* (eds. A. Williamson, C. Gunn, A. Young & T. Clear), volume 2, Auckland, New Zealand, 8-11 December. Unitec Institute of Technology, Auckland, New Zealand, pp. 711-720.

Agency Publications

U.S. Census Bureau (2009). *World Population: 1950 – 2050*. U.S. Census Bureau, Washington DC, USA.

Department of Health (2008). *Health Inequalities: Progress and Next Step* (pdf). Department of Health, London, UK. Available at *http:// PublicationsPolicyAndGuidance/ DH _ 08 5307* , Accessed 9 June 2008.

Other

Robinson L.J. (2003) Spatial scale and depletion models of farmland birds in a fragmented landscape. *PhD thesis*, University of Reading, Reading, UK.

Efford M.G. (2008). Density 4.3: software for spatially explicit capture-recapture. Available at *http://www.otago.ac.nz/density* , Accessed 15 March 2009.

Abbreviations and Symbols: Unless common, these should be defined when first used, and not included in the abstract. The SI System of units should be used wherever possible. If measurements were made in units other than SI, the data should be reported in the same units followed by SI units in brackets, e.g. 5290 ft (1610 m).

Formulae and Equations: Equations should be typewritten and quadruple spaced. They should be started on the left margin and the number placed in parentheses to the right of the equation.

Nomenclature: Scientific names of plants and animals should be printed in italics. In the first citation, genus, species and authority must be given. e.g. *Borassus flabellifer* Linn. In latter citations, the generic name may be abbreviated, for example, *B. flabellifer* L.

Tables and figures: Tables and Figures should be clear and intelligible and kept to a minimum, and should not repeat data available elsewhere in the paper. Any reproduction of illustrations, tabulations, pictures etc. in the manuscript should be acknowledged.

Tables: Tables should be numbered consecutively with Arabic numerals and placed at the appropriate position in the manuscript. If a Table must be continued, a second sheet should be used and all the headings repeated. The number of columns or rows in each Table should be minimized. Each Table should have a title, which makes its general meaning clear, without reference to the text. All Table columns should have explanatory headings. Units of measurement, if any, should be indicated in parentheses in the heading of each column. Vertical lines should not be used and horizontal lines should be used only in the heading and at the bottom of the table. Footnotes to Tables should be placed directly below the Table and should be indicated by superscript lower case italic letters (^{a}, ^{b}, ^{c}, etc.).

Figures: All illustrations are considered as figures, and each graph, drawing or photograph should be numbered consecutively with Arabic numerals and placed at the appropriate position in the manuscript. Any lettering to appear on the illustrations should be of a suitable size for reproduction and uniform lettering should be used in all the Figures of the manuscript. Scanned figures or photographs should be of high quality (**300 dpi**), to fit the proportions of the printed page (12 × 17 cm). Each figure should carry a legend so that the general meaning of the figure can be understood without reference to the text. Where magnifications are used, they should be stated.

Units of measurement

Length: km, m, mm, µm, nm

Area: ha, km^2, m^2

Capacity: kL, L, mL, µL

Volume: km^3, m^3, cm^3

Mass: t, kg, g, mg, µg

Time: year(s), month(s), wk(s), d(s), h, min, s

Concentration: M, mM, N, %, g/L, mg/L, ppm

Temperature: °C, K

Gravity: x g

Molecular weight: mol wt

Others: Radio-isotopes: 32P

Radiation dose: Bq

Oxidation-reduction potential: rH

Hydrogen ion concentration: pH